2020

Mathematical modelling of the impact of HIV intervention strategies in Kenya.

Omondi, Evans Otieno
Strathmore Institute of Mathematical Sciences
Strathmore University

Mathematical modelling of the impact of HIV intervention strategies in Kenya

Evans Otieno Omondi

Submitted in total fulfilment of the requirements for the degree of Doctor of Philosophy in Biomathematics of Strathmore University

Institute of Mathematical Sciences

Strathmore University

Nairobi, Kenya

June 2020

Declaration

I declare that this work has not been previously submitted and approved for award of a degree by this or any other University. To the best of my knowledge and belief, the thesis contains no material previously published or written by another person except where due reference is made in the thesis itself.

Name: **Evans Otieno Omondi**

Signature: 

Date: April 24, 2020

Approval

The thesis of Evans Otieno Omondi was reviewed and approved by the following:

Professor Livingstone Serwadda Luboobi

Supervisor,

Institute of Mathematical Sciences, Strathmore University.

Professor Rachel Waema Mbogo

Supervisor,

Institute of Mathematical Sciences, Strathmore University.

Ferdinand Othieno

Dean,

Institute of Mathematical Sciences, Strathmore University.

Dr. Bernard Shibwabo

Director,

Office of Graduate Studies, Strathmore University.

Abstract

Since the identification of the first cases of AIDS almost three and half decades ago, HIV/AIDS continues to inflict major public health and socio-economic challenges. Although various intervention strategies have been employed, cases of new infections are still quite high especially in sub-Saharan Africa. At the end of 2018, nearly 37.9 million people were infected with HIV globally. In Kenya, approximately 1.6 million people are living with HIV with 25,000 deaths resulting from AIDS-related illness yearly. The rise in the cases of infections obviously poses danger in the efforts to contain HIV pandemic. HIV prevention and intervention measures need to be enhanced in order to achieve an HIV free society.

In this work, mathematical models for HIV transmission dynamics with focus on the impacts of testing and counselling, PrEP uptake and ART treatment are formulated and analysed. Vital analyses that include positivity, steady states and their stability conditions for the models are precisely established. Numerical results from fitting the models to real-time surveillance data to show the evolution of populations over time are obtained. Through Pontryagin's maximum principle, qualitative optimal control measure against HIV is established.

Results are indicative of the fact that combination of various control measures lead to reduction in cases of new infections. Our findings show that the introduction of PrEP has a positive effect on the limitation of spread of HIV when the coverage is maintained at 40%. Furthermore, a combination of PrEP uptake, condom use and ART treatment is likely to offer the best control measure against HIV infections. It is thus critical to devote more resources to education on HIV preventive measures and treatment programmes.

In summary, control of new cases of HIV infections should take into account PrEP uptake and combination of condom use and ART treatment. However, PrEP program coverage and individual-level adherence is very critical. These results have the potential to help in escalating programs against HIV infections in high risk populations by modifying the implementation of current interventions, or by adding new control measures.

Table of contents

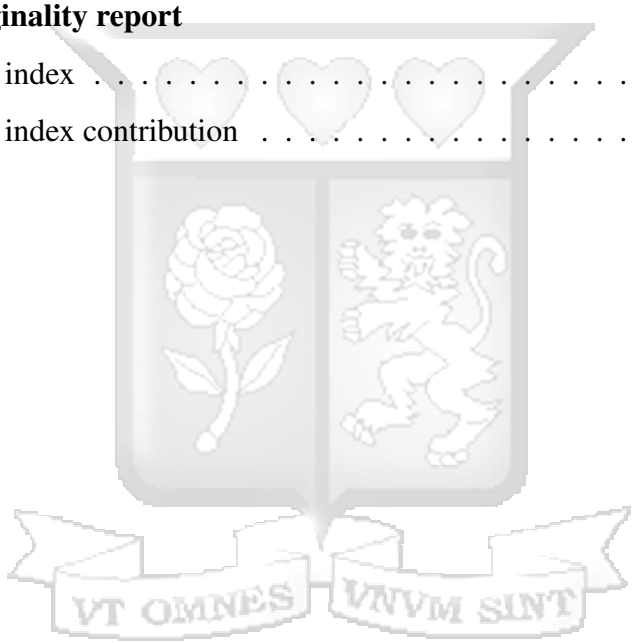

List of figures

List of tables

List of abbreviations

AIDS	Acquired Immune deficiency Syndrome	MCMC	Markov chain monte carlo
ART	Antiretroviral Therapy	MMC	Medical Male Circumcision
CSW	Commercial sex workers	MOH	Ministry of Health
DNA	Deoxyribonucleic acid	MSM	Males who have sex with males
HIV	Human Immunodeficiency Virus	NACC	Kenya National AIDS Control Council
HTC	HIV Testing and Counseling	NGOs	Non-governmental organizations
IDU	Injection drug users	PrEP	Pre-Exposure Prophylaxis
KHIS	Kenya Health Information System	PRCC	Partial rank correlation coefficients
KNBS	Kenya National Bureau of Statistics	UNAIDS	Joint United Nations Programme on HIV/AIDS
LHS	Latin hypercube sampling	WHO	World Health Organization

List of Publications

The following publications were derived from the work in this thesis.

- Omondi, E. O., Mbogo, R. W., and Luboobi, L. S. (2018), "Modelling the Trend of HIV Transmission and Treatment in Kenya", *International Journal of Applied and Computational Mathematics*, 4(5):123, doi: https://doi.org/10.1007/s40819-018-0558-y. See Omondi et al. (2018d).

- Omondi, E. O., Mbogo, R., and Luboobi, L. (2018). "Mathematical modelling of the impact of testing, treatment and control of HIV transmission in Kenya", *Cogent Mathematics & Statistics*, 5(1):1475590, doi: https://www.tandfonline.com/doi/abs/10.1080/25742558.2018.1475590. See Omondi et al. (2018b).

- Omondi, E. O., Mbogo, R., and Luboobi, L. (2018). "Mathematical analysis of sex structured population model of HIV infection in Kenya", *Letters in Biomathematics*, 5(1):174–194. See Omondi et al. (2018c).

- Omondi, E. O., Mbogo, R., and Luboobi, L. "A mathematical modelling study of HIV infection between two heterosexual age groups in Kenya", *Infectious Disease Modelling*, Vol 4 (2019):83–98. See Omondi et al. (2019).

- Omondi, E. O., Mbogo, R., and Luboobi, L. "A mathematical model of HIV transmission between commercial sex workers and injection drug users and analysis of optimal control strategy", *Acta Biotheoretica*, Manuscript accepted for publication.

Conference presentations

The following articles and papers presented at conferences were built from the work in this thesis.

- Omondi, E. O., Mbogo, R. W., and Luboobi, L. S. (2018), "Modelling the Trend of HIV Transmission and Treatment in Kenya", *International Journal of Applied and Computational Mathematics*, 4(5):123, doi: https://doi.org/10.1007/s40819-018-0558-y.

  The results in this paper were presented at the Annual Southern Africa Mathematical Sciences Association (SAMSA) conference held in Arusha, Tanzania, from 20th to 23rd November 2017.

- Omondi, E. O., Mbogo, R. W., and Luboobi, L. S. (2018), "A mathematical modelling study of HIV infection between two heterosexual age groups in Kenya", *Infectious Disease Modelling*, 4(2019):83–98.

  The results in this paper were presented at the the 2nd Workshop on Dynamical Systems and Their Applications in Mathematical Physics, Engineering and Economics (WDS 2019) held at Kulliyyah of Science, International Islamic University Malaysia Kuantan Campus from 26th to 28th August 2019.

Acknowledgement

First and above all, I thank God, the Almighty for the good health and for providing me this opportunity to successfully finish this PhD programme. My God, my good Father, You led me through all the difficulties. I have experienced Your guidance day by day. I will keep on trusting You for my future. Thank you, Lord.

Second, I would like to express my sincere gratitude to my esteemed academic supervisors Prof. Livingstone Luboobi and Prof. Rachel Mbogo for the trust, insightful discussion, valuable advice and support during the period of the study and most important your patience and guidance during this thesis write-up. You have been tremendous mentors to me. May I thank both of you for encouraging my research and for allowing me to grow as a research scientist. Special thanks go to the Institute of Mathematical Sciences, Strathmore University for giving me this opportunity and making my study a memorable one. Thank you. I would also wish to give my humble thanks to all my friends, colleague students for their assistance and encouragements.

Third, special thanks go to my beloved family. Words cannot express how grateful I am to my mother Mrs. Helida Omondi, and father Mr. Leonard Omondi, for all of the sacrifices that you've made on my behalf. Your prayers sustained me thus far. To my brothers (George, Cornel and Kennedy) and sisters (Celline, Maurine, Lilian, Josephine and Jackline) thank you so much for your support and prayers. Many thanks to my eldest sister Dr. Celline Omondi, thank you for leading from the front. Your support and encouragements made this journey an incredible one. More gratitude goes to my lovely wife Eunice Achieng. Thank you for supporting me in everything, and especially I can't thank you enough for encouraging me, praying for me and always loving me throughout this experience. To my beloved daughter Noeline Lakicia, I would like to express my thanks for being such a good girl and always cheering me up. May God Almighty bless you all.

Dedication

This thesis is dedicated to God Almighty for giving me wisdom and good health. To my dad and mum Leonard and Helida Omondi for their love and support. To my siblings George, Celline, Cornel, Maurine, Lillian, Josephine, Jackline and Kennedy Omondi. To my lovely wife and the best friend of my life Eunice Achieng and my beloved daughter Noeline Lakicia. I love you. May God bless you.

Chapter 1

Introduction

1.1 Background to the study

HIV stands for human immunodeficiency virus; this is a virus that causes the immune system to become defenceless against other opportunistic diseases it could normally fight off (Barley et al., 2012). The last stage of HIV infection is acquired immune deficiency syndrome (AIDS). Since it's inception in the 1980s (Sharp and Hahn, 2011), HIV/AIDS continues to inflict major public health and socio-economic challenges in many parts of the world (Barley et al., 2012; CGD, 2016). In addition to the over 20 million people that have so far died of HIV/AIDS, data from the UNAIDS show that nearly 37.9 million people live with HIV/AIDS globally (UNAIDS, 2018a) as at the end of year 2018. Of these, an estimated 1.8 million are children under the age of 15 years and approximately 19.8 million are women constituting about 60% of the new infections (AIDS, 2016b; UNAIDS, 2015a). An estimated 2.1 million individuals worldwide become newly infected with HIV each year of which about 150,000 are children below 15 years of age (AIDS, 2016b). However, AIDS-related deaths have been reduced by more than 51% since the peak in 2004. In 2017, 940 000 people died from AIDS-related illnesses worldwide, compared to 1.4 million in 2010 and 1.9 million in 2004 (AIDS, 2016b; UNAIDS, 2015a). Even though the interventions aimed at reducing the epidemic globally have borne fruits through reduction in the incidence rate, the epidemic continues to inflict major public health and developmental problem. In particular the situation still remains a challenge in sub-Saharan African which bears more than 70% of the global burden (Blaizot et al., 2016; Kharsany and Karim, 2016; UNAIDS, 2016a). The prevalence of HIV globally is given in Figure 1.1.

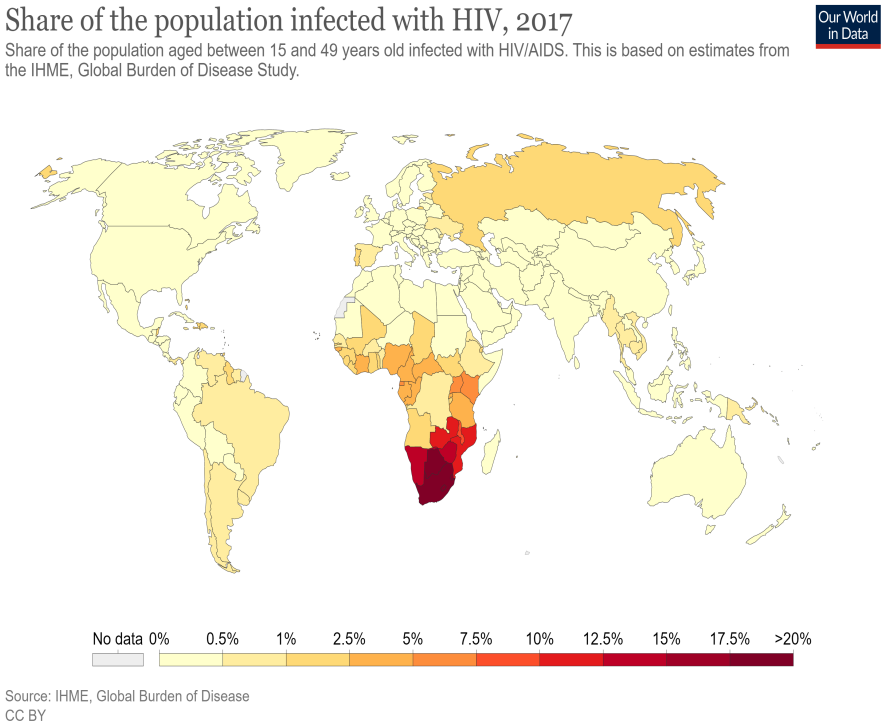

Figure 1.1: Global HIV prevalence. Souce: World Bank (2019).

The HIV epidemic has been evolving in Kenya since the detection of the first case in 1984. Kenya has the fourth highest number of HIV infection globally (UNAIDS, 2015c). The number of people living with HIV was estimated to be 1.6 million at the end of the year 2018 with 25,000 deaths resulting from AIDS-related illness (AVERT, 2019). Based on the sentinel surveillance data, the HIV prevalence peaked at 10.5% in 1996 and fell to 6.0% in 2015 (NACC, 2016). It is estimated that 30% of the new infections in Kenya is deeply rooted among sex workers, men who have sex with men and people who inject drugs (NACC, 2014a). The young people (aged 15-24 years) significantly contribute to high HIV burden in the country. They constitute the largest proportion of people living with HIV. Notably, they contribute 51% of all new HIV infections showing rapid rise from 29% in 2013 (NACC, 2016). In addition, women continue to be disproportionately affected by HIV epidemic. The most affected cohort is the young women between the age of 15 and 24 accounting for approximately 21% of all the new infections (MOH, 2016a; NACC, 2016).

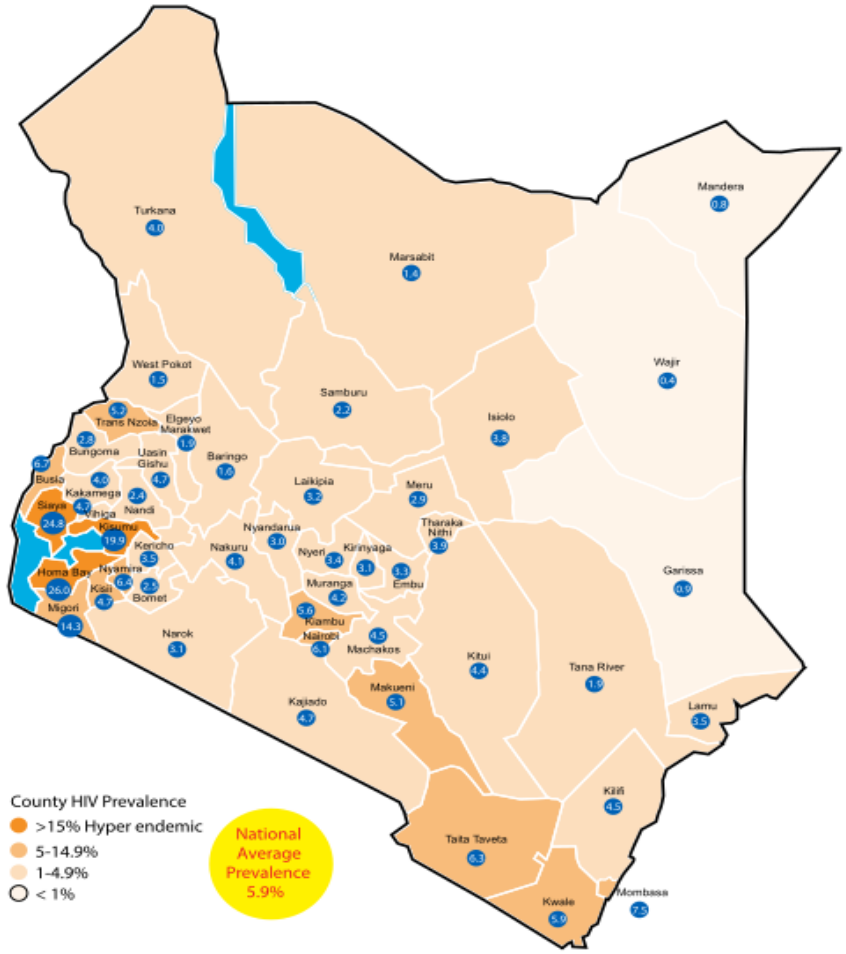

Figure 1.2: HIV prevalence by Counties. Souce: MOH (2016a).

Although progress is being made to control new HIV infections, Kenya still remains one of the six HIV high burden countries in Africa (UNAIDS, 2014). According to MOH (2014b), it is reported that about 65% of the new cases of HIV infections occur in nine out of the 47 counties mainly coastal and western parts of Kenya. Western region that comprises Homabay, Siaya and Kisumu counties are the most affected with HIV prevalence of 25.7%, 23.7% and 19.3% respectively (OPTIONS, 2016; UNAIDS, 2014). The prevalence of HIV by county is given in Figure 1.2. Figure 1.3 shows the prevalence since the identification of HIV/AIDS infection per former provinces.

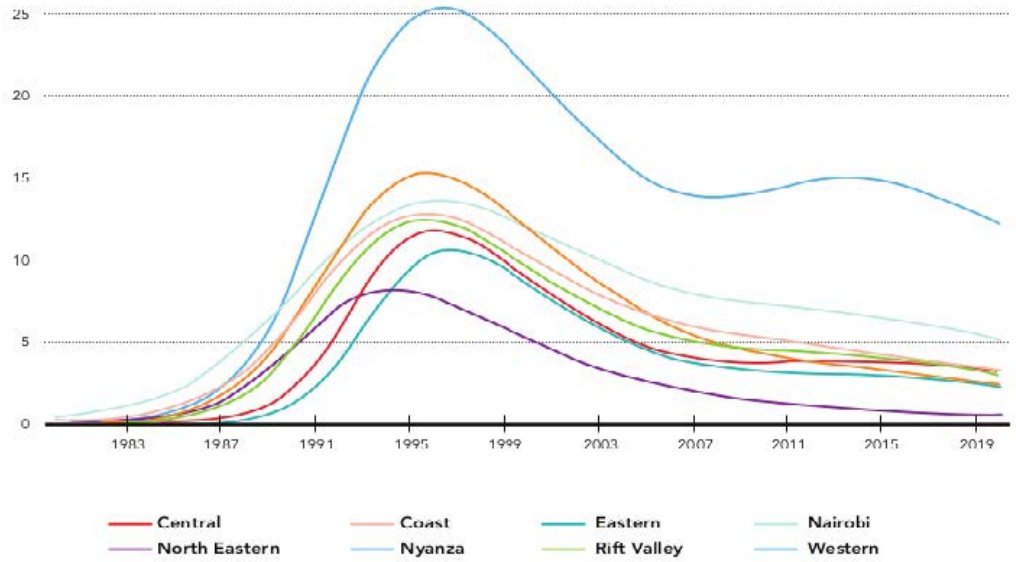

Figure 1.3: HIV prevalence by Provinces. Souce: MOH (2014a).

1.2 HIV life cycle

Understanding the biology of HIV infection in the body is critical in explaining how HIV drugs work to fight the virus. HIV can be transmitted in various ways that can be classified as either horizontal or vertical. Vertical can result from direct transfer of HIV from an infected mother to an unborn or newborn child. Vertical transmission of HIV/AIDS can occur during pregnancy, delivery or breastfeeding and is influenced by many factors, including maternal viral load and the type of delivery (Janini, 1998; Schmid et al., 2004). On the other hand, horizontal transmission of HIV can result from direct physical contact between an infected individual and a susceptible individual. HIV is transmitted through direct contact with certain body fluids that include blood, semen and pre-seminal fluids, rectal fluids,vaginal fluids and breast milk from an HIV infected person with detectable viral load . Sexual intercourse is the most common mode of HIV transmission. Blood to blood contact, such as sharing needles for intravenous injection or blood transfusion can also transmit HIV (De Cock and Weiss, 2000; Morison, 2001).

HIV transmitted through sexual intercourse enters the bloodstream through mucous membranes lining the vagina, foreskin and urethra on the penis, rectum and mouth (Doms and

Trono, 2000). Upon entry into the body, the virion binds to molecules on the surface of the **CD4** cells. It first attaches itself to a **CD4** + T cell receptor then either a **CCR5** or **CXCR4** co-receptors on the surface of a CD**4**$^{+}$ T-lymphocyte (UNR-Med, 2005). The virus then fuses with the host cell after which the virus releases its RNA into the host cell. RNA refers to Ribonucleic Acid interference which is the HIV genetic material (Capodici et al., 2002; UNR-Med, 2005). An HIV enzyme known as reverse transcriptase then converts the single stranded HIV RNA to double stranded HIV-DNA. Reverse transcription yields the HIV preintegration complex (PIC), composed of double-stranded viral cDNA, integrase, matrix, Vpr, reverse transcriptase, and the high mobility group DNA-binding cellular protein HMGI(Y) (Cann and Karn, 1989; UNR-Med, 2005). The newly formed HIV DNA then enters the host cell's nucleus, where it is integrated within the host cell's own DNA by integrase. The integrated HIV-DNA is known as provirus.

When the host cell receives a signal to become active, the pro-virus uses a host enzyme known as RNA polymerase to create copies of the HIV genomic material, as well as shorter strands of RNA known as messenger RNA (mRNA). The mRNA is used as a blueprint to make long chains of HIV proteins. The HIV enzyme protease cuts the long chains of HIV proteins into smaller individual proteins. As the smaller HIV proteins come together with copies of HIV's RNA genetic material, a new virus particle is assembled. The newly assembled virus pushes out ("buds") from the host cell. During budding, the new virus steals part of the cell's outer envelope. This envelope, which acts as a covering, is studded with protein/sugar combinations called HIV glycoproteins. These HIV glycoproteins are necessary for the virus to bind **CD4**+T cells and co-receptors (UNR-Med, 2005). The new copies of HIV can now move on to infect other cells (Kirchhoff, 2013; UNR-Med, 2005). The summary of the life cycle of HIV is given in Figure 1.4.

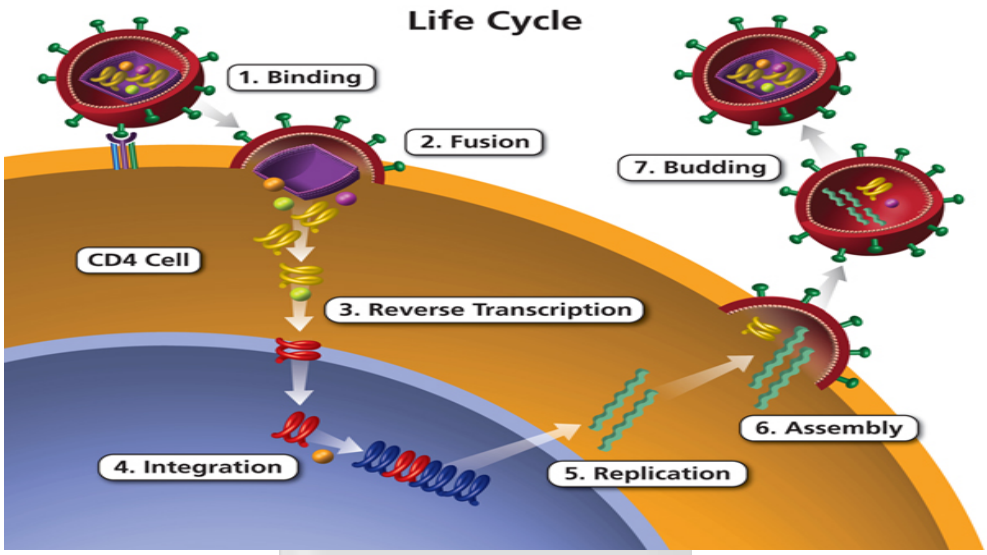

Figure 1.4: The HIV life cycle and stages of infection. Souce: AIDSINFO (2017).

1.3 HIV in Kenya

1.3.1 HIV transmission in Kenya

HIV transmission is primarily through sexual intercourse in heterosexual means and vertical transmission (mother-to-child). Other ways through which HIV is transmitted include homosexuality (men having sex with men) and people who inject drugs (UNAIDS, 2015b). Men who have sex with men commonly known as males who have sex with males acronymed as MSM, are male persons who engage in sexual activity with fellow males (Young and Meyer, 2005). Homosexuality in Africa is widely perceived to be abnormal and against the societal cultural norms believed as an influence from the western countries (Geibel, 2012). In most African countries, same-sex sexual behaviour is criminalized. As a result there exists high level of stigmatization and discrimination of the participants. This stigmatization extends to other members of lesbian, bisexual and transgender community (KLGBTIR, 2017). According to UNAIDS (2015b), HIV prevalence among men who have sex with men in Kenya is estimated at 18.2%. In 2011, an estimated 18.3% of injection drug users (IDU) in Kenya were living with HIV. The majority of people who inject drugs are concentrated

in specific geographical areas such as Nairobi and Mombasa (KLGBTIR, 2017; UNAIDS, 2015b). A summary of the prevalence by modes of transmission is given in Figure 1.5. On the other hand Table 1.1 shows the summary of prevalence by modes of transmission in the three worst affected provinces in terms of HIV infection.

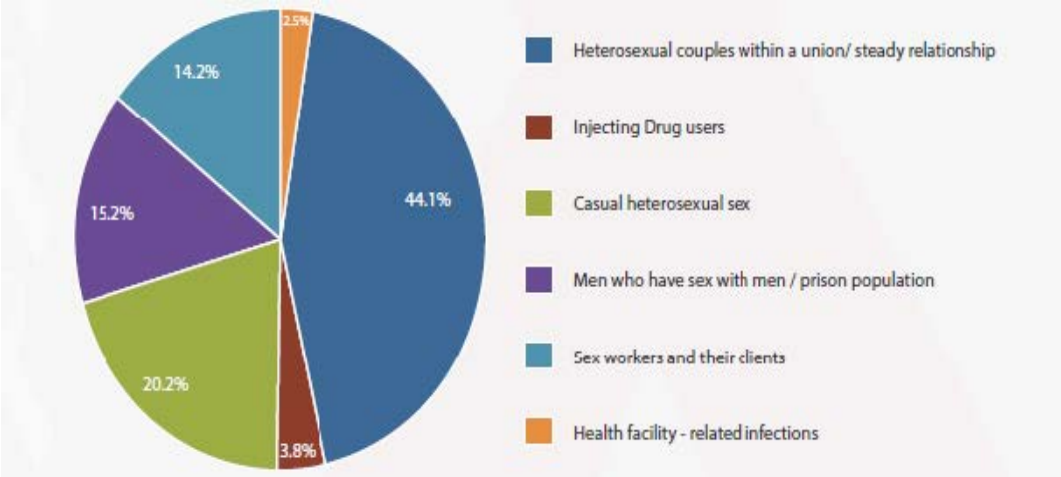

Figure 1.5: Prevalence of HIV infections by modes of transmission in Kenya. Souce: NACC (2009).

Table 1.1: HIV prevalence by modes of transmission for the worst three affected provinces in Kenya. Souce: NACC (2009).

Groups	National	Nyanza	Nairobi	Coast
Heterosexual sex within union/regular partnership	44.1%	38.5%	37.4%	37.9%
Casual heterosexual sex	20.3%	30.5%	23.0%	14.9%
Sex workers and their clients	14.1%	23.1%	14.7%	18.2%
MSM and prison	15.2%	6.0%	16.4%	20.5%
Injecting drug users (IDUs)	3.8%		5.8%	6.1%
Health facility related	2.5%	1.9%	2.7%	2.3%

HIV is also spread through transactional sex. This is defined as an exchange of gifts or money for sex (Kwena et al., 2012; Stoebenau et al., 2016). Relationships arising from transactional sex are described to be non-commercial (Wamoyi et al., 2016). People who take part in these relationships consider themselves as lovers (boyfriends and girlfriends) and not sex workers (Wamoyi et al., 2016). Exchange of sex for goods and services is believed to be a way of life

for many fishing families around Lake Victoria. The high HIV prevalence in western Kenya in the communities living around the Lake Victoria region whose main economic activity is fishing has been largely attributed to "Fish for Sex" (Kwena et al., 2012). The history of "Fish for Sex" in Lake Victoria fishing communities is thought to be associated with the prevailing socio-economic and cultural factors (Mojola, 2011). "Fish for Sex" between men and women is a manifestation of poverty where men and women exploit unequal economic power disparity by demanding sex for any goods or services that either person may need (Gillespie et al., 2007). It is estimated that about 14.5% of men and 5.5% of women aged 15-49 engage in transactional sex (Robinson and Yeh, 2011).

HIV infection alters the the clinical manifestation of tuberculosis (TB). It increases the risk of latent TB and exogenous infections (DeRiemer et al., 2007). TB and HIV co-infection in Kenya has remained high. In 2014, it was estimated that Kenya made up 3.3% of the total number of people living with an HIV/TB co-infection globally (NACC, 2016). It is estimated 38% of people with TB in Kenya are co-infected with HIV. However, it is reported that 83% of people with a co-infection are being treated for both illnesses (NACC, 2014a, 2016). Nonetheless, efforts to prevent co-infection have been slower and only 11% of people living with HIV were enrolled on TB preventative therapy in 2016 (UNAIDS, 2015a). On alcohol use, the unhealthy consumption leads to behaviours that are risk factors for HIV infection and spread (Jaquet et al., 2010; Wamoyi et al., 2016). Kenya in particular and sub-Saharan Africa in general register the highest rates of heavy alcohol use and drinking globally leading to convergence of alcohol and HIV-related diseases (Braithwaite et al., 2014; Chersich and Rees, 2010; Hahn et al., 2011).

1.3.2 Intervention strategies

Key interventions championed by various organs of the government and non-governmental organizations (NGOs) have been highly effective in reducing the risk of HIV transmission. These intervention strategies include HIV testing and counselling, voluntary medical male

circumcision, uptake of pre-exposure prophylaxis (PrEP) and early initiation of antiretroviral therapy (ART).

HIV testing and counselling

Diagnosis of HIV infection is a prerequisite for treatment. Detection of anti-HIV antibodies as a marker of HIV exposure is the most widely used approach for serodiagnosis of HIV (Mehra et al., 2014). Enzyme linked immunosorbent assay (ELISA) has been a preferred screening procedure in this regard (Mehra et al., 2014; Torane and Shastri, 2008). They were the first HIV tests available in the 1980s. However, the labour intensive and time consuming format of the assay as well as the requirement of instrumentation and technical expertise has resulted in a shift from an ELISA based approach to rapid diagnostic tests (RDTs), particularly in resource constrained settings. There are four types of simple/rapid tests: agglutination assays, comb/dipstick assays, flow-through membrane assays, and chromatographic membrane assays (AIDS-Action, 2005). While some studies have reported the performance of RDTs and ELISA to be comparable Lien et al. (2000), results from others have raised concerns regarding sensitivity and specificity of the rapid assays (Claassen et al., 2006; Gray et al., 2007). Most commercially available ELISA have a high sensitivity and specificity and are able to detect all subtypes of HIV-1 and HIV-2 in comparison to RDTs. Another technique of testing HIV is based on amplification of the pro-viral DNA from infected peripheral blood mononuclear cells (PBMC) and detection by DNA. This method of testing HIV is known as Nucleic Acid Amplification Testing (NAAT) (Medscape, 2010). Nucleic acid amplification technologies (NAATs), such as polymerase chain reaction (PCR) tests, work by detecting the genetic material of the virus. The HIV NAAT test is a very sensitive test designed to detect HIV RNA in blood and is capable of detecting 1-10 copies/ml of HIV proviral DNA (RNA) (Medscape, 2010). RNA is the viral equivalent to human DNA. The NAAT test is able to detect HIV RNA as early as seven to 14 days after infection with HIV (Fiebig et al., 2003; Sickinger et al., 2008; Stekler et al., 2007). Unlike the RDTs, the NAAT test will always give a positive result as long as there is HIV in someone's blood. Like viral culture, PCR

testing is expensive, requires sophisticated facilities and highly trained technicians, and is not feasible in most developing countries.

In Kenya, rapid diagnostic tests (RDTs) and ELISA based testing are carried out through voluntary counselling and testing which refers to the process initiated by an individual who wishes to know his HIV status. According to the WHO regulations, all forms of HIV testing and counselling should be voluntary and adhere to the five Cs namely: consent, confidentiality, counselling, correct test results and connection to care, treatment and prevention services (WHO, 2014). Identification of recent HIV infections and their role in driving the HIV epidemics is critical in understanding the spread of HIV and the deployment of relevant control measures (Quinn et al., 2000; Yerly et al., 2001). According to NACC (2014a), an estimated 53% of the 1.6 million people living with HIV in Kenya are not aware of their HIV status. In addition, approximately 260,000 couples in HIV sero-discordant couples significantly contribute to new infections. Therefore, HIV testing and counselling (HTC) has been encouraged significantly by the Kenyan government.

In its efforts to reduce HIV spread, HTC has been adopted through targeted community – based testing and door-to-door testing initiatives. In order to boost these efforts, Kenyan government announced plans to introduce self-test kits in 2015 (UNAIDS, 2016b) which were subsequently approved and launched in 2017 (Kelvin et al., 2019). In 2008, approximately 860,000 people were being tested annually for HIV totalling to about 6.4 million people by the end of 2013 (NACC, 2014b). Furthermore, the report from (NACC, 2014b) indicate that HTC coverage among the pregnant women have risen substantially. Between 2009 and 2013, the number of pregnant women tested for HIV increased from 68% to 92%.

Uptake of Pre-Exposure Prophylaxis (PrEP)

Pre-exposure prophylaxis (PrEP) is the prophylactic use of anti-retroviral drugs (ARVS) by people who do not have HIV but are at high risk of acquiring it to prevent HIV infection (AIDS, 2016a; HIV/AIDS, 2016). Injectable cabotegravir (CAB) is considered better than a combination of daily oral HIV drugs – Tenofovir disoproxil fumarate 300mg plus

Emtricitabine 200 mg (TDF/FTC) (McPherson et al., 2018; Oral-PrEP, 2017). The only drug regimen currently licensed for HIV pre-exposure prophylaxis, or PrEP, in Kenya, is the anti-HIV medication Truvada taken daily as an oral tablet (Oral-PrEP, 2017). Oral PrEP contains two antiretroviral drugs: tenofovir disoproxil fumarate (TDF) and emtricitabine (FTC) (Oral-PrEP, 2017). When someone is exposed to HIV through sex or injection drug use, these pills can potentially work to keep the virus from establishing a permanent infection. PrEP has been shown to reduce the risk of HIV infection in people who are at high risk by up to 92% (HIV/AIDS, 2016). However, PrEP is much less effective if it is not taken consistently (Bush et al., 2016; HIV/AIDS, 2016). In 2016, Kenyan government issued full regulatory approval of PrEP, becoming the second country in sub-Saharan Africa to make such approval (UNAIDS, 2016b). However, much of the successes are yet to be reported since research into the uptake and impact of PrEP, specifically with young women and girls in high-incidence areas is still on-going (UNAIDS, 2016b). In addition, Kenya is among seven African countries carrying out large-scale clinical trials of a long-lasting injectable PrEP in sexually active women. The trials, called HPTN 084 and sponsored by the US National Institutes of Health will examine whether a long-acting form of the investigational anti-HIV drug cabotegravir injected once every eight weeks can safely protect women at risk of HIV infection.

Medical male circumcision

Medical male circumcision is a surgical procedure that involves the removal of the foreskin of the penis. It is estimated that approximately 30% to 39% of the global male population is circumcised (Morris et al., 2016; WHO, 2008). Most randomized studies conducted in the mid-2000s established that male circumcision reduces the female-to-male sexual transmission of HIV by 60% (Auvert et al., 2005, 2006; Bailey et al., 2007; Morris et al., 2016; Prodger and Kaul, 2017; Weiss et al., 2008). Since then, WHO/UNAIDS recommended that male circumcision should be considered an efficacious intervention for HIV prevention in countries and regions with heterosexual epidemics, high HIV and low male circumcision prevalence (Njeuhmeli et al., 2011; WHO et al., 2009). As a result, in 2008 Kenya rolled

out the voluntary male medical circumcision for HIV prevention prioritizing the areas with high HIV prevalence among uncircumcised men (CDC, 2012). By 2015 this initiative had circumcised 860,000 males between the ages 15 and 49 years (AVERTS, 2007; UNAIDS, 2016b).

ART treatment

Antiretroviral therapy (ART) refers to the use of a combination of three or more antiretroviral drugs (ARVs) to achieve the suppression of the viral load (WHO, 2014). According to Pau and George (2014) the current classes of drugs included in antiretroviral therapies include:

- **Entry or fusion inhibitors:-** These inhibitors block the virus's ability to enter the body's CD4 cells.
- **Nucleoside reverse transcriptase inhibitors (NRTIs):-** HIV requires an enzyme called reverse transcriptase (RT) in order to replicate. By offering faulty versions of RT to the virus, NRTIs block HIV's ability to replicate. There are many approved NRTIs that include:- Emtriva (emtricitabine or FTC), Epivir (lamivudine or 3TC), Retrovir (zidovudine or AZT), Tenofovir alafenamide fumarate, Videx (didanosine or ddI), Viread (Tenofovir disoproxil fumarate or TDF), Zerit (stavudine or d4T) and Ziagen (abacavir).
- **Non-nucleoside reverse transcription inhibitors (NNRTIs):-** These inhibitors disable a key protein that HIV requires to replicate. The approved NNRTIs include:- Edurant (rilpivirine or RPV), Intelence (etravirine or ETR), Rescriptor (delavirdine), Sustiva (efavirenz) and Viramune (nevirapine).
- **Protease inhibitors (PIs):-** This inhibitor disables the protein called protease, another key building block required by HIV to replicate. Such approved drugs include:- Aptivus (tipranivir), Crixivan (indinavir), Invirase (saquinavir), Kaletra (lopinavir plus ritonavir), Lexiva (fosamprenavir), Norvir (ritonavir), Prezista (darunavir), Reyataz (atazanavir) and Viracept (nelfinavir).

- **Integrase inhibitors (INSTIs):-** Once HIV has penetrated a CD4 cell, it inserts genetic material into the cells with the assistance of a protein called integrase. These inhibitors block the virus' ability to complete this crucial replication step.

- **Fixed-Dose Combinations:-** Although not a separate class, there are fixed-dose drugs that combine two or more HIV drugs from one or more classes in just one pill. This can make taking the medication easier. Fifteen combination pills have been approved that include:- Atripla (Sustiva plus Emtriva plus Viread), Biktarvy (Bictegravir plus Descovy), Combivir (Retrovir plus Epivir), Complera (Emtriva plus Viread plus Edurant), Descovy (Emtriva plus tenofovir alafenamide (TAF)), Epzicom (Epivir plus Ziagen), Evotaz (Reyataz plus Tybost), Genvoya (Vitekta plus Tybost plus Emtriva plus tenofovir alafenamide fumarate (TAF)), Juluca (Tivicay plus Edurant), Odefsey (Emtriva plus tenofovir alafenamide (TAF) plus Edurant), Prezcobix (Prezista plus Tybost), Stribild (Emtriva plus Viread plus Vitekta plus Tybost), Triumeq (Ziagen plus Tivicay plus Epivir), Trizivir (Retrovir plus Epivir plus Ziagen) and Truvada (Emtriva plus Viread).

- **Boosting Agents:-** These drugs do not affect HIV's lifecycle; rather, they improve, or 'boost', the level of other drugs in the bloodstream so that the other HIV drugs can be taken at a lower dose. They include:- Norvir (ritonavir) and Tybost (cobicistat).

The drugs do not kill or cure the virus and are lifelong treatment for HIV patients. The major intervention for HIV infection is that when people are infected with HIV they should start ART treatment as soon as possible, an approach referred to as "universal test and treat" (UTT), to reduce the risk of dying (Williams, 2014; Williams et al., 2010). The UTT approach represents a set of strategies that aim to advance a broader project of expanding HIV testing and scaling up access to ART, with concerns for the health and rights of those living with HIV at its core. As this shift has taken place, HIV researchers have also increasingly focused on developing strategies for implementing the series of steps involved in diagnosing, treating, and keeping HIV-positive individuals engaged in ongoing care often referred to as the "treatment cascade" or "care continuum" (Gardner et al., 2011).

As at June 2016, an estimated 18.2 million people living with HIV were receiving antiretroviral treatment (ART) representing 46% of all adults and 49% of all children living with HIV globally (UNAIDS, 2017). In its efforts to reduce HIV infections, in 2015, Kenya began to adopt 2015 WHO recommendations to immediately offer treatment to people diagnosed with HIV in order to increase the ART access. It is estimated that about 826,000 adults and 71,500 children were receiving ART treatment in 2015 (UNAIDS, 2016b). The fact that ART has the potential to stop transmission of HIV, United Nations Programme on HIV and AIDS (UNAIDS) called for an end to HIV/AIDS centred on 90-90-90 target by 2020 (United Nations Programme on HIV/AIDS, 2014). The strategy implies that 90% of all those living with HIV should have been tested within the last one year, unless they already know that they are infected with HIV, 90% of these should be on treatment and 90% of these should have plasma viral loads below 1,000 copies/mL.

There is no doubt that ART is beneficial, but it is also associated with toxicities and resistance. Pre-clinical and clinical studies have demonstrated short-and long-term adverse events on ART, including haematological, renal, cardiovascular, bone and metabolic abnormalities (Nolan et al., 2005). The short term side effects are frequently observed on initiation of ART, with dizziness and gastrointestinal disorders (diarrhoea, nausea and vomiting) (Tukei et al., 2012). The long term effects observed are particularly important as they impact quality of life in adulthood. Lipodystrophy, as described by abnormalities of fat loss (lipoatrophy), fat accumulation (lipohypertrophy), dyslipidemia, insulin resistance, diabetes, lactic acidosis or mixed forms, has been observed to occur in 20–50% of patients on ART for prolonged periods. These abnormalities have been associated with specific antiretroviral drugs, such as stavudine, lopinavir/ritonavir, zidovudine and efavirenz; older age; puberty; and longer ART duration (Blázquez et al., 2015; Tukei et al., 2012). The numbers of people with drug resistant virus has increased over time as a result of the largely growing levels of resistance to NNRTI drugs in sub-Saharan Africa (Gupta et al., 2012). One reason for this is that just one mutation-notably the K103N mutation – causes high-level resistance to the NNRTIs efavirenz and nevirapine and cross-resistance between the two drugs. This leaves few treatment options for drugs in this class (Gupta et al., 2012).

1.4 HIV vaccine and global efforts towards its eradication

The search for HIV vaccine to prevent HIV infections has been on since 2016 in South Africa. The first HIV vaccine efficacy study is being tested to establish whether an experimental vaccine regimen safely prevents HIV infection among adult South Africans (NIH, 2019). The study named HVTN 702, involves a new version of the HIV vaccine candidate that has been shown to provide some protection against the virus (Vaccine, 2018). This study targets 5,400 men and women for trial effectively making it the largest and most advanced HIV vaccine clinical trial to take place in South Africa (NIH, 2019). Development of a safe and effective HIV vaccine will probably be essential to achieve a durable end to the HIV pandemic. Moreover, additional HIV vaccine candidates are being pursued as the research into HIV vaccine awaits efficacy results from HVTN 702 (Barouch, 2018). These include adenovirus vectors expressing mosaic immunogens with an env gp140 protein boost, cytomegalovirus vectors that induce persistent T-cell responses, native-like env trimers, and sequential env immunisation approaches that aim to induce broadly neutralising antibodies (Stephenson et al., 2016).

1.5 Statement of the problem

Since the detection of the first cases of HIV/AIDS in early 1980's, it has remained one of the global health and developmental problem. At the end of the year 2018, it was estimated that 37.9 million people were living with HIV with approximately 770,000 deaths resulting from HIV-related illness globally (UNAIDS, 2018a). There is no cure or vaccine against HIV but various control programmes such as use of condoms, medical male circumcision and PrEP uptake in addition to treatment with ART have been rolled out across the world to stop new HIV infections. Treatment with ART has proven to have enormous benefits to the HIV patients due to its ability to reduce the patients' risk of dying through suppression of viral load in the blood to undetectable levels. Due to these benefits, WHO and UNAIDS made

recommendations for HIV treatment centred on 90-90-90 to be achieved by 2020 (United Nations Programme on HIV/AIDS, 2014).

Despite the intense and aggressive interventions put in place, there is still growing number of new HIV infections more so in sub-Saharan Africa where adult prevalence stands at 7.0% (AVERT, 2018). In Kenya, the number of people living with HIV was estimated to be 1.6 million at the end of the year 2018 with 25,000 deaths resulting from HIV-related illness (AVERT, 2019). The adult HIV prevalence was reported to be 4.7% at the end of the same year. Furthermore, there were 46,000 new cases of HIV infection in 2018 of which approximately 51% occurred among the young adults aged between 15 years and 24 years. To reduce the effect of HIV pandemic, Kenyan government adopted WHO and UNAIDS recommendations for HIV treatment centred on 90-90-90 which has seen 64% of the adults aged between 15 years to 49 years and 65% of children (aged 0-14 years) living with HIV receiving ART treatment. In addition to ART treatment, the Kenyan government is currently encouraging the up-take of PrEP following its roll-out in May 2017 in order to limit the spread of HIV and contain new infections by 2030.

Owing to the dramatic rise in the occurrence of new cases of HIV infection in Kenya especially amongst young adults aged between 15 years and 24 years, the need to understand the transmission dynamics and the need for eradication of further infections so as to meet the Kenya's vision 2030 is today greater than ever. Elimination of HIV infection offers the potential to the government for focusing to other essential economic matters of the society. Therefore, this research intends to provide theoretical insights on the dynamics of HIV infection in the adults aged 15 years and above as well as sex workers and injection drug users using real-time surveillance data. Impacts of HIV testing and counselling (HTC), ART treatment and PrEP uptake are investigated in this study. We extend the existing HIV models to determine the effectiveness of PrEP in containing new cases of HIV infections and combination of these intervention measures while at the same time providing valuable insights into shaping the intervention policies in limiting HIV spread.

1.6 Research objectives

1.6.1 General objective

The main aim of this research is to develop deterministic mathematical models to determine the potential impact of HIV intervention strategies that include HTC, ART treatment and PrEP on HIV incidence in Kenya.

1.6.2 Specific objectives

(i) To develop a mathematical model for investigating the dynamics of HIV transmission amongst the adults population aged 15 years and above in order to determine the impact HTC and ART treatment.

(ii) To extend the model to a sex structured mathematical model to analyse the impact PrEP in limiting the spread of HIV.

(iii) To mathematically determine the epidemiological differences of HIV infections between young adults (age 15-24 years) adults (aged 25 years and above).

(iv) To extend the sex structured mathematical model to one for the analysis of the dynamics of HIV between commercial sex workers and injection drug users.

(v) To determine an optimal therapy for HIV transmission between commercial sex workers and injection drug.

1.7 Significance of the study

In the current era mulled by significant number of new HIV infections, understanding the transmission dynamics and potential control measures is vital in the fight to eradicate HIV. Our study is therefore, important in the following aspects:

(i) It adds onto the platform for research in mathematical modelling of HIV/AIDS infections and gives an insight into the predictions of the cause of the epidemic given different transmission patterns among different risk groups.

(ii) It gives an insight into shaping the intervention policies in limiting HIV spread thereby contributing to the Kenya vision 2030 aimed at eradicating HIV infections and consequently reducing the country's disease burden.

(iii) The mathematical framework adds to the elaborate bank of knowledge and procedure for carrying out analyses related to mathematical models for HIV infection.

Due to the fact that no effort towards containing diseases is insignificant, a critical look at the aspects presented in this thesis not fully considered previously were valuable. HIV transmission, manifestation and global spread follows a chain of events some of which are related to human movement, lifestyle, social economic status and policies made in communities.

1.8 Sources of data

HIV incidence and sentinel data were obtained from Kenya Health information System available at KHIS and Kenya National AIDS Control Council (NACC). Details of the data are explained in each chapter where data are used. Least squares and Markov chain Monte Carlo (MCMC) methods would be used to estimate parameters with the aim of determining the key parameters that would aid possibility of eliminating new transmissions as well as containing HIV infection from the population.

1.9 Outline of the thesis

In Chapter 2 we provide a brief literature review of the modelling work done on the transmission, spread and control of HIV/AIDS. The review consists of the highlights on the

transmission routes of HIV/AIDS, classification of patients, control measures incorporated as well as mathematical techniques applied in the models.

In Chapter 3, we study the general trend of HIV transmission and treatment with ART. Mathematical analysis of the model is done and the model is fitted to surveillance data representing the adult population aged 15 years and above.

In Chapter 4, we develop a sex structured model to study the difference in transmission between male and female adults. Projections up to the year 2030 are made and recommendations drawn.

In Chapter 5, an age and sex-structured model is analysed with the aim of gaining qualitative insight into the effect of age on HIV transmission dynamics and establish whether there are statistical significant differences in HIV infection in Kenya within and between different age groups.

In Chapter 6, a model incorporating the transmission of HIV between commercial sex workers and injection drug users is formulated with a coupling between these risk groups. Mathematical analysis of the model is done. Optimal control of HIV between coupled risk groups is studied. The permissible controls are assumed to be non-linear and that implementation of controls may contain the infection in about half the time it would take the infection under self-limitation.

In Chapter 7, we discuss the thesis results by linking the results to the already published results from other authors and works. We then conclude the thesis by discussing the limitations of the study and making recommendations for future consideration.

Chapter 2

Literature review

2.1 Introduction

Mathematical modelling plays a vital role in understanding HIV/AIDS epidemiology (Auvert et al., 2000; Garnett, 2002). Modelling the population level impact and cost-effectiveness of an HIV prevention method helps to inform policy (Pretorius et al., 2010). Modelling is particularly helpful in evaluating the possible impact of a combination of prevention methods, showing how results are likely to vary depending on levels of acceptability, product adherence and whether there might be synergy or antagonism between prevention methods. Modelling is also useful in the context of trial designs for multi-component prevention methods, identifying the intervention components that are most critical to maximizing effectiveness. It is therefore plausible to believe that with the progressive research on the HIV infection, more factors that drive the epidemic are identified. In this chapter, we outline and review previous studies and models that focus on HIV transmission and the various prevention methods under consideration as well as the key results.

2.2 Mathematical models that studied the dynamics of HIV transmission

In an attempt to study the HIV transmission pathways, various epidemiological models have been developed. Apenteng and Ismail (2017) developed and used mathematical models that described how to model the spread of HIV/AIDS epidemics with constant inflow of migration into the male and female populations. They included migration to assess its effect

on the spread of HIV/AIDS in the generation population. The model developed in their work comprised of six differential equations within the male and female populations, depicting the dynamics of the spread of HIV/AIDS epidemics. The basic reproduction number for each of the two categories of the population (males and females) was separately determined to establish the global stability of the disease-free equilibrium. However, in this model, no account of control strategies were considered. Furthermore, this model was not tested against real-world data to determine its fitness and accuracy.

Mathematical models in Mukandavire and Garira (2007a,b), described the heterosexual interactions of males and females using integro-differential equations with a time delay due to incubation period. While these two models incorporated the effects of male and female condom use as the main mode of preventing HIV infection, there was no explicit consideration of test and treat in addition to application of real-time surveillance data to establish the trend of infection was not considered.

Hethcote (1989) proposed a model for transmission of HIV/AIDS. In this work, a description of infection process by interactions within and between risk groups such as homosexual men, bisexual men, female prostitutes, intravenous drug abusers and heterosexually active men and women was given. The model developed in this work was proposed for suitable modification to specifically study the transmission of HIV infection and the incidence of AIDS in risk groups in the U.S.A. Related to this, Castillo-Chavez et al. (1989) formulated and analysed a single and multiple group susceptible-infectious (S-I) mathematical models for the spread of HIV/AIDS. The results from these models were stated for specific and arbitrary survivorship functions. They established that the reproductive number is not significantly affected by the shape of the survivorship function. It is important to note that in these studies, there were not attempts made to fit the models to data and estimate the parameters.

Baryarama et al. (2006) proposed a model that considers the dynamics of HIV/AIDS with gradual behaviour change. The model in this work consists of three differential equations as

presented in (2.1)

$$\left.\begin{aligned} \dot{S} &= p\lambda[\varepsilon I(t-\alpha)+S(t-\alpha)] - \frac{\omega(t)SI}{N} - \mu S, \\ \dot{I} &= \frac{\omega(t)SI}{N} - (\nu+\mu)I, \\ \dot{A} &= \nu I - (\tau+\mu)A. \end{aligned}\right\} \tag{2.1}$$

The variables S, I and A describe susceptibles, infectives and AIDS symptomatic cases respectively. The variable force of infection $\omega(t) = \beta(t)c(t)$ is used instead of the constant force of infection β_c to allow for incorporation of behaviour change from behavioural surveillance data. $\beta(t)$ represents HIV transmission probability while $c(t)$ is the average number of sexual acts per year. The quanties p and ε are proportions α is the mean age and $\lambda, \nu, \mu,$ and τ are constant rates. The model was used to study the dynamics of HIV and behaviour change in Uganda. The model was used to make comparison of model projections for urban, semi-urban and rural Uganda made against HIV prevalence trends from corresponding antenatal clinic data. In the obtained results, the authors observed that a decrease in the behaviour parameter directly leads to a decrease in the number of secondary infections. This study focused on the mathematical analysis of the model with no application of data for model validation.

Isdory et al. (2015) presented a SIR meta-population model to study the impact of human mobility to the transmission of HIV/AIDS. In their model, the dynamics in each sub-population included only individuals aged 15-64 years with the assumption that this age group are most sexually active and hence susceptible to HIV. The model comprises of thirteen differential equations. The basic reproduction number was computed and the parameter estimates obtained from fitting the model to census data, HIV data and mobile phone data adopted to track human mobility from different regions in Kenya. The authors established that movement between different regions appears to have a relatively small overall effect on the total increase in HIV infection in Kenya. The results suggest that the consequence of movement patterns is the transmission of the disease from high infection to low prevalence areas. The authors concluded that mobility slightly increases HIV incidence rates in regions with initially low HIV prevalences and slightly decreases incidences in regions with initially high HIV prevalence.

In as much as data were used in this study, there was no consideration of test and treat which is critical in limiting spread of HIV.

Okongo et al. (2013) used a mathematical model to investigated the effects of social behaviour, treatment of and vaccination against HIV. The model's stability analysis was performed and numerical simulations carried out. They established that treatment which does not reduce infectivity may not reduce spread of HIV. The incorporation of practical control measures such as behaviour change and treatment in models present an opportunity to assess the benefits of the intervention of public health authorities (Sahu and Dhar, 2015; Yan et al., 2007).

Liu et al. (2007) studied the psychological impact on periodic oscillations of emerging infectious diseases. They established that an increment in the infection level decreases the effective contacts. Kiss et al. (2010) developed a deterministic model to study the impact of information transmission on sexually transmitted diseases. Their model accounted for the diffusion of health information disseminated as a result of the presence of a disease and an 'active' host population that can respond to it by taking measures to avoid infection or if infected by seeking treatment early. In their findings they concluded that only a proportion of the population chooses to respond to the risks by limiting effective contacts and subsequently seeking immediate treatment. While these models incorporated the effects of HIV prevention through such means as behaviour change and as well as treatment with ART, they did not consider the immediate enrollment of new HIV infected individuals to treatment following the WHO and UNAIDS recommendation for HIV treatment centred on 90-90-90 (United Nations Programme on HIV/AIDS, 2014).

2.3 Mathematical models that assessed the impact of PrEP

Clinical trials have in the recent past demonstrated the effectiveness of PrEP in preventing HIV infection. Various mathematical models have been developed to evaluate the impact of PrEP on HIV incidence and prevalence. While investigating the impact of HIV prevention measures including PrEP on HIV incidence in South Korea, Kim et al. (2014) formulated a

seven state deterministic model. The basic reproduction number was computed and sensitivity analysis of the outcome to the model parameters carried out. The model was then fitted to HIV incidence data. The results obtained suggested that the most effective prevention measure against HIV would be PrEP and would greatly reduce HIV incidence in South Korea.

Simpson and Gumel (2017) developed deterministic model for HIV/AIDS that incorporated PrEP and used to assess the population-level impact of the use of PrEP on the transmission dynamics of the disease within an MSM population. They performed detailed mathematical analysis. Data relevant to HIV transmission dynamics in the MSM community in the U.S. State of Minnesota were used to carry out both uncertainty and sensitivity analysis. This was done mainly to determine the effect of the uncertainties in the parameter values on the outcome (response) variable (the associated reproduction number) and to identify the parameters that have the most effect on the disease transmission dynamics. The results from their numerical simulations showed that, if the current rate of administration of antiretroviral treatment is maintained, HIV burden decreases with increasing PrEP coverage. This study suggested that HIV can be effectively controlled in the MSM population if, in addition to the current rate of administration of antiretroviral therapy in the community, at least 61-77% (with mean of about 70%) of the susceptible members of the MSM community are on PrEP.

Li et al. (2018) developed a deterministic mathematical model to study the biomedical interventions for HIV prevention among men who have sex with men in China. They used the model for projection over 20 years to assess the impact of the PrEP, biomedical interventions and their combinations. Incidence and prevalence of HIV were measured, and cost-effectiveness was assessed using incremental cost per quality-adjusted life year gained. They established that the optimal cost-effectiveness path is from test-and-treat to the combination strategy of test-and-treat and PrEP. These strategies could almost eliminate new HIV infections over the next 20 years. Thus, PrEP is an important and cost-effective addition to current policy geared towards eliminating HIV infections.

Afassinou et al. (2017) developed a deterministic model for HIV/AIDS to be utilised to assess the impact of combining PrEP and ARVs use interventions. Detailed the mathematical

analysis was carried out. Their results predicted a significant decrease in the number of new HIV infections when PrEP and ARVs are concurrently implemented at high levels (90%-100%). The results also reveal that PrEP drug resistance has the potential to slow down or reverse the impact of PrEP, especially at low efficacy levels. It is important to note that the model analysed in this study was not validated using data.

Silva and Torres (2017) developed a model for HIV/AIDS transmission including PrEP. The existence, uniqueness and global stability of the disease free and endemic equilibria were proved. They then calibrated the model with no PrEP with the cumulative cases of infection by HIV and AIDS reported in Cape Verde from 1987 to 2014, showing that it predicts well such reality. Key results from this work through numerical simulations, showed that PrEP reduces HIV transmission significantly. While the results from this work are interesting, it would be plausible to extend this model to include the interaction between key populations, more specifically the interaction between sex workers and injection drug users.

2.4 Mathematical models that incorporated HIV testing, ART and circumcision

Early diagnosis and immediate treatment of HIV infection as well as suppression of the viral load remain the key interventions in reducing the HIV incidence. To understand the severity of the HIV epidemics as well as establishing a baseline in Lianshan in China, Su et al. (2016) constructed a deterministic transmission model. This model consisted of four differential equations as given in (2.2)

$$\left.\begin{aligned} \dot{S} &= \Lambda - \lambda\frac{S}{N} - d_S S, \\ \dot{I} &= \lambda\frac{S}{N} - \alpha I - d_I I, \\ \dot{D} &= \alpha I + \rho T - \gamma D - d_D D, \\ \dot{T} &= \gamma D - \rho T - d_T T. \end{aligned}\right\} \tag{2.2}$$

In their model, S represents the number of susceptible people, I represents the number of undiagnosed HIV positive people, D denotes the number of people who are diagnosed with HIV but are not in a treatment program, and T denotes the number of people who are diagnosed with HIV and are enrolled in a treatment program. The force of infection λ is expressed as $\lambda = \beta_I I + \beta_D D + \beta_T T$. The model was calibrated using surveillance and treatment data for the period 2005–2008. The authors then validated the model by comparing its predicted value of HIV prevalence in 2010 to the prevalence data of 2010. The validated model produced estimations on the new infections, people living with HIV (PLWHIV) and HIV-AIDS related deaths. From their results, it is established that HIV control programs have drastically scaled up the HIV testing and treatment. This was reflected in the new treatments for HIV. The results affirm that population-wide screening programs has tested 50% and 99% of the population in Jiudu and Muer townships respectively. However, the heterogeneity of the people living with HIV was not considered hence a limitation in this model.

On the other hand, Kok et al. (2015) constructed a system of dynamic model of the continuum of HIV care in Vancouver, Canada. This model incorporated the main activities and decisions in the delivery of antiretroviral therapy that included HIV testing, linkage to care and long-term retention in care and treatment. The system model developed was coupled to a non-linear compartmental HIV transmission model. In the development of the model, the authors considered four sub-populations namely; men who have sex with men, injection drug users, female sex workers and the general population. Each of the models in the sub-populations consisted of 17 compartments representing the stocks of undiagnosed and diagnosed groups. The model was then used to find optimal allocation of testing resources which minimize the total number of new infections. The model was fit to data obtained from public health sources that included British Columbia Centre for Excellence in HIV/AIDS. The findings predicted a lower than expected number of new diagnoses among MSM. Furthermore, their findings suggested that optimal resource allocation favours routine testing in high prevalence settings over targeted testing and that a greater impact would be achieved by allocating more resources to routine testing in high prevalence settings for MSM.

Elbasha and Gumel (2006) analysed a number of deterministic models for theoretically assessing the potential impact of an imperfect prophylactic HIV-1 vaccine that had five biological modes of action, namely “take," “degree," “duration," “infectiousness", and “progression," and could lead to increased risky behavior. The key findings of the study included the idea that, if the vaccinated reproduction number is greater than unity, each of the models considered had a locally unstable disease-free equilibrium and a unique endemic equilibrium. Owing to the vaccine-induced backward bifurcation in these models, the classical epidemiological requirement of vaccinated reproduction number being less than unity would not guarantee disease elimination in these models. Furthermore, an imperfect vaccine will reduce HIV prevalence and mortality if the reproduction number for a wholly vaccinated population is less than the corresponding reproduction number in the absence of vaccination.

Podder et al. (2011) developed a ten state deterministic model for evaluating the impact of anti-retroviral drugs (ARVs), voluntary testing (using standard antibody-based and a DNA-based testing methods) and condom use on the transmission dynamics of HIV in a community. Effective reproduction number was determined. Their mathematical analysis showed that the model had a globally-stable disease-free equilibrium whenever the effective reproduction number, is less than unity. In addition, the authors conducted numerical simulations and established that the use of the combined testing and treatment strategy is more effective than the use of the standard ELISA testing method with ARV treatment, even for the use of condoms as a singular strategy. Furthermore, the universal strategy (which involves the use of condoms, the two testing methods and ARV treatment) is always more effective than the combined use of the standard ELISA testing method and ARVs. However, application of the model to data was not considered hence a limitation.

While evaluating the quantitative assessment of the role of male circumcision in HIV transmission, Alsallaq et al. (2009) constructed a deterministic compartmental model consisting of a system of twelve coupled non-linear differential equations for different risk groups. The risk groups included in their study represent low, low to intermediate, intermediate to high and high risk groups. The model stratifies the population into compartments according to

sex, circumcision status, HIV status and disease stage and sexual risk activity for each of the four risk groups. The model was numerically solved using data from Kisumu in Kenya and Rakai in Uganda. The model predicted a large gap between HIV prevalence at reported level of circumcision coverage and that in a counter-factual scenario at universal circumcision coverage. The results of the model indicated that circumcision is an effective intervention against HIV infectious spread and would be of utility in both high and intermediate HIV prevalence settings. While the results from this work are interesting, it would be plausible to extend this model to include test and treat strategy.

Hallett et al. (2008) investigated the effect of male circumcision on the spread of HIV in Southern Africa. They used published data from eastern Zimbabwe to inform the parameters of the model. Men and women were stratified into risk groups that form different number of sexual partners to account for heterogeneity in the model. The numerical results from this model suggested that circumcision alone may not halt HIV infection but reduces the HIV incidence by 25-30% if high coverage levels are achieved. Furthermore, the findings suggested that the indirect benefit of circumcision interventions to women is mediated by reduction in HIV prevalence among their circumcised male sexual partners.

Boily et al. (2008) used a dynamical stochastic model of HIV and STI infections in a Kenyan population to simulate the impact of circumcision offered to a minority of trials participants or to a large fraction of men in order to study the protective role of male circumcision on HIV infection at the individual-level and at the population-level, respectively. They established that the protection of male circumcision against STI contributes little to the overall effect of male circumcision on HIV in the trials. They suggested that additional work is needed to identify if the protective effect of MC efficacy against STIs can have a significant incremental benefit on the HIV epidemic. Closely related, Podder et al. (2007) presented a compartmental model for the transmission dynamics of HIV in a community where male circumcision is practised. Through the use of partial data from South Africa, the study showed that male circumcision at 60% efficacy level could prevent up to 220,000 cases and 8,200 deaths in the country within a year. Further, it was shown that male circumcision could significantly reduce, but not eliminate, HIV burden in a community. Furthermore, they showed that the

combined use of male circumcision and ARVs is more effective in reducing disease burden than the combined use of male circumcision and condoms for a moderate condom compliance rate.

Other deterministic models which have been developed by many others (Douraki, 2017; Gumel et al., 2006; Tan and Wu, 2005), explored mathematical analysis of the dynamics of HIV/AIDS and are pertinent to this work. Furthermore, this model considered the dynamics of HIV/AIDS as well as its control through treatments and preventions.

2.5 Statistical models for the transmission dynamics of HIV

Statistical modelling has been instrumental in studying the dynamics of infectious diseases. It is helpful in projection and planning. Several statistical models have been proposed and analysed to explain the transmission and control of HIV infection. Zeh et al. (2016) while studying the transmission dynamics of recent and long term HIV-1 infections in two populations in rural western Kenya, used logistic regression to identify independent factors associated with recent infections. The blood samples were obtained from participants in two large cross-sectional surveys conducted in Asembo and Gem located on the shores of Lake Victoria. Differences in subtype distribution between recent and long term infections were assessed by Pearson chi-square test. In their findings, they established that recent HIV-1 infection was more frequent among the 13-19 year olds population as compared with older age groups. This underscored the ongoing risk and susceptibility of younger persons for acquiring HIV infection. Furthermore, their findings also provided evidence of existence of sexual networks. The findings suggested that early infections may be contributing significant proportions of onward transmission highlighting the need for early diagnosis and treatment.

Means et al. (2016) used a hierarchical nonlinear mixed effects (NLME) model to fit $CD4^{+}T$ cell count progression following ART initiation in their attempt to investigate the impact of age and sex on CD4+ cell count following the initiation of treatment on HIV patients. They used longitudinal data of the HIV patient obtained from the outpatient monitoring system of the National AIDS Control Program in Tanzania. The study restricted the analysis to

individuals of age 19 years and above at the initiation of ART, sex and baseline $CD4^+$T cell count. Their findings suggested that earlier ART initiation is associated with greater long term $CD4^+$T cell counts. In addition, their findings suggested that immune reconstruction in older patients is lower than that of the younger patients and there is need to initiate early treatment in the disease progression.

Other models on HIV transmission and treatment include "Assessing evidence for behaviour change affecting the course of HIV epidemics" (Hallett et al., 2009). This model focused on evaluating the evidence for changes in risk behaviour altering the course of an HIV epidemic in Zimbabwe. Bailey et al. (2007) and Amornkul et al. (2009) assesed the protective effect of male circumcision against HIV infection as well as its safety and sexual behaviour in Kisumu-Kenya. In both the models they established that male circumcision has a significant reduction in the risk of HIV acquisition in young men. They recommended that voluntary, safe and affordable circumcision services should be integrated with other HIV preventive interventions to reduce the spread of HIV.

Okango et al. (2016) performed a spatial modelling of HIV and HSV-2 among women in Kenya by allowing the covariate age to have a non-linear effect on HIV and HSV-2 prevalence using random walk model. They used data from the 2007 Kenya AIDS indicator survey where women aged 15-49 years were surveyed. They established that age has a non-linear relationship with both HIV and HSV-2 prevalence. The findings of their research could be used in informing tailor made strategies for tackling HIV and HSV-2 in different counties in Kenya.

2.6 The gaps identified

Some questions to answer, observations from aforementioned models and possible modifications that can be made are highlighted below.

- It is clear from the aforementioned studies that substantial studies have been conducted to model HIV/AIDS. However, most of these models have been theoretically analysed with little calibration of the models with real-time series data.

- In the aforementioned transmission models; little consideration has been given with regards to the interaction between the key risk populations in the HIV transmission chain. For example, the interaction between sex workers and the injection drug users. These interactions, if accounted for, can give a plausible basis for proper control of the HIV infection.

- In the literature, PrEP has been given attention specific to MSM communities. This leaves a key question as to whether this control measure can help forecast the eradication of HIV by 2030. In addition, there are concerns on the control of HIV and the efforts needed to contain further occurrence of infections.

From the literature, it is shown that many epidemiological, mathematical and statistical models have been used to explain and understand the dynamics of HIV transmission and its control. Based on the problem we have described so far, our objectives are to develop mathematical models that can specifically characterize the dynamics of HIV in Kenya with special interest in its transmission and control.

Chapter 3

Modelling the dynamics of HIV transmission and treatment

3.1 Introduction

HIV epidemic has been evolving in Kenya since the detection of the first case in 1984. Kenya has the fourth highest number of HIV infections globally (UNAIDS, 2015c). By the end of the year 1985, about 26 cases of AIDS were reported in Kenya mainly from sex workers in Nairobi. This placed the prevalence amongst this group at 29% (UNAIDS, 2015b). By the end of 1987 HIV appeared to be spreading rapidly with an estimated 1-2% of adults in Nairobi having been infected. HIV prevalence continued soaring from 6.5% to about 13% between 1989 and 1991 (UNAIDS, 2015b). Due to the devastating effects of HIV, plans to develop preventive measures were drawn and consequently a condom factory was built in Nairobi in the year 2000. HIV prevalence began to decline from its peak of 10.5% in 2000 and continued to decrease steadily to 6.9 percent in 2006 (NACC, 2016; UNAIDS, 2015b,c). The decrease in prevalence coincided with the rapid expansion of preventative interventions since 2000, which resulted in a change in sexual behaviour and the increased use of condoms (UNAIDS, 2004). The reports from Kenyan National AIDS Control Council (NACC) approximated that 1.6 million people were living with HIV by end of year 2015 with 36,000 deaths resulting from AIDS-related illness (OPTIONS, 2016; UNAIDS, 2015c). Adults aged 15 to 49 years constituted about 51% of the new infections in Kenya (NACC, 2016). This is the aged group that significantly contributed to high HIV burden in Kenya through heterosexual means (NACC, 2016). Thus, in this chapter, we aim to develop a mathematical model to integrate to real-time series of HIV infection data amongst the people

aged 15 years and above. We also seek to investigate the global dynamics of the developed HIV epidemic model. We analyse the global stability of the model equilibria and fit the model to data. Our aim is to examine the trend of HIV/AIDS in Kenya so as to propose effective strategies that can help combat HIV epidemic in order to achieve the vision 2030.

3.2 Model formulation

A number of mathematical models have been developed to study the dynamics of HIV infection. (Baryarama et al., 2006; Okango et al., 2016; Wodarz and Nowak, 2002). These models have focused on steady states and their stability as well as computer simulations. None of the existing mathematical models, however, explicitly considers the HIV trends data specific to Kenya. For example, Okongo et al. (2013) used a mathematical model to investigated the effects of social behaviour, treatment and vaccination of HIV. The model's stability analysis was performed and numerical simulations carried out. Kiss et al. (2010) developed a deterministic model to study the impact of information dissemination on sexually transmitted diseases. Their model accounted for the diffusion of health information disseminated as a result of the presence of a disease and an 'active' host population that can respond to it by taking measures to avoid infection or if infected by seeking treatment early. While these models incorporated the effects of HIV prevention through such means as behaviour change and as well as treatment with ART, they did not consider the immediate enrolment of new HIV infected individuals to treatment following the WHO and UNAIDS recommendation for HIV treatment centred on 90-90-90 (United Nations Programme on HIV/AIDS, 2014).

We use a mathematical model to analyse the trend of HIV infection in Kenya. We propose a five state compartmental model. The structure of the model is such that it comprises susceptible individuals (S) who are at high risk of HIV infection. Upon acquiring infection, individuals in class S move to infection class which is divided into two stages according to CD4$^+$T cell counts in the blood. These include: stage 1 comprising of individuals with CD4$^+$T cell counts $\geq 350/\mu L$, (I_1). The infected individuals in (I_1) are assumed to be the new infections. The second stage of infection consists of individuals with $200/\mu L <$ CD4$^+$T

cell counts $< 350/\mu L$, (I_2). HIV positive individuals in stages I_1 and I_2 enter into I_1^A and I_2^A if they receive antiretroviral treatment (ART) respectively. This is consistent with the WHO recommendation of immediate enrollment into ART irrespective of the CD4$^+$T cell counts in the blood in order to achieve viral load suppression (AIDS, 2015; Williams, 2014). Figure 4.3 shows the schematic flow diagram of the model structure.

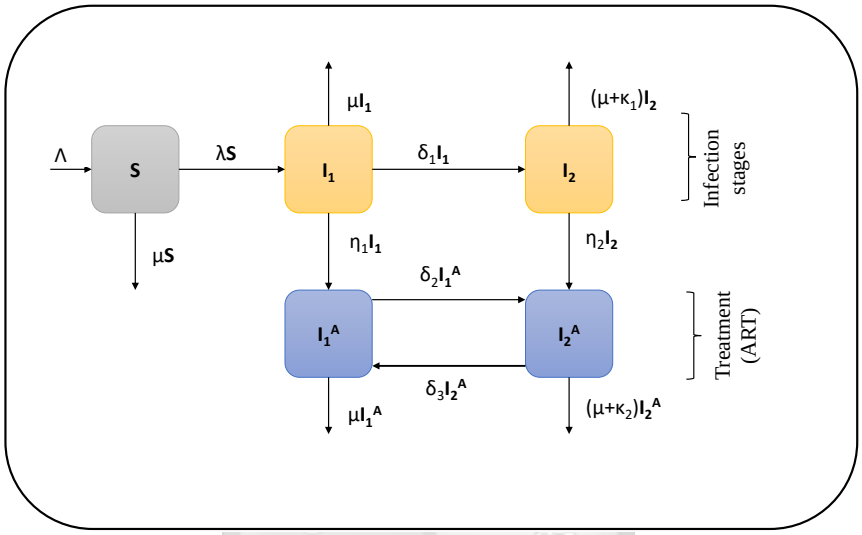

Figure 3.1: Schematic diagram of HIV transmission.

The variable population denoted by $N(t)$ is described by (3.1).

$$N(t) = S(t) + I_1(t) + I_2(t) + I_1^A(t) + I_2^A(t). \tag{3.1}$$

The susceptible individuals are recruited into the system at a constant rate Λ. The susceptible individuals then acquire infections at the rate λ, expressed as

$$\lambda = \frac{\beta_1 I_1 + \beta_2 I_2 + \beta_3 I_1^A + \beta_4 I_2^A}{N}. \tag{3.2}$$

Here, β_i, where $(i = 1,\ 2,\ 3,\ 4)$, define the effective contact rates between susceptible individuals and infectious individuals in the classes I_1, I_2, I_1^A and I_2^A, respectively. The natural death rate for all classes is μ. The progression rate from I_1 stage I_2 is given by δ_1. The progression rates from I_1 stage to I_1^A stage and from I_2 stage to I_2^A stage are given by η_1 and η_2 upon enrollment to ART treatment respectively. The rates δ_2 and δ_3 refers to the

movement from I_1^A to I_2^A and from I_2^A to I_1^A. The disease related death rate is assumed to be κ_1 and κ_2 for I_2 and I_2^A respectively. The summary of the state variables and the parameters are given in Tables 3.1 and 3.2, respectively.

3.2.1 Model assumptions

- In our modelling attempt, we consider the case where HIV patients get enrolled to ART treatment irrespective of their CD4$^+$T cell counts in addition to studying the trend of HIV infections.
- The movement between I_1^A and I_2^A is assumed to be bi-directional due to adherence of HIV patients to ART treatment and improvement or decline of the immunological status of the HIV patients on ART treatment.
- The AIDS class is not considered in this model given that full blown AIDS patients are usually hospitalized and/or sexually inactive. It is assumed that they are not able to engage in HIV transmission activities hence do not contribute to HIV infection. Similar assumptions were made by Yang et al. (2017) while modelling the global dynamics of HIV among female sex workers and their senior male clients.
- Different effective contact rates are used based on the assumption that infected individuals in different stages may have different effective contact rates due to difference in CD4$^+$T cell counts in the blood, ART treatment and behaviour change.

Table 3.1: Symbols and definition of the state variables.

Variable	Description
S	The number of susceptible individuals at time t
I_1	The number of the infected individuals with **CD4$^+$T** cell counts $\geq 350/\mu L$ at time t
I_2	The number of the infected individuals with **CD4$^+$T** cell counts $< 350/\mu L$ at time t
I_1^A	The number of the infected individuals with **CD4$^+$T** cell counts $\geq 350/\mu L$ on ART at time t
I_2^A	The number of the infected individuals with **CD4$^+$T** cell counts $< 350/\mu L$ on ART at time t

Table 3.2: Symbols and description of the parameters.

Parameter	Description
Λ	The recruitment rate into susceptible class
β_1	Effective contact rate between susceptible and infected individuals in class I_1
β_2	Effective contact rate between susceptible and infected individuals in class I_2
β_3	Effective contact rate between susceptible and infected individuals in class I_1^A
β_4	Effective contact rate between susceptible and infected individuals in class I_2^A
μ	The natural death rate
δ_1	The progression rate from stage I_1 to stage I_2
η_1	The progression rate from I_1 to I_1^A
η_2	The progression rate from I_2 to I_2^A
δ_2	Progression from I_1^A to I_2^A
δ_3	Progression from I_2^A to I_1^A
κ_1	The disease related death rate in I_2
κ_2	The disease related death rate in I_2^A

3.2.2 Model equations

The descriptions in Section 3.2 and assumptions in sub-section 3.2.1 translate in the following non-linear ordinary differential equations.

$$\left.\begin{aligned}
\frac{dS}{dt} &= \Lambda - \lambda S - \mu S, \\
\frac{dI_1}{dt} &= \lambda S - (\delta_1 + \eta_1 + \mu) I_1, \\
\frac{dI_2}{dt} &= \delta_1 I_1 - (\eta_2 + \mu + \kappa_1) I_2, \\
\frac{dI_1^A}{dt} &= \eta_1 I_1 + \delta_3 I_2^A - (\delta_2 + \mu) I_1^A, \\
\frac{dI_2^A}{dt} &= \delta_2 I_1^A + \eta_2 I_2 - (\delta_3 + \mu + \kappa_2) I_2^A.
\end{aligned}\right\} \tag{3.3}$$

We assume that at $t = 0$, $S(0) > 0$, $I_1(0) \geq 0$, $I_2(0) \geq 0$, $I_1^A(0) \geq 0$ and $I_2^A(0) \geq 0$.

3.3 Model basic properties

In this section, we explore the basic dynamical features of the system (3.3). For the system (3.3) to be mathematically tractable and epidemiologically meaningful, it is important to prove that all the state variables and all the associated parameters are non-negative for all time $t > 0$.

Theorem 3.1. *The solutions of system* (3.3) *exist and are non-negative for any given positive initial conditions for all* $t \in [0, \infty)$.

Proof. Here, we prove that all the stated variables remain non-negative and the solutions of the system (3.3) with non-negative initial conditions will remain positive for all $t > 0$. Following the work in Nyabadza et al. (2013); Omondi et al. (2017a), assume that

$$\hat{t} = \sup\{t > 0 : S > 0,\ I_1 > 0,\ I_2 > 0,\ I_1^A > 0,\ I_2^A > 0\} \in (0, t].$$

Thus $\hat{t} > 0$, and it follows directly from the first equation of the system (3.3) that

$$\dot{S} = \Lambda - \lambda S - \mu S = \Lambda - (\lambda + \mu)S. \tag{3.4}$$

Equation (3.4) can be written as

$$\frac{d}{dt}\left(S\exp\left\{\int_0^t \lambda(u)du + \mu t\right\}\right) = \Lambda\exp\left\{\int_0^t \lambda(u)du + \mu(t)\right\},$$

Integrating both sides from $t = 0$ to $t = \hat{t}$, we obtain

$$S(\hat{t})\exp\left\{\int_0^{\hat{t}} \lambda(u)du + \mu\hat{t}\right\} - S(0) = \int_0^{\hat{t}} \Lambda\exp\left\{\int_0^x \lambda(x)dx + \mu y\right\}dy,$$

then multiplying both sides by $\exp\left\{-\int_0^{t^*} \lambda(u)du - \mu_v\hat{t}\right\}$, we have

$$\begin{aligned} S(\hat{t}) = S(0)\exp\left\{-\int_0^{\hat{t}} \lambda(u)du - \mu\hat{t}\right\} + \exp\left\{-\int_0^{\hat{t}} \lambda_v(u)du - \mu\hat{t}\right\} \\ \times \int_0^{\hat{t}} \Lambda\exp\left\{\int_0^x \lambda(x)dx + \mu y\right\}dy > 0. \end{aligned} \tag{3.5}$$

Since, the right-hand side of the expression (3.5) is always positive, the solution $S(t)$ will always remain positive for all $t > 0$. Using the same argument, it can be shown that the quantities I_1, I_2, I_1^A, and I_2^A are positive for all $t > 0$. □

Theorem 3.2. *The feasible region* Ω *represented by the set*

$$\Omega := \left\{(S, I_1, I_2, I_1^A, I_2^A) \in \mathbb{R}_+^5 : S + I_1 + I_2 + I_1^A + I_2^A \leq \max\left\{N(0), \frac{\Lambda}{\mu}\right\}\right\},$$

with initial conditions $S(0) > 0$, $I_1(0) \geq 0$, $I_2(0) \geq 0$, $I_1^A(0) \geq 0$ *and* $I_2^A(0) \geq 0$, *is attracting and positively invariant with respect to the flow of the model system* (3.3).

Proof. If $S(0)$, $I_1(0)$, $I_2(0)$, $I_1^A(0)$, $I_2^A(0)$ are non-negative, so are $S(t)$, $I_1(t)$, $I_2(t)$, $I_1^A(t)$, $I_2^A(t)$ for all time $t > 0$. Summing up the five differential equations of the system (3.3) with the

condition that $N(0) > 0$, the total population evolves according to the following inequality.

$$\frac{dN(t)}{dt} \leq \Lambda - \mu N(t). \tag{3.6}$$

Using, the standard comparison theorem as given in Smith and Waltman (1995), we solve equation (3.6) by integrating factor technique to obtain

$$N(t) \leq \frac{\Lambda}{\mu} + \left(N(0) - \frac{\Lambda}{\mu}\right)\exp(-\mu t), \quad \text{for all } t \geq 0. \tag{3.7}$$

The solution in (3.7) yields two possible scenarios in studying the behaviour of $N(t)$. In the first scenario, we consider $N(0) > \frac{\Lambda}{\mu}$ so that, at time $t = 0$, the right-hand side of (3.7) experiences the largest possible value of $N(0)$. That is, $N(t) \leq N(0)$ for all time $t \geq 0$. In the second scenario, we consider $N(0) < \frac{\Lambda}{\mu}$, so that the largest possible value of the right-hand side of (3.7) approaches $\frac{\Lambda}{\mu}$ as time t tends infinity. Thus, $N(t) \leq \frac{\Lambda}{\mu}$ for all time $t \geq 0$. From these two scenarios, we conclude that $N(t) \leq \max\left\{N(0), \frac{\Lambda}{\mu}\right\}$ for all time $t \geq 0$.

□

The solutions in Ω are all non-negative and bounded. Hence the domain of biological significance is positively invariant and attracting. Thus, all solutions starting in Ω remain in Ω. Furthermore, the system (3.3) is well-posed epidemiologically and we will consider dynamic behaviour of the system (3.3) in Ω.

3.4 Stability analysis

3.4.1 Basic reproduction number

The disease-free steady state (DFE) of system (3.3) is given by

$$\mathscr{E}_0 = \{S_0,\ 0,\ 0,\ 0,\ 0\}.$$

$S_0 = \frac{\Lambda}{\mu}$, represents the susceptible individuals when no one is infected with HIV. To obtain basic reproduction number, denoted by $\mathscr{R}_0$, we employ the next generation method (Van den Driessche and Watmough, 2002). The matrices that describe the rate at which the new infectives are produced and the transfer of infectives between compartments are respectively given by

$$\mathbf{F} = \begin{pmatrix} \beta_1 & \beta_2 & \beta_3 & \beta_4 \\ 0 & 0 & 0 & 0 \\ 0 & 0 & 0 & 0 \\ 0 & 0 & 0 & 0 \end{pmatrix} \quad \text{and} \quad \mathbf{V} = \begin{pmatrix} Q_1 & 0 & 0 & 0 \\ -\delta_1 & Q_2 & 0 & 0 \\ -\eta_1 & 0 & Q_3 & -\delta_3 \\ 0 & -\eta_2 & -\delta_2 & Q_4 \end{pmatrix}.$$

Thus, $\mathscr{R}_0$ is the dominant eigenvalue of $\mathbf{FV}^{-1}$ given by

$$\mathscr{R}_0 = \mathscr{R}_1 + \mathscr{R}_2 + \mathscr{R}_1^A + \mathscr{R}_2^A, \tag{3.8}$$

where

$$\mathscr{R}_1 = \frac{\beta_1}{Q_1}, \quad \mathscr{R}_2 = \frac{\beta_2\delta_1}{Q_1Q_2}, \quad \mathscr{R}_1^A = \frac{\beta_3(Q_2Q_4\eta_1 + \delta_1\delta_3\eta_2)}{Q_1Q_2Q_3Q_4(1-\Phi_1)}, \quad \mathscr{R}_2^A = \frac{\beta_4(Q_2\delta_2\eta_1 + Q_3\delta_1\eta_2)}{Q_1Q_2Q_3Q_4(1-\Phi_1)}$$

with

$$Q_1 = \delta_1 + \eta_1 + \mu, \quad Q_2 = \eta_2 + \mu + \kappa_1, \quad Q_3 = \delta_2 + \mu, \quad Q_4 = \delta_3 + \mu + \kappa_2, \quad \Phi_1 = \frac{\delta_2\delta_3}{Q_3Q_4}.$$

Note that $0 < \Phi_1 < 1$. The expression for $\mathscr{R}_0$ in (3.8) is carefully written to reflect the contribution of each stage of the infected individuals in the initiation of new infections. Here, $\mathscr{R}_0$ is interpreted as the expected cases of secondary HIV infections arising from a single HIV infected individual during his or her entire infectious period, in an otherwise disease-free population (Heffernan et al., 2005; Omondi et al., 2017b; Van den Driessche and Watmough, 2002).

From Theorem 2 in Van den Driessche and Watmough (2002), we establish following result.

Theorem 3.3. *The disease-free equilibrium of system* (3.3) *is locally asymptotically stable whenever* $\mathscr{R}_0 < 1$ *and unstable otherwise.*

Theorem 3.3 implies that HIV infection will disappear from the population when $\mathscr{R}_0 < 1$ if the initial sizes of the of the sub-populations of the system (3.3) are in the basin of attraction of the disease-free equilibrium.

Theorem 3.4. *The disease-free steady state,* $\mathscr{E}_0$*, of the model system* (3.3) *is globally asymptotically stable when* $\mathscr{R}_0 < 1$ *and unstable otherwise.*

Proof. We define a candidate Lyapunov function as follows

$$L(I_1,\, I_2,\, I_1^A,\, I_2^A) = \Psi_1 I_1 + \Psi_2 I_2 + \Psi_3 I_1^A + \Psi_4 I_2^A, \tag{3.9}$$

where $\Psi_1,\ \Psi_2,\ \Psi_3$ and Ψ_4 are non-negative constants to be determined. The derivative of (3.9) is given by

$$\begin{aligned}
\frac{dL}{dt} &= \Psi_1 \frac{dI_1}{dt} + \Psi_2 \frac{dI_2}{dt} + \Psi_3 \frac{dI_1^A}{dt} + \Psi_4 \frac{dI_2^A}{dt}, \\
&= \Psi_1 \left[\left(\frac{\beta_1 I_1 + \beta_2 I_2 + \beta_3 I_1^A + \beta_4 I_2^A}{N} \right) S - Q_1 I_1 \right] + \Psi_2 \left[\delta_1 I_1 - Q_2 I_2 \right] \\
&\quad + \Psi_3 \left[\eta_1 I_1 + \delta_3 I_2^A - Q_3 I_1^A \right] + \Psi_4 \left[\delta_2 I_1^A + \eta_2 I_2 - Q_4 I_2^A \right], \\
&\leq \Psi_1 \left[\beta_1 I_1 + \beta_2 I_2 + \beta_3 I_1^A + \beta_4 I_2^A - Q_1 I_1 \right] + \Psi_2 \left[\delta_1 I_1 - Q_2 I_2 \right] + \Psi_3 \left[\eta_1 I_1 + \delta_3 I_2^A - Q_3 I_1^A \right] \\
&\quad + \Psi_4 \left[\delta_2 I_1^A + \eta_2 I_2 - Q_4 I_2^A \right], \\
&= [\Psi_1 \beta_1 + \Psi_2 \delta_1 + \Psi_3 \eta_1 - \Psi_1 Q_1] I_1 + [\Psi_1 \beta_2 + \Psi_4 \eta_2 - \Psi_2 Q_2] I_2 \\
&\quad + [\Psi_1 \beta_3 + \Psi_4 \delta_2 - \Psi_3 Q_3] I_1^A + [\Psi_1 \beta_4 + \Psi_3 \delta_3 - \Psi_4 Q_4] I_2^A.
\end{aligned}$$

Setting the coefficients of I_2, I_1^A and I_2^A which are not primary contributors to the force of infection to zero and solving, we get

$$\Psi_1 = Q_2Q_3Q_4(1-\Phi_1), \quad \Psi_2 = Q_3Q_4\beta_2(1-\Phi_1)+\eta_2(\beta_3\delta_3+\beta_4Q_3),$$
$$\Psi_3 = Q_2(\beta_3Q_4+\beta_4\delta_2), \quad \Psi_4 = Q_2(Q_3\beta_4+\beta_3\delta_3).$$

Using these coefficients, the time derivative of (3.9) can be expressed as

$$\frac{dL}{dt} \leq Q_1Q_2Q_3Q_4(1-\Phi_1)[\mathscr{R}_0-1]. \tag{3.10}$$

Clearly from (3.10), when $\mathscr{R}_0 \leq 1$, $\frac{dL}{dt}$ is negative semi-definite, with equality at $\mathscr{R}_0 = 1$. In addition, $\frac{dL}{dt} = 0$ if and only if $I_1 = I_2 = I_1^A = I_2^A = 0$. Hence, the largest compact invariant set in $\{(S,\, I_1,\, I_2,\, I_1^A,\, I_2^A) \in \Omega : \frac{dL}{dt} = 0\}$, when $\mathscr{R}_0 \leq 1$ is the singleton $\mathscr{E}_0$. Thus, $\mathscr{E}_0$ is the only steady state when $\mathscr{R}_0 \leq 1$. Using LaSalle Invariance Principle La Salle (1976), this implies that $\mathscr{E}_0$ is globally attractive in Ω if $\mathscr{R}_0 \leq 1$. □

Epidemiological implications of Theorem 3.4 is that when $\mathscr{R}_0 < 1$, a small influx of HIV infected individuals into the community will not result in an outbreak. The subsequent numbers of those infected will be less than that of their predecessors and eventually the disease will be contained.

3.5 Existence of endemic equilibrium

The results in Theorem 3.3, show that the system (3.3) has an disease-free steady state when $\mathscr{R}_0 < 1$. When $\mathscr{R}_0 > 1$, the disease-free steady state ($\mathscr{E}_0$), is unstable and the system (3.3) has a non-trivial endemic equilibrium. Let the endemic equilibrium be represented by the phase space

$$\mathscr{E}_1 = \left(S^*,\, I_1^*,\, I_2^*,\, I_1^{A*},\, I_2^{A*}\right) \in \mathbb{R}_+^5.$$

Therefore, solving system (3.3) in terms of the force of infection in (3.2), we obtain

$$S^* = \frac{\Lambda}{\lambda^* + \mu}, \quad I_1^* = \frac{\Lambda\lambda^*}{Q_1(\lambda^* + \mu)}, \quad I_2^* = \frac{\Lambda\lambda^*\delta_1}{Q_1Q_2(\lambda^* + \mu)},$$
$$I_1^{A*} = \frac{\Lambda\lambda^*(Q_2Q_4\eta_1 + \delta_1\delta_3\eta_2)}{Q_1Q_2Q_3Q_4(1-\Phi_1)(\lambda^* + \mu)}, \quad I_2^{A*} = \frac{\Lambda\lambda^*(Q_2\delta_2\eta_1 + Q_3\delta_1\eta_2)}{Q_1Q_2Q_3Q_4(1-\Phi_1)(\lambda^* + \mu)}.$$

Substituting the expressions for I_1^*, I_2^*, I_1^{A*} and I_2^{A*} into (3.2) at the equilibrium, we either obtain $\lambda^* = 0$, which corresponds to the disease-free equilibrium previously obtained or

$$\lambda^* = \frac{\mu(\mathscr{R}_0 - 1)}{Q_1Q_2Q_3Q_4(1-\Phi_1)}. \tag{3.11}$$

Since the solution of the system (3.3) is only feasible in the invariant region Ω, the expression (3.11) is only feasible when $\mathscr{R}_0 > 1$. Hence the system (3.3) has a unique endemic equilibrium whenever $\mathscr{R}_0 > 1$ and this equilibrium approaches zero as $\mathscr{R}_0$ tends to one. These results are summarized in the following theorem.

Theorem 3.5. *The model system* (3.3) *has a unique endemic equilibrium whenever* $\mathscr{R}_0 > 1$ *and no positive endemic equilibrium otherwise.*

We then study the global stability of the endemic equilibrium of system (3.3) by construction of Lyapunov function. Thus, we begin by stating the following theorem.

Theorem 3.6. *The endemic equilibrium,* $\mathscr{E}_1$*, of system* (3.3) *is globally asymptotically stable when* $\mathscr{R}_0 > 1$ *and unstable otherwise.*

In order to prove the global asymptotic stability of the unique endemic steady state $\mathscr{E}_1$, we linearise system (3.3) based on the assumption that $N = I_1 + I_2 + I_1^A + I_2^A$ so that we have

$$s = \frac{S}{N}, \quad x = \frac{I_1}{N}, \quad y = \frac{I_2}{N}, \quad w = \frac{I_1^A}{N}, \quad z = \frac{I_2^A}{N}.$$

Our new system therefore becomes

$$\left.\begin{aligned}
\frac{ds}{dt} &= \mu - (\beta_1 x + \beta_2 y + \beta_3 w + \beta_4 z)s - \mu s,\\
\frac{dx}{dt} &= (\beta_1 x + \beta_2 y + \beta_3 w + \beta_4 z)s - Q_1 x,\\
\frac{dy}{dt} &= \delta_1 x - Q_2 y,\\
\frac{dw}{dt} &= \eta_1 x + \delta_3 z - Q_3 w,\\
\frac{dz}{dt} &= \delta_2 w + \eta_2 y - Q_4 z.
\end{aligned}\right\} \tag{3.12}$$

Next, without loss of generality, we provide the proof to the global asymptotic stability of the system (3.3) using system (3.12).

Proof. Let

$$\begin{aligned}
V = &\left(s - s^* - s^* \ln \frac{s}{s^*}\right) + \Phi_2 \left(x - x^* - x^* \ln \frac{x}{x^*}\right) + \Phi_3 \left(y - y^* - y^* \ln \frac{y}{y^*}\right)\\
&+ \Phi_4 \left(w - w^* - w^* \ln \frac{w}{w^*}\right) + \Phi_5 \left(z - z^* - z^* \ln \frac{z}{z^*}\right),
\end{aligned} \tag{3.13}$$

be a suitable Lyapunov function such that Φ_2, Φ_3, Φ_4 and Φ_5 are non-negative constants to be determined. Hence, differentiating (3.13) along the trajectories of (3.12), we obtain

$$\left.\begin{aligned}
\frac{dV}{dt} &= \left(1 - \frac{s^*}{s}\right)\frac{ds}{dt} + \Phi_2 \left(1 - \frac{x^*}{x}\right)\frac{dx}{dt} + \Phi_3 \left(1 - \frac{y^*}{y}\right)\frac{dy}{dt} + \Phi_4 \left(1 - \frac{w^*}{w}\right)\frac{dw}{dt}\\
&\quad + \Phi_5 \left(1 - \frac{z^*}{z}\right)\frac{dz}{dt},\\
&= \left[\mu - (\beta_1 x + \beta_2 y + \beta_3 w + \beta_4 z)\, s - \mu s\right]\left(1 - \frac{s^*}{s}\right) + \Phi_2 \Big[(\beta_1 x + \beta_2 y + \beta_3 w + \beta_4 z)\, s\\
&\quad - Q_1 x\Big]\left(1 - \frac{x^*}{x}\right) + \Phi_3 \left[\delta_1 x - Q_2 y\right]\left(1 - \frac{y^*}{y}\right) + \Phi_4 \left[\eta_1 x + \delta_3 z - Q_3 w\right]\left(1 - \frac{w^*}{w}\right)\\
&\quad + \Phi_5 \left[\delta_2 w + \eta_2 y - Q_4 z\right]\left(1 - \frac{z^*}{z}\right).
\end{aligned}\right\} \tag{3.14}$$

Using system (3.3) at endemic steady state, (3.14) admits the following set of solutions

$$\left.\begin{aligned} \mu &= (\beta_1 x^* + \beta_2 y^* + \beta_3 w^* + \beta_4 z^*)\, s^* + \mu s^*, \quad Q_1 = \left(\frac{\beta_1 x^* + \beta_2 y^* + \beta_3 w^* + \beta_4 z^*}{x^*}\right) s^*, \\ Q_2 &= \frac{\delta_1 x^*}{y^*}, \quad Q_3 = \frac{\eta_1 x^* + \delta_3 z^*}{w^*}, \quad Q_4 = \frac{\delta_2 w^* + \eta_2 y^*}{z^*}. \end{aligned}\right\} \tag{3.15}$$

We now substitute the terms in (3.15) into (3.14) to obtain

$$\left.\begin{aligned} \frac{dV}{dt} &= \left(1 - \frac{s^*}{s}\right)\left[\mu s^*\left(1 - \frac{s}{s^*}\right) + \beta_1 s^* x^*\left(1 - \frac{sx}{s^* x^*}\right) + \beta_2 s^* y^*\left(1 - \frac{sy}{s^* y^*}\right)\right. \\ &\quad \left. + \beta_3 s^* w^*\left(1 - \frac{sw}{s^* w^*}\right) + \beta_4 s^* z^*\left(1 - \frac{sz}{s^* z^*}\right)\right] + \Phi_2\left(1 - \frac{x^*}{x}\right) \\ &\quad \left[-\beta_1 s^* x^*\left(\frac{x}{x^*} - \frac{sx}{s^* x^*}\right) - \beta_2 s^* y^*\left(\frac{x}{x^*} - \frac{sy}{s^* y^*}\right) - \beta_3 s^* w^*\left(\frac{x}{x^*} - \frac{sw}{s^* w^*}\right)\right. \\ &\quad \left. - \beta_4 s^* z^*\left(\frac{x}{x^*} - \frac{sz}{s^* z^*}\right)\right] + \Phi_3\left(1 - \frac{y^*}{y}\right)\left[-\delta_1 x^*\left(\frac{y}{y^*} - \frac{x}{x^*}\right)\right] \\ &\quad + \Phi_4\left(1 - \frac{w^*}{w}\right)\left[-\eta_1 x^*\left(\frac{w}{w^*} - \frac{x}{x^*}\right) - \delta_3 z^*\left(\frac{w}{w^*} - \frac{z}{z^*}\right)\right] + \Phi_5\left(1 - \frac{z^*}{z}\right) \\ &\quad \left[-\delta_2 w^*\left(\frac{z}{z^*} - \frac{w}{w^*}\right) - \eta_2 y^*\left(\frac{z}{z^*} - \frac{y}{y^*}\right)\right]. \end{aligned}\right\} \tag{3.16}$$

Let

$$\frac{s}{s^*} = \Pi_1, \quad \frac{x}{x^*} = \Pi_2, \quad \frac{y}{y^*} = \Pi_3, \quad \frac{w}{w^*} = \Pi_4, \quad \frac{z}{z^*} = \Pi_5. \tag{3.17}$$

In order to cancel the coefficients of x, w, y and z, we set $\Phi_2 = 1$ and substituting (3.17) into (3.16), the derivative of V in (3.16) reduces to

$$\frac{dV}{dt} = \mu s^*\left(2 - \frac{1}{\Pi_1} - \Pi_1\right) + \Gamma(\Pi_1, \Pi_2, \Pi_3, \Pi_4, \Pi_5), \tag{3.18}$$

where

$$\left.\begin{aligned}\Gamma = \beta_1 s^* x^* \left[2 - \frac{1}{\Pi_1} - \Pi_1\right] + \beta_2 s^* y^* \left[\left(2 - \frac{1}{\Pi_1} - \Pi_1\right) - \frac{(\Pi_3 - \Pi_2)(\Pi_1 - \Pi_2)}{\Pi_2}\right] \\ + \beta_3 s^* w^* \left[\left(2 - \frac{1}{\Pi_1} - \Pi_1\right) - \frac{(\Pi_4 - \Pi_2)(\Pi_1 - \Pi_2)}{\Pi_2}\right] + \beta_4 s^* z^* \left[\left(2 - \frac{1}{\Pi_1} - \Pi_1\right)\right. \\ \left. - \frac{(\Pi_5 - \Pi_2)(\Pi_1 - \Pi_2)}{\Pi_2}\right] + \Phi_3 \delta_1 x^* \left[(1 - \Pi_3) - \Pi_2 \left(\frac{1}{\Pi_3} - 1\right)\right] \\ + \Phi_4 \left[\eta_1 x^* \left((1 - \Pi_4) - \Pi_2 \left(\frac{1}{\Pi_4} - 1\right)\right) + \delta_3 z^* \left((1 - \Pi_4) - \Pi_5 \left(\frac{1}{\Pi_4} - 1\right)\right)\right] \\ + \Phi_5 \left[\delta_2 w^* \left((1 - \Pi_5) - \Pi_4 \left(\frac{1}{\Pi_5} - 1\right)\right) + \eta_2 y^* \left((1 - \Pi_5) - \Pi_3 \left(\frac{1}{\Pi_5} - 1\right)\right)\right].\end{aligned}\right\}$$

Here, Γ is obtained after setting the coefficients of Π_2, Π_3, Π_4 and Π_5 to zero so that

$$\Phi_3 = \frac{\beta_1 s^* x^* + \beta_2 s^* y^* + \beta_3 s^* w^* + \beta_4 s^* z^*}{\delta_1 x^*}, \quad \Phi_4 = \delta_2 w^*, \quad \Phi_5 = \eta_1 x^* + \delta_3 z^*. \tag{3.19}$$

Using the arithmetic-mean/geometric-mean inequality, we note that the following expressions

$$\left[2 - \frac{1}{\Pi_1} - \Pi_1\right], \quad \left[\left(2 - \frac{1}{\Pi_1} - \Pi_1\right) - \frac{(\Pi_3 - \Pi_2)(\Pi_1 - \Pi_2)}{\Pi_2}\right],$$
$$\left[\left(2 - \frac{1}{\Pi_1} - \Pi_1\right) - \frac{(\Pi_4 - \Pi_2)(\Pi_1 - \Pi_2)}{\Pi_2}\right], \quad \left[\left(2 - \frac{1}{\Pi_1} - \Pi_1\right) - \frac{(L - \Pi_2)(\Pi_1 - \Pi_2)}{\Pi_2}\right],$$

are less or equal to zero , with equality if and only if $\Pi_1 = 1$ and $\Pi_2 = \Pi_3 = \Pi_4 = \Pi_5$. Similar conclusions can be drawn from the remaining parts of expression (3.18). Therefore $\frac{dV}{dt} \leq 0$ with equality if and only if $s = s^*$, $x = x^*, y = y^*$, $w = w^*$ and $z = z^*$. By LaSalle's invariance principle La Salle (1976), this implies that the solution lies in an invariant set contained in

$$\Omega = \left\{(s,\ x,\ y,\ w,\ z) : s = s^*, \frac{x}{x^*} = \frac{y}{y^*} = \frac{w}{w^*} = \frac{z}{z^*}\right\}.$$

Thus, the only invariant set contained in Ω is the singleton $\mathscr{E}_1$. This shows that each solution that intersects $\mathbb{R}^5_+$ tends to the endemic equilibrium $\mathscr{E}_1$. □

The global asymptotic stability of the endemic equilibrium has serious implications on the spread of HIV. If the population is constant and $\mathscr{R}_0 > 1$, HIV infection will always persist

regardless of the initial conditions. It is therefore imperative to reduce $\mathscr{R}_0 > 1$ to a value less than one so as to contain the spread of HIV.

3.6 Data and parameter estimation

To fit system (3.3) to data, we determine the baseline values of known parameters from the literature that correspond to available experimental data and biological facts. The unknown parameters are estimated on the basis of the available data. The estimation process attempts to find the best concordance between computed and observed data. It can be carried out by trial and error or by the use of software programs designed to find parameters that give the best fit. Here, the fitting process involves the use of the least squares-curve fitting method. The known parameter baseline values are approximated as follows: Λ which is defined as the recruitment rate into the susceptible is estimated based on the birth rate given as 23.9 births/1,000 population (WB, 2017). Thus the constant recruitment rate $\Lambda = 0.0239N$ per year. The natural death rate μ is estimated based on life expectancy which is reported to be 58 years (WB, 2017). Thus $\mu = 0.0172$ per year. AIDS related death rate in I_2, κ_1 is estimated at 0.089 per year while that in class I_2^A, κ_2 per year is estimated at 0.095.

The initial conditions are estimated as follows.

(i) $N = 17,528,707$, adult population that were found in 2000 (KNBS, 2017; KNBS2, 2017).

(ii) $S(0) = N - I_1(0) - I_2(0) - I_1^A(0) - I_2^A(0) = 17,196,488$.

(iii) $I_1(0) = 77,219$, reported number of new HIV infections at the end of 2000 (NACC, 2013).

(iv) $I_2(0) = 150,000$ (assumed), $I_1^A(0) = 60,000$ and $I_2^A(0) = 45,000$ (assumed).

The data used in this chapter was obtained from National AIDS Control Council (NACC, 2014a) and is given in in Table 3.3. The data was extracted for the period spanning over 17

years from the year 2000–2017. This data represents new infections for the adults aged 15 years and above.

Table 3.3: Reported new HIV infections in Kenya.

Year	2000	2001	2002	2003	2004	2005	2006	2007	2008
HIV+	77219	72329	71875	74074	77729	81523	85201	91082	105292
Year	2009	2010	2011	2012	2013	2014	2015	2016	2017
HIV+	108764	105072	98263	91949	85569	90986	71034	69491	70570

3.7 Curve fitting

Curve fitting can be defined as a process that enables us to quantitatively estimate the trend of the outcomes. In this process, equations of approximating curves are fitted to raw data. In order to fit the system (3.3)to data, we employ least squares method in matlab where unknown parameters are given both lower and upper bounds from which we obtain parameter values that provide the best fit. These set of parameter values are presented in Table 3.4.

Table 3.4: Estimated parameter ranges per year and parameter point values generated by curve fitting.

Parameter	Description	Min	Max	Point value
β_1	Contact for susceptible with I_1	0.0	2.0	0.912
β_2	Contact for susceptible with I_2	0.0	2.0	0.894
β_3	Contact for susceptible with I_1^A	0.0	2.0	0.095
β_4	Contact for susceptible with I_2^A	0.0	2.0	0.091
η_1	Progression rate from I_1 to I_1^A	0.1	1.5	0.084
η_2	Progression rate from I_1 to I_2^A	0.1	1.0	0.091
δ_1	Progression rate from I_1 to I_2	0.1	1.0	1.000
δ_2	Progression rate from I_1^A to I_2^A	0.1	1.0	0.096
δ_3	Progression rate from I_2^A to I_1^A	0.1	1.0	0.112

The results in Figure 3.2, panel (a) presents the results of the curve fitting where the trend of the data as reported in Table 3.3 and the curve representing the estimated values given

the model for the new HIV infected persons. It is seen that the cases of new HIV infections estimated by the model for the set of parameter values in Table 3.4 are closer to the reported new HIV infection data in Kenya. The study findings in Figure 3.2, panel (b) shows HIV incidence as estimated by the incidence function λS. It is seen that the estimated incidence reached the peak between 2010–2014. Our results show of a short-term increase of HIV epidemic in which there is a significant rise in new HIV infections for a considerably short time, followed by a significant decline in the generation of new cases. Nonetheless, this may not give a similar pattern with regards to prevalence, since recovery from HIV is not possible due to HIV being incurable. Hence, the cases of HIV infection is projected to remain significantly high over a long time. It is therefore suggested educational campaigns on safe sex be increased so as to stop further spread.

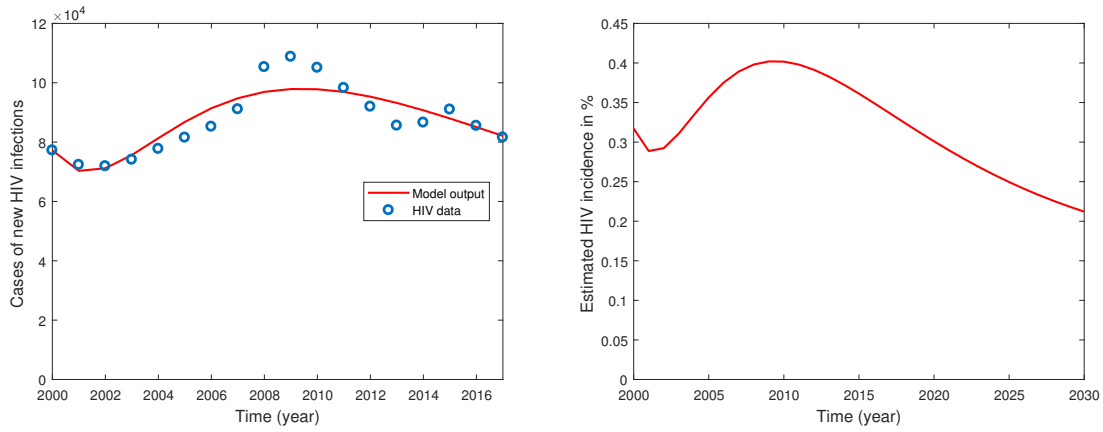

(a) (b)

Figure 3.2: Model system (3.3) fitted to data for the reported new HIV positive cases. Panel (a) shows the model fit to HIV data. Panel (b) gives the estimated disease incidence.

3.8 Numerical simulations

In this section, we carry out numerical simulations to see the dynamical behaviour of the system (3.3) using the initial conditions as as given in Section 3.6. The numerical results depend on the parameter values in Table 3.4. To investigate the contribution of linkage of new infected individuals to ART as well as the effectiveness of ART treatment on increasing

the CD4+T cell counts, we show the variation over time of prevalence of HIV for different rates of η_1 and δ_3. This is shown in Figure 3.3, panels (a) and (b), respectively. We note an increase in the values of η_1 decreases the prevalence of HIV. The decrease in prevalence can be attributed to the protective effect of ART in increasing the level of CD4+T cell counts. Similarly, an improvement in the immunological status of HIV patients in I_2 following effectiveness of ART maintaining the level of CD4+T cell counts high results in a decrease in the HIV prevalence as shown by the effect of δ_3. This shows that effectiveness in the up-take of ART reduces the risk at which an infected individual may spread HIV.

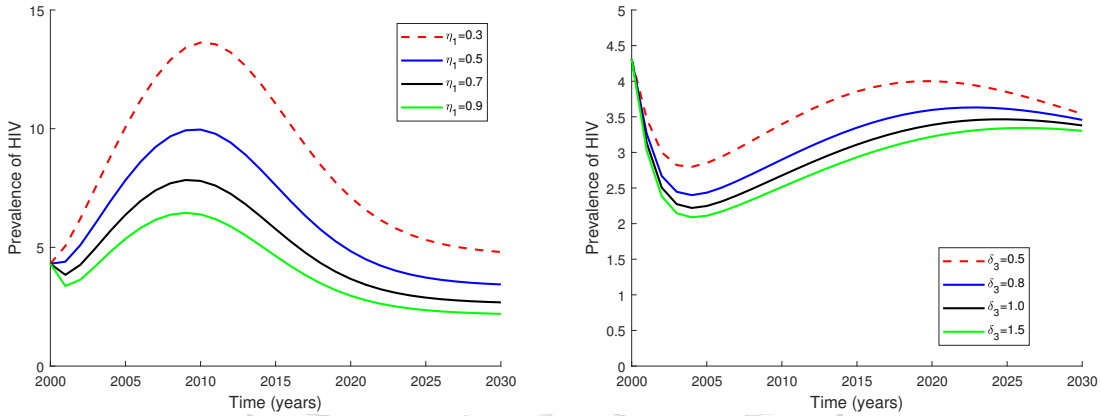

(a) (b)

Figure 3.3: Impact of enrollment to ART and improvement in the immunological status of HIV patient on the HIV prevalence. Panel (a) shows the impact of linkage to ART of the new infections on prevalence of HIV and panel (b) shows the impact of improvement in the immunological status on prevalence of HIV.

The results in Figure 3.4 indicate that $\mathscr{R}_0$ exponentially decreases with the increase in the rate of progression from I_1 to I_2, that is, η_1 and progression rate from I_2^A to I_1^A, that is, δ_3. Therefore, increasing the treatment with ART and its effective up-take reduces the chances of a susceptible person being infected with HIV through contact with HIV patients on ART treatment. The reduction in the likelihood of infection is due to the fact that high ART efficacy increases the level of CD4+T cell counts in the blood and as a result lowers the disease viral load. It is imperative to note that, even though increased drug efficacy may reduce incidence and consequently prevalence of HIV, it does not lead to its subsequent eradication from the community.

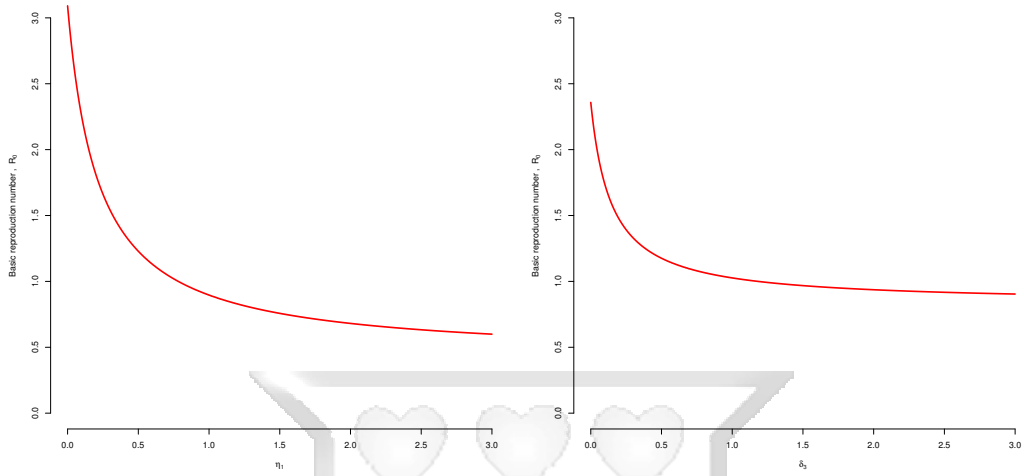

(a) (b)

Figure 3.4: Effect of η_1 and δ_3 on $\mathscr{R}_0$.

3.9 Conclusion

In this chapter, a simple deterministic model that takes into account new cases of HIV infections as well as HIV patients on ART was formulated to study the trend of HIV infection in Kenya amongst adults aged 15 years and above. Important mathematical features of the model that include the threshold for the epidemic, steady states, positivity and boundedness of solutions as well as the region of biological significance were determined. It is shown that when $\mathscr{R}_0$ is less than one, the disease-free equilibrium is both locally globally asymptotically stable. This disease-free equilibrium is unstable when the disease threshold is greater than one. The model has a unique endemic equilibrium when $\mathscr{R}_0$ is greater than one.

With the help of least squares method in Matlab, the model was fitted to data on cases of new HIV infections for the patients aged 15 years and above. The parameter values obtained from the curve fitting have been used to predict future infection trends. The results suggest that there is a general decline in the HIV infection which is predicted to eventually converge asymptotically over the next few years. The most important observation from our findings is that there is a short-term rise in HIV infection in which there is a significant increase in new HIV infections followed by a significant decline in the generation of new infections. Both treatment of the new infected individuals and the drug efficacy/adherence is seen to greatly

reduce HIV prevalence. Therefore, treatment applied immediately to someone who is found to have acquired HIV as well close attention to ART efficacy and adherence is paramount.

The model presented in this chapter is not exhaustive and may be extended to involve the study, the difference in HIV infections between adults males and females, transmission of HIV between different risk groups as well as studying the effect of testing, roll out of PrEP, ART up-take and epidemiological impact of media on the spread and control of HIV. Taking into account these suggestions will undoubtedly enhance the understanding of HIV transmission and control in Kenya. Thus, in the next chapter, proposed improvements of the model include, consideration of a gender and use of PrEP in the control of new HIV infections.

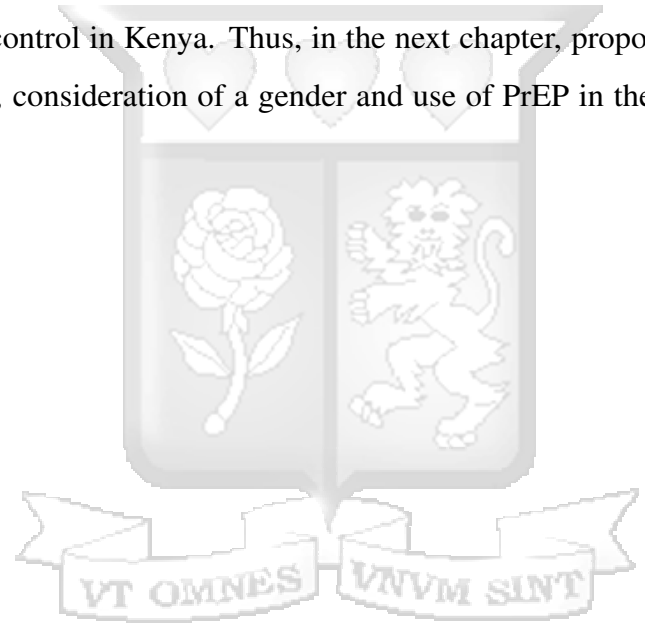

Chapter 4

Sex-structured mathematical model of HIV dynamics

4.1 Introduction

HIV remains a major global health problem affecting approximately 70 million people worldwide causing significant morbidity and mortality (WHO, 2018). In Kenya, the number of persons living with HIV was approximated to be 1.6 million in the year 2016, with women accounting for 910,000 (OPTIONS, 2016; UNAIDS, 2015c). The main transmission route is through sexual intercourse in heterosexual means with estimated 30% of the new infections deeply rooted among sex workers (NACC, 2014a). High HIV infections amongst sex workers in Kenya is attributed to unprotected sex. According to Shields (2012), most sex workers are constantly harassed by the police and/or physically and sexually abused for carrying condoms. In addition, the sex workers have no power to negotiate for safe sex. This is due to the fact that clients may decline to pay if they have to use a condom and hence use intimidation or violence to force unsafe sex (Ghimire et al., 2011). Furthermore, the clients may offer more money for unprotected sex, a proposal that is unlikely to be rejected by the sex workers. According to NACC (2014b), an estimated 29.3% of female sex workers were living with HIV in 2011. In addition, the findings from the Sex Workers Outreach Project reported an HIV prevalence of 30% among female sex workers and 40% among male sex workers in 2011 (UNAIDS, 2015b). Young women (aged 15 to 24 years) are more than three times more likely to be exposed to sexual violence than young men (KNBS, 2015). Among women aged 15-19 years, HIV prevalence was 23.0%, compared to 3.5% among men of the same age (KNBS, 2015; Voeten et al., 2007). Approximately 33% of the girls in

Kenya have been raped by the time they reach 18 years with about 22% aged 15-19 years reporting that their first sexual encounter was forced (NACC, 2014a). In addition, women continue to face discrimination in terms of access to education, employment and healthcare (UNAIDS, 2018b). Consequently, men often dominate sexual relationships, with women not always able to practice safer sex even when they know the risks involved (UNAIDS, 2015b, 2018b). For instance, in 2014, 35% of adult women (aged 15-49 years) who were or had been married had experienced spousal violence and 14% had experienced sexual violence (UNAIDS, 2018b).

Quite a number of mathematical models have been developed to investigate the dynamics of HIV and spread in the population (Athithan and Ghosh, 2014; Baryarama et al., 2006; Doyle et al., 1998; Kaur et al., 2014; Okango et al., 2016; Van Sighem et al., 2012; Wodarz and Nowak, 2002). However, to the author's knowledge, little attention has been given in incorporating sexual orientation of individuals using real-time series of HIV infection trend data. For example, the mathematical models in Mukandavire and Garira (2007a,b), describe the heterosexual interactions of males and females using integro-differential equations with a time delay due to incubation period. While these two models incorporated the effects of male and female condom use as the main mode of preventing HIV infection, they did not consider applying real-time surveillance data to establish the trend of infection. Additionally, in our modelling attempt, we consider a scenario in which individuals with HIV are enrolled to ART treatment. A study by Mukandavire et al. (2009) modelled a sex-structured model for heterosexual transmission of HIV/AIDS with explicit incubation period and provided an in-depth qualitative mathematical analysis. However, there was no numerical results to show the effect HIV prevention intervention measures as well as trend within these two sexes. Bhunu et al. (2011) derived an HIV model and examined the effect of counselling and testing coupled with decrease in sexual activity on HIV spread in resource-limited communities. The results from this model suggested that effective counselling and testing have a great potential to partially control the epidemic especially when HIV positive individuals willingly withdraw from sexual activities.

While these models elucidated the importance of prevention to reduce HIV burden, they did not take into account the fact that the immediate linkage of HIV patients to ART treatment can reduce the risk of dying as well as preventing further occurrence of new infections. The work in this chapter is motivated by the desire to understand HIV epidemic in Kenya by developing a mathematical model that aims at integrating data on HIV within males and females. In our modelling attempt, we consider a scenario in which individuals with HIV are linked to ART treatment. We extend the modelling framework in Bhunu et al. (2011); Mukandavire et al. (2009); Mukandavire and Garira (2007a,b) to fit into the Kenyan situation. We consider a population model for HIV describing disease transmission between males and females. Our main goals are: first, to develop a mathematical model that takes into account the treatment of HIV patients with ART and carry out qualitative analysis of the model and find the necessary threshold for controlling the spread of the disease. Second, to fit the model to observed data of new infections to show the trend between males and females using the parameter values that produce the best fit to the data. The model can help in planning and designing effective control measures to reduce the risk of new infections. In addition, the model and its predictions provide a framework for evaluating the success or failure of the current HIV intervention measures.

4.2 Model formulation

The model proposed in this work is an extension of the previous models studied in Mukandavire et al. (2009); Mukandavire and Garira (2007a,b), by enrolling the HIV patients regardless of the stage of infection or $CD4^{+}T$ cell counts. It extends the models stated by allowing for back-and-forth transitions between treatment classes thereby accounting for treatment failure. It is worth noting that when there is one failure in one level of ART treatment, the patients are usually placed on another level of ART treatment (WHO, 2014). We keep the model as simple as possible consistent with the available data. The model proposed here represents the sexually mature age group in Kenya (age 15 years and over). It is believed that this is the age group that is responsible for the spread of HIV (UNAIDS,

2015b). It is assumed that the male and female populations are divided into compartments described by time-dependent state variables. These compartments are: Susceptible (S_i), infected individuals with CD4$^+$T cell counts $\geq 350/\mu L$ who are considered to be new infections (I_{i1}) and infected individuals with CD4$^+$T cell counts $< 350/\mu L$ (I_{i2}). The infected individuals are then enrolled on ART which is divided into two depending the CD4$^+$T cell counts, that is, T_{i1} and T_{i2}. This is consistent with the WHO recommendation of immediate treatment with ART of HIV to attain viral load suppression (AIDS, 2015; Williams, 2014). Here, $i = m, f$ denoting male and female, respectively. The total variable population at time t, denoted by $N(t)$ is described by (4.1).

$$N(t) = N_m(t) + N_f(t), \tag{4.1}$$

where

$$N_m(t) = S_m(t) + I_{m1}(t) + I_{m2}(t) + T_{m1}(t) + T_{m2}(t),$$
$$N_f(t) = S_f(t) + I_{f1}(t) + I_{f2}(t) + T_{f1}(t) + T_{f2}(t).$$

The recruitment in the susceptible compartment is at the constant rate Λ of which a proportion α are assumed to be males and $(1-\alpha)$ are assumed to be females. Each individual compartment goes out from the system at natural mortality rate μ. The susceptible in either male or female populations is decreased following infection, which can be acquired via effective contact through sexual intercourse in heterosexual means with an infectious person at the respective rates given by λ_m and λ_f. These rates are obtained as follows: the probability that a male or female person chooses a particular partner of the opposite sex can be assumed as $\frac{1}{N_m}$ and $\frac{1}{N_f}$, respectively. Thus, a male or female receives in average $\frac{c_{mj}N_f}{N_m}$ and $\frac{c_{fj}N_m}{N_f}$ partners per unit of time, respectively. The total number of sexual contacts by males equals that of the females (conservation law). Then, the infection rate per susceptible male or female are, respectively, given by

$$\left.\begin{aligned}\lambda_m &= \frac{\left(\frac{N_f}{N_m}\right)\left[\sum_{j=k=1}^{j=k=2}\beta_{fj}c_{mj}I_{fk}+\sum_{j=3,k=1}^{j=4,k=2}\beta_{fj}c_{mj}T_{fk}\right]}{N_f},\\ \lambda_f &= \frac{\left(\frac{N_m}{N_f}\right)\left[\sum_{j=k=1}^{j=k=2}\beta_{mj}c_{fj}I_{mk}+\sum_{j=3,k=1}^{j=4,k=2}\beta_{mj}c_{fj}T_{mk}\right]}{N_m}.\end{aligned}\right\} \tag{4.2}$$

Here, $k=1,2$, representing the two stages of infectious population, β_{ij}, where $i=m,f$ and $j=1,\cdots,4$, are the probabilities of HIV transmission per partnership and c_{ij} are the rates at which an individual acquires sexual partners associated with the four infectious compartments, respectively. Thus, the expressions in (4.2) can be simplified to the following

$$\left.\begin{aligned}\lambda_m &= \left(\frac{\beta_{f1}c_{m1}I_{f1}+\beta_{f2}c_{m2}I_{f2}+\beta_{f3}c_{m3}T_{f1}+\beta_{f4}c_{m4}T_{f2}}{N_m}\right),\\ \lambda_f &= \left(\frac{\beta_{m1}c_{f1}I_{m1}+\beta_{m2}c_{f2}I_{m2}+\beta_{m3}c_{f3}T_{m1}+\beta_{m4}c_{f4}T_{m2}}{N_f}\right).\end{aligned}\right\} \tag{4.3}$$

Infectious individuals in class (I_{i1}) progress to class (I_{i2}) at rate γ_h, for $h=1,2$. Infectious individuals in classes (I_i^1) and (I_{i2}) move to (T_{i1}) and (T_{i2}) at a constant rate τ_p, for $p=1,\cdots,4$, as consequence of treatment with ART. The infectious individuals on ART in class (T_{i1}) progress to (T_{i2}) at a rate ψ_h as a result of decline in the immunological status. Similarly, infectious individuals on ART in class (T_{i2}) progress to (T_{i1}) at a rate ω_h as a consequence of improvement in the immunological status. Infectious individuals in classes I_{i2} and T_{i2} may die as a consequence of infection, at a disease-induced death rate δ_1 and δ_2 respectively.

4.2.1 Model assumptions

The following key assumptions have been made.

(i) The modelling framework is purely based on the assumption that HIV infection is through sexual intercourse in heterosexual means.

(ii) The proportion of the infected individuals on treatment is bi-directional due to attrition or adherence to ART and decline or improvement of immunological status.

(iii) The standard HIV transmission incidence has been used to model the disease transmission. This is the form most commonly used for sexually transmitted diseases (Hethcote, 2000).

(iv) There is homogeneous mixing of both males and females so that the average number of sexual contacts received depends on the population sizes of males and females and the transmission of HIV is assumed to be mainly through heterosexual means.

(v) An exit due to death as a consequence of development of AIDS has been included hence AIDS class is considered redundant and thus left out. Furthermore, AIDS patients are usually too ill to remain sexually active and they are unable to transmit HIV through sexual activity. Similar assumption was also made by Yang et al. (2017) while modelling the global dynamics of an HIV model incorporating senior male clients.

Figure 4.1 shows the schematic diagram for the compartmental model structure.

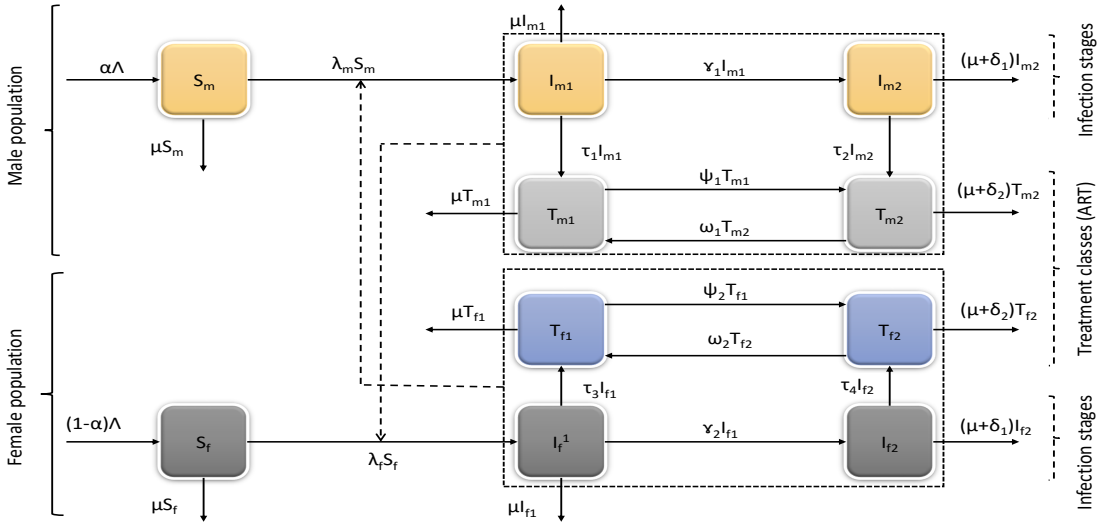

Figure 4.1: A compartmental model for the transmission dynamics of HIV, which takes into account treatment with ART.

In 2016, the Kenyan government issued full regulatory approval of PrEP, becoming the second country in sub-Saharan Africa after South Africa, to make such approval (UNAIDS, 2016b). PrEP is used by people who do not have HIV but are at high risk of acquiring it to prevent

HIV infection (AIDS, 2016a; HIV/AIDS, 2016). The successes of PrEP use in Kenya are yet to be reported since research into the uptake and impact of PrEP, specifically with young women and girls in high-incidence areas is still on-going (UNAIDS, 2016b). The challenges posed by the continued occurrence of new infections call for a better understanding of the disease transmission and development of effective strategies for prevention and control of the spread of HIV. Therefore, we add control $0 \leq \phi \leq 1$ to measure the effectiveness of PrEP in the prevention against acquiring HIV infection. Thus the infection terms given in (4.3) are, respectively, modified as follows

$$\lambda_{mq} = (1-\phi)\lambda_m \text{ and } \lambda_{fq} = (1-\phi)\lambda_f. \tag{4.4}$$

Similar modelling approach of PrEP was done by Afassinou et al. (2017) where they developed a model for HIV/AIDS which can be utilized to assess the impact of combining PrEP and ARVs interventions.

Table 4.1: Definition of the state variables.

Variable	Description
S_i	The number of susceptible individuals at time t
I_{i1}	The number of the infected individuals with **CD4$^+$T** cell counts $\geq 350/\mu L$ at time t
I_{i2}	The number of the infected individuals with **CD4$^+$T** cell counts $< 350/\mu L$ at time t
T_{i1}	The number of the infected individuals with **CD4$^+$T** cell counts $\geq 350/\mu L$ on ART at time t
T_{i2}	The number of the infected individuals with **CD4$^+$T** cell counts $< 350/\mu L$ on ART at time t

Table 4.2: Description of the parameters.

Parameter	Description
Λ	The per capita recruitment rate of the susceptibles
α	proportion of male susceptibles among the recruits
β_{ij}	The rate of HIV transmission per effective contact with sexual partner of opposite sex
c_{ij}	The rates at which an individual acquires sexual partners
μ	The per capita natural death rate
δ_h	The disease-induced death rate in I_{i2} and T_{i2}
γ_h	The rate at which infectious individuals in class I_{i1} progress to class I_{i2}
τ_p	Progression rate from I_{i1} and I_{i2} to T_{i1} and T_{i2}
ψ_h	Progression rate from T_{i1} to T_{i2}
ω_h	Progression rate from T_{i2} to T_{i1}

4.2.2 Model equations

The above assumptions and descriptions lead to the following ten non-linear system of ordinary differential equations.

$$\left.\begin{aligned}
\frac{dS_m}{dt} &= \alpha\Lambda - \lambda_{mq}S_m - \mu S_m, & \frac{dS_f}{dt} &= (1-\alpha)\Lambda - \lambda_{fq}S_f - \mu S_f,\\
\frac{dI_{m1}}{dt} &= \lambda_{mq}S_m - (\gamma_1+\tau_1+\mu)I_{m1}, & \frac{dI_{f1}}{dt} &= \lambda_{fq}S_f - (\gamma_2+\tau_3+\mu)I_{f1},\\
\frac{dI_{m2}}{dt} &= \gamma_1 I_{m1} - (\tau_2+\mu+\delta_1)I_{m2}, & \frac{dI_{f2}}{dt} &= \gamma_2 I_{f1} - (\tau_4+\mu+\delta_1)I_{f2},\\
\frac{dT_{m1}}{dt} &= \tau_1 I_{m1} + \omega_1 T_{m2} - (\psi_1+\mu)T_{m1}, & \frac{dT_{f1}}{dt} &= \tau_3 I_{f1} + \omega_2 T_{f2} - (\psi_2+\mu)T_{f1},\\
\frac{dT_{m2}}{dt} &= \tau_2 I_{m2} + \psi_1 T_{m1} - (\omega_1+\mu+\delta_2)T_{m2}, & \frac{dT_{f2}}{dt} &= \tau_4 I_{f2} + \psi_2 T_{f1} - (\omega_2+\mu+\delta_2)T_{f2},
\end{aligned}\right\} \tag{4.5}$$

subject to the following initial conditions

$$S_i(0) \geq 0,\ I_{i1}(0) \geq 0,\ I_{i2}(0) \geq 0,\ T_{i1}(0) \geq 0,\ T_{i2}(0) \geq 0,\ \text{for } i = m, f. \tag{4.6}$$

The total population of both male and female sub-populations, respectively, evolve according to the following

$$\frac{dN_m}{dt} = \alpha\Lambda - \mu N_m \text{ and } \frac{dN_f}{dt} = (1-\alpha)\Lambda - \mu N_f. \tag{4.7}$$

The solutions to each of the equations in system (4.7) are given by

$$N_m = \frac{\alpha\Lambda}{\mu} + \left[N_{0m} - \frac{\alpha\Lambda}{\mu}\right]\exp(-\mu t) \text{ and } N_f = \frac{(1-\alpha)\Lambda}{\mu} + \left[N_{0f} - \frac{(1-\alpha)\Lambda}{\mu}\right]\exp(-\mu t),$$

respectively. Here, N_{0m} and N_{0f} are the initial populations for the males and females, respectively. The solution of the equations from system (4.5) remain non-negative for all $t \geq 0$. The total population $\{N_m;\ N_f\}$ in each of the sub-populations is bounded by $\frac{\alpha\Lambda}{\mu}$ and $\frac{(1-\alpha)\Lambda}{\mu}$, respectively. The total population in both sub-populations is given by $N = N_m + N_f$ such that the evolution of the total population over a specified period is given by

$$\frac{dN}{dt} = \Lambda - \mu N.$$

It can easily be seen that $\limsup_{t\to\infty} N \leq \frac{\Lambda}{\mu}$. Therefore, the phase space of the system (4.5) is given by

$$\Omega := \left\{(S_i, I_{i1}, I_{i2}, T_{i1}, T_{i2}) : S_i + I_{i1} + I_{i2} + T_{i1} + T_{i2} \leq \frac{\Lambda}{\mu}\right\}.$$

The solutions in Ω are all non-negative and bounded. Hence the domain of biological significance is positively invariant and attracting. Therefore, all solutions starting in Ω remain in Ω.

4.3 Equilibrium points

To better understand the dynamics of the proposed model, we begin by examining the model's behaviour about the steady states. This analysis is crucial for identifying the parameters of the model that help to achieve an HIV-free state. Since the rate of change in each compartment is constant at equilibrium, we set the right-hand side of equations in the system (4.5) to zero

and solve for the state variables in terms of the infection terms λ_{mq} and λ_{fq} and obtain the following;

$$\left.\begin{aligned}
S_m^* &= \frac{\alpha\Lambda}{\mu+\lambda_{mq}^*}, \quad I_{m1}^* = \frac{\alpha\Lambda\lambda_{mq}^*)}{Q_1(\mu+\lambda_{mq}^*)}, \quad I_{m2}^* = \frac{\alpha\gamma_1\Lambda\lambda_{mq}^*}{Q_1Q_2(\mu+\lambda_{mq}^*)}, \\
T_{m1}^* &= \frac{\alpha\Lambda\lambda_{mq}^*(\gamma_1\tau_2\omega_1+Q_2Q_4\tau_1)}{Q_1Q_2Q_3Q_4(\mu+\lambda_{mq}^*)(1-\Phi_1)}, \quad T_{m2}^* = \frac{\alpha\Lambda\lambda_{mq}^*(\gamma_1Q_3\tau_2+Q_2\tau_1\psi_1)}{Q_1Q_2Q_3Q_4(\mu+\lambda_{mq}^*)(1-\Phi_1)}, \\
S_f^* &= \frac{(1-\alpha)\Lambda}{\mu+\lambda_{fq}^*}, \quad I_{f1}^* = \frac{(1-\alpha)\Lambda\lambda_{fq}^*}{Q_5(\mu+\lambda_{fq}^*)}, \quad I_{f2}^* = \frac{(1-\alpha)\gamma_2\Lambda\lambda_{fq}^*}{Q_5Q_6(\mu+\lambda_{fq}^*)}, \\
T_{f1}^* &= \frac{(1-\alpha)\Lambda\lambda_{fq}^*(\gamma_2\tau_4\omega_2+Q_6Q_8\tau_3)}{Q_5Q_6Q_7Q_8(\lambda_{fq}^*+\mu)(1-\Phi_2)}, \quad T_{f2}^* = \frac{(1-\alpha)\Lambda\lambda_{fq}^*(\gamma_2Q_7\tau_4+Q_6\tau_3\psi_2)}{Q_5Q_6Q_7Q_8(\lambda_{fq}^*+\mu)(1-\Phi_2)},
\end{aligned}\right\} \tag{4.8}$$

where

$$Q_1 = \gamma_1+\tau_1+\mu, \quad Q_2 = \tau_2+\mu+\delta_1, \quad Q_3 = \psi_1+\mu, \quad Q_4 = \omega_1+\mu+\delta_2, \quad \Phi_1 = \frac{\psi_1\omega_1}{Q_3Q_4},$$
$$Q_5 = \gamma_2+\tau_3+\mu, \quad Q_6 = \tau_4+\mu+\delta_1, \quad Q_7 = \psi_2+\mu, \quad Q_8 = \omega_2+\mu+\delta_2, \quad \Phi_2 = \frac{\psi_2\omega_2}{Q_7Q_8}.$$

Substituting the expressions for the state variables I_{i1}^*, I_{i2}^*, T_{i1}^* and T_{i2}^* in (4.8) into infection terms in (4.4) then simplifying, the following polynomial is obtained.

$$\lambda_{mq}^*[A_1\lambda_{mq}^*+A_0] = 0, \tag{4.9}$$

where

$$\begin{aligned}
A_0 &= -Q_1Q_2Q_3Q_4Q_5Q_6Q_7Q_8\mu(1-\Phi_1)(1-\Phi_2)(1-\alpha)[\mathscr{R}_0-1], \\
A_1 &= Q_5Q_6Q_7Q_8(1-\Phi_2)[(1-\phi)\alpha(Q_3Q_4(1-\Phi_1)(Q_2\beta_{m1}c_{f1}+\gamma_1\beta_{m2}c_{f2}) \\
&\quad +(Q_2Q_4\tau_1+\gamma_1\tau_2\omega_1)\beta_{m3}c_{f3}+(Q_3\gamma_1\tau_2Q_2\tau_1\psi_1)\beta_{m4}c_{f4}) \\
&\quad +Q_1Q_2Q_3Q_4\mu(1-\Phi_1)(1-\alpha)].
\end{aligned}$$

The expression for $\mathscr{R}_0$ is computed in (4.13). Note that the case $\lambda^*_{mq} = 0$ corresponds to the disease-free equilibrium which can be expressed as

$$\mathscr{E}_0 = \left[\frac{\alpha\Lambda}{\mu},\ 0,\ 0,\ 0,\ 0,\ \frac{(1-\alpha)\Lambda}{\mu},\ 0,\ 0,\ 0,\ 0\right]. \tag{4.10}$$

The disease-free equilibrium refers to a scenario in which HIV infection is not present in a population. The solutions to the remaining part of (4.9), given by equation (4.11) give possible disease-persistent state ($\mathscr{E}_1$).

$$A_1\lambda^*_{mq} + A_0 = 0. \tag{4.11}$$

The existence of disease-persistent state refers to a scenario in which HIV infection persists in the population. We note that $A_0 > 0$ if $\mathscr{R}_0 < 1$ and expression (4.11) does not have a positive solution. However, $B_0 < 0$ if $\mathscr{R}_0 > 1$ and expression (4.11) does have a positive solution implying that there exists a unique endemic equilibrium if and only if $\mathscr{R}_0 > 1$.

4.3.1 The basic reproduction number

The basic reproduction number is defined as the average number of new infections generated by one infected individual throughout his/her period of infectiousness, via sexual intercourse in heterosexual means, in a completely susceptible population (Van den Driessche and Watmough, 2002). The basic reproduction number, R_0, which is a measure of the infection on the susceptible populations, for the system (4.5) is obtained using the next generation method described in (Van den Driessche and Watmough, 2002). Following the explanation given in Van den Driessche and Watmough (2002), we obtain **F** which is the matrix of new infections and **V** which is the matrix of transfers between compartments given by

$$\mathbf{F} = \begin{bmatrix} \mathbf{F}_1 & \mathbf{F}_2 \\ \mathbf{F}_3 & \mathbf{F}_4 \end{bmatrix} \text{ and } \mathbf{V} = \begin{bmatrix} Q_1 & 0 & 0 & 0 & 0 & 0 & 0 & 0 \\ -\gamma_1 & Q_2 & 0 & 0 & 0 & 0 & 0 & 0 \\ -\tau_1 & 0 & Q_3 & -\omega_1 & 0 & 0 & 0 & 0 \\ 0 & -\tau_2 & -\psi_1 & Q_4 & 0 & 0 & 0 & 0 \\ 0 & 0 & 0 & 0 & Q_5 & 0 & 0 & 0 \\ 0 & 0 & 0 & 0 & -\gamma_2 & Q_6 & 0 & 0 \\ 0 & 0 & 0 & 0 & -\tau_3 & 0 & Q_7 & -\omega_2 \\ 0 & 0 & 0 & 0 & 0 & -\tau_4 & -\psi_2 & Q_8 \end{bmatrix}, \quad (4.12)$$

where

$$\mathbf{F}_1 = \begin{bmatrix} 0 & 0 & 0 & 0 \\ 0 & 0 & 0 & 0 \\ 0 & 0 & 0 & 0 \\ 0 & 0 & 0 & 0 \end{bmatrix}, \quad \mathbf{F}_2 = \begin{bmatrix} (1-\phi)c_{m1}\beta_{f1} & (1-\phi)c_{m2}\beta_{f2} & (1-\phi)c_{m3}\beta_{f3} & (1-\phi)c_{m4}\beta_{f4} \\ 0 & 0 & 0 & 0 \\ 0 & 0 & 0 & 0 \\ 0 & 0 & 0 & 0 \end{bmatrix}$$

$$\mathbf{F}_3 = \begin{bmatrix} (1-\phi)c_{f1}\beta_{m1} & (1-\phi)c_{f2}\beta_{m2} & (1-\phi)c_{f3}\beta_{m3} & (1-\phi)c_{f4}\beta_{m4} \\ 0 & 0 & 0 & 0 \\ 0 & 0 & 0 & 0 \\ 0 & 0 & 0 & 0 \end{bmatrix}, \quad \mathbf{F}_4 = \begin{bmatrix} 0 & 0 & 0 & 0 \\ 0 & 0 & 0 & 0 \\ 0 & 0 & 0 & 0 \\ 0 & 0 & 0 & 0 \end{bmatrix}.$$

If there is an existence of an infection in the population, then the corresponding threshold number for the persistence or eradication of HIV obtained from the spectral radius of $\mathbf{FV}^{-1}$ is given by

$$R_0 = \sqrt{\mathscr{R}_{0m}\mathscr{R}_{0f}}, \quad (4.13)$$

where

$$\mathscr{R}_{0m} = \mathscr{R}_{0m1} + \mathscr{R}_{0m2} + \mathscr{R}_{0m3} + \mathscr{R}_{0m4}, \quad \mathscr{R}_{0f} = \mathscr{R}_{0f1} + \mathscr{R}_{0f2} + \mathscr{R}_{0f3} + \mathscr{R}_{0f4},$$

with

$$
\left.
\begin{aligned}
\mathscr{R}_{0m1} &= \left(\frac{1-\phi}{Q_1\mu}\right)\beta_{m1}c_{f1}, \quad \mathscr{R}_{0m2} = \left(\frac{1-\phi}{Q_1Q_2\mu}\right)\gamma_1\beta_{m2}c_{f2},\\
\mathscr{R}_{0m3} &= \left(\frac{(Q_2Q_4\tau_1+\gamma_1\tau_2\omega_1)(1-\phi)}{Q_1Q_2Q_3Q_4\mu(1-\Phi_1)}\right)\beta_{m3}c_{f3},\\
\mathscr{R}_{0m4} &= \left(\frac{(Q_3\gamma_1\tau_2+Q_2\tau_1\psi_1)(1-\phi)}{Q_1Q_2Q_3Q_4\mu(1-\Phi_1)}\right)\beta_{m4}c_{f4},\\
\mathscr{R}_{0f1} &= \left(\frac{1-\phi}{Q_5\mu}\right)\beta_{f1}c_{m1}, \quad \mathscr{R}_{0f2} = \left(\frac{1-\phi}{Q_5Q_6\mu}\right)\gamma_2\beta_{f2}c_{m2},\\
\mathscr{R}_{0f3} &= \left(\frac{(Q_6Q_8\tau_3+\gamma_2\tau_4\omega_2)(1-\phi)}{Q_5Q_6Q_7Q_8\mu(1-\Phi_2)}\right)\beta_{f3}c_{m3},\\
\mathscr{R}_{0f4} &= \left(\frac{(Q_7\gamma_2\tau_4+Q_6\tau_3\psi_2)(1-\phi)}{Q_5Q_6Q_7Q_8\mu(1-\Phi_2)}\right)\beta_{f4}c_{m4}.
\end{aligned}
\right\}
$$

The components of the basic reproduction numbers, R_0, are explained as follows:-

(i) $\mathscr{R}_{0mj}$, for $j = 1,\cdots,4$, represents the basic reproductive number associated with each category of the male infected patients in compartments I_{mk} and T_{mk}, for $k = 1,2$, when introduced into a population, respectively.

(ii) $\mathscr{R}_{0fj}$, for $j = 1,\cdots,4$, represents the basic reproductive number associated with each category of the female infected patients in compartments I_{fk} and T_{fk}, for $k = 1,2$, when introduced into a population, respectively.

The term $\Phi_1 = \frac{\psi_1\omega_1}{Q_3Q_4}$ represents the fraction of male individuals in compartments T_{m1} and T_{m2} who move from either the compartments due to either improvement or decline in their immunological status. The same explanation applies to the term $\Phi_2 = \frac{\psi_2\omega_2}{Q_7Q_8}$ in the female population. The values $\frac{1}{Q_3}$, $\frac{1}{Q_4}$ represent the average time male individuals in compartments T_{m1} and T_{m2} stay in their respective compartments. A similar explanation is given for the values $\frac{1}{Q_7}$, $\frac{1}{Q_8}$ in the female population. Therefore, $(1-\Phi_1)$ and $(1-\Phi_2)$ refer to the fraction of individuals who do not cycle between compartments T_{i1} and T_{i2} in the male and female populations respectively. Note that the square root arises due to the fact that it takes two generations for infected individuals to produce new infections.

From Theorem 2 in Van den Driessche and Watmough (2002), fundamental results about the equilibria analyses of the system (4.5) are given by the following results:

Theorem 4.1. *The disease-free equilibrium point $\mathscr{E}_0$ is locally asymptotically stable when $R_0 < 1$ and unstable otherwise.*

It is important to note that If $R_0 < 1$, then on average, an infected individual produces less than one new infected individual over the course of its infectious period and the infection cannot grow. The converse is true for $R_0 > 1$.

4.4 Local stability of the disease-persistent equilibrium

Theorem 4.2. *The disease-persistent equilibrium point $\mathscr{E}_1$ given by the solution of expression (4.11) is locally asymptotically stable in Ω when $R_0 > 1$ and unstable otherwise.*

Proof. The local stability of the disease-persistent equilibrium point $\mathscr{E}_1$ is proved based on the centre manifold theory as described in (Castillo-Chavez and Song, 2004). We avoid re-stating the theorem and compute the components of **a** and **b** as explained in the theorem. Let $\vartheta = \beta_{m1} c_{f1}$ be our bifurcation parameter so that for

$$\mathscr{R}_0 = 1, \quad \vartheta = \vartheta^* = \left[\frac{Q_1}{1-\phi}\right]\left[\frac{1}{\mathscr{R}_{0f1}+\mathscr{R}_{0f2}+\mathscr{R}_{0f3}+\mathscr{R}_{0f4}} - (\mathscr{R}_{0m2}+\mathscr{R}_{0m3}+\mathscr{R}_{0m4})\right]. \tag{4.14}$$

Furthermore, to linearise the system (4.5), we define

$$S_m = x_1, \quad I_{m1} = x_2, \quad I_{m2} = x_3, \quad T_{m1} = x_4, \quad T_{m2} = x_5,$$
$$S_f = x_6, \quad I_{f1} = x_7, \quad I_{f2} = x_8, \quad T_{f1} = x_9, \quad T_{f2} = x_{10},$$

and

$$\frac{dx}{dt} = f(x, \vartheta), f : \mathbb{R}^{10} \times \mathbb{R} \to \mathbb{R} \text{ and } f \in \mathbf{C}^2(\mathbb{R}^{10} \times \mathbb{R}).$$

Thus, we linearise the system (4.5) at disease-free equilibrium with the bifurcation parameter ϑ to obtain

$$\mathbf{J} = \begin{bmatrix} J_1 & J_2 \\ J_3 & J_4 \end{bmatrix} \tag{4.15}$$

where

$$J_1 = \begin{bmatrix} -\mu & 0 & 0 & 0 & 0 \\ 0 & -Q_1 & 0 & 0 & 0 \\ 0 & \gamma_1 & -Q_2 & 0 & 0 \\ 0 & \tau_1 & 0 & -Q_3 & \omega_1 \\ 0 & 0 & \tau_2 & \psi_1 & -Q_4 \end{bmatrix}, \quad J_4 = \begin{bmatrix} -\mu & 0 & 0 & 0 & 0 \\ 0 & -Q_5 & 0 & 0 & 0 \\ 0 & \gamma_2 & -Q_6 & 0 & 0 \\ 0 & \tau_3 & 0 & -Q_7 & \omega_2 \\ 0 & 0 & \tau_4 & \psi_2 & -Q_8 \end{bmatrix}.$$

$$J_2 = \begin{bmatrix} 0 & -\frac{(1-\phi)\beta_{f1}c_{m1}S_m^*}{N_m} & -\frac{(1-\phi)\beta_{f2}c_{m2}S_m^*}{N_m} & -\frac{(1-\phi)\beta_{f3}c_{m3}S_m^*}{N_m} & -\frac{(1-\phi)\beta_{f4}c_{m4}S_m^*}{N_m} \\ 0 & \frac{(1-\phi)\beta_{f1}c_{m1}S_m^*}{N_m} & \frac{(1-\phi)\beta_{f2}c_{m2}S_m^*}{N_m} & \frac{(1-\phi)\beta_{f3}c_{m3}S_m^*}{N_m} & \frac{(1-\phi)\beta_{f4}c_{m4}S_m^*}{N_m} \\ 0 & 0 & 0 & 0 & 0 \\ 0 & 0 & 0 & 0 & 0 \\ 0 & 0 & 0 & 0 & 0 \end{bmatrix},$$

$$J_3 = \begin{bmatrix} 0 & -\frac{(1-\phi)\beta_{m1}c_{f1}S_f^*}{N_f} & -\frac{(1-\phi)\beta_{m2}c_{f2}S_f^*}{N_f} & -\frac{(1-\phi)\beta_{m3}c_{f3}S_f^*}{N_f} & -\frac{(1-\phi)\beta_{m4}c_{f4}S_f^*}{N_f} \\ 0 & \frac{(1-\phi)\beta_{m1}c_{f1}S_f^*}{N_f} & \frac{(1-\phi)\beta_{m2}c_{f2}S_f^*}{N_f} & \frac{(1-\phi)\beta_{m3}c_{f3}S_f^*}{N_f} & \frac{(1-\phi)\beta_{m4}c_{f4}S_f^*}{N_f} \\ 0 & 0 & 0 & 0 & 0 \\ 0 & 0 & 0 & 0 & 0 \\ 0 & 0 & 0 & 0 & 0 \end{bmatrix}.$$

It is important to note that with the bifurcation parameter expressed in (4.14), the linearised system (4.15) has a zero eigenvalue while the rest of the eigenvalues are negative. The left eigenvector of (4.15), $\mathbf{V} = (v_1, v_2, v_3, v_4, v_5, v_6, v_7, v_8, v_9, v_{10})$ and the right eigenvector $\mathbf{W} = (w_1, w_2, w_3, w_4, w_5,\ w_6, w_7, w_8, w_9, w_{10})^T$ both associated to the eigenvalue zero are solutions of the linearised system (4.15) such that $\mathbf{VJ} = [0,0,0,0,0,0,0,0,0,0]$, $\mathbf{JW} = [0,0,0,0,0,0,0,0,0,0]^T$ and $\mathbf{VW} = 1$. The associated left eigenvectors are given by

$$\left.\begin{aligned}
&v_1 = v_6 = 0, \quad v_7 = 1, \quad v_2 = \frac{Q_5Q_6(Q_7(\delta_2+\mu)+\mu\omega_2)}{\mu(1-\phi)(Q_9+Q_{10}+Q_{11})},\\
&v_3 = \frac{(1-\phi)(\omega_1(\mu c_{f2}\beta_{m2}+\tau_2 c_{f3}\beta_{m3})+Q_3((\delta_2+\mu)c_{f2}\beta_{m2}+\tau_2 c_{f4}\beta_{m4}))}{Q_2(\mu\omega_1+Q_3(\delta_2+\mu))},\\
&v_4 = \frac{(1-\phi)(Q_4 c_{f3}\beta_{m3}+\psi_1 c_{f4}\beta_{m4})}{\mu\omega_1+Q_3(\delta_2+\mu)}, \quad v_5 = \frac{(1-\phi)(\omega_1 c_{f3}\beta_{m3}+Q_3 c_{f4}\beta_{m4})}{\mu\omega_1+Q_3(\delta_2+\mu)},\\
&v_8 = \frac{Q_5(\beta_{f2}c_{m2}(\mu\omega_2+Q_7(\delta_2+\mu))+\tau_4(\omega_2\beta_{f3}c_{m3}+Q_7\beta_{f4}c_{m4}))}{(Q_9+Q_{10}+Q_{11})},\\
&v_9 = \frac{Q_5Q_6(Q_8\beta_{f3}c_{m3}+\psi_2\beta_{f4}c_{m4})}{(Q_9+Q_{10}+Q_{11})}, \quad v_{10} = \frac{Q_5Q_6(\omega_2\beta_{f3}c_{m3}+Q_7\beta_{f4}c_{m4})}{(Q_9+Q_{10}+Q_{11})},
\end{aligned}\right\}$$

while the associated right eigenvectors are given by

$$\left.\begin{aligned}
&w_1 = \frac{-Q_1}{\mu}, \quad w_2 = 1, \quad w_3 = \frac{\gamma_1}{Q_2}, \quad w_4 = \frac{\gamma_1\tau_2\omega_1+Q_2Q_4\tau_1}{Q_2(\mu\omega_1+Q_3(\mu+\delta_2))},\\
&w_5 = \frac{Q_2\tau_1\omega_1+Q_3\gamma_1\tau_2}{Q_2(\mu\omega_1+Q_3(\mu+\delta_2))}, \quad w_6 = \frac{-Q_1Q_5Q_6(\mu\omega_2+Q_7(\delta_2+\mu))}{\mu(1-\phi)(Q_9+Q_{10}+Q_{11})},\\
&w_7 = \frac{Q_1Q_6(Q_7(\delta_2+\mu)+\mu\omega_2)}{\mu(1-\phi)(Q_9+Q_{10}+Q_{11})}, \quad w_8 = \frac{(Q_1\gamma_2(Q_7(\delta_2+\mu)+\mu\omega_2)}{\mu(1-\phi)(Q_9+Q_{10}+Q_{11})},\\
&w_9 = \frac{Q_1(\gamma_2\tau_4\omega_2+Q_6Q_8\tau_3)}{\mu(1-\phi)(Q_9+Q_{10}+Q_{11})}, \quad w_{10} = \frac{(Q_1(Q_7\gamma_2\tau_4+Q_6\tau_3\psi_2)}{\mu(1-\phi)(Q_9+Q_{10}+Q_{11})},
\end{aligned}\right\}$$

with

$$Q_9 = (\mu\omega_2+Q_7(\delta_2+\mu))(Q_6\beta_{f1}c_{m1}+\gamma_2\beta_{f2}c_{m2}), \quad Q_{10} = \beta_{f3}c_{m3}(\gamma_2\tau_4\omega_2+Q_6Q_8\tau_3),$$
$$Q_{11} = \beta_{f4}c_{m4}(\gamma_2Q_7\tau_4+Q_6\tau_3\psi_2).$$

According Castillo-Chavez and Song (2004), the local dynamics of the system (4.5) around zero are governed by the the signs of **a** and **b**, where

$$\mathbf{a} = \sum_{k,i,j=1}^{n} v_k w_i w_j \frac{\partial^2 f_k}{\partial x_i \partial x_j}(0,0), \quad \mathbf{b} = \sum_{k,i=1}^{n} v_k w_i \frac{\partial^2 f_k}{\partial x_i \partial \vartheta}(0,0). \tag{4.16}$$

To compute **a** and **b** we, respectively, evaluate the non-zero second-order mixed derivatives with respect to variables and the non-zero partial derivatives with respect to bifurcation

parameter. These are given by

$$\frac{\partial^2 f_7}{\partial x_6 \partial x_2} = \frac{\partial^2 f_7}{\partial x_2 \partial x_6} = \frac{\mu\vartheta}{(1-\alpha)\Lambda}, \quad \frac{\partial^2 f_7}{\partial x_2 \vartheta} = 1. \tag{4.17}$$

Now, substituting the expressions into (4.16) and simplifying, we obtain

$$\left.\begin{aligned} \mathbf{a} &= -\frac{Q_1Q_5Q_6(\mu\omega_2 + Q_7(\delta_2+\mu))[Q_1Q_2Q_3Q_4Q_5Q_6Q_7Q_8(1-\Phi_1)(1-\Phi_2)-\Psi_1]}{Q_3Q_4\Lambda(1-\alpha)(1-\phi)^3(1-\Phi_1)(Q_9+Q_{10}+Q_{11})\Psi_2}, \\ \mathbf{b} &= 1, \end{aligned}\right\} \tag{4.18}$$

where

$$\left.\begin{aligned} \Psi_1 &= (1-\phi)^2(\gamma_1Q_3Q_4(1-\Phi_1)c_{f2}\beta_{m2} + c_{f3}\beta_{m3}(\gamma_1\tau_2\omega_1 + Q_2Q_4\tau_1) + c_{f4}\beta_{m4}(\gamma_1Q_3\tau_2 \\ &\quad + Q_2\tau_1\psi_1))(Q_6Q_7Q_8\beta_{f1}c_{m1}(1-\Phi_2) + \beta_{f3}c_{m3}(Q_6Q_8\tau_3 + \gamma_2\tau_4\omega_2) \\ &\quad + Q_7Q_8\beta_{f2}c_{m2}\gamma_2(1-\Phi_2) + \beta_{f4}c_{m4}(Q_7\gamma_2\tau_4 + Q_6\tau_3\psi_2)), \\ \Psi_2 &= (Q_6Q_7Q_8\beta_{f1}c_{m1}(1-\Phi_2) + \beta_{f3}c_{m3}(Q_6Q_8\tau_3 + \gamma_2\tau_4\omega_2) + Q_7Q_8\beta_{f2}c_{m2}\gamma_2(1-\Phi_2) \\ &\quad + \beta_{f4}c_{m4}(Q_7\gamma_2\tau_4 + Q_6\tau_3\psi_2)). \end{aligned}\right\}$$

From expressions in (4.18), it can be seen that $\mathbf{a} < 0$ and $\mathbf{b} > 0$ for all parameter values. Therefore the disease-persistent equilibrium point $\mathscr{E}_1$ is locally asymptotically stable close to $\mathscr{R}_0 = 1$. □

4.5 Data and parameter estimation

4.5.1 Parameter estimation

Some of the parameter ranges used in this paper have been estimated from previously published articles, while others are estimated intuitively. The baseline parameter values are obtained through curve fitting and presented under the caption of Figure 4.4. The full list of parameter ranges used in the simulation is given in Table 4.3.

Table 4.3: Parameter ranges of the model (4.5) given per month.

Parameter	Min	Max	Source
Λ	0.0013N	0.00265N	(WB, 2017)
β_{ij}	0.0	1.0	Assumed
c_{ij}	1.0	4.0	Estimated
α	0.35	0.60	(POP, 2017)
μ	0.00119	0.00167	(POP, 2017; WB, 2017)
δ_h	0.0069	0.0104	(Okosun et al., 2013)
γ_h	0.18	1.0	Estimated
τ_p	0.1	1.0	Estimated
ψ_h	0.1	1.0	Estimated
ω_h	0.1	0.8	Estimated

4.5.2 HIV data

The data were obtained from Kenya Health Information System (KHIS) (KHIS, 2017). The data used represent new HIV infection for both males and females in Kenya. Data are collected routinely on a monthly basis and were retrieved for the period beginning January 2011 to December 2017. Only variables of interest were pulled out to excel spreadsheet. Data were stored in excel and thereafter analysed in **R**. The pictorial representation of the raw data is given in Figure 4.2.

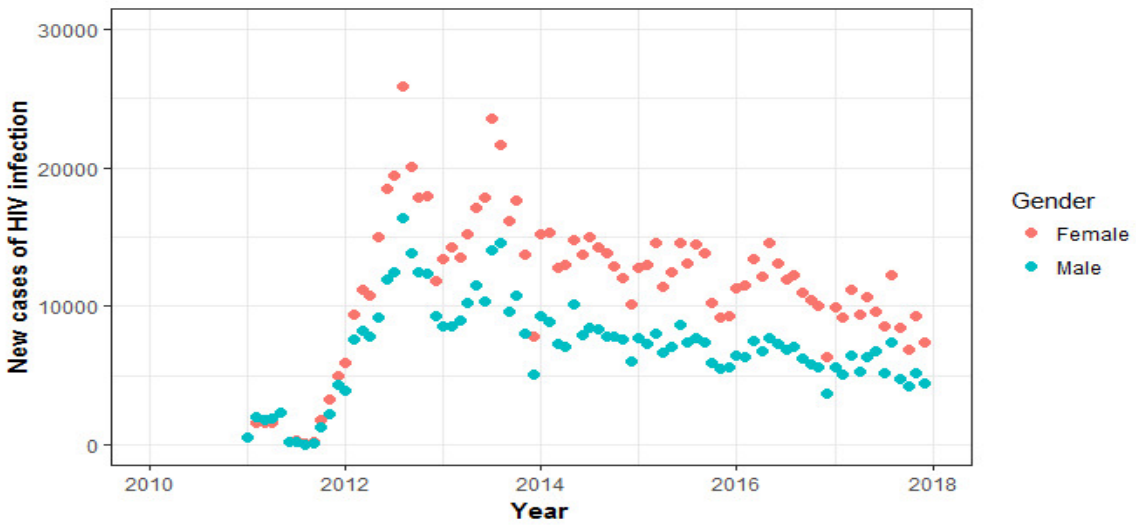

Figure 4.2: The graphical representation of the data for the new cases of HIV infections in Kenya in the male and female populations.

4.5.3 Initial conditions

To fit and validate model (4.5) to the data on reported cases of new HIV infections in Kenya, the initial conditions are set as follows. The total population of Kenya at the end of 2010 was estimated to be 41.35 million according to KNBS (2015). Of this, 57.6% was aged 15 years and above. Therefore the total population (N) considered in this paper is 23.8176 million. The population of male (N_m) is estimated to be 49% and that of female (N_f) is estimated at 51%. The reported number of adults living with HIV in January 2011 was 1.2 million with approximated 661,515 on ART treatment (NACC, 2013). From here, the number of new HIV infections (I_{m1} and I_{fm}) have been estimated based on the data reported in January 2011 to be 500 and 530, respectively (KHIS, 2017). The susceptible population for each gender is estimated using the following relations

$$S_m = N_m - \sum_{k=1}^{2} I_{mk} - \sum_{k=1}^{2} T_{mk} \text{ and } S_f = N_f - \sum_{k=1}^{2} I_{fk} - \sum_{k=1}^{2} T_{fk}.$$

The breakdown of the initial populations used in the curve fitting is given in Table 4.4. We therefore resort to curve fitting and numerical simulation to understand the effect of PrEP on the evolution of HIV.

Table 4.4: Estimates of the ranges of the state variables of model (4.5).

Variable	Male	Female	Source
S	11,589,991	11,764,344	(NACC, 2013)
I_1	500	530	KHIS (2017)
I_2	35,000	40,000	Assumed
T_1	30,000	35,000	(NACC, 2013)
T_2	45,000	50,000	Assumed

4.6 Descriptive statistical analysis of the data

Input data were summarized using error bar and density plot to illustrate the extent of variability and presented in Figure 4.3. For process indicators, the mean number of infections

are reported and the 95% confidence intervals are presented using the error bar in Figure 4.3, panel (a). The results suggest that there is a significant difference in HIV infections between males and females. This is supported by the non-overlapping standard deviation error bars. Furthermore, it can easily be seen that the mean number of new cases of infections in the female population is higher than that in males. From results in Figure 4.3, panel (b), it can clearly be seen that the data for the two sets do not follow a normal distribution. Thus, there is need to perform further tests to establish any significance difference. To establish whether there is significant difference in the male and female infections, Mann-Whitney U-test is used. This is a non-parametric test that is used to compare means of two groups that do not follow a normal distribution. The results in Table 4.5 show that there is significant difference in the mean infections between male and female given that the p-value $= 3.686e-10 < 0.05$, performed at 95% confidence level.

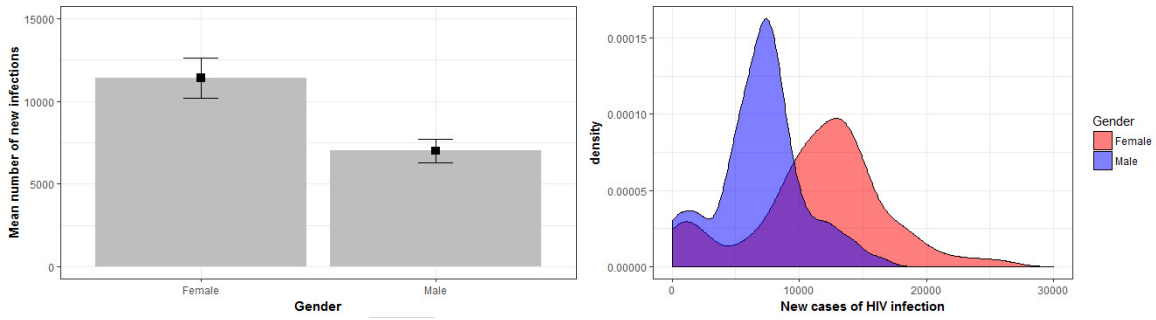

(a) (b)

Figure 4.3: The graphical representation of the variability of the data. Panel (a) shows the means with error bars for two variables (females and males): $n = 84$ for each variable. The column denotes the data mean (M). The bars show confidence interval (CI). CI error bars encompass 95% of the data. Panel (b) shows the density distribution of the data.

Table 4.5: Wilcoxon test results for the difference in the male and female infections

w	p-value
5504	3.686e-10

4.7 Cuve fitting

In this section, we fit system (4.5) to data to determine the trend of HIV in male and female populations. Curve fitting is a process that allows us to quantitatively estimate the trend of the outcomes. The curve fitting process fits equations of approximating curves to the raw field data. However, for a given set of data, the fitting curves of a given type are generally not unique. Thus, a curve with a minimal deviation from all data points is desired. This best-fitting curve can be obtained by the method of least squares. In this method, the unknown parameters are approximated through minimization of the sum of the squared deviations between the data and the model predictions. It minimizes the sum of squared distances between the observed values and the model predicted values. This can be mathematically expressed as

$$RSS = \sum_{i=1}^{n} \theta_i^2 = \sum_{i=1}^{n} (y_1 - \hat{y})^2,$$

where $\theta_i = (y - \bar{y})$ and n refers to the data points and RSS refers to the sum of square error estimate which is assumed to follow a normal distribution.

The FME package (A flexible modelling environment for inverse modelling, sensitivity, identifiability and Monte Carlo Analysis) in **R** (Soetaert et al., 2010) is used to fit the model to data. An **R** code is used in which, the parameters with unknown values are given lower and upper bounds from which the set of parameter values that produce the best fit are obtained. The following parameters were fixed at the values: $\Lambda = 0.0014N$, $\mu = 0.00139$, $\delta_1 = 0.00915$, $\delta_2 = 0.00725$, $c_{m1} = c_{f1} = 3$, $c_{m2} = c_{m3} = c_{m4} = c_{f2} = c_{f3} = c_{f4} = 2, \alpha = 0.49$. The parameter ranges/values in Table 4.3 are used in the curve fitting and the resulting point values estimated are presented under the caption of Figure 4.4.

We observe in Figure 4.4, panels (a) and (b) that the model fits well to the data. It is important to note that the cases of new infection reached their peak in the year 2014. The results show that there was a rise in HIV infection between 2011 and 2014, accompanied by a noticeable decline in the occurrences of of new cases of HIV infection. The projected trends in Figure 4.5, panel (b) show that infection will decline towards 2030 when PrEP

uptake is maintained slightly above 40%. Note that the government of Kenya approved PrEP uptake in 2017 and much of its successes are yet to be reported. The effect of introduction of PrEP is seen in Figure 4.5, panel (b) where there is a sudden fall in 2017 following the government approval. Thus, there is need to emphasise preventive measures through educational campaigns and social programmes that ensure minimal or reduced infections. Although, the trend shows a general fall in HIV infections, the female population will still continue to be disproportionately affected by the epidemic compared to the the male population as reflected in Figure 4.5, panel (a). This finding agrees with the finding in the report by Kenya National AIDS Control Council (NACC) (MOH, 2016a; NACC, 2016).

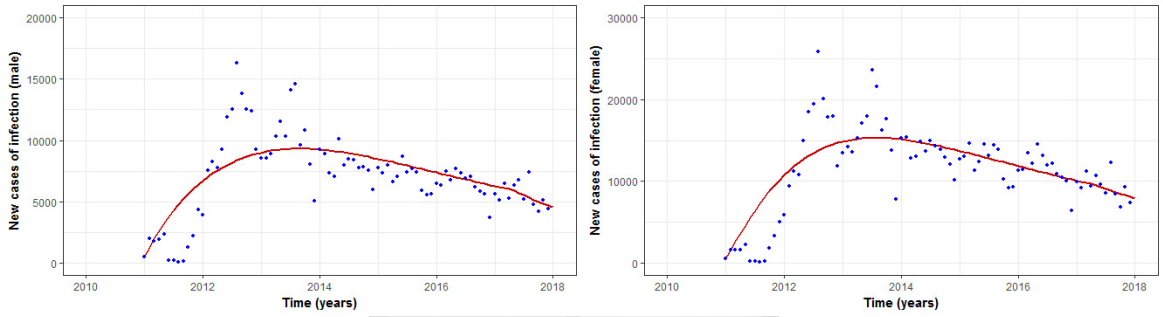

(a) (b)

Figure 4.4: Model system (4.5) fitted to data for the reported new cases of HIV infection. The panel (a) shows the model fitted to the data for the male while panel (b) shows the model fitted to data for the female. The blue dots indicate the actual data and the red line indicates the model fit to the data. The baseline parameter values obtained from the curve fitting are: $\beta_{m1} = 0.110, \beta_{m2} = 0.0031, \beta_{m3} = 0.0062, \beta_{m4} = 0.149, \beta_{f1} = 0.243, \beta_{f2} = 0.127, \beta_{f3} = 0.003, \beta_{f4} = 0.0014, \gamma_1 = 0.550, \gamma_2 = 0.126, \tau_1 = 0.999, \tau_2 = 1.000, \tau_3 = 0.613, \tau_4 = 0.483, \psi_1 = 0.005, \psi_2 = 0.002, \omega_1 = 0.540, \omega_2 = 0.002$.

In order to establish the correlation between the parameters with respect to variables I_{m1} and I_{f1}, we present pairs plot of the markov chain monte carlo (MCMC) samples for the model parameters. As seen Figure 4.6, the scatter plot matrix in the upper panel describes the pairwise relationship between parameters with corresponding correlation coefficients shown in the lower panel. The marginal distribution for each parameter is shown on the diagonal. The scatter in blue and green correspond to I_{m1} and I_{f1} respectively. It is shown in Figure 4.6 that there is a negative correlation between β_{m1} and ω_1 as well as β_{f1} and ω_2. This implies that that an increase in the drug efficacy (ART) results in a decrease in the infection terms.

This is particularly true with regards to treatment of HIV due to the fact that an increase in the drug efficacy results in an increase in viral load suppression which in turn lowers the chances of infection through heterosexual means.

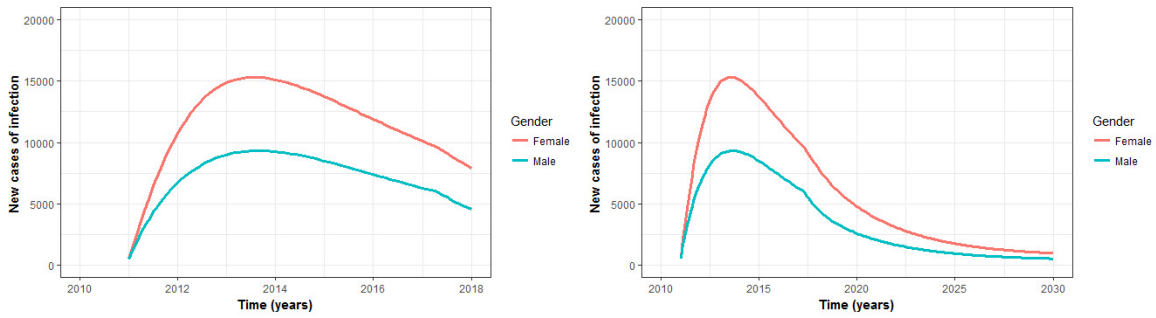

(a) (b)

Figure 4.5: Panel (a) shows the comparison of the new cases of infections between male and females as fitted to the data. Panel (b) shows the projection of infection to 2030 with a constant up-take of PrEP at 40% following its approval and its subsequent use in 2017 by the Kenyan government.

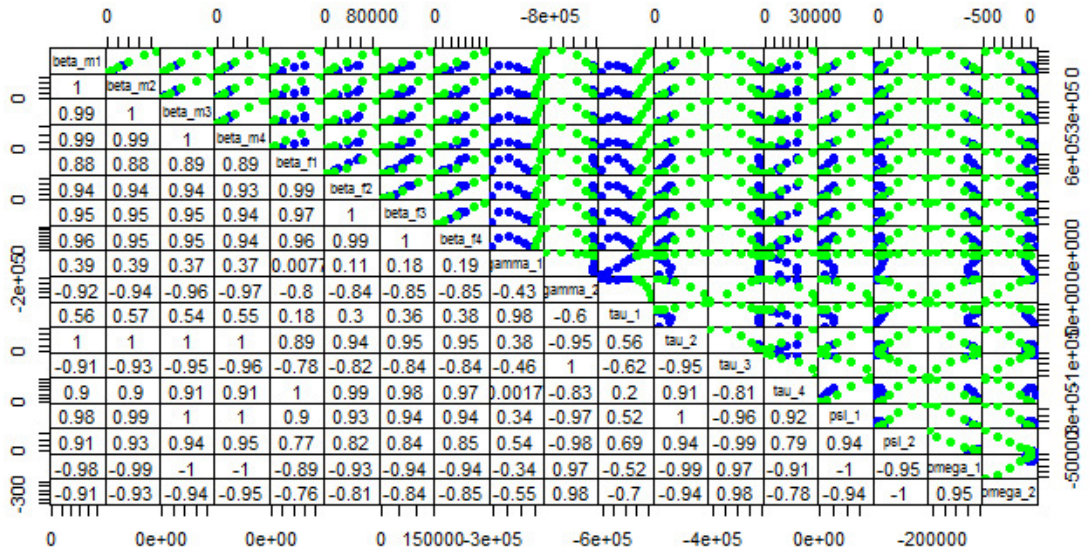

Figure 4.6: Pairs plot of the markov chain monte carlo (MCMC) samples for the model parameters.

4.7.1 Sensitivity analysis

We performed sensitivity analysis to examine the output's (basic reproduction number) response to the simultaneous variation of the parameter values within a range in the parameter space is given in Table 4.3. Following the work in Marino et al. (2008); Stein (1987); Wu et al. (2013), we use Latin Hypercube Sampling (LHS) to determine the Partial Rank Correlation Coefficients (PRCCs) with 5000 simulations per run in Matlab. PRCC takes values between -1 and $+1$ in which the sign indicates how the model output is qualitatively related to each model parameter. The parameters are assumed to be drawn distributions of random variables with uniform distribution with their range values given in Table 4.3 and point values given under the caption of Figure 4.4. We observe from Figure 4.7 that the parameters with the greatest potential to increase the HIV infection are the effective person to person contact rates. Moreover, the uptake of PrEP, ϕ is the parameter with the greatest potential to make the epidemic better when increased. This is supported by the results in Figure 4.5 sub-figure (b).

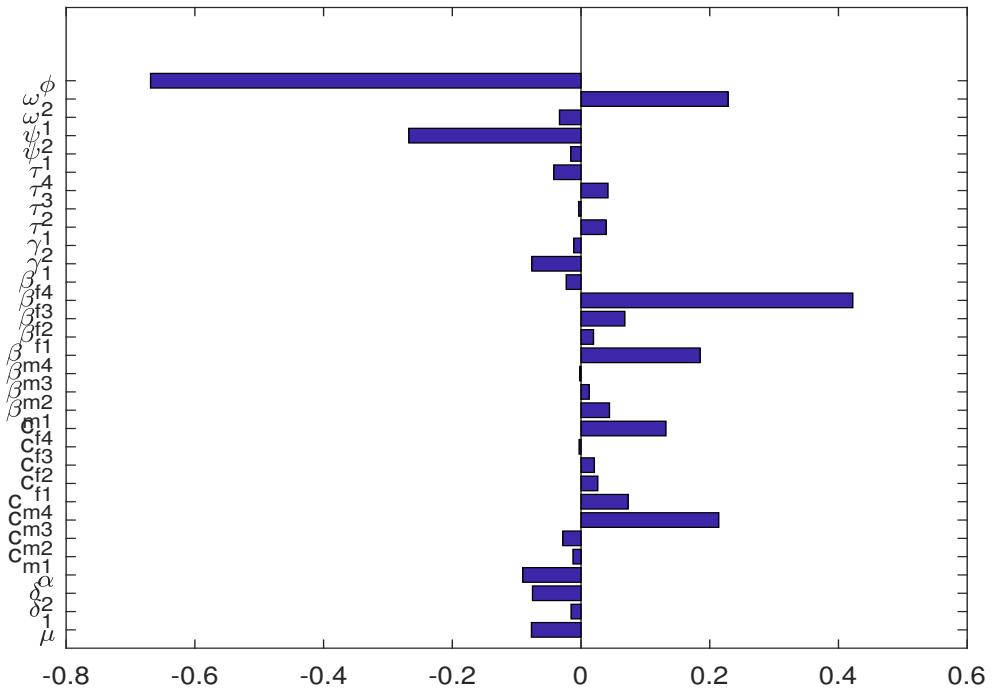

Figure 4.7: Sensitivity indices of the model parameters with I_{m1} and I_{f1} taken as baseline PRCC analysis variables.

4.8 Conclusion

In this chapter, we have analysed a sex-structured population model and studied the HIV infection trends in males and females. The model assumed that the main mode of HIV transmission is through intercourse in heterosexual means. The basic reproduction number and equilibrium points are computed and their stability analysed. From our computation, we deduce that the model exhibits two equilibria namely the disease-free equilibrium and the endemic equilibrium. The data representing new cases of HIV infection for both males and females were extracted from Kenya Health Information System (KHIS) and analysed. The descriptive statistics of the data shows that there exists a higher number of cases of infection in females as compared to males. This difference has been established to be significant through Mann-Whitney U-test. The model has been fitted to data using least squares method in **R**. The trend shows that the females are still disproportionately affected with HIV as compared to males. In order to establish the impact of the recent roll-out of PrEP, we investigated its role in limiting HIV infection. We fixed the rate of PrEP use to zero for the period before May 2017 when the PrEP use was launched in Kenya and after May 2017, the rate of PrEP use was fixed at 0.40 representing 40% coverage. From the trend projection to year 2030, we conclude that PrEP plays an important role in reducing the number of new cases of HIV. We notice that when the value of parameter (ϕ) is fixed at 0.40, the cases of infection declines towards 2030 to a near complete eradication of HIV. This implies that controlling and eventual eradication of HIV in Kenya requires aggressive campaigns by the government in favour of PrEP use. Furthermore, sensitivity analysis has been carried out using Latin Hypercube Sampling (LHS) technique. It is seen that the model output (basic reproduction number) is highly sensitive to the effective contact rates suggesting that efforts made to reduce the contacts between uninfected individuals and the infected individuals will be most appropriate in limiting the occurrence of new cases infections.

HIV patients under ART treatment are possibly capable of aiding the eradication of HIV by convincing their sexual partners of the need to adhere to protection via use of PrEP or any other protection means and ART treatment. The model presented in this chapter is a simplified description of HIV infection in Kenya and therefore it has some cogent

limitations. The model presented in this study does not take into account the full stages of HIV. Even though, the model recognizes the fact that there is need for immediate treatment once an individual is found to be positive in line with WHO regulations of 2015 based on viral load suppression, the model did not factor in the viral load levels. This limitation can be circumvented in various ways. First, there is a need to link the model to laboratory experiments for a clearer determination of parameter values based on the viral load of the patients. Second, the development of mathematical models elucidating all the HIV stages will greatly advance our understanding of HIV spread in Kenya. Despite the limitations highlighted, the model results have significant bearings on HIV dynamics and its treatment with ART. In the next chapter, we develop an age and sex structured mathematical model to project future time trends in the epidemic allowing for current and future levels of ART coverage.

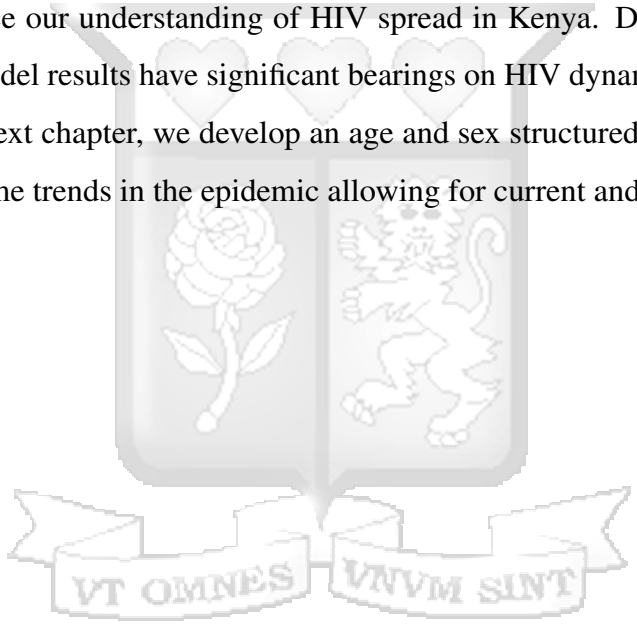

Chapter 5

A mathematical model of HIV dynamics in two heterosexual age groups

5.1 Introduction

Kenya's HIV epidemic is driven by sexual transmission and is generalized, meaning it affects all sections of the population including children (aged 0-14 years), young people (aged 15-24 years), adults (aged 25 years and over), women and men (AV, 2017). While the prevalence of HIV infection considerably reduced to 6.0% in 2010 from 10% in 1996, women still continue to be disproportionately affected by the HIV infections since men often dominate sexual relationships, with women not always able to practice safer sex even when they know the risks (AV, 2017). Young women are almost twice as likely to acquire HIV as their male counterparts. At the end of 2015, young women accounted for 33% of the total number of new infections in comparison to young men that accounted for 16% (MOH, 2016b). Control of HIV requires different interventions for different age groups. HIV education and awareness is an important component of HIV prevention. In Kenya, 73% of young women and 82% of young men in 2014 demonstrated adequate knowledge of HIV prevention (MOH, 2016b). However, incorrect perception of HIV risk, and having unprotected sexual intercourse under influence of alcohol or drugs have been cited as some of the factors that contribute to the rise in HIV infection among young people (AV, 2017).

Mathematical modelling is a common tool for studying the dynamics of infectious disease, and propose mitigation measures to control disease outbreaks (Keeling and Rohani, 2011). As such, a number of HIV models have been constructed and analysed to understand the transmission dynamics of the disease. Aldila (2018) studied HIV transmission dynamics

using a compartmental model. They considered the awareness of individuals both infected and uninfected with HIV as well as ART treatment intervention. In another study, Kim et al. (2014) studied HIV prevention measures including PrEP on HIV incidence and established that PrEP use was more beneficial in prevention of HIV infection in South Korea. Mukandavire et al. (2009) modelled a sex-structured model for heterosexual transmission of HIV/AIDS with explicit incubation period and provided an in-depth and complete qualitative analysis. However, the model neglected stratification by age. In another study,Mukandavire and Garira (2007a,b) considered heterosexual interactions of males and females using integro-differential equations with a time delay due to incubation period. While they incorporated the effects of male and female condom use as the main mode of preventing HIV infection, no real-time surveillance data to establish the trend of infection using using MCMC technique to infer the parameters. To the best of our knowledge, all the above research works focused on the mathematical analysis of the models and few papers of HIV infection exist, where gender and age is modelled using real-time surveillance data.

The work in this chapter is motivated by the desire to understand the difference in HIV infections within and between different age groups. We develop a deterministic transmission model to gain qualitative insight into the effect of age on HIV transmission dynamics and establish whether there is difference in HIV infection in Kenya within and between different age groups by extending the model in Mukandavire and Garira (2007a). A notable feature of our model is the incorporation of two different age classes involving the young adults (aged 15-24 years) and adults (aged 25 years and over) for which data are available. The model is a classic susceptible, infectious and treatment (SIT) model that involves infectious classes and those who have been enrolled into treatment programme mainly ART. While both the impact and the cost of different combinations of interventions vary, in this chapter, we are concerned with the population impact that can be achieved for a given reduction in the individual risk of transmission irrespective of how it is brought about.

5.2 Mathematical model

5.2.1 Model formulation

We consider a simple mathematical model to understand the dynamics of HIV within and between two different age categories in Kenya. A similar modelling approach was carried out by Forouzannia and Gumel (2014) where they developed a model to assess the role of age-structure on the transmission dynamics of malaria in a community. The population is divided into young adults (aged 15-24) and adult (age 25 and over) sub-populations. Each sub-population is divided into susceptible individuals (S), infected individuals (I) and those who have been enrolled into treatment programme mainly ART (T). The total variable population at time t is described by

$$N(t) = N_m(t) + N_f(t), \tag{5.1}$$

where the subscripts m and f denote male and female and the individual sex oriented population described by

$$\left.\begin{aligned} N_m(t) &= S_{dm} + S_{am} + I_{dm} + I_{am} + T_{dm} + T_{am}, \\ N_f(t) &= S_{df} + S_{af} + I_{df} + I_{af} + T_{df} + T_{af}. \end{aligned}\right\} \tag{5.2}$$

Here, d and a represent the young adults (aged between 15-24 years) and the adults (aged over 25 years), respectively. The population of the susceptible young adults is generated at the rate Π via birth or immigration of which a proportion τ are assumed to be males and $(1-\tau)$ females. The population is reduced by young adults maturation at the rate α and by natural death at the rate μ_d. The infection rate of the young adults in both males and females is respectively given by

$$\lambda_{dm} = \frac{\beta_1\gamma_1(I_{df} + \theta_1 I_{af} + \theta_2 T_{df} + \theta_3 T_{af})}{N_m} \text{ and } \lambda_{df} = \frac{\beta_2\gamma_2(I_{dm} + \theta_4 I_{am} + \theta_5 T_{dm} + \theta_6 T_{am})}{N_f}. \tag{5.3}$$

The parameters $\beta_1,\ \beta_1\theta_1,\ \beta_1\theta_2,\ \beta_1\theta_3,\ \beta_2,\ \beta_2\theta_4,\ \beta_2\theta_5$ and $\beta_2\theta_6$ are the probabilities of HIV infection through contacts with individuals in Iij and T_{ij}, where i, j refers to young adults and adults, respectively. The infected young adults for both males and females are connected to ART treatment and care at the rates ϕ_1 and δ_1, respectively. The male and female adults acquire infection at the rates, respectively given by

$$\lambda_{am} = \frac{\beta_3\gamma_3(I_{df} + \eta_1 I_{af} + \eta_2 T_{df} + \eta_3 T_{af})}{N_m} \text{ and } \lambda_{af} = \frac{\beta_4\gamma_4(I_{dm} + \eta_4 I_{am} + \eta_5 T_{dm} + \eta_6 T_{am})}{N_f}, \tag{5.4}$$

where the parameters $\beta_3,\ \beta_3\eta_1,\ \beta_3\eta_2,\ \beta_3\eta_3,\ \beta_4,\ \beta_4\eta_4,\ \beta_4\eta_5$ and $\beta_4\eta_6$ are the probabilities of HIV infection through contacts with individuals in Iij and T_{ij}, respectively. The infected male and female adults are connected to ART treatment and care at the respective rates given by ϕ_2 and δ_2. The adult classes are reduced by the natural death rate μ_a. The parameters γ_k, for $k = 1, \cdots, 4$, are the average number of sexual partnerships formed per unit time in each age category.

5.2.2 Model assumptions

(i) In our modelling framework, it is assumed that HIV transmission is mainly through sexual intercourse in heterosexual means.

(ii) We assume that all the infected individuals are connected to ART treatment.

(iii) The AIDS class is not considered in this model given that full blown AIDS patients are usually hospitalized and/or sexually inactive. It is assumed that they are not able to engage in HIV transmission activities hence do not contribute to HIV infection.

(iv) Since the current study is looking at the trend of new HIV infections within and between these two age groups, it is assumed that there is no vertical transmission or immigration of infectious individuals; thus there is no inflow into the infectious classes.

The model compartments are schematically illustrated in Figure 5.1.

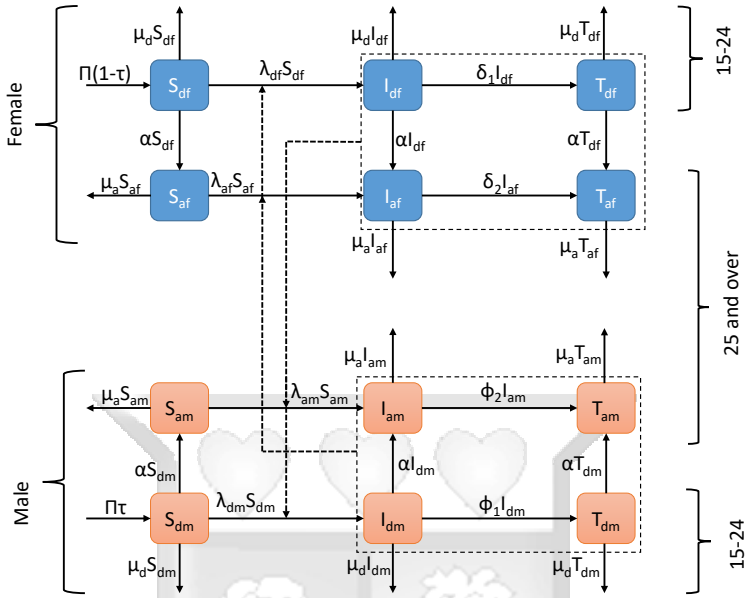

Figure 5.1: Flow chart of the compartmental model.

Table 5.1: Definition of the state variables considered in the model (5.5).

Variable	Description
$S_{dm}(t)$	The number of susceptible male young adults at time t
$I_{dm}(t)$	The number of infected male young adults not on ART at time t
$T_{dm}(t)$	The number of infected male young adults on ART at time t
$S_{df}(t)$	The number of susceptible female young adults at time t
$I_{df}(t)$	The number of infected female young adults not on ART at time t
$T_{fm}(t)$	The number of infected female young adults on ART at time t
$S_{am}(t)$	The number of susceptible male adults at time t
$I_{am}(t)$	The number of infected male adults not on ART at time t
$T_{am}(t)$	The number of infected male adults on ART at time t
$S_{af}(t)$	The number of susceptible female adults at time t
$I_{af}(t)$	The number of infected female adults not on ART at time t
$T_{af}(t)$	The number of infected female adults on ART at time t

Table 5.2: Description of the parameters used in the model (5.5).

Parameter	Description
β_1	The probability of HIV infection by S_{dm} through contacts with infected individuals
β_2	The probability of HIV infection by S_{df} through contacts with infected individuals
β_3	The probability of HIV infection by S_{am} through contacts with infected individuals
β_4	The probability of HIV infection by S_{af} through contacts with infected individuals
θ_1	The modification parameter accounting for reduced infectiousness in I_{af}
θ_2	The modification parameter accounting for reduced infectiousness in T_{df}
θ_3	The modification parameter accounting for reduced infectiousness in T_{af}
θ_4	The modification parameter accounting for reduced infectiousness in I_{am}
θ_5	The modification parameter accounting for reduced infectiousness in T_{dm}
θ_6	The modification parameter accounting for reduced infectiousness in T_{am}
η_1	The modification parameter accounting for reduced infectiousness in I_{af}
η_2	The modification parameter accounting for reduced infectiousness in T_{df}
Π	The total rate of generation of the susceptible into the system
η_3	The modification parameter accounting for reduced infectiousness in T_{af}
τ	The proportion male susceptible generated into the system
η_4	The modification parameter accounting for reduced infectiousness in I_{am}
μ_d	The natural death rate of young adults
η_5	The modification parameter accounting for reduced infectiousness in T_{dm}
μ_a	The natural death rate of the adults
η_6	The modification parameter accounting for reduced infectiousness in T_{am}
γ_1	The average number of sexual partnership formed by male young adults
γ_2	The average number of sexual partnership formed by female young adults
γ_3	The average number of sexual partnership formed by male adults
γ_4	The average number of sexual partnership formed by female adults
ϕ_1	The rate at which infected young male adults are connected to ART treatment
ϕ_2	The rate at which infected male adults are connected to ART treatment
δ_1	The rate at which infected young female adults are connected to ART treatment
δ_2	The rate at which infected female adults are connected to ART treatment
α	The maturation rate of young adults to adults

5.2.3 Model equations

Given the above descriptions and assumptions, the dynamics of HIV in the population is given by the following deterministic system of non-linear differential equations.

$$\left.\begin{aligned}
\frac{dS_{dm}}{dt} &= \Pi\tau - \lambda_{dm}S_{dm} - (\mu_d+\alpha)S_{dm}, & \frac{dS_{df}}{dt} &= \Pi(1-\tau) - \lambda_{df}S_{df} - (\mu_d+\alpha)S_{df},\\
\frac{dI_{dm}}{dt} &= \lambda_{dm}S_{dm} - (\phi_1+\alpha+\mu_d)I_{dm}, & \frac{dI_{df}}{dt} &= \lambda_{df}S_{df} - (\alpha+\delta_1+\mu_d)I_{df},\\
\frac{dT_{dm}}{dt} &= \phi_1 I_{dm} - (\alpha+\mu_d)T_{dm}, & \frac{dT_{df}}{dt} &= \delta_1 I_{df} - (\alpha+\mu_d)T_{df},\\
\frac{dS_{am}}{dt} &= \alpha S_{dm} - \lambda_{am}S_{am} - \mu_a S_{am}, & \frac{dS_{af}}{dt} &= \alpha S_{df} - \lambda_{af}S_{af} - \mu_a S_{af},\\
\frac{dI_{am}}{dt} &= \lambda_{am}S_{am} + \alpha I_{dm} - (\phi_2+\mu_a)I_{am}, & \frac{dI_{af}}{dt} &= \lambda_{af}S_{af} + \alpha I_{df} - (\delta_2+\mu_a)I_{af},\\
\frac{dT_{am}}{dt} &= \phi_2 I_{am} + \alpha T_{dm} - \mu_a T_{am}, & \frac{dT_{af}}{dt} &= \delta_2 I_{af} + \alpha T_{df} - \mu_a T_{af},
\end{aligned}\right\} \tag{5.5}$$

subject to the following initial conditions

$$S_{ijm}(0)\geq 0,\ I_{ijm}(0)\geq 0,\ T_{ijm}(0)\geq 0,\ S_{ijf}(0)\geq 0,\ I_{ijf}(0)\geq 0,\ T_{ijf}(0)\geq 0,\ \text{for } i,\ j=d,a. \tag{5.6}$$

5.3 Model analysis

5.3.1 Well-posedness of the model

In this section, we show that the system (5.5) is mathematically well defined and biologically feasible. For convenience in mathematical analysis, we let $Q_1=\mu_d+\alpha$, $Q_2=\phi_1+\alpha+\mu_d$, $Q_3=\phi_2+\mu_a$, $Q_4=\alpha+\delta_1+\mu_d$, $Q_5=\delta_2+\mu_a$. The system (5.5) can be rewritten in the following form

$$\frac{dX}{dt} = A(X)X + F,$$

where $X = (S_{dm},\ I_{dm},\ T_{dm},\ S_{am},\ I_{am},\ T_{am},\ S_{df},\ I_{df},\ T_{df},\ S_{af},\ I_{af},\ T_{af})^t$. Thus, the matrix A is given by

$$A(X) = \begin{bmatrix}
-Q_6 & 0 & 0 & 0 & 0 & 0 & 0 & 0 & 0 & 0 & 0 & 0 \\
\lambda_{dm} & -Q_2 & 0 & 0 & 0 & 0 & 0 & 0 & 0 & 0 & 0 & 0 \\
0 & \phi_1 & -Q_1 & 0 & 0 & 0 & 0 & 0 & 0 & 0 & 0 & 0 \\
\alpha & 0 & 0 & -Q_7 & 0 & 0 & 0 & 0 & 0 & 0 & 0 & 0 \\
0 & \alpha & 0 & \lambda_{am} & -Q_3 & 0 & 0 & 0 & 0 & 0 & 0 & 0 \\
0 & 0 & \alpha & 0 & \phi_2 & -\mu_a & 0 & 0 & 0 & 0 & 0 & 0 \\
0 & 0 & 0 & 0 & 0 & 0 & -Q_8 & 0 & 0 & 0 & 0 & 0 \\
0 & 0 & 0 & 0 & 0 & 0 & \lambda_{df} & -Q_4 & 0 & 0 & 0 & 0 \\
0 & 0 & 0 & 0 & 0 & 0 & 0 & \delta_1 & -Q_1 & 0 & 0 & 0 \\
0 & 0 & 0 & 0 & 0 & 0 & \alpha & 0 & 0 & -Q_9 & 0 & 0 \\
0 & 0 & 0 & 0 & 0 & 0 & 0 & \alpha & 0 & \lambda_{af} & -Q_5 & 0 \\
0 & 0 & 0 & 0 & 0 & 0 & 0 & 0 & 0 & \alpha & \delta_2 & -\mu_a
\end{bmatrix}$$

and $F = (\Pi\tau,\ 0,\ 0,\ 0,\ 0,\ 0,\ \Pi(1-\tau),\ 0,\ 0,\ 0,\ 0,\ 0)^T$. Here, $Q_6 = (\lambda_{dm} + Q_1)$, $Q_7 = (\lambda_{am} + \mu_a)$, $Q_8 = (\lambda_{df} + Q_1)$, $Q_9 = (\lambda_{af} + \mu_a)$. It is important to note that $A(X)$ is a Metzler matrix, that is, a matrix such that off diagonal entries are non-negative, for all $Y \in \mathbb{R}^{12}_+$. Thus, using the fact that $F \geq 0$, the system (5.5) is positively invariant in $\mathbb{R}^{12}_+$ (see, Abate et al. (2009); Berman and Plemmons (1994)). This implies that any trajectory of the system (5.5) starting from an initial state in $\mathbb{R}^{12}_+$ forever remains in $\mathbb{R}^{12}_+$. Using the initial condition $N(0) > 0$, the evolution of the system (5.5) is described by $\frac{dN}{dt} \leq \Pi - \mu N$. Solving for $N(t)$ using integrating factor method we get

$$N(t) \leq \frac{\Pi}{\mu} + e^{-\mu t}\left(N(0) - \frac{\Pi}{\mu}\right). \tag{5.7}$$

There are two possible cases in studying the behaviour of $N(t)$ in (6.5). In the first case, we consider $N(0) > \frac{\Pi}{\mu}$ so that, at time t = 0, the right-hand side (RHS) of (6.5) experiences the largest possible value of $N(0)$. That is, $N(t) \leq N(0)$ for all time $t \geq 0$. In the second case, we consider $N(0) < \frac{\Pi}{\mu}$, so that the largest possible value of the RHS of (6.5) approaches $\frac{\Pi}{\mu}$

as time t approaches infinity. Thus, $N(t) \leq \frac{\Pi}{\mu}$ for all time $t \geq 0$. From these two cases, we conclude that $N(t) \leq \max\left\{N(0), \frac{\Pi}{\mu}\right\}$ for all time $t \geq 0$. Therefore, we can study the system (5.5) in the feasible region given by

$$\Omega = \left\{(S_{ijm}(t), I_{ijm}(t), T_{ijm}(t), S_{ijf}(t), I_{ijf}(t), T_{ijf}(t)) \in \mathbb{R}_+^{12} : N(t) \leq \max\left\{N(0), \frac{\Pi}{\mu}\right\}\right\},$$

which is positively invariant with respect to systems (5.5). This implies that the systems (5.5) is well posed epidemiologically and all the solutions starting in Ω remain in Ω for all $t \geq 0$.

5.3.2 Basic reproduction number

According to Diekmann and Heesterbeek (2000); Diekmann et al. (1990), the basic reproduction number commonly denoted as $\mathscr{R}_0$ is defined as the number of secondary cases of infections arising from the introduction of a single infected individual in a wholly susceptible population. The system (5.5) has a unique disease-free equilibrium given by

$$\mathscr{E}_0 = \left(\frac{\Pi\tau}{Q_1}, 0, 0, \frac{\alpha\Pi\tau}{Q_1\mu_a}, 0, 0, \frac{\Pi(1-\tau)}{Q_1}, 0, 0, \frac{\alpha\Pi(1-\tau)}{Q_1\mu_a}, 0, 0\right). \tag{5.8}$$

Since the model system (5.5) allows for free mixing of the individuals from the two stated age groups, there are two ways of the disease transmission. These are within age group transmission and between age groups transmission. We begin by finding the reproduction numbers within the age groups. For the young adults, the disease-free equilibrium is given by

$$\mathscr{E}_d = \left(\frac{\Pi\tau}{\mu_d}, 0, 0, \frac{\Pi(1-\tau)}{\mu_d}, 0, 0\right). \tag{5.9}$$

Following the approach given in Van den Driessche and Watmough (2002), we let F and V be the matrices of new infections and transmission, respectively. Thus, at the disease-free

equilibrium defined in (5.9), these matrices are respectively given by

$$F = \begin{bmatrix} 0 & 0 & \beta_1\gamma_1 & \beta_1\gamma_1\theta_2 \\ 0 & 0 & 0 & 0 \\ \beta_2\gamma_2 & \beta_2\gamma_2\theta_5 & 0 & 0 \\ 0 & 0 & 0 & 0 \end{bmatrix}, \quad V = \begin{bmatrix} \mu_d+\phi_1 & 0 & 0 & 0 \\ -\phi_1 & \mu_d & 0 & 0 \\ 0 & 0 & \delta_1+\mu_d & 0 \\ 0 & 0 & -\delta_1 & \mu_d \end{bmatrix}.$$

The young adults transmission reproduction number which is the spectral radius of the next-generation matrix (NGM) for the epidemic of HIV given by FV^{-1} is obtained as

$$\mathscr{R}_{0d} = \sqrt{\left[\frac{\beta_1\gamma_1(\delta_1\theta_2+\mu_d)}{\mu_d(\mu_d+\phi_1)}\right]\left[\frac{\beta_2\gamma_2(\mu_d+\theta_5\phi_1)}{\mu_d(\mu_d+\delta_1)}\right]}. \tag{5.10}$$

Similarly, the disease-free equilibrium within the adult age group is defined as

$$\mathscr{E}_a = \left(\frac{\Pi\tau}{\mu_d},\ 0,\ 0,\ \frac{\Pi(1-\tau)}{\mu_d},\ 0,\ 0\right). \tag{5.11}$$

The matrices of new infections and transmission within adult (age group 25+) evaluated at disease-free in (5.11) are, respectively given as

$$F = \begin{bmatrix} 0 & 0 & \beta_3\gamma_3\eta_1 & \beta_3\gamma_3\eta_3 \\ 0 & 0 & 0 & 0 \\ \beta_4\gamma_4\eta_4 & \beta_4\gamma_4\eta_6 & 0 & 0 \\ 0 & 0 & 0 & 0 \end{bmatrix}, \quad V = \begin{bmatrix} \mu_a+\phi_2 & 0 & 0 & 0 \\ -\phi_2 & \mu_a & 0 & 0 \\ 0 & 0 & \delta_2+\mu_a & 0 \\ 0 & 0 & -\delta_2 & \mu_a \end{bmatrix}.$$

Therefore, the transmission reproduction number is given by

$$\mathscr{R}_{0a} = \sqrt{\left[\frac{\beta_3\gamma_3(\eta_1\mu_a+\delta_2\eta_3)}{\mu_a(\mu_a+\phi_2)}\right]\left[\frac{\beta_4\gamma_4(\eta_4\mu_a+\eta_6\phi_2)}{\mu_a(\mu_a+\delta_2)}\right]}. \tag{5.12}$$

If the HIV infection exists in a single age group connected to another age group through maturation, then the movement of the individuals must be reflected in the basic reproduction

number. The matrices for new infection terms and the transfer terms at the disease-free equilibrium (5.8) are given by

$$F = \begin{bmatrix} 0 & 0 & \frac{\beta_1\gamma_1\theta_1\mu_a}{\alpha+\mu_a} & \frac{\beta_1\gamma_1\theta_3\mu_a}{\alpha+\mu_a} \\ 0 & 0 & 0 & 0 \\ \frac{\alpha\beta_4\gamma_4}{\alpha+\mu_a} & \frac{\alpha\beta_4\gamma_4\eta_5}{\alpha+\mu_a} & 0 & 0 \\ 0 & 0 & 0 & 0 \end{bmatrix}, \quad V = \begin{bmatrix} Q_2 & 0 & 0 & 0 \\ -\phi_1 & Q_1 & 0 & 0 \\ 0 & 0 & Q_5 & 0 \\ 0 & 0 & -\delta_2 & \mu_a \end{bmatrix}$$

Thus, the basic reproduction number between the male young adults and the female adults (aged 25+ years) is given by

$$\mathscr{R}_{0mdfa} = \sqrt{\left[\frac{\alpha\beta_4\gamma_4\left(\eta_5\phi_1+Q_1\right)}{Q_1Q_2\left(\mu_a+\alpha\right)}\right]\left[\frac{\beta_1\gamma_1\left(\theta_1\mu_a+\delta_2\theta_3\right)}{Q_5\left(\mu_a+\alpha\right)}\right]}. \tag{5.13}$$

On the other hand, the matrices for new infection terms and the transfer terms at the disease-free equilibrium in (5.8) for the female young adults and male adults are given by

$$F = \begin{bmatrix} 0 & 0 & \frac{\alpha\beta_3\gamma_3}{\alpha+\mu_a} & \frac{\alpha\beta_3\gamma_3\eta_2}{\alpha+\mu_a} \\ 0 & 0 & 0 & 0 \\ \frac{\beta_2\gamma_2\theta_4\mu_a}{\alpha+\mu_a} & \frac{\beta_2\gamma_2\theta_6\mu_a}{\alpha+\mu_a} & 0 & 0 \\ 0 & 0 & 0 & 0 \end{bmatrix}, \quad V = \begin{bmatrix} Q_3 & 0 & 0 & 0 \\ -\phi_2 & \mu_a & 0 & 0 \\ 0 & 0 & Q_4 & 0 \\ 0 & 0 & -\delta_1 & Q_1 \end{bmatrix}.$$

Hence, the basic reproduction number between the female young adults and the male adults is given by

$$\mathscr{R}_{0fdma} = \sqrt{\left[\frac{\beta_2\gamma_2\left(\theta_4\mu_a+\theta_6\phi_2\right)}{Q_3\left(\mu_a+\alpha\right)}\right]\left[\frac{\alpha\beta_3\gamma_3\left(\delta_1\eta_2+Q_1\right)}{Q_1Q_4\left(\mu_a+\alpha\right)}\right]}. \tag{5.14}$$

The matrices of representing new infections and transfer at the disease-free equilibrium in (5.8) are respectively by

$$F = \begin{bmatrix} 0 & 0 & 0 & 0 & \beta_1\gamma_1 & \beta_1\gamma_1\theta_1 & \beta_1\gamma_1\theta_2 & \beta_1\gamma_1\theta_3 \\ 0 & 0 & 0 & 0 & 0 & 0 & 0 & 0 \\ 0 & 0 & 0 & 0 & \beta_3\gamma_3 & \beta_3\gamma_3\eta_1 & \beta_3\gamma_3\eta_2 & \beta_3\gamma_3\eta_3 \\ 0 & 0 & 0 & 0 & 0 & 0 & 0 & 0 \\ \beta_2\gamma_2 & \beta_2\gamma_2\theta_4 & \beta_2\gamma_2\theta_5 & \beta_2\gamma_2\theta_6 & 0 & 0 & 0 & 0 \\ 0 & 0 & 0 & 0 & 0 & 0 & 0 & 0 \\ \beta_4\gamma_4 & \beta_4\gamma_4\eta_4 & \beta_4\gamma_4\eta_5 & \beta_4\gamma_4\eta_6 & 0 & 0 & 0 & 0 \\ 0 & 0 & 0 & 0 & 0 & 0 & 0 & 0 \end{bmatrix},$$

$$V = \begin{bmatrix} Q_2 & 0 & 0 & 0 & 0 & 0 & 0 & 0 \\ -\alpha & Q_3 & 0 & 0 & 0 & 0 & 0 & 0 \\ -\phi_1 & 0 & Q_1 & 0 & 0 & 0 & 0 & 0 \\ 0 & -\phi_2 & -\alpha & \mu_a & 0 & 0 & 0 & 0 \\ 0 & 0 & 0 & 0 & Q_4 & 0 & 0 & 0 \\ 0 & 0 & 0 & 0-\alpha & Q_5 & 0 & 0 & \\ 0 & 0 & 0 & 0 & -\delta_1 & 0 & Q_1 & 0 \\ 0 & 0 & 0 & 0 & 0 & -\delta_2 & -\alpha & \mu_a \end{bmatrix}$$

The basic reproduction number, $\mathscr{R}_0$, of the whole system (5.5) is given as the maximum of between age groups specific reproduction numbers. Thus, we have

$$\mathscr{R}_0 = \max\left\{\mathscr{R}_{0mdfa}, \mathscr{R}_{0fdma}\right\}.$$

From Theorem 2 in Van den Driessche and Watmough (2002), we establish following result.

Theorem 5.1. *The disease-free equilibrium of system* (5.5) *is locally asymptotically stable whenever* $\mathscr{R}_0 < 1$ *and unstable otherwise.*

Theorem 5.1 implies that HIV infection will be contained in the population when $\mathscr{R}_0 < 1$ if the initial sizes of the of the sub-populations of the system (5.5) are in the basin of attraction of the disease-free equilibrium. To understand the trend of HIV infection, we perform data analysis and present results in section 5.4.

5.4 Numerical analysis results

5.4.1 Epidemiological data and Ethical considerations

To study the extent and trend of HIV infection, we analyse the confirmed cases of new infections in Kenya from January 2011 to September 2018. The data analysed was routinely collected on a monthly basis and retrieved from Kenya Health information System available at KHIS. Only variables of interest were pulled out to excel spreadsheet and thereafter analysed in **R**. The data analysed is publicly available. Thus, the datasets used in our study were de-identified and fully anonymised in advance, and the analysis of publicly available data without identity information does not require ethical approval.

5.4.2 Parameter inference and estimation

The natural death rate was estimated to be $\mu_d = 0.0013$ per month,$\mu_a = 0.00128$ per month based on the life expectancy in Kenya (WHR, 2018). The young adults maturation at the rate $\alpha = 0.0083$. The rate at young adults acquire sexual partners is assumed to be 3, that is, $\gamma_1 = \gamma_2 = 3$, while that of the adults has been assumed to be 2 ($\gamma_3 = \gamma_4 = 2$). Initiating and staying on treatment is particularly problematic for young adults. In 2014, it was estimated that only 34,800 out of 141,000 young adults with known HIV positive status were on ART (AV, 2017). Thus, the rates at which adolescents (males and females) are connected to ART treatment are assumed to be $\phi_1 = 0.24$ per month and $\delta_1 = 0.28$ per month, respectively. On the other hand, based on the estimates from AV (2017), the rates at which the male and female adults are connected to ART treatment is assumed to be $\phi_2 = 0.58$ per month and $\delta_2 = 0.68$ per month, respectively. Table 5.3 gives the description of the parameters and the initial conditions estimates used in this work. The initial conditions for S_{dm}, S_{df}, S_{am} and S_{af} are estimated from Kenya demographics profile of both 2010 and 2018 (see KD (2018)) while other initial conditions for I_{dm}, T_{dm}, I_{df}, T_{fm}, I_{am}, T_{am}, I_{af} and T_{af} are estimated based on the retrieved data that is used in curve fitting.

Table 5.3: Description of the parameters and the initial conditions estimates for the system (5.5). The parameters are given per month.

Par/var	Range	Value	Source	Par	Range	Value	Source
$S_{dm}(0)$	4,148,153–4,552,448	Est.	KD (2018)	β_1	0.0–1.0	Est.	
$I_{dm}(0)$	0–8,000	Est.		β_2	0.0–1.0	Est.	
$T_{dm}(0)$	0–6,000	Est.		β_3	0.0–1.0	Est.	
$S_{df}(0)$	4,147,896–4,567,894	Est.	KD (2018)	β_4	0.0–1.0	Est.	
$I_{df}(0)$	0–11,000	Est.		θ_1	0.0–1.0	Est.	
$T_{fm}(0)$	0–8,000	Est.		θ_2	0.0–1.0	Est.	
$S_{am}(0)$	8,460,138–9,641,107	Est.	KD (2018)	θ_3	0.0–1.0	Est.	
$I_{am}(0)$	0–11,000	Est.		θ_4	0.0 – 1.0	Est.	
$T_{am}(0)$	0–9,000	Est.		θ_5	0.0–1.0	Est.	
$S_{af}(0)$	8,624,799–9,799,146	Est.	KD (2018)	θ_6	0.0–1.0	Est.	
$I_{af}(0)$	0–17,000	Est.		η_1	0.0–1.0	Est.	
$T_{af}(0)$	0–14,000	Est.		η_2	0.0–1.0	Est.	
Π	40,000–85,000	44,000	KD (2018)	η_3	0.0–1.0	Est.	
τ	0.0–1.0	0.48	WHR (2018)	η_4	0.0–1.0	Est.	
μ_d	0.0011–0.0017	0.0013	WHR (2018)	η_5	0.0–1.0	Est.	
μ_a	0.0011–0.0017	0.00128	WHR (2018)	η_6	0.0–1.0	Est.	
γ_1	1–4	3	Assumed	γ_2	1–4	3	Assumed
γ_3	1–4	2	Assumed	γ_4	1–4	2	Assumed
ϕ_1	0.0–1.0	0.24	AV (2017)	ϕ_2	0.0 – 1.0	0.58	AV (2017)
δ_1	0.0–1.0	0.28	AV (2017)	δ_2	0.0–1.0	0.68	AV (2017)
α		0.0083					

The unknown parameters, that is, β_1, β_2, β_3, β_4, θ_1, θ_2, θ_3, θ_4, θ_5, θ_6, η_1, η_2, η_3, η_4, η_5 and η_6, were estimated on the basis of the available data. Bayesian approach that is implemented to the Markov Chain Monte Carlo (MCMC) technique is used in parameter estimation. We minimize the sum of the squared error between the model and data, which is given by

$$SS(\hat{\vartheta}) = \sum_{i=1}^{n} \left(Y_h - P(t_h,\ \hat{\vartheta})\right)^2, \tag{5.15}$$

where

$$P(t_h, \hat{\vartheta}) = \int_{t_h-1}^{t_h} p\left(\lambda_{dm}S_{dm} + \lambda_{df}S_{df} + \lambda_{am}S_{am} + \lambda_{af}S_{af}\right) dt,$$

which is the number of new HIV cases of infection for each age group. Note that, there are D independent observations from the dataset that represent the number of new HIV cases of infection at the hth month, for $h = 1, 2, 3, \cdots, D$. Now considering ε is the error of fit, which

follows an independent Gaussian distribution having unknown variance σ^2, then it follows from (5.15) that

$$Y_h = P(t_h, \hat{\vartheta}) + \varepsilon, \quad \varepsilon \sim \mathcal{N}(0,\ I^*_{ij}\sigma^2),$$

with $*$ referring to males and females, i and j remain as earlier defined. We assume an independent Gaussian prior specification for the unknown parameters $\hat{\vartheta}$, that is, $\vartheta_r \sim \mathcal{N}(\nu_r,\ \psi_r^2)$, where $r = 1, 2, 3, \cdots, D$. Furthermore, it is assumed that the inverse of the error variance follows a Gaussian distribution as prior taking the following form

$$\upsilon\left(\sigma^{-2}\right) \sim \Gamma\left(\frac{x_0}{2},\ \frac{x_0 S_0^2}{2}\right).$$

Here, x_0 and S_0^2 respectively, give the prior accuracy and prior mean of σ^2. Considering the conditional conjugacy property of Gamma distribution (*see*, Sardar et al. (2016)), the conditional distribution of $\upsilon(\sigma^{-2}|Y, \hat{\vartheta})$ is also a Gamma distribution with

$$\upsilon\left(\sigma^{-2}|Y,\ \hat{\vartheta}\right) = \Gamma\left(\frac{x_0 + R}{2},\ \frac{x_0 S_0^2 + SS(\hat{\vartheta})}{2}\right).$$

The above property makes it possible to sample and update σ^{-2} within each Metropolis Hastings simulation step for the other parameters. Since an independent Gaussian prior specification for $\hat{\vartheta}$ is assumed, the prior sum of squares for $\hat{\vartheta}$ is given by

$$SS_{\text{pri}}(\hat{\vartheta}) = \sum_{h=1}^{D} \left(\frac{\vartheta_h - \nu_h}{\psi_h}\right)^2.$$

For a fixed value of σ^2, the posterior distribution of $\hat{\vartheta}$ is given by

$$\upsilon\left(\hat{\vartheta}|Y, \sigma^2\right) \propto \exp\left[-\frac{1}{2}\left(\frac{SS(\hat{\vartheta})}{\sigma^2} + SS_{\text{pri}}(\hat{\vartheta})\right)\right],$$

with the posterior ratio needed in the Metropolis-Hastings acceptable probability given as

$$\frac{\upsilon\left(\hat{\vartheta}^1|Y, \sigma^2\right)}{\upsilon\left(\hat{\vartheta}^2|Y, \sigma^2\right)} = \exp\left[-\frac{1}{2}\left(\left(\frac{SS(\hat{\vartheta}^1)}{\sigma^2} - \frac{SS(\hat{\vartheta}^2)}{\sigma^2}\right) + \frac{1}{2}\left(SS_{\text{pri}}(\hat{\vartheta}^2) + SS_{\text{pri}}(\hat{\vartheta}^1)\right)\right)\right].$$

The modCost, modFit and modMCMC routine in package FME package (A flexible modelling environment for inverse modelling, sensitivity, identifiability and Monte Carlo Analysis) in **R** is used to estimate the unknown ϑ for the model. A **R** code is used in which, the unknown parameter values are given a lower bound and an upper bound from which the set of parameter values that produce the best fit are obtained. The parameter estimates and other results arising from the model fitting to data are given in sub-section 5.4.6.

5.4.3 The basic description of data

In this section, we carry out simple descriptive statistical analysis of the dataset and results presented in Table 5.4. The mean number of new HIV infections in the male young adults age group is 1337 (95% Confidence Intervals (CI), 1114, 1560) while the average number of new infections in the females of the same age group is 3164.7 (95% Confidence Intervals (CI), 2775, 3554), for the period from January 2011 to September 2018. The average number of new infections in male and female adults are given by 5319 (95% Confidence Intervals (CI), 4818, 5821) and 7693 (95% Confidence Intervals (CI), 6952, 8433), respectively. Overall, the mean number of HIV infections in males is 3328.1 while that in females is 5429. It can be seen that females in both age categories are disproportionately affected with HIV more than the males. In order to establish the extent of variation in the mean number of cases of infections in the two age categories along the gender line, an error bar is plotted and presented in Figure 5.2. It can be seen that the non-overlapping error bars may be significantly different. This implies that further test is required to indicate the nature of differences in the means. Thus, in sub-section 5.4.4, we carry out probability distribution test in order to choose an appropriate test to establish the mean differences.

5.4.4 The probability distribution of the data

The probability distribution of the given dataset plays an important role in determining which tests between parametric and non-parametric to conduct. There are various methods used to test for the probability distribution of a given dataset. The methods can be to test for normality

Table 5.4: Descriptive characteristics of the dataset retrieved for the duration spanning from January 2011 to September 2018.

Age group	Male				Female			
	Mean	SD	SE	95% CI[1]	Mean	SD	SE	95% CI[1]
15-24 years	1337	1082	112.2	[1114, 1560]	3165	1891	196.1	[2775, 3554]
25+ years	5319	2434	252.4	[4818, 5821]	7693	3597	373	[6952, 8433]
d[2] and a[3]	3328	2742	201.0	[2932, 3725]	5429	3656	268.1	[4900, 5958]

[1] 95% Confidence Interval
[2] The young adults aged 15-24 years
[3] The adults aged 25 and over years

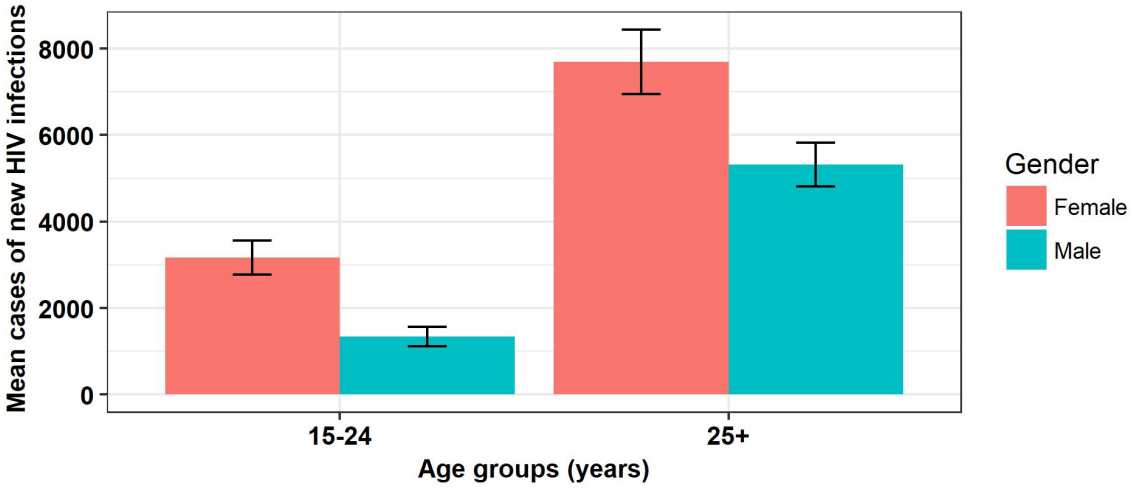

Figure 5.2: The distribution of the average number of new HIV infections in two age groups for males and females. Error bars are 95% confidence intervals.

or any other distribution. For normality tests, methods used include kolmogorov-smirnov, Anderson Darling, Shapiro Wilk and Lilliefors test (Shapiro and Wilk, 1965). In this study, we use the Shapiro Wilk test. This is the most powerful test when compared to the Anderson Darling, Kolmogorov-Smirnov and Lilliefors tests (Razali and Wah, 2011). The test statistics proposed in Shapiro and Wilk (1965) is given by

$$W = \frac{(a'y)^2}{S^2} = \frac{\left(\sum_{q=1}^{n} a_q y_q\right)^2}{\sum_{q=1}^{n}(y_q - \bar{y})^2},$$

where a' are set of weights given by

$$a' = (a_1, \cdots, a_n) = \frac{m'V^{-1}}{\sqrt{(m'V^{-1}V^{-1}m)}}.$$

Here, y_q, for $q = 1, 2, \cdots, n$, is the qth order statistics whose similarity scores are sorted in either descending or ascending order, $\bar{y}$ is the sample mean similarity score, $m = (m_1, \cdots, m_n)'$ are the first moments of the order statistics which are independent and identically normally distributed random variables, S^2 is the estimator for the population variance σ^2 and V is the covariance matrix of the order statistics. The dataset is assumed not to follow a normal distribution when the test statistics W is small, that is, $0 < \frac{na_1^2}{n-1} \leq W \leq 1$ or when p-value $< \alpha$, the significance level. Otherwise the dataset follows a normal distribution.

Table 5.5: Shapiro Wilk test for normality of the dataset.

Age group	Male		Female	
	W	P-value	W	P-value
15-24 years	0.8585	0.0000	0.9549	0.0028
25+ years	0.9692	0.0268	0.9600	0.0061

Table 5.5 shows results from Shapiro Wilk test for normality of the dataset. The test was carried out at alpha level equal to 0.05, that is, at 95% Confidence Interval. Given that the p-value for each age category for males and females is less than 0.05, then the null hypothesis that the data are normally distributed is rejected. Thus, there is no enough evidence to assume that the data follows a normal distribution. Figure 5.3 shows density plot to visualise the distribution of data. This chart uses kernel smoothing to plot values, allowing for smoother distributions by smoothing out the noise. The peaks of a density plot help display where values are concentrated over the interval. It can be easily seen that the data are positively skewed. Since the results show that the data does not follow a normal distribution, we conduct Friedman test, a non-parametric test, to establish if there exists any significant differences in mean number number of HIV infections between the two age groups for the males and females.

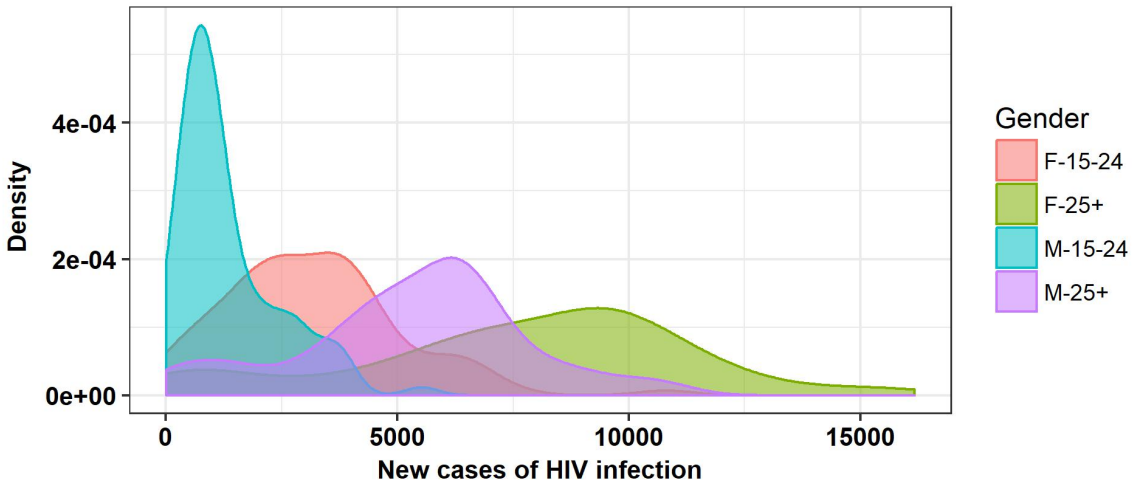

Figure 5.3: Density distribution of the dataset.

5.4.5 Kruskal–Wallis test

Kruskal–Wallis's test is a non-parametric method for testing the equality of several independent samples. It is useful in analysing experimental data from completely randomized designs (Kruskal and Wallis, 1952). To compute the Kruskal–Wallis test statistic, all the observations are first ranked in ascending order where the smallest observation takes rank 1 and the largest observation takes rank N. The sum and average of the ranks of the observations pertaining to each sample are obtained next. If the sample effects are equal, then the average ranks are expected to be the same and if there is any difference then that is due to sampling fluctuations. The Kruskal–Wallis test statistic is based on the assessment of the differences among the average ranks. That is, let R_{ij} be the rank of $y_{ij}, i = 1,2,3,\cdots,b; \quad j = 1,2,\cdots,t$ (where b refers to the samples (treatments) and the ith treatment is replicated t_1 times, $i = 1,2,\cdots,b$, $R_i = \sum_{j=1}^{t} R_{ij}$ be the sum of the ranks of the observations pertaining to the ith treatment, $\bar{R}_i = \frac{R_i}{t_i}$ be the average of the ranks of the observations pertaining to the ith treatment, and $\bar{R}$ be the mean of all the $\bar{R}_i$. The Kruskal–Wallis test statistic is then given by

$$H = \frac{12}{N(N+1)} \sum_{i=1}^{b} t_i (\bar{R}_i - \bar{R})^2 \sim \chi^2_{b-1}. \tag{5.16}$$

Since $\sum_{i=1}^{b} R_i = \frac{N(N+1)}{2}$, it follows that $\bar{R} = \frac{N+1}{2}$. Thus, expression (5.16) reduces to

$$H = \frac{12}{N(N+1)} \sum_{i=1}^{b} \frac{R_i^2}{t_i} - 3(N+1) \sim \chi^2_{b-1}. \tag{5.17}$$

Note that the coefficient $\frac{12}{N(N+1)}$ is known as a suitable normalization factor (see, Manoukian (1986)). The expressions in (5.16) and (5.17) are computed if there are no ties in the observations. In the event there are ties, each observation is given the mean of the ranks for which it is tied. The Kruskal–Wallis statistics in (5.17) is then divided by the correction factor given by

$$cf = 1 - \frac{\sum_{i=1}^{k}(m_i^3 - m_i)}{N^3 - N},$$

where m_i refers to the number of ties in ith group of k tied groups. Hence, the corrected Kruskal–Wallis test statistic for ties is expressed as

$$H^m = \frac{12}{N(N+1)} \sum_{i=1}^{b} \frac{R_i^2}{t_i} - \frac{3N(N+1)^2(N-1)}{N(N^2-1) - \sum_{i=1}^{k}(m_i^3 - m_i)} \sim \chi^2_{b-1}.$$

It is important to note that the correction factor is included when there are ties to increase the value of the test statistics so as to make the results more significant. Furthermore, the Kruskal–Wallis test statistic has a chi-square distribution with $(b-1)$ degrees of freedom under the null hypothesis. The test results obtained in **R** are given as:

$$\text{Kruskal-Wallis chi-squared} = 180.11, \text{ df} = 3, \text{ p-value} < 2.2e-16.$$

The results give $\chi^2_{3,\alpha=0.05} = 180.11$ and p-value< 0.05, the level of significance. There is very strong evidence to suggest a significant difference in HIV infection between at least one pair of the groups. Since there is a significant difference in HIV infections as the results suggest, a post-hoc analysis is performed to determine which group of the individuals differ from each other in HIV infections. We use Nemenyi test which is appropriate for groups with equal number of observations as in our case (Zar, 2010). The results are presented in Table 5.6. Since all the p-values are less that 0.05, the level of significance, there are significant differences in HIV infections between the groups.

Table 5.6: Pairwise comparisons using Tukey and Kramer (Nemenyi) test. F-15-24 and M-15-24 means the female and male young adults while F-25+ and M-25+ means the female and male adults, respectively. The lower triangles of the matrices respectively contain the χ^2 and p-values of the pairwise comparisons.

	χ^2 output				P-value		
	F-15-24	F-25+	M-15-24		F-15-24	F-25+	M-15-24
F-25+	10.978			F-25+	0.0000		
M-15-24	6.828	17.806		M-15-24	0.00001	0.0000	
M-25+	6.377	4.601	13.205	M-25+	0.00004	0.006	0.0000

5.4.6 Model fitting

The results in Figure 5.4 clearly show that the model fits well with the available data points. It is important to observe that the cases of infection peaked in the year 2013. The results show that there was a rise in HIV infection between 2011 and 2013, followed by a significant slow down in the occurrences of of new cases of HIV infection. In Figure 5.5, we make a comparison of new cases of HIV infection for the two groups. Our results are indicative of a long-term fall in cases of HIV infection in which there is a significant decline in the cases of infection by 2030. However, it can be clearly seen that the occurrence of new cases of HIV infection is more prominent in the adult population as compared to the young adults' population. The most important observation is there is high number of cases of HIV infection amongst the female adults (aged 25 and over) in comparison to the remaining groups. It is known that women in this group are disproportionately affected by the HIV infections since it is men often dominate sexual relationships leaving women with no ability to always practice safer sex despite the known risks involved (AV, 2017). The results show that new cases of HIV infection amongst the young male adults would be contained by 2025 while that of their female counterparts is likely to be contained after 2030 should the current interventions against HIV in Kenya be maintained. Tables 5.7-5.9 give the estimated variable values, estimated parameter values and the transmission reproduction numbers, respectively. The computation of the reproduction numbers within and between age groups in Table 5.9 provides insights into control that cannot be deduced simply from observations on the prevalence of infection. More specifically, the analysis showed that the per capita rate

of HIV transmission was highest when there is interaction between young adults to adults and most HIV infections occurred in adult population.

Table 5.7: Estimates of state variable values from the model fitting to data.

	Male			Female		
	Mean	SE	95% CI[1]	Mean	SE	95% CI[1]
S_d	4326140	1665	[4325114, 4327166]	4333384	548.6	[4332309, 4334459]
I_d	180	0.4845	[179.05, 180.95]	191	1.766	[187.54, 194.46]
T_d	105	0.4625	[104.09, 105.91]	126	0.2417	[125.53, 126.47]
S_a	9011930	1418	[9009150, 9014710]	9312839	1417	[9310062, 9315616]
I_a	665	1.671	[661.73, 668.28]	370	0.9102	[368.22, 371.78]
T_a	144	0.4261	[143.16, 144.84]	333	0.6121	[331.8, 334.2]

[1] 95% Confidence Interval

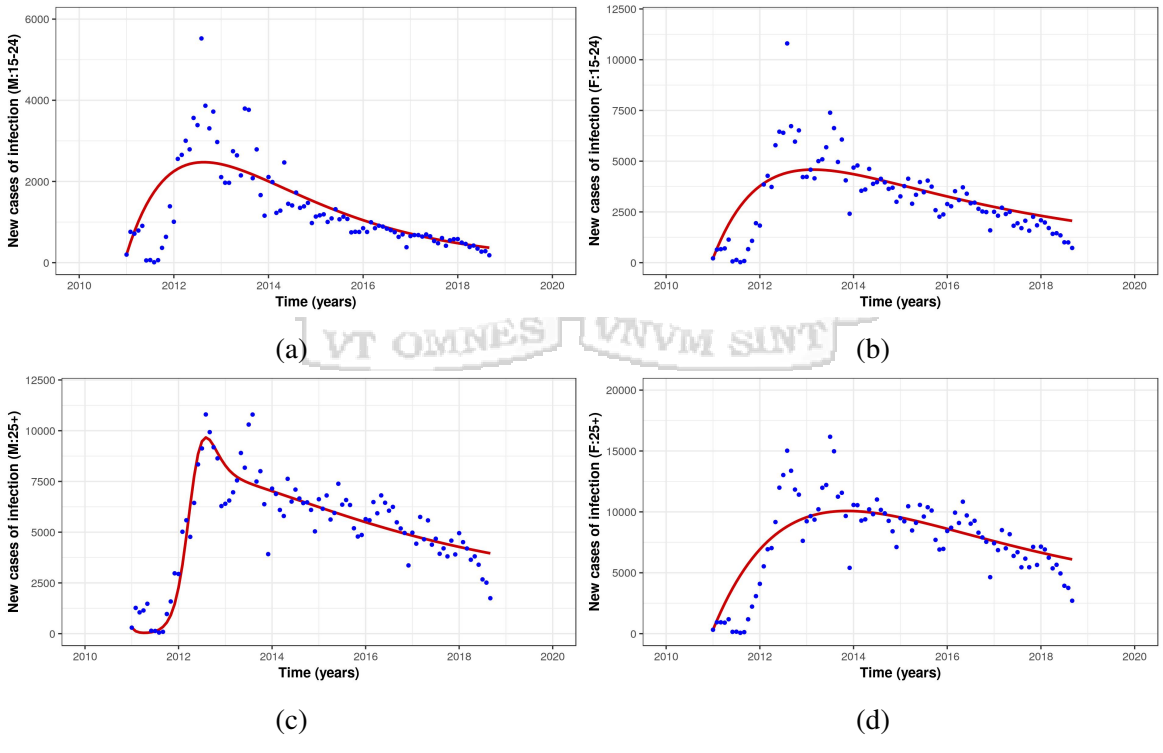

Figure 5.4: Model system (5.5) fitted to data for the reported new cases of HIV infection. Panel (a) shows the model fitted to the data for the young male adults (aged 15-24 years). Panel (b) shows the model fitted to data for the young female adults (aged 15-24 years). On the other hand panel (c) shows the model fitted to the data for the male adults (aged 25+ years). Panel (d) shows the model fitted to data for the female adults (aged 25+ years). The blue dots indicate the actual data and the red line indicates the model fit to the data. All the fitted curves are done with 95% confidence limits.

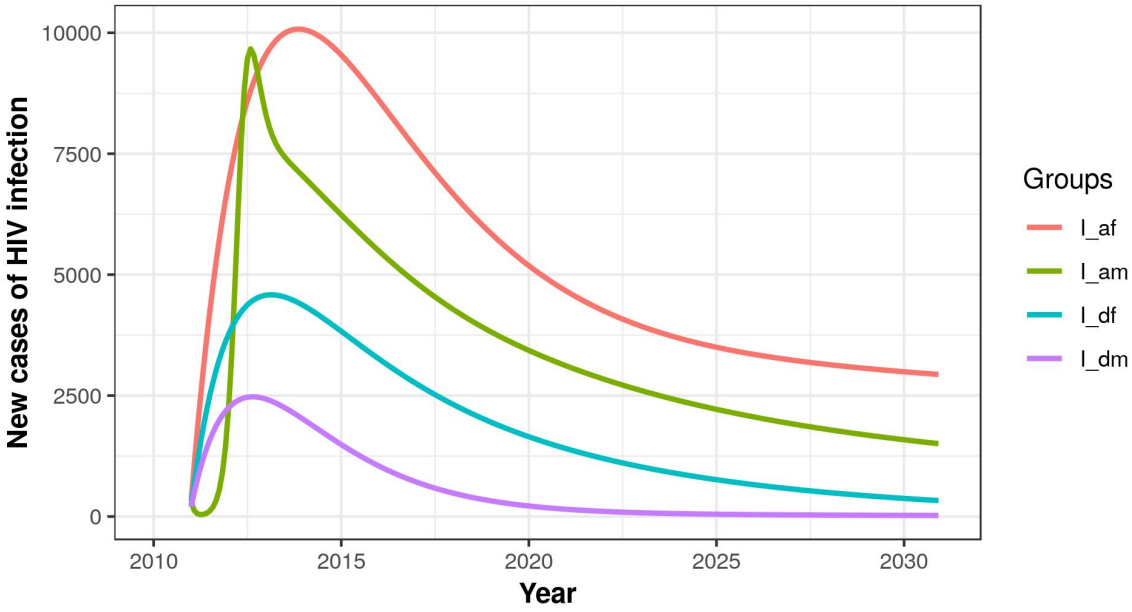

Figure 5.5: The projected cases of new HIV infection within the age groups as fitted in Figure 5.4.

Table 5.8: Estimated parameter values of the system (5.5) obtained from model fitting.

Par	Mean	SE	95% CI	Par	Mean	SE	95% CI
β_1	0.3743	7.8e-4	[0.3728, 0.3758]	β_2	0.4.01e-3	5.0e-6	[4.0e-3, 4.02e-3]
β_3	4.2e-5	5.33e-8	[4.23e-5, 4.25e-5]	β_4	0.7451	0.0015	[0.7421, 0.7481]
θ_1	0.1698	2.86e-4	[0.1693, 0.1704]	θ_2	2.76e-4	4.57e-7	[2.7e-4, 2.8e-4]
θ_3	1.282e-5	8.2e-9	[1.28e-5, 1.29e-5]	θ_4	0.0422	1.301e-4	[0.0419, 0.0425]
θ_5	0.0248	7.531e-5	[0.0246, 0.0250]	θ_6	0.2195	2.712e-4	[0.2189, 0.2202]
η_1	0.0432	1.167e-4	[0.0429, 0.0434]	η_2	0.6256	1.0704e-3	[0.6235, 0.6277]
η_3	0.0680	1.078e-4	[0.0678, 0.0683]	η_4	5.181e-4	1.181e-6	[5.15e-4, 5.2e-4]
η_5	5.494e-3	1.735e-5	[5.46e-3, 5.53e-3]	η_6	0.2169	2.392e-4	[0.2165, 0.2174]

Table 5.9: Estimation of young adults transmission reproduction number $\mathscr{R}_{0d}$, adults transmission reproduction number $\mathscr{R}_{0a}$, basic reproduction number between the male young adults and the female adults $\mathscr{R}_{0mdfa}$, basic reproduction number between the female young adults and the male adults $\mathscr{R}_{0fdma}$ and the system (5.5) basic reproduction number $\mathscr{R}_0$.

Statistics	$\mathscr{R}_{0d}$	$\mathscr{R}_{0a}$	$\mathscr{R}_{0mdfa}$	$\mathscr{R}_{0fdma}$
Mean	1.135	1.921	2.432	2.432
Std. error	0.000035	0.00014	0.00089	0.00089
95% Confidence Interval	1.131–1.139	1.901–1.941	2.397–2.467	2.397–2.467

5.4.7 Sensitivity analysis

Sensitivity analysis is introduced to study the strength of the basic reproduction numbers as listed in Table 5.9 for the model parameters. Here, we perform sensitivity analysis to examine the model's response to parameter variation within a wider range in the parameter space. Following the work by Marino et al. (2008), partial rank correlation coefficients (PRCC) between the basic reproduction number R_0 and each parameter are derived from 1,000 runs of the Latin hypercube sampling (LHS) method (Stein, 1987). The parameters are assumed to be random variables with uniform distributions with their mean value listed in Tables 5.3 and 5.8. Tornado plots for the normalised sensitivity index for different parameters are given in Figure 5.6.

If the sensitivity index is positive, then the reproduction number increases along with increasing value of the parameter. On the other hand, if the sensitivity index is negative, then reproduction decreasing with the increasing value of the parameter. Figure 5.6, panels (a) and (b) are produced assuming that the HIV infection is localised only the young adults (15-24 years) and adults (15+ years) age groups respectively. From the figures, the parameters related to the probabilities of HIV transmission have reasonably significant PRCCs and cannot be ignored. The parameters ϕ_1, δ_1, ϕ_2 and δ_2 have the lowest PRCCs with respect to the corresponding disease thresholds. However, their direction of influence is clearly visible. In this regard, since no effort toward reducing disease spread is rendered insignificant, any action that increases the number of individuals under ART treatment reduces the infection. Figure 5.6, panels (c) and (d) are produced assuming that there is interaction between young male adults (15-24 years) and adult females (15+ years) and young female adults (15-24 years) and male adults (15+ years), respectively. It is also seen that probabilities of HIV transmission have the potential of making the epidemic worse if increased while parameters related to treatment of infected individuals into ART have the potential of reducing infections.

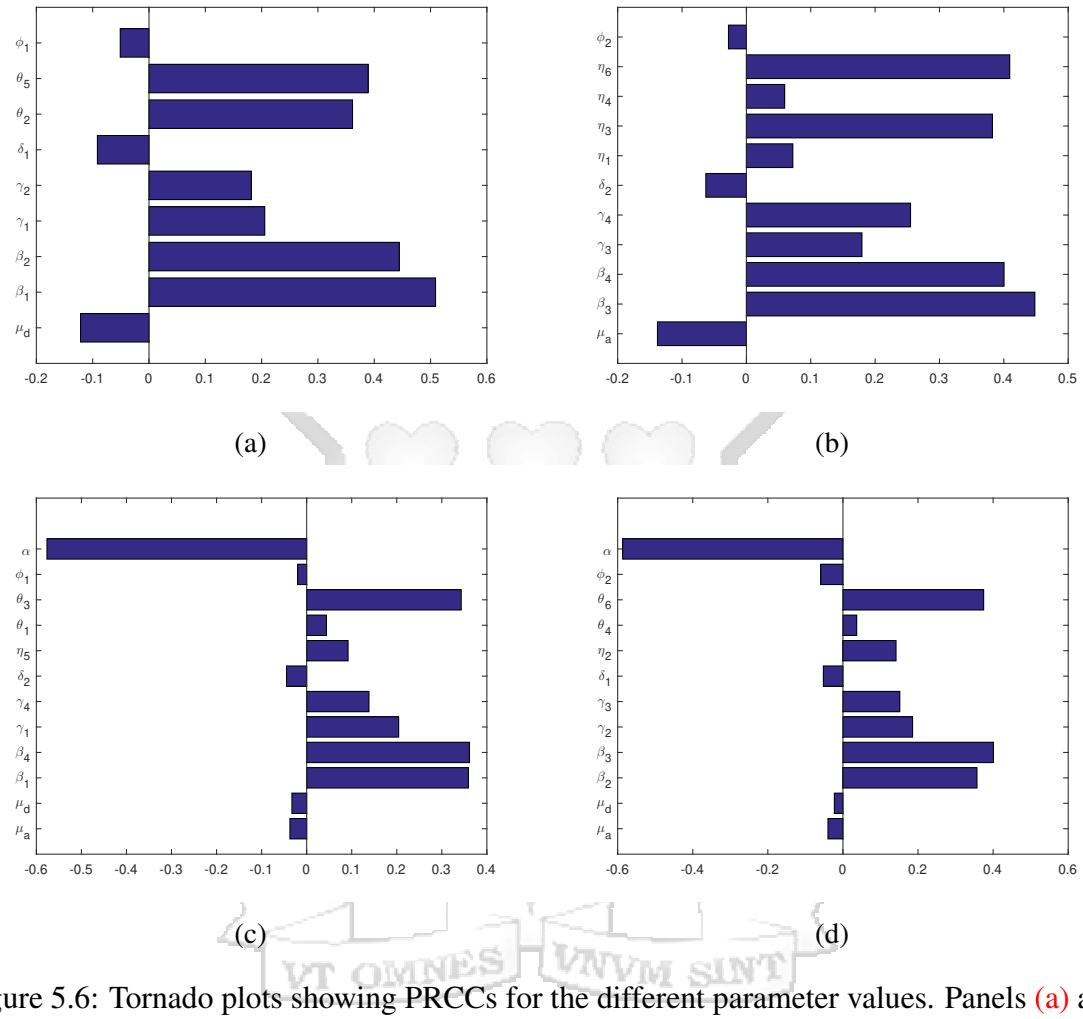

Figure 5.6: Tornado plots showing PRCCs for the different parameter values. Panels (a) and (b) are produced assuming that the HIV infection is localised only the young adults (15-24 years) and adults (15+ years) age groups respectively. On the other hand panels (c) and (d) are produced assuming that there is interaction between young male adults (15-24 years) and adult females (15+ years) and young female adults (15-24 years) and male adults (15+ years), respectively.

5.5 Conclusion

In this chapter, we modelled the trend of new HIV infections in Kenya, for which a considerable amount of data are available. Thus, a deterministic model for HIV dynamics within and between age groups that takes into consideration the sexual orientation of individuals is presented. Vital mathematical characteristics of the model have been presented. These include the invariant region of biological significance, the age group specific basic transmission numbers and inter age group specific basic transmission numbers. MCMC method has been

used to estimate the parameter values based on the available data. The basic descriptive and inferential statistics of the data have been computed and presented. Our analysis of the data shows that that females in both age categories are disproportionately affected with HIV more than the males. This is in agreement with the Kruskal-Wallis results which are indicative of very strong evidence that there exist significant differences in HIV infections between the groups.

The model was then fitted to on the new cases of HIV infections with the objective of using the model parameters that give the best fit to examine the trend of HIV infection. It has been established that the occurrence of new cases of HIV infection is more prominent in the adult population as compared to the young adults' population. It is important to note that there is high number of cases of HIV infection amongst the female adults (aged 25 and over). This can be attributed to the fact that men often dominate sexual relationships leaving women with no ability to always practice safer sex despite the known risks involved. The results show that new cases of HIV infection amongst the young male adults would be contained by 2025 while that of their female counterparts is likely to be contained after 2030 should the current interventions against HIV in Kenya be maintained. Furthermore, computation of the reproduction numbers within and between age groups provides insights into control that cannot be deduced simply from observations on the prevalence of infection. More specifically, the analysis showed that the per capita rate of HIV transmission was highest when there is interaction between young adults to adults and most HIV infections occurred in adult population.

Sensitivity of parameters was also considered. The results demonstrate that the transmission probabilities and treatment rates have the greatest impacts on the reproduction numbers. This suggests that control of HIV pivots around transmission prevention programmes. The programmes aimed at individuals at high risks of HIV infection that encourage them to use preventive measures such as condoms and PrEP will be particularly effective. Furthermore, enrolling more infected individuals on ART treatment would be ideal in reducing the cases of new infections for it is known that it helps in suppressing the viral load in the body thus limiting further HIV infections. It is thus critical to to devote more resources to education

on HIV preventive measures and treatment programs that are especially targeted to both the susceptible and infected individuals.

The model considered in this chapter is consistent with the dynamics of HIV infection in Kenya and it has some lucid limitations. In fact, lack of sufficient data on the number of HIV patients enrolled in ART treatment and care limited the numerical analysis and interpretation. This work has only considered the new cases of HIV infections. It is well known that the goodness of fit measures the discrepancy between observed data and values expected from the model. In this work, no goodness of fit tests were performed. However, we relied on the MCMC method for the model fitting. We argue that MCMC method of fitting models to data provides useful insights into how the model can be linked to data despite the challenge of using statistical tools to test the goodness of fit of the model.

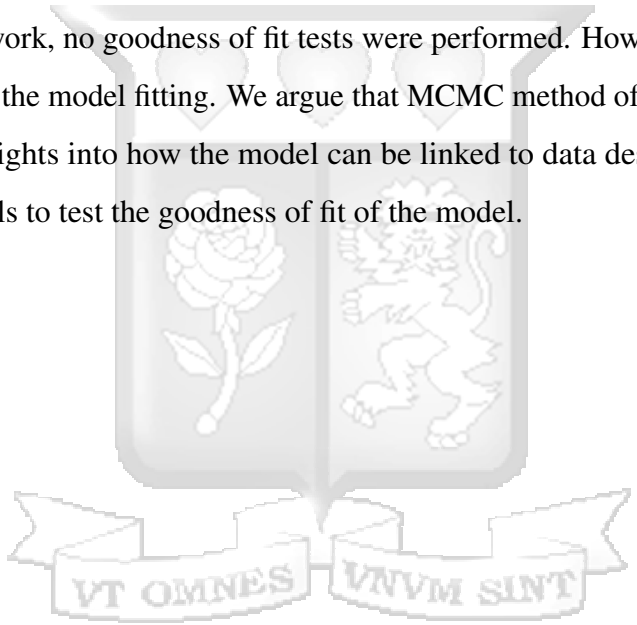

Chapter 6

Optimal control of HIV transmission dynamics between commercial sex workers and injection drug users

6.1 Introduction

HIV is characterised as a generalised epidemic among the adult population but has a more concentrated epidemic among commercial sex workers and injection drug users who are considered to be at a heightened risk of HIV acquisition and transmission (KNASP, 2009). Sex workers refers women or men and trans-gender people who receive money or goods in exchange for sexual services and define the activities as income generating (Overs, 2002). However, these activities are considered illegal and participants are highly stigmatised in many countries (Musyoki et al., 2015). For instance, a sex worker may not press charges against an attacker in the case of rape due to stigmatisation and the illegality of the activities. Lack of protection of the sex workers makes them vulnerable to abuse, violence and rape thereby creating an environment which facilitates transmission of HIV (Wechsberg et al., 2005).

High HIV infections amongst sex workers in Kenya is attributed to unprotected sex. According to Shields (2012), most sex workers are constantly harassed by the police officers who physically and sexually abuse them for carrying condoms. In addition, the sex workers have no power to negotiate for safe sex. This is due to the fact that clients may decline to pay if they have to use condom and hence use intimidation or violence to force unprotected sex

(Ghimire et al., 2011). Furthermore, the clients may offer more money for unprotected sex a proposal that is unlikely to be rejected by the sex workers.

In comparison to the general population, sex workers have a high number of sexual partners. However, the risk of becoming HIV infected may be greatly reduced if there is correct and consistent use of condoms (WHO et al., 2009). In Kenya, sex workers bear a high burden of HIV infection compared to any group in Kenya. According to NACC (2014b) an estimated 29.3% of female sex workers were living with HIV in 2011. Furthermore, the findings from the Sex Workers Outreach Project reported a HIV prevalence of 30% among female sex workers and 40% among male sex workers in 2011 (UNAIDS, 2015b).

In Kenya, transmission of HIV among people who inject drugs (PWID) is becoming increasingly recognised (Gelmon, 2009; Kurth et al., 2015). PWID are highly vulnerable to HIV and considered a bridge for HIV transmission to the general population. Sharing of needles and other high risk behaviours such as flashblood where users who cannot afford heroin inject the blood of a PWID who recently injected are the main ways through which HIV is spread among the participants of PWID (Beckerleg et al., 2005, 2006; McCurdy et al., 2010; McNeil Jr, 2010). The majority of people who inject drugs are concentrated in specific geographical areas such as Nairobi and Mombasa. According to Gelmon (2009); Kurth et al. (2015); UNAIDS (2015b), an estimated 18% of HIV infections on the Kenyan coast and 7.5% of the national HIV infections are attributed to people who inject drugs.

Optimality, costs and cost-effectiveness of the interventions which may sometimes be limited by availability of resources in the presence of transmission between these two risk groups is of great concern. More precisely, carrying out comparative analysis, knowing costs and the results of the alternative control measures is significant to the policy makers who are often faced with challenges of resource allocation. Therefore, application of optimal control theory can be an important tool to estimate the efficacy of various policies and control strategies against the cost of implementation. Optimal control is a powerful mathematical tool in decision making that involves employing appropriate strategies to eradicate epidemics from the population (Makinde and Okosun, 2011). The application of this theory includes the optimization of the costs of using active and passive immunization in control infectious

diseases (Gupta and Rink, 1973). Optimal control has been used to study the dynamics of some diseases such as malaria (Okosun et al., 2011), onchocerciasis (Omondi et al., 2017b), West Nile virus (Blayneh et al., 2009; Blayneh, 2010) and HIV/AIDS (Silva and Torres, 2017). For instance, Castilho (2006); Sethi and Staats (1978) used optimal control theory to investigate the best strategy for educational campaigns during outbreak of an epidemic and at the same time minimizing the number of infected humans. It has also been applied in modelling Leukemia (Aïnseba and Benosman, 2010; Nanda et al., 2007). Okosun et al. (2013) studied the impact of optimal control on the treatment of HIV/AIDS and screening of unaware infectives on the transmission dynamics of the disease in a homogeneous population with constant immigration of susceptibles. They incorporated use of condoms, screening of unaware infectives and treatment of the infected. Other HIV models that incorporated optimal controls include (Gromov et al., 2017; Kwon et al., 2012).

In this chapter, we propose a mathematical model of HIV transmission between sex workers and injection drug users that takes into account treatment with ART and prevention with PrEP. It is important to note that sex workers and injection drug users usually consist of both women and men thus we consider the inflow from sex workers and injection drug users. We use optimal control theory to study the effectiveness of combination of three HIV/AIDS control measures, namely (i) use of PrEP, (ii) use of educational campaigns and condoms and (iii) treatment with ART. For this, we consider an HIV transmission model and incorporate three time dependent controls representing these interventions. We carry out detailed qualitative optimal control analysis of the model and find the necessary conditions for optimal control of the disease using Pontryagin's maximum principle (Bohner et al., 2017) in order to determine optimal strategies for controlling the spread of HIV/AIDS.

6.2 Model formulation

In this section, we propose a mathematical model that describes the transmission of HIV between two different risk groups, namely:- commercial sex workers and drug injection users as well as incorporating optimal control measures. The model we propose here is an

extension of the previous model studied in (Silva and Torres, 2017), and is based on the modelling approach given in (Njagarah and Nyabadza, 2014; Williams and Dye, 2018). In this model, there is transition between these risk groups. We compartmentalise our model into eight (8) classes. These are:- S_s, U_s, T_s, S_d, U_d, T_d, P_s and P_d. The subscripts s and d define commercial sex workers and the injection drug users, respectively. The HIV patients in each risk group are divided into two groups, the HIV-positive individuals not on treatment (U) and the HIV-positive individuals receiving antiretroviral therapy (ART) treatment (T) to suppress the viral load, respectively. Note that S class represent the populations at high risk of HIV infection and (P) class represent the population at high risk of HIV infection on PrEP. The total populations for each risk group are governed by the following at any time, t.

$$N_1(t) = S_s(t) + U_s(t) + T_s(t) + P_s(t), \quad N_2(t) = S_d(t) + U_d(t) + T_d(t) + P_d(t).$$

The total population is the sum of the populations of the two risk groups given by $N(t) = N_1(t) + N_2(t)$. The rates at which the susceptible (S_s and S_d) acquire infection are respectively given by

$$\lambda_1 = \psi\beta\left[\frac{U_s + \theta_1 T_s + \theta_2 U_d + \theta_3 T_d}{N}\right], \quad \lambda_d = \lambda_2 + \lambda_3, \tag{6.1}$$

where

$$\lambda_2 = \eta\psi\beta\left[\frac{U_s + \theta_1 T_s + \theta_2 U_d + \theta_3 T_d}{N}\right], \quad \lambda_3 = \frac{\delta U_d}{1 + \tau U_d}.$$

The function λ_3 denotes the HIV infection rate of susceptible IDUs initiated by sharing of needles resulting in flash blood. δ is positive and τ is nonnegative. The parameter τ accounts for the concentration of injection drug users. It is worth noting that for small U_d, the infection rate λ_3 reduces to $\lambda_3 \approx \delta U_d$, while for large U_d it reduces to $\lambda_3 \approx \frac{\delta}{\tau}$, which characterizes the concentration phenomenon. In addition, if $\tau = 0$ the infection rate becomes $\lambda_3 = \delta U_d$ which is the usual linearly density-dependent infection rate. The rest of the parameters of the model and other assumptions made are described as follows:

- Π_1, Π_2 : the recruitment rates at which individuals enter the CSW and IDU susceptible populations, respectively. During this modelling time, we only consider individuals

aged 15 years and above. This group of individuals is assumed to be adult population, and hence the recruitment rate defines the demographic process of individuals attaining age 15. In addition, all those recruited into the population of CSW and IDU are assumed susceptible.

- $\beta, \beta\theta_1, \beta\theta_2, \beta\theta_3$: the probabilities of susceptible individuals acquiring HIV infection through contact with the infected HIV individuals in classes U_s, T_s, U_d and T_d, respectively.

- ψ : the average number of contacts a susceptible individual makes with the infected individuals per unit time.

- η : modification rate for the probabilities of susceptible IDU individuals acquiring HIV infection through contact with infected HIV individuals in classes U_s, T_s, U_d and T_d.

- α_1, α_2 : the rates at which the HIV-positive individuals not on treatment are tested and connected to ART treatment. This treatment is assumed to conform to WHO guidelines on HIV treatment based on test and treat strategy to attain viral load suppression in order to achieve the 90-90-90 plan (WHO, 2015).

- μ : the natural death rate of the general population at any given time.

- κ_1, κ_2 : the respective rates of transition from susceptible CSW to susceptible IDU and from susceptible IDU to susceptible CSW.

- ω_1, ω_2 : the respective rates of transition of HIV-positive individuals not on treatment in CSW to HIV-positive individuals not on treatment in IDU and vice versa.

- ρ_1, ρ_2 : the respective rates of transition from T_s (infected sex workers on ART treatment) to T_d (infected drug users on ART treatment) and vice versa.

- The proportions of susceptible individuals in CSW and IDU that take PrEP are denoted by ξ_1 and ξ_3, respectively. The individuals that stop using PrEP become susceptible individuals again, at rates ξ_2 and ξ_4 for CSW and IDU, respectively.

6.2.1 Model assumptions

(i) It is assumed that HIV-positive individuals on ART treatment in IDU do not contribute to new infections as a result of flash blood due to educational awareness on effective HIV prevention services.

(ii) The AIDS class is not considered in this model, given that full blown AIDS patients are usually hospitalized and/or sexually inactive. It is assumed that they are not able to engage in HIV transmission activities, hence do not contribute to HIV infection. Furthermore, during the modelling time we consider the asymptomatic stage of HIV infection that includes a 2-4 week acute HIV infection stage followed by a 10 year long clinical latency stage before the onset of AIDS. During the asymptotic stage, individuals infected with HIV experience no symptoms or only mild ones. Thus, HIV-related death during this stage is assumed to be negligible.

(iii) The total population is assumed a homogeneous mixing. This means that susceptible individuals are equally likely to be infected by an infectious individual in the case of a contact.

The flow and interactions between the compartments is described in Figure 6.1.

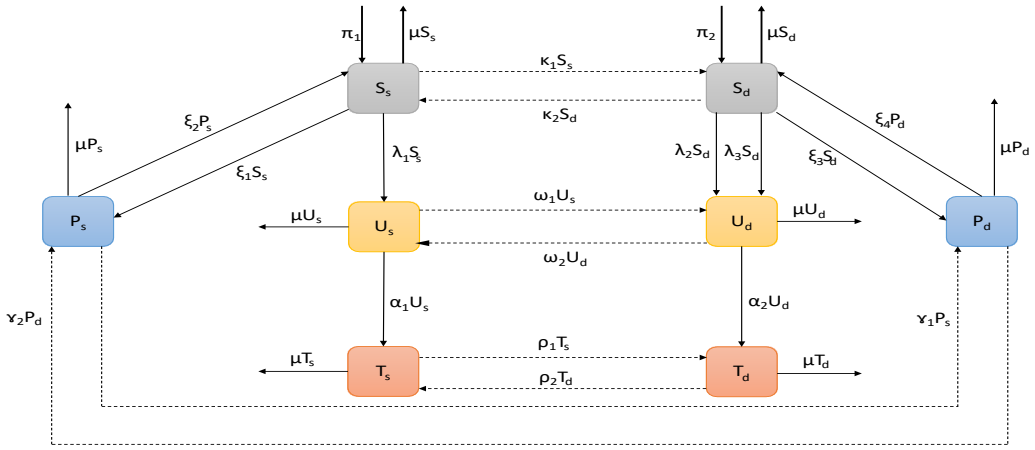

Figure 6.1: A compartmental representation of the model for HIV transmission. The dotted lines point to the transitions between the risk groups, while a solid line points to a transition within the same risk group.

Our model explores the interaction between CSW and IDU in HIV spread and we have not modelled genders separately. Including gender in the model, would add a lot of complexity (parameters), and is not necessary for addressing our question, since evidence suggests that the gender-specific proportion of index cases and probabilities of transmission are at least roughly similar (Bellan et al., 2013; Boily et al., 2009; Eyawo et al., 2010).

There are several possible interventions in order to reduce or limit the proliferation of HIV and the explosion of the number of infected HIV. Thus, we introduce three time dependent controls to reduce the spread of HIV/AIDS. The following interventions have been added to the model

- Following WHO, making PrEP drugs available for safe, effective prevention outside the clinical trial setting is the current challenge. However, it is important to highlight that PrEP is not for general use and is only meant for people who are HIV-negative and at very high risk of acquiring infection (AIDS, 2016a). Thus, the first control $0 \leq u_1(t) \leq 1$ represents efforts made to protect susceptible individuals from infections. It mainly consists of the use of PrEP. We assume that the fraction of individuals that takes PrEP, at each instant of time, is a control function, that is, $\xi_i^c = \xi_i u_1(t)$, for i=1,2.

- The second control is concerned with educational campaigns and condom use on the prevention of new infections. Thus, the infection terms given in (6.1) are modified as follows

$$\lambda_i^c = (1 - u_2(t))\lambda_i, \text{ for } i = 1,2,3, \tag{6.2}$$

- The third control $0 \leq u_3(t) \leq 1$ represents efforts made for ART treatment. It mainly consists of up-take of ARV drugs to reduce the risk of dying (Williams, 2014; Williams et al., 2010). Thus, we modify α_i to $\alpha_i^c = \alpha_i u_3(t)$, for $i = 1,2$.

Note that $0 \leq u_i \leq 1$, for $i = 1,\ 2,\ 3$, means that when the control is zero there is no any effort invested, i.e. no control and when it is one, the maximum control effort is invested.

Following the above description, the following non-linear ordinary differential equations are obtained.

For the commercial sex workers we have

$$\left.\begin{aligned}
\frac{dS_s}{dt} &= \Pi_1 + \xi_2 P_s + \kappa_2 S_d - \lambda_1^c S_s - (\mu + u_1(t)\xi_1 + \kappa_1) S_s, \\
\frac{dU_s}{dt} &= \lambda_1^c S_s + \omega_2 U_d - (\alpha_1 u_3(t) + \omega_1 + \mu) U_s, \\
\frac{dT_s}{dt} &= \alpha_1 u_3(t) U_s + \rho_2 T_d - (\rho_1 + \mu) T_s, \\
\frac{dP_s}{dt} &= \xi_1 u_1(t) S_s + \gamma_2 P_d - (\gamma_1 + \xi_2 + \mu) P_s.
\end{aligned}\right\} \text{CSW} \tag{6.3}$$

For the injection drug users we have

$$\left.\begin{aligned}
\frac{dS_d}{dt} &= \Pi_2 + \kappa_1 S_s + \xi_4 P_d - (\lambda_2^c + \lambda_3^c) S_d - (\mu + \kappa_2 + u_1(t)\xi_3) S_d, \\
\frac{dU_d}{dt} &= (\lambda_2^c + \lambda_3^c) S_d + \omega_1 U_s - (\alpha_2 u_3(t) + \omega_2 + \mu) U_d, \\
\frac{dT_d}{dt} &= \alpha_2 u_3(t) U_d + \rho_1 T_s - (\rho_2 + \mu) T_d, \\
\frac{dP_d}{dt} &= \xi_3 u_1(t) S_d + \gamma_1 P_s - (\gamma_2 + \xi_4 + \mu) P_d.
\end{aligned}\right\} \text{IDU} \tag{6.4}$$

The system of equations in (6.3)–(6.4) is subject to the following initial conditions, $S_s(0) \geq 0$, $U_s(0) \geq 0$, $T_s(0) \geq 0$, $P_s(0) \geq 0$, $S_d(0) \geq 0$, $U_d(0) \geq 0$, $T_d(0) \geq 0$, $P_d(0) \geq 0$. The two populations namely (CSW and IDU) are connected by migration of individuals from one key population to the next and back.

6.2.2 Parameter and initial data estimation

The natural death rate was estimated to be $\mu = 0.0161$ based on the life expectancy in Kenya (WHR, 2018). It is important to note that $\Pi_1 = \mu N_s$ and $\Pi_2 = \mu N_d$. It follows that the in-flow per unit of time equals out-flow per unit of time. Thus, the total population size N remains constant. According to UNAIDS (2015b), the ART coverage is markedly lower among key populations, ranging from 15% amongst injection drug users to 34% among sex workers. Hence the rates of ART treatment α_1, α_2 have been estimated to be 0.34 and 0.15 respectively. Other unknown parameters are estimated on the basis of the numerical simulations carried out in Section 6.7. The estimates from PKPK (2014) show

that there are about 150,675 commercial sex workers and 18,327 injection drug users in Kenya. The Kenya's HIV prevalence within the key populations were reported to be 29.3% and 18.3% for CSW and IDU, respectively, in 2013 (Bhattacharjee et al., 2015). Therefore, the initial starting values are $S_s(0) = 110,000$; $U_s(0) = 20,000$; $T_s(0) = 10,000$; $P_s(0) = 10,000$; $S_d(0) = 12,000$; $U_d(0) = 2,500$; $T_d(0) = 2,000$; $P_d(0) = 2,000$.

Table 6.1: Parameter ranges and baseline values per year.

Par	Min	Max	Baseline	Source	Par	Min	Max	Baseline	Source
Π_1	-	-	μN_1	WHR (2018)	κ_1	0.0	1.0	0.0055	Assumed
Π_2	-	-	μN_2	WHR (2018)	κ_2	0.0	1.0	0.0075	Assumed
ψ	0.0	3.0	3.0	Assumed	β	0.0	1.0	0.75	Assumed
η	0.1	1.0	0.58	Assumed	ω_1	0.0	1.0	0.0065	Assumed
ω_2	0.0	1.0	0.0085	Assumed	δ	0.1	1.0	0.92	Assumed
θ_1	0.1	1.0	0.98	Assumed	θ_2	0.1	1.0	0.88	Assumed
θ_3	0.1	1.0	0.91	Assumed	ρ_1	0.0	1.0	0.045	Assumed
ρ_2	0.0	1.0	0.075	Assumed	μ	-	-	0.0161	WHR (2018)
α_1	-	-	0.34	UNAIDS (2015b)	τ	0.1	1.0	0.28	Assumed
α_2	-	-	0.15	UNAIDS (2015b)	ξ_1	0.0	1.0	0.40	Assumed
ξ_2	0.0	1.0	0.0512	Assumed	ξ_3	0.0	1.0	0.40	Assumed
ξ_4	0.0	1.0	0.0615	Assumed	γ_1	0.0	1.0	0.0037	Assumed
γ_2	0.0	1.0	0.0046	Assumed					

6.3 Analysis of the model with constant controls

All the model parameters are assumed to be positive. Thus, the positivity of the solutions of the model system (6.3)–(6.4) can easily be established provided $S_s(0) \geq 0, U_s(0) \geq 0, T_s(0) \geq 0, P_s(0) \geq 0, S_d(0) \geq 0, U_d(0) \geq 0, T_d(0) \geq 0, P_d(0) \geq 0$. See Huo and Feng (2013); Nyabadza et al. (2013); Omondi et al. (2018a, 2017b) for the proof.

6.3.1 Invariant region

The system (6.3)–(6.4) can be rewritten in the following form

$$\frac{dY}{dt} = A(Y) + D,$$

where $Y = (S_s, U_s, T_s, P_s, S_d, U_d, T_d, P_d)^T$. For convenience and ease in the computation, we define some combination of parameters of the system (6.3)–(6.4) as follows; $Q_1 = \mu + \kappa_1 + u_1\xi_1$, $Q_2 = \alpha_1 u_3 + \omega_1 + \mu$, $Q_3 = \rho_1 + \mu$, $Q_4 = \gamma_1 + \xi_2 + \mu$, $Q_5 = \mu + \kappa_2 + u_1\xi_3$, $Q_6 = \alpha_2 u_3 + \omega_2 + \mu$, $Q_7 = \rho_2 + \mu$, $Q_8 = \rho_2 + \xi_4 + \mu$. Thus, the matrix A is given by

$$A(Y) = \begin{bmatrix} -(\lambda_1^c + Q_1) & 0 & 0 & \xi_2 & \kappa_2 & 0 & 0 & 0 \\ \lambda_1^c & -Q_2 & 0 & 0 & 0 & \omega_2 & 0 & 0 \\ 0 & \alpha_1 u_3 & -Q_3 & 0 & 0 & 0 & \rho_2 & 0 \\ \xi_1 u_1 & 0 & 0 & -Q_4 & 0 & 0 & 0 & \gamma_2 \\ \kappa_1 & 0 & 0 & 0 & -(\lambda_2^c + \lambda_3^c + Q_5) & 0 & 0 & \xi_4 \\ 0 & \omega_1 & 0 & 0 & (\lambda_2^c + \lambda_3^c) & -Q_6 & 0 & 0 \\ 0 & 0 & \rho_1 & 0 & 0 & \alpha_2 u_3 & -Q_7 & 0 \\ 0 & 0 & 0 & \gamma_1 & \xi_3 u_1 & 0 & 0 & -Q_8 \end{bmatrix}.$$

On the other hand, the vector $D = (\Pi_1, 0, 0, 0, \Pi_2, 0, 0, 0)^T$ is positive. It is important to note that $A(Y)$ has all off diagonal entries non-negative. This implies that $A(Y)$ is a Metzler matrix, for all $Y \in \mathbb{R}^9_+$. Using the fact that $D \geq 0$, the system (6.3)–(6.4) is positively invariant in $\mathbb{R}^8_+$ (see, Abate et al. (2009); Berman and Plemmons (1994)). This means that any trajectory of the system (6.3)–(6.4) starting from an initial state in $\mathbb{R}^8_+$ forever remains in $\mathbb{R}^8_+$.

It is easy to see that the evolution of the system (6.3)–(6.4) is described by $\frac{dN}{dt} = \Pi^* - \mu N$, where $\Pi^* = \Pi_1 + \Pi_2$. Thus, solving for $N(t)$ we get

$$N(t) \leq \frac{\Pi^*}{\mu} + e^{-\mu t}\left(N(0) - \frac{\Pi^*}{\mu}\right). \tag{6.5}$$

There are two possible cases in studying the behaviour of $N(t)$ in (6.5). In the first case, we consider $N(0) > \frac{\Pi^*}{\mu}$ so that, at time t = 0, the right-hand side (RHS) of (6.5) experiences the largest possible value of $N(0)$. That is, $N(t) \leq N(0)$ for all time $t \geq 0$. In the second case, we consider $N(0) < \frac{\Pi^*}{\mu}$, so that the largest possible value of the RHS of (6.5) approaches $\frac{\Pi^*}{\mu}$ as time t approaches infinity. Thus, $N(t) \leq \frac{\Pi^*}{\mu}$ for all time $t \geq 0$. From these two cases, we conclude that $N(t) \leq \max\left\{N(0), \frac{\Pi^*}{\mu}\right\}$ for all time $t \geq 0$. Therefore, we can study the system (6.3)–(6.4) in the feasible region given by

$$\Omega = \left\{(S_s(t), U_s(t), T_s(t), P_s(t), S_d(t), U_d(t), T_d(t), P_d(t)) \in \mathbb{R}^8_+ : N(t) \leq \max\left\{N(0), \frac{\Pi^*}{\mu}\right\}\right\},$$

which is positively invariant with respect to systems (6.3)–(6.4). This implies that the systems (6.4)–(6.4) is well posed epidemiologically and all the solutions starting in Ω remain in Ω for all $t \geq 0$. Since the region Ω is positively-invariant, the usual existence, uniqueness, continuation results hold for the system hence, it is sufficient to consider the dynamics of the flow generated by the system (6.3)–(6.4) in the region Ω (Hethcote, 2000).

6.4 Model equilibrium points

The system (6.3)–(6.4) has the following four (4) equilibrium points

$$\mathscr{E}_0 = \{S_s^*, 0, 0, P_s^*, S_d^*, 0, 0, P_d^*\}, \tag{6.6}$$

$$\mathscr{E}_1 = \{S_s^*, U_s^*, T_s^*, P_s^*, S_d^*, 0, 0, P_d^*\}, \tag{6.7}$$

$$\mathscr{E}_2 = \{S_s^*, 0, 0, P_s^*, S_d^*, U_d^*, T_d^*, P_d^*\}, \tag{6.8}$$

$$\mathscr{E}_3 = \{S_s^*, U_s^*, T_s^*, P_s^*, S_d^*, U_d^*, T_d^*, P_d^*\}. \tag{6.9}$$

Note that $\mathscr{E}_0$ refers to the HIV-free equilibrium whereas $\mathscr{E}_1$ and $\mathscr{E}_2$ refer to the first and second boundary endemic equilibria. On the other hand, $\mathscr{E}_3$ defines the interior endemic equilibrium in the domain Ω. The HIV-free equilibrium $\mathscr{E}_0$ in the two risk populations is obtained from the systems (6.3)–(6.4) which reduces to

$$\left.\begin{aligned}
\frac{dS_s}{dt} &= \Pi_1 + \xi_2 P_s + \kappa_2 S_d - Q_1 S_s, \\
\frac{dP_s}{dt} &= \xi_1 u_1 S_s + \gamma_2 P_d - Q_4 P_s, \\
\frac{dS_d}{dt} &= \Pi_2 + \kappa_1 S_s + \xi_4 P_d - Q_5 S_d, \\
\frac{dP_d}{dt} &= \xi_3 u_1 S_d + \gamma_1 P_s - Q_8 P_d.
\end{aligned}\right\} \tag{6.10}$$

Setting the right-hand side of the system (6.10) to zero and solving, we obtain

$$\left.\begin{aligned}
S_s^* &= \frac{\kappa_2 S_d^* + \xi_2 P_s^* + \Pi_1}{Q_1}, \quad P_s^* = \frac{\gamma_2 Q_1 P_d^* + \xi_1 u_1 \left(\kappa_2 S_d^* + \Pi_1\right)}{Q_1 Q_4 (1-\Phi_1)}, \\
S_d^* &= \frac{P_d^* \left(\gamma_2 \kappa_1 \xi_2 + Q_1 Q_4 (1-\Phi_1)\xi_4\right) + Q_4 \left(\kappa_1 \Pi_1 + \Pi_2 Q_1\right) - \xi_1 \xi_2 \Pi_2 u_1}{Q_4 \left(1-\Phi_5\right) - \xi_1 \xi_2 Q_5 u_1}, \\
P_d^* &= \frac{u_1 \left(\gamma_1 \kappa_2 \xi_1 \Pi_2 \left(1-\Phi_3\right) + \gamma_1 \xi_1 \Pi_1 Q_5 + \xi_3 Q_4 \left(\kappa_1 \Pi_1 + \Pi_2 Q_1\right)\right)}{\gamma_1 \gamma_2 \kappa_1 \kappa_2 \left(1-\Phi_3\right)\left(1-\Phi_4\right) + Q_1 Q_5 \left(Q_4 Q_8 \left(1-\Phi_2\right) - \gamma_1 \gamma_2\right) - Q_9},
\end{aligned}\right\} \tag{6.11}$$

where $Q_9 = \kappa_1 \kappa_2 Q_4 Q_8 + \xi_1 \xi_2 Q_5 Q_8 u_1$, $\Phi_1 = \frac{\xi_1 \xi_2 u_1}{Q_1 Q_4}$, $\Phi_2 = \frac{u_1 \xi_3 \xi_4}{Q_5 Q_8}$, $\Phi_3 = \frac{u_1 \xi_2 \xi_3}{\gamma_1 \kappa_2}$, $\Phi_4 = \frac{u_1 \xi_1 \xi_4}{\gamma_2 \kappa_1}$, $\Phi_5 = \frac{\kappa_1 \kappa_2}{Q_1 Q_5}$. Here Φ_1 indicates the fraction of individuals who move from either S_s or P_s and back. Furthermore, $(1-\Phi_1)$ shows the fraction of susceptible individuals who do not cycle between S_s and P_s. Similarly, Φ_2 indicates the fraction of susceptible individuals who move from S_d or P_d and vice versa. Furthermore, $(1-\Phi_2)$ shows the fraction of susceptible individuals who do not cycle between S_d and P_d. Φ_3 refers to the fraction of susceptible individuals on PrEP who move from either P_s to P_d or S_s to S_d and back. $(1-\Phi_2)$ shows the fraction of susceptible individuals who do not cycle from either P_s or P_d and S_s or S_d. On the other hand Φ_4 refers to the fraction of susceptible individuals who move from either S_s to P_s, or P_s to P_d, or P_d to S_d and vice versa. $(1-\Phi_4)$ shows the fraction of susceptible individuals who do not cycle from either S_s to P_s or P_s to P_d or P_d to S_d. Finally, Φ_5 indicates the fraction of susceptible individuals who move from either S_s or S_d and back with $(1-\Phi_5)$ defining the fraction of susceptible individuals who do not cycle between S_s and S_d.

6.4.1 The basic reproduction number, $\mathscr{R}_0$

The threshold parameter $\mathscr{R}_0$ is defined as the average cases of secondary infections generated by a single infectious individual in a completely susceptible population during his/her period of infectiousness (Diekmann et al., 1990; Van den Driessche and Watmough, 2002). Here, $\mathscr{R}_0$ is used to determine whether HIV will persist in the population. Thus, following the next-generation matrix operator defined in Van den Driessche and Watmough (2002), we begin by computing the threshold numbers for persistence of HIV in each risk group assuming that HIV is existent in a single isolated risk group. The HIV–free equilibrium in each isolated risk groups, that is, CSW and IDU are respectively given by

$$\left.\begin{aligned}\mathscr{E}_{\mathrm{s}}^0 &= \left[S_s^0, 0, 0, P_s^0\right] = \left[\frac{\Pi_1\left(\mu+\xi_2\right)}{\mu\left(\mu+\xi_2+\xi_1 u_1\right)}, 0, 0, \frac{\xi_1\Pi_1 u_1}{\mu\left(\mu+\xi_2+\xi_1 u_1\right)}\right],\\ \mathscr{E}_{\mathrm{d}}^0 &= \left[S_d^0, 0, 0, P_d^0\right] = \left[\frac{\Pi_2\left(\mu+\xi_4\right)}{\mu\left(\mu+\xi_4+\xi_3 u_1\right)}, 0, 0, \frac{\xi_3\Pi_2 u_1}{\mu\left(\mu+\xi_4+\xi_3 u_1\right)}\right].\end{aligned}\right\} \tag{6.12}$$

Let F and V define the matrix of new infection and the transmission, respectively. At the HIV–free equilibrium given in (6.12), the matrices F and V isolated in CSW are given by:

$$F = \begin{bmatrix} \frac{\beta\psi(1-u_2)(\mu+\xi_2)}{\mu+u_1\xi_1+\xi_2} & \frac{\beta\psi(1-u_2)\theta_1(\mu+\xi_2)}{\mu+u_1\xi_1+\xi_2} \\ 0 & 0 \end{bmatrix}, \quad V = \begin{bmatrix} \mu+u_3\alpha_1 & 0 \\ -u_3\alpha_1 & \mu \end{bmatrix}.$$

Similarly, the matrices F and V isolated in IDU are given by:

$$F = \begin{bmatrix} \frac{\delta(\mu+u_1\xi_3+\xi_4)+\beta\eta\psi(1-u_2)\theta_2(\mu+\xi_4)}{\mu+u_1\xi_3+\xi_4} & \frac{\beta\eta\psi(1-u_2)\theta_3(\mu+\xi_4)}{\mu+u_1\xi_3+\xi_4} \\ 0 & 0 \end{bmatrix}, V = \begin{bmatrix} \mu+u_3\alpha_2 & 0 \\ -u_3\alpha_2 & \mu \end{bmatrix}.$$

Thus, the threshold numbers evaluated at the respective HIV-free equilibrium of the isolated risk groups are given by

$$\left.\begin{aligned}\mathscr{R}_0^s &= \frac{(1-u_2)\beta\psi\left(\mu+\xi_2\right)\left(\mu+\alpha_1\theta_1 u_3\right)}{\mu\left(\mu+\alpha_1 u_3\right)\left(\mu+\xi_2+\xi_1 u_1\right)},\\ \mathscr{R}_0^d &= \frac{(1-u_2)\beta\eta\psi\left(\mu+\xi_4\right)\left(\theta_2\mu+\alpha_2\theta_3 u_3\right)+\delta\mu\left(\mu+\xi_4+\xi_3 u_1\right)}{\mu\left(\mu+\alpha_2 u_3\right)\left(\mu+\xi_4+\xi_3 u_1\right)}.\end{aligned}\right\} \tag{6.13}$$

Note that the threshold numbers in (6.13) correspond to CSW and IDU, respectively. However, if the HIV infection exists in a single risk group connected to another risk group through migration, then the movement of the individuals must be reflected in the threshold number. The matrices of new infection and transmission for CSW connected to IDU are respectively given by

$$F = \begin{bmatrix} \frac{(1-u_2)\psi\beta S_s}{N} & \frac{(1-u_2)\psi\beta\theta_1 S_s}{N} \\ 0 & 0 \end{bmatrix}, \quad V = \begin{bmatrix} Q_2 & 0 \\ -u_3\alpha_1 & Q_3 \end{bmatrix}.$$

On the other hand, the matrices of new infection and transmission for IDU connected to CSW are respectively given by

$$\begin{bmatrix} S_d(1-u_2)\left(\delta + \frac{\beta\eta\psi\theta_2}{N_1}\right) & \frac{\beta\eta\psi S_d(1-u_2)\theta_3}{N_1} \\ 0 & 0 \end{bmatrix}, \quad V = \begin{bmatrix} Q_6 & 0 \\ -u_3\alpha_2 & Q_7 \end{bmatrix}.$$

Thus, at HIV-free equilibrium $\mathscr{E}_0$, the risk group specific threshold numbers are respectively given by

$$\mathscr{R}_{0s} = \frac{\beta(1-u_2)\psi S_s(Q_3+\alpha_1\theta_1 u_3)}{NQ_2Q_3}, \quad \mathscr{R}_{0d} = \frac{(1-u_2)S_d(\delta N_1 Q_7 + \beta\eta\psi(\theta_2 Q_7 + \alpha_2\theta_3 u_3))}{NQ_6Q_7}, \tag{6.14}$$

where S_s and S_d are as defined in (6.11). To find the threshold number, $\mathscr{R}_0$, of the system (6.3)–(6.4), let F and V be the matrices of new infections and transmission, respectively. At the HIV-free equilibrium, $\mathscr{E}_0$, of the system (6.3)–(6.4), the matrices F and V are given by

$$F = \begin{bmatrix} \frac{(1-u_2)\beta\psi S_s}{N} & \frac{(1-u_2)\beta\psi\theta_1 S_s}{N} & \frac{(1-u_2)\beta\psi\theta_2 S_s}{N} & \frac{(1-u_2)\beta\psi\theta_3 S_s}{N} \\ 0 & 0 & 0 & 0 \\ \frac{(1-u_2)\eta\beta\psi S_d}{N} & \frac{(1-u_2)\eta\beta\psi\theta_1 S_d}{N} & S_d(1-u_2)\left(\delta + \frac{\beta\eta\psi\theta_2}{N_1}\right) & \frac{(1-u_2)\eta\beta\psi\theta_3 S_d}{N} \\ 0 & 0 & 0 & 0 \end{bmatrix},$$

$$V = \begin{bmatrix} Q_2 & 0 & -\omega_2 & 0 \\ -\alpha_1 u_3 & Q_3 & 0 & -\rho_2 \\ -\omega_1 & 0 & Q_6 & 0 \\ 0 & -\rho_1 & -\alpha_2 u_3 & Q_7 \end{bmatrix}.$$

Thus, the $\mathscr{R}_0$ which is the spectral radius of the matrix FV^{-1} is given as

$$\mathscr{R}_0 = \max\{\mathscr{R}_{0s}, \mathscr{R}_{0d}\}. \tag{6.15}$$

From Theorem 2 in (Van den Driessche and Watmough, 2002), the following result is established.

Theorem 6.1. *The HIV-free equilibrium $\mathscr{E}_0$ is locally asymptotically stable whenever $\mathscr{R}_0 < 1$ and unstable otherwise.*

6.5 HIV persistent equilibrium

In this section, we determine the number of possible HIV persistent steady states as expressed in (6.7)–(6.9).

6.5.1 HIV persistent state $\mathscr{E}_1$

In order to determine the possible solutions of the system around $\mathscr{E}_1$, we solve system (6.16) in terms of the infection term λ_1^c.

$$\left.\begin{aligned}
\frac{dS_s}{dt} &= \Pi_1 + \xi_2 P_s + \kappa_2 S_d - \lambda_1^c S_s - Q_1 S_s,\\
\frac{dU_s}{dt} &= \lambda_1^c S_s - Q_2 U_s,\\
\frac{dT_s}{dt} &= \alpha_1 u_3 U_s - Q_3 T_s,\\
\frac{dP_s}{dt} &= \xi_1 u_1 S_s + \gamma_2 P_d - Q_4 P_s,\\
\frac{dS_d}{dt} &= \Pi_2 + \kappa_1 S_s + \xi_4 P_d - Q_5 S_d,\\
\frac{dP_d}{dt} &= \xi_3 u_1 S_d + \gamma_1 P_s - Q_8 P_d.
\end{aligned}\right\} \tag{6.16}$$

Note that the existence of $\mathscr{E}_1$ is based on the assumption that there is no infection in IDU population. This implies that $I_d = T_d = 0$. Thus, equating the right-hand side of (6.16) to zero and solving, we get

$$S_s^* = \frac{\kappa_2 S_d^* + \xi_2 P_s^* + \Pi_1}{\lambda_1^{c*} + Q_1}, \quad U_s^* = \frac{\lambda_1 \left(\kappa_2 S_d^* + \xi_2 P_s^* + \Pi_1\right)}{Q_2 \left(\lambda_1^{c*} + Q_1\right)}, \quad T_s^* = \frac{\alpha_1 \lambda_1^{c*} u_3 \left(\kappa_2 S_d^* + \xi_2 P_s^* + \Pi_1\right)}{Q_2 Q_3 \left(\lambda_1^{c*} + Q_1\right)},$$
$$P_s^* = \frac{\gamma_2 P_d^* \left(\lambda_1^{c*} + Q_1\right) + \xi_1 u_1 \left(\kappa_2 S_d^* + \Pi_1\right)}{Q_4 \left(\lambda_1^{c*} + Q_1\right) - \xi_1 \xi_2 u_1}, \quad S_d^* = \frac{\left(\lambda_1^{c*} + Q_1\right)\left(\xi_4 P_d^* + \Pi_2\right) + \kappa_1 \left(\xi_2 P_s^* + \Pi_1\right)}{Q_5 \left(\lambda_1^{c*} + Q_1\right) - \kappa_1 \kappa_2},$$
$$P_d^* = \frac{u_1 \left(\gamma_1 \kappa_2 \xi_1 \Pi_2 \left(1 - \Phi_3\right) + \gamma_1 \xi_1 \Pi_1 Q_5 + \xi_3 Q_4 \left(\kappa_1 \Pi_1 + \Pi_2 \left(\lambda_1 + Q_1\right)\right)\right)}{\lambda_1 Q_4 Q_5 Q_8 - \xi_4 u_1 \left(\gamma_1 \kappa_2 \xi_1 \left(1 - \Phi_3\right) + \xi_3 Q_4 \left(\lambda_1 + Q_1\right)\right) - \xi_1 \xi_2 Q_5 Q_8 u_1 + Q_1 Q_4 Q_5 Q_8 + \Phi_{10}},$$

with $\Phi_9 = \frac{\gamma_1 \gamma_2}{Q_4 Q_8}$, $\quad \Phi_{10} = -\gamma_1 \gamma_2 \lambda_1 Q_5 - \gamma_1 \gamma_2 Q_1 Q_5 - \kappa_1 \kappa_2 Q_4 Q_8 \left(1 - \Phi_9\right) - \gamma_2 \kappa_1 \xi_2 \xi_3 u_1$. Substituting the expressions for U_s^* and T_s^* into λ_1^{c*} as defined in (6.2), we obtain the following expression

$$\begin{aligned} \lambda_1^{c*} \Pi^* Q_2 Q_3 ((Q_4 Q_5 Q_8 (1 - \Phi_2) - \gamma_1 \gamma_2 Q_5) \lambda_1^{c*} + (\gamma_1 \gamma_2 \kappa_1 \kappa_2 (1 - \Phi_3)(1 - \Phi_4) \\ - Q_1 Q_5 (\gamma_1 \gamma_2 - Q_4 Q_8 (1 - \Phi_2)) - \Phi_7)[1 - \mathscr{R}_{0s}]) = 0. \end{aligned} \tag{6.17}$$

The equation (6.17) gives $\lambda_1^{c*} = 0$ as one of the solutions. This solution corresponds to the HIV-equilibrium expressed in (6.6). If $\lambda_1^{c*} \neq 0$, then the following equation indicates the existence of endemic equilibrium.

$$\begin{aligned} (Q_4 Q_5 Q_8 (1 - \Phi_2) - \gamma_1 \gamma_2 Q_5) \lambda_1^{c*} + (\gamma_1 \gamma_2 \kappa_1 \kappa_2 (1 - \Phi_3)(1 - \Phi_4) \\ + Q_1 Q_5 (Q_4 Q_8 (1 - \Phi_2) - \gamma_1 \gamma_2) - \Phi_7)[1 - \mathscr{R}_{0s}] = 0. \end{aligned} \tag{6.18}$$

Equation (6.18) no positive solution for λ_1^{c*} when $\mathscr{R}_{0s} < 1$. However, if $\mathscr{R}_{0s} > 1$, equation (6.18) has one positive solution . Thus, we conclude that when $\mathscr{R}_{0s} > 1$ we have a unique HIV persistent equilibrium localized in the CSW population.

6.5.2 HIV persistent state $\mathscr{E}_2$

We note that with the absence of infection in CSW and IDU populations, we have the following system of equations.

$$\left.\begin{aligned}
\frac{dS_s}{dt} &= \Pi_1 + \xi_2 P_s + \kappa_2 S_d - Q_1 S_s,\\
\frac{dP_s}{dt} &= \xi_1 u_1 S_s + \gamma_2 P_d - Q_4 P_s,\\
\frac{dS_d}{dt} &= \Pi_2 + \kappa_1 S_s + \xi_4 P_d - (\lambda_2^c + \lambda_3^c) S_d - Q_5 S_d,\\
\frac{dU_d}{dt} &= (\lambda_2^c + \lambda_3^c) S_d - Q_6 U_d,\\
\frac{dT_d}{dt} &= \alpha_2 u_3 U_d - Q_7 T_d,\\
\frac{dP_d}{dt} &= \xi_3 u_1 S_d + \gamma_1 P_s - Q_8 P_d.
\end{aligned}\right\} \tag{6.19}$$

We express all the state variables in terms of λ_2^c, λ_3^c and U_d to obtain the following expressions.

$$S_s^* = \frac{\kappa_2 S_d^* + \xi_2 P_s^* + \Pi_1}{Q_1}, \quad P_s^* = \frac{\gamma_2 Q_1 P_d^* + \xi_1 u_1 \left(\kappa_2 S_d^* + \Pi_1\right)}{Q_1 Q_4 (1-\Phi_1)},$$
$$S_d^* = \frac{P_d^* \left(\gamma_2 \kappa_1 \xi_2 + \xi_4 Q_1 Q_4 (1-\Phi_1)\right) + Q_4 \left(\kappa_1 \Pi_1 + \Pi_2 Q_1\right) - \xi_1 \xi_2 \Pi_2 u_1}{Q_4 \left(Q_1 \left(\lambda_2^{c*} + \lambda_3^{c*} + Q_5\right) - \kappa_1 \kappa_2\right) - \xi_1 \xi_2 u_1 \left(\lambda_2^{c*} + \lambda_3^{c*} + Q_5\right)}, \quad T_d^* = \frac{\alpha_2 u_3 U_d^*}{Q_7},$$
$$P_d^* = \frac{u_1 \left(\Pi_1 \left(\gamma_1 \xi_1 \left(\lambda_2^{c*} + \lambda_3^{c*} + Q_5\right) + \kappa_1 \xi_3 Q_4\right) + \Pi_2 \left(\gamma_1 \kappa_2 \xi_1 + \xi_3 Q_1 Q_4 (1-\Phi_1)\right)\right)}{\Phi_{11} + Q_1 \left(Q_4 Q_8 (1-\Phi_9) \left(\lambda_2^{c*} + \lambda_3^{c*} + Q_5\right) - \xi_3 \xi_4 Q_4 u_1\right) - \xi_1 \xi_2 Q_8 u_1 \left(\lambda_2^{c*} + \lambda_3^{c*} + Q_5\right)},$$

where $\Phi_{11} = \gamma_1 \gamma_2 \kappa_1 \kappa_2 (1-\Phi_3)(1-\Phi_4) - \kappa_1 \kappa_2 Q_4 Q_8$. Now substituting the expressions for $S_d^*, T_d^*, \lambda_2^{c*}$ and λ_3^{c*} into the fourth equation in (6.19), we obtain the following equation.

$$U_d^* [V_2 U_d^{*2} + V_1 U_d^* + V_0] = 0, \tag{6.20}$$

where

$$V_2 = \beta \psi \eta \mu Q_6 \tau (1-u_2) (\theta_2 Q_7 + \alpha_2 \theta_3 u_3) (\xi_1 \xi_2 Q_8 u_1 - Q_1 Q_4 Q_8 (1-\Phi_{10})),$$
$$V_0 = \Pi^* Q_6 Q_7 (\gamma_1 \gamma_2 \kappa_1 \kappa_2 (1-\Phi_3)(1-\Phi_4) - Q_1 Q_5 (\gamma_1 \gamma_2 - Q_4 Q_8 (1-\Phi_2)) - \Phi_7) [1 - \mathscr{R}_{0d}].$$

$$V_1 = Q_6(\alpha_2\beta\eta\theta_3\mu\xi_1\xi_2Q_8u_1(1-u_2)u_3\psi + Q_7(Q_8(\kappa_1\kappa_2\Pi^*Q_4\tau + \xi_1\xi_2u_1(\Pi^*(\delta+Q_5\tau) + \beta\eta\theta_2\mu(1-u_2)\psi)) - \gamma_1\gamma_2\kappa_1\kappa_2\Pi^*\tau(1-\Phi_3)(1-\Phi_4))) + Q_1(\gamma_1\gamma_2(Q_6(Q_7(\Pi^*(\delta+Q_5\tau) + \beta\eta\theta_2\mu(1-u_2)\psi) + \alpha_2\beta\eta\theta_3\mu(1-u_2)u_3\psi) - \beta\eta\mu\Pi_2\tau(1-u_2)\psi(\theta_2Q_7+\alpha_2\theta_3u_3)) + Q_4(Q_6(Q_7(Q_8(-\Pi^*(\delta+Q_5\tau) - \beta\eta\theta_2\mu(1-u_2)\psi) + \xi_3\xi_4\Pi^*\tau u_1) - \alpha_2\beta\eta\theta_3\mu Q_8(1-u_2)u_3\psi) + \beta\eta\mu\Pi_2 Q_8\tau(1-u_2)\psi(\theta_2Q_7+\alpha_2\theta_3u_3))) + \beta\eta\mu\tau(1-u_2)\psi(\theta_2Q_7+\alpha_2\theta_3u_3)(\kappa_1\Pi_1Q_4Q_8 - \xi_1\xi_2\Pi_2Q_8u_1 - \gamma_1\gamma_2\kappa_1\Pi_1(1-\Phi_4)),$$

Note that the case $U_d^* = 0$, corresponds to the HIV-free equilibrium described previously. The remaining part of the equation (6.20) given by

$$V_2U_d^{*2} + V_1U_d^* + V_0 = 0, \tag{6.21}$$

gives the existence and the number of HIV persistent equilibria for the system (6.19). Note that when $\tau = 0$, equation (6.21) reduces to

$$\hat{V}_1U_d^* + V_0 = 0, \tag{6.22}$$

where

$$\hat{V}_1 = Q_6(\xi_1\xi_2Q_8u_1 - Q_1Q_4Q_8(1-\Phi_{10}))(Q_7(\delta(\Pi_1+\Pi_2) + \beta\eta\theta_2\mu(1-u_2)\psi) + \alpha_2\beta\eta\theta_3\mu(1-u_2)u_3\psi),$$

so that the system (6.19) has a unique HIV persistent equilibrium if and only if $\mathscr{R}_{0d} > 1$. These results can be summarized as follows:

Remark 6.1. *When $\tau = 0$, the system (6.19) has a unique positive HIV persistent equilibrium whenever $\mathscr{R}_{0d} > 1$ and no positive HIV persistent equilibrium otherwise.*

On the other hand $\tau \neq 0$, the solution of the polynomial (6.21) depends on the signs of V_1 and V_0, since $V_2 > 0$. Hence the following observations are made

- When $V_0 < 0$ (that is, when $\mathscr{R}_{0d} > 1$), we have exactly one solution for all values of V_1.

- When $V_0 > 0$ (that is, when $\mathscr{R}_{0d} < 1$), we have no positive solution if $V_1 > 0$ and two distinct positive solutions when $V_1 < 0$ expressed as

$$I^*_{d(1,1)} = \frac{-V_1 + \sqrt{V_1^2 - 4V_2V_0}}{2V_2}, \quad I^*_{d(1,2)} = \frac{-V_1 - \sqrt{V_1^2 - 4V_2V_0}}{2V_2}.$$

This scenario suggests that the system (6.19) exhibits backward bifurcation phenomenon. Epidemiologically, the existence of two positive roots when $\mathscr{R}_{0d} < 1$ implies that bringing $\mathscr{R}_{0d}$ below unity does not suffice for the eradication of HIV. The existence of backward bifurcation indicates that in the neighbourhood of 1, for $\mathscr{R}_{0d} < 1$, a stable HIV-free equilibrium coexists with two HIV persistent equilibria, that is , a smaller equilibrium (smaller number of infectious individuals) which is unstable and a larger equilibrium (with a larger number of infectious individuals) which is stable. These two HIV persistent equilibria disappear by saddle-node bifurcation when the basic reproduction $\mathscr{R}_{0d}$ is decreased below the critical value $\mathscr{R}^c_{0d}$ below which the HIV-free equilibrium (6.6) is globally stable. This critical threshold is obtained by setting the discriminant of the equation (6.21) to zero. Thus, we have

$$\mathscr{R}^c_{0d} = 1 - \frac{V_1^2}{4V_2[\Pi^* Q_6 Q_7 (\gamma_1\gamma_2\kappa_1\kappa_2 (1-\Phi_3)(1-\Phi_4) - Q_1 Q_5 (\gamma_1\gamma_2 - Q_4 Q_8 (1-\Phi_2)) - \Phi_7)]}. \tag{6.23}$$

From the equation (6.23), the following results are established.

Theorem 6.2.

- *Whenever $\mathscr{R}_{0d} > 1$, the system (6.19) has a unique HIV persistent equilibrium.*
- *If $\mathscr{R}^c_{0d} < \mathscr{R}_{0d} < 1$, then the system (6.19) has two HIV persistent equilibria which implies that the system (6.19) exhibits backward bifurcation.*
- *If $\mathscr{R}_{0d} < \mathscr{R}^c_{0d} < 1$, then the system (6.19) has only an HIV-free equilibrium, $\mathscr{E}_0$, which implies that HIV infection dies out of the population.*

6.5.3 Bifurcation analysis

This is a qualitative change in the behaviour and/or dynamics of a dynamical system produced by varying a parameter in the equation (Kuznetsov, 2013). Bifurcation occurs when $\mathscr{R}_{0d}$ changes its stability at 1. We investigate the nature of the bifurcation by employing the method introduced in Castillo-Chavez and Song (2004) which is based on the use of center manifold theory (Guckenheimer and Holmes, 2013). Therefore, we have the following Theorem.

Theorem 6.3. *The system* (6.19) *has a backward bifurcation at* $\mathscr{R}_{0d} = 1$ *if and only if* $V_1 < 0$ *and* $V_1^2 - 4V_2V_0 = \Delta > 0$.

Proof. We adopt the notations in Castillo-Chavez and Song (2004) and directly compute the values of a and b whose signs determine local dynamics of the system (6.19) without necessarily re-stating Theorem **4.1** in Castillo-Chavez and Song (2004). Let us set β as our bifurcation parameter, so that

$$\beta^* = \frac{NQ_7\left(\delta\left(1-u_2\right)S_d + Q_6\right)}{\eta\left(u_2-1\right)\psi S_d\left(\theta_2 Q_7 + \alpha_2\theta_3 u_3\right)},$$

where S_d is given in (6.11). We observe that the eigenvalues of the matrix, $J(\mathscr{E}_0, \beta^*)$,

$$\begin{bmatrix} -Q_1 & \xi_2 & \kappa_2 & 0 & 0 & 0 \\ \xi_1 u_1 & -Q_4 & 0 & 0 & 0 & \gamma_2 \\ \kappa_1 & 0 & -Q_5 & -\left(1-u_2\right)S_d\left(\delta + \frac{\beta^*\eta\theta_2\psi}{N}\right) & -\frac{\beta^*\eta\theta_3(1-u_2)\psi S_d}{N} & \xi_4 \\ 0 & 0 & 0 & \left(1-u_2\right)S_d\left(\delta + \frac{\beta^*\eta\theta_2\psi}{N}\right) - Q_6 & \frac{\beta^*\eta\theta_3(1-u_2)\psi S_d}{N} & 0 \\ 0 & 0 & 0 & \alpha_2 u_3 & -Q_7 & 0 \\ 0 & \gamma_1 & \xi_3 u_1 & 0 & 0 & -Q_8 \end{bmatrix},$$

admits a simple zero eigenvalue and the other eigenvalues are real and negative. Therefore, the HIV-free equilibrium $\mathscr{E}_0$, is non-hyperbolic equilibrium thereby verifying the assumption **A1** of Theorem **4.1** in Castillo-Chavez and Song (2004). To verify assumption **A2** of Theorem **4.1** in Castillo-Chavez and Song (2004), we denote a left and a right eigenvector associated with the zero eigenvalue as $\mathbf{v} = (v_1, v_2, v_3, v_4, v_5)$ and $\mathbf{w} = (w_1, w_2, w_3, w_4, w_5)^T$ respectively,

such that $\mathbf{v}.\mathbf{w} = 1$. It follows that the component of the left eigenvector associated with the zero eigenvalue are given in (6.24).

$$\left.\begin{aligned}
&v_1 = v_2 = v_3 = v_6 = 0, \quad v_4 = 1,\\
&v_5 = -\theta_3(1-u_2)(\mu+\delta(u_2-1)(\kappa_1(\Pi_1+\Pi_2)((\mu+\xi_2)(\mu+\xi_4+\rho_2)+\gamma_1(Q_8-\gamma_2))+\mu\Pi_2\\
&\quad(\gamma_1(Q_8-\gamma_2)+Q_8(\mu+\xi_2))+\xi_1u_1(\gamma_1(\xi_4(\Pi_1+\Pi_2)+\Pi_2(Q_7-\gamma_2))+\mu\Pi_2Q_8))/\gamma_1(\mu\xi_4Q_5\\
&\quad+\gamma_2(-Q_5(\mu+\xi_1u_1)-\kappa_1(\mu+\xi_3u_1))+\kappa_1(\mu Q_8+\xi_3Q_7u_1)+\rho_2Q_5(\mu+\xi_1u_1)+\mu Q_5(\mu\\
&\quad+\xi_1u_1))+\kappa_1(\xi_2(\mu Q_8+\xi_3u_1(Q_7-\gamma_2t))+\mu(\mu Q_8+\xi_3Q_7u_1))+\mu(\mu+\xi_2+\xi_1u_1)(\kappa_2Q_8\\
&\quad+\mu Q_8+\xi_3Q_7u_1t)+\alpha_2u_3+\omega_2)/(u_2-1)(\theta_2Q_7+\alpha_2\theta_3u_3).
\end{aligned}\right\} \tag{6.24}$$

Furthermore, the components of the right eigenvector associated with the zero eigenvalue are given in (6.25).

$$\left.\begin{aligned}
&w_1 = \frac{-(Q_6(\kappa_2Q_8(\gamma_1+\mu+\xi_2)+\gamma_2(\xi_2\xi_3u_1-\gamma_1\kappa_2))}{D}, \quad w_2 = \frac{-Q_6u_1w_4(\gamma_2\xi_3Q_1+\kappa_2\xi_1Q_8)}{D},\\
&w_3 = \frac{-Q_6(\gamma_1Q_1(Q_8-\gamma_2)+Q_8(\kappa_1(\mu+\xi_2)+\mu(\mu+\xi_2+\xi_1u_1)))}{D}, \quad w_4 = 1, \quad w_5 = \frac{\alpha_2u_3}{Q_7},\\
&w_6 = \frac{-Q_6u_1(\gamma_1(\kappa_2\xi_1+\xi_3Q_1)+\xi_3(\kappa_1(\mu+\xi_2)+\mu(\mu+\xi_2+\xi_1u_1)))}{D}.
\end{aligned}\right\} \tag{6.25}$$

where

$$\begin{aligned}
D = {}&\gamma_1(\kappa_1(\mu Q_8+\xi_3Q_7u_1)+\rho_2Q_5(\mu+\xi_1u_1)+\gamma_2(-\kappa_1(\mu+\xi_3u_1)-(\mu+\xi_1u_1)(\kappa_2+\mu+\xi_3u_1))\\
&+\mu(\mu+\xi_1u_1)(\kappa_2+\mu+\xi_3u_1)+\mu\xi_4(\kappa_2+\mu+\xi_1u_1))+\kappa_1(\mu Q_8(\mu+\xi_2)+\xi_3u_1(Q_7(\mu+\xi_2)\\
&-\gamma_2\xi_2))+\mu(\mu+\xi_2+\xi_1u_1)(Q_8(\kappa_2+\mu)+\xi_3Q_7u_1)
\end{aligned}$$

We can thus compute the coefficient a and b defined in Theorem **4.1** in Castillo-Chavez and Song (2004), i.e.

$$a = \sum_{k,i,j=1}^{3} v_k w_i w_j \frac{\partial^2 f_k}{\partial x_1 \partial x_j}(\mathscr{E}_0, \beta^*), \quad b = \sum_{k,i=1}^{3} v_k w_i \frac{\partial^2 f_k}{\partial x_1 \partial \beta^*}(\mathscr{E}_0, \beta^*).$$

Taking into account of system (6.19) and considering in a and b only the nonzero derivatives for the terms $\frac{\partial^2 f_k}{\partial x_1 \partial x_j}(\mathscr{E}_0, \beta^*)$ and $\frac{\partial^2 f_k}{\partial x_1 \partial \beta^*}(\mathscr{E}_0, \beta^*)$, it follows that

$$a = v_4 w_3 w_4 \frac{\partial^2 f_4}{\partial S_d \partial U_d}(\mathscr{E}_0, \beta^*) + v_4 w_3 w_5 \frac{\partial^2 f_4}{\partial S_d \partial T_d}(\mathscr{E}_0, \beta^*), \tag{6.26}$$

$$b = v_4 w_4 \frac{\partial^2 f_4}{\partial U_d \partial \beta^*}(\mathscr{E}_0, \beta^*) + v_4 w_5 \frac{\partial^2 f_4}{\partial T_d \partial \beta^*}(\mathscr{E}_0, \beta *). \tag{6.27}$$

In view of (6.24) and (6.25), the expressions in (6.26) and (6.27) can be explicitly expressed as given in (6.28) and (6.29), respectively.

$$\begin{aligned} a = & -[(Q_6^2(\gamma_1 Q_1(Q_8 - \gamma_2) + Q_8(\kappa_1(\mu + \xi_2) + \mu(\mu + \xi_2 + \xi_1 u_1))))/((1 - u_2)(\kappa_1(\Pi_1 + \Pi_2) \\ & (Q_8(\gamma_1 + \mu + \xi_2) - \gamma_1\gamma_2) + \mu\Pi_2(Q_8(\gamma_1 + \mu + \xi_2) - \gamma_1\gamma_2) + \xi_1 u_1(\gamma_1(\xi_4\Pi_1 + \Pi_2(\xi_4 \\ & + Q_7 - \gamma_2)) + \mu\Pi_2 Q_8)))]. \end{aligned} \tag{6.28}$$

$$\begin{aligned} b = & [(\eta\psi(\theta_2 Q_7 + \alpha_2\theta_3 u_3)(\kappa_1(\Pi_1 + \Pi_2)(Q_8(\gamma_1 + \mu + \xi_2) - \gamma_1\gamma_2) + \mu\Pi_2(Q_8(\gamma_1 + \mu + \xi_2) - \gamma_1\gamma_2) \\ & + \xi_1 u_1(\gamma_1(\xi_4\Pi_1 + \Pi_2(-\gamma_2 + \xi_4 + Q_7)) + \mu\Pi_2 Q_8)))/(Q_7(\Pi_1(\gamma_1(\mu^2 + \kappa_1 Q_8 + \rho_2 Q_5 - \gamma_2(\kappa_1 \\ & + \kappa_2 + \mu + \xi_3 u_1) + u_1(\mu\xi_1 + \xi_3(\kappa_1 + \mu + \xi_1 u_1)) + \kappa_2(\mu + \xi_4 + \xi_1 u_1) + \xi_4(\mu + \xi_1 u_1)) \\ & + \kappa_1(Q_8(\mu + \xi_2) + \xi_3 u_1(\gamma_2 + \mu + \xi_2)) + (\mu + \xi_2 + \xi_1 u_1)(Q_8(\kappa_2 + \mu) + \xi_3 Q_7 u_1)) \\ & + \Pi_2(\gamma_1(\gamma_2(-Q_1) + \kappa_1 Q_8 + \kappa_2(-\gamma_2 + \mu + \xi_4 + \rho_2 + \xi_1 u_1) + u_1(\kappa_1\xi_3 + \xi_1(\xi_4 + \rho_2 + \xi_3 u_1)) \\ & + \mu(\mu + \xi_4 + \rho_2 + (\xi_1 + \xi_3)u_1)) + (\mu + \xi_2 + \xi_1 u_1)(Q_8(\kappa_2 + \mu) + \xi_3 u_1(\gamma_2 + \mu)) \\ & + \kappa_1(Q_8(\mu + \xi_2) + \xi_3 u_1(\gamma_2 + \mu + \xi_2)))))]. \end{aligned} \tag{6.29}$$

Thus, $a < 0$ and $b > 0$. Hence, applying item (iv) of Theorem **4.1** in Castillo-Chavez and Song (2004), system (6.19) exhibits backward of forward bifurcation at $\mathscr{R}_{0d} = 1$. □

We summarize the above results in the following proposition:

Proposition 6.1. *If $\mathscr{R}_{0d} < 1$, system (6.19) exhibits a backward bifurcation when $\mathscr{R}_{0d} = 1$.If $\mathscr{R}_{0d} > 1$, system (6.19) exhibits a forward bifurcation when $\mathscr{R}_{0d} = 1$.*

The local dynamics in the neighbouring of the bifurcation value $\mathscr{R}_{0d} = 1$ is described in the former case in 6.1 by item (i) of Theorem **4.1** and in the latter case in 6.1 by the (iv)

of the same Theorem. These two scenarios are represented by the bifurcation diagrams in Figure 6.2(a) and Figure 6.2(b), obtained by considering suitable numerical values for the parameters of system (6.19). Figures 6.2(a) and 6.2(b) illustrate different bifurcations and show the effect of increased parameter values on the disease endemicity. A change in the qualitative behaviour of the system (6.19) is observed when $\mathscr{R}_{0d} = 1$. At $\mathscr{R}_{0d} = 1$, the epidemic is sustained in the population since each existing infection causes one new infection. In addition, it has been proven that sub-critical endemic equilibrium exists for values of the reproduction number less than one, which is unusual since HIV persistent steady state in general exists when the values of the reproduction number are above one. So the coexistence of the HIV-free equilibrium and the HIV persistent equilibrium when $\mathscr{R}_{0d} < 1$ makes it difficult to clear HIV from the population. In this case, there is no secondary transmission of HIV but it remains persistent. This describes the backward bifurcation, as shown in Figure 6.2(b). Figure 6.2(a) is obtained from Figure 6.2(b) by decreasing the value of τ. Figure 6.2(a) shows how reduction in drug user saturation changes a backward bifurcation into a forward bifurcation, making easier the control of HIV infection.

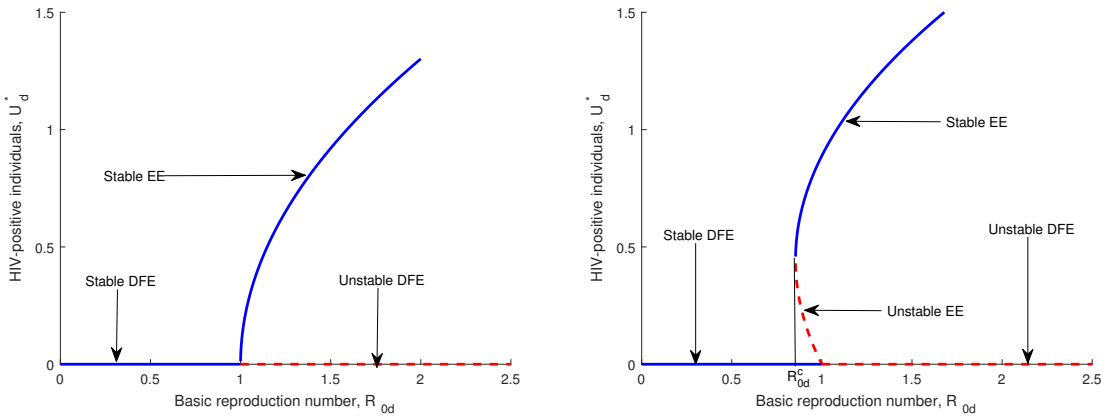

(a) (b)

Figure 6.2: Forward bifurcation in (a) for $\tau = 0.20$ and backward bifurcation in (b) for $\tau = 0.98$. The other parameters were fixed at the following values; $\Pi_1 = 100, \Pi 2 = 100, \psi = 2, \theta_2 = 0.0017, \theta_3 = 0.0021, \eta = 0.17, \alpha_2 = 0.0066, u_1 = 1, u_2 = 0, u_3 = 1, \mu = 0.0170, \delta = 0.000083, \tau = 0.20, \kappa_1 = 0.00036, \kappa_2 = 0.0023, \xi_1 = 0.0068, \xi_2 = 0.0036, \xi_3 = 0.0016, \xi_4 = 0.000011, \gamma_1 = 0.039, \omega_2 = 0.00018, \rho_2 = 0.00125, \gamma_2 = 0.00025$.

6.6 Numerical simulations

In this section, we investigate the impact of PrEP in the reduction of HIV infection. We use the parameter values and the initial conditions presented in sub-section 6.2.2. We begin our simulations with the assumption that at the start only 10% have been taking PrEP ($\xi_1 = 0.1, \xi_3 = 0.1$) and the default rates leading to relapse to susceptible classes are fixed at 0.05 and 0.06 for ξ_2 and ξ_4, respectively. The rates of PrEP uptake are increased gradually from 0.1 to 0.4 and then to 0.9, to check any changes in the HIV infections. From the results in Figure 6.3, we observe that PrEP reduces the number of individuals with HIV infection (*see*, Figures 6.3(a) and 6.3(b)). It is important to note that with an increase in the PrEP uptake, there is a decline in the HIV infections which consequently leads to a decrease in the number of individuals under the ART treatment (*see*, Figures 6.3(c) and 6.3(d)). On the other hand, the simulation results show that the number of susceptible individuals taking PrEP will gradually increase with its uptake. This can be seen in Figures 6.3(e) and 6.3(f). Thus, it is important to establish the optimal proportion of susceptible individuals that should take PrEP by taking into consideration the cost of PrEP uptake. An optimal control problem is formulated in Section 6.7. The results in Table 6.2 show that if

Table 6.2: The number of secondary cases of infection in each group as well as for the two groups combined. The reproduction numbers are given as defined by the interaction between the rows and columns. Note that the dash mark cells are assumed to be identically zero.

	$\xi_1 = \xi_3 = 0.1$				$\xi_1 = \xi_3 = 0.4$				$\xi_1 = \xi_3 = 0.9$			
	$\mathscr{R}_0^s$	$\mathscr{R}_0^d$	$\mathscr{R}_{0s}$	$\mathscr{R}_{0s}$	$\mathscr{R}_0^s$	$\mathscr{R}_0^d$	$\mathscr{R}_{0s}$	$\mathscr{R}_{0s}$	$\mathscr{R}_0^s$	$\mathscr{R}_0^d$	$\mathscr{R}_{0s}$	$\mathscr{R}_{0s}$
$\mathscr{R}_0^s$	15.92	-	-	-	5.698	-	-	-	2.753	-	-	-
$\mathscr{R}_0^d$	-	10.07	-	-	-	3.744	-	-	-	1.829	-	-
$\mathscr{R}_{0s}$	-	-	1.318	-	-	-	0.3081	-	-	-	0.1342	-
$\mathscr{R}_{0d}$	-	-	-	2.055	-	-	-	0.5779	-	-	-	0.2629
$\mathscr{R}_0$		2.055				0.5779				0.2629		

the connections between groups were broken, the epidemic would still be self-sustaining in CSW given that $\mathscr{R}_0^s = 15.92, 5.698, 2.753$. Similarly, the epidemic in CSW and IDU would each be self-sustaining but transmission in these groups is much easier to control since the reproduction numbers are smaller with increase in PrEP uptake. Thus, controlling HIV infection in the whole network will ultimately depend on controlling much of the infections in CSW.

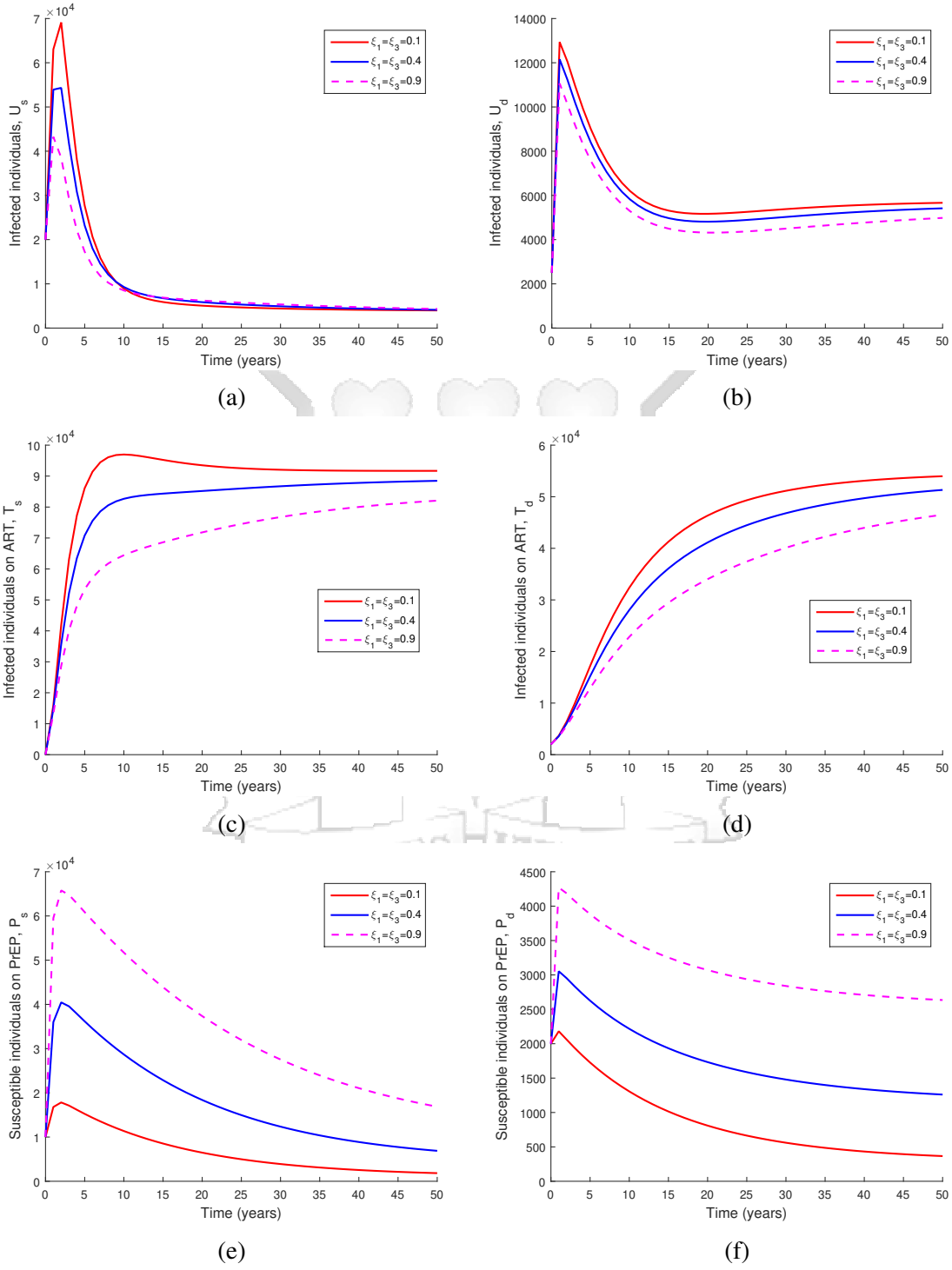

Figure 6.3: Simulation results of the system (6.3)–(6.4). The panels (a)–(f), respectively, show the evolution of the $U_{s,d}$, $T_{s,d}$ and $P_{s,d}$. The parameter values and the initial conditions used are presented in sub-section 6.2.2.

6.7 Optimal control problem

For the non-autonomous system (6.3)–(6.4), the rate of change of the total population is given by

$$\frac{dN}{dt} = \Pi^* - \mu N.$$

For bounded Lebesgue measurable controls and non-negative initial conditions, non-negative bounded solutions to the state system exist (Lukes, 1982). The objective of control is to minimize the number of new HIV infections while keeping the costs of the control as low as possible. To achieve this objective we must incorporate the relative costs associated with each policy (control) or combination of policies directed towards controlling the spread of HIV. We define the objective function as

$$J(u_1,u_2,u_3) = \int_0^{t_f} \left[A_1 P_{s,d} + A_2 U_{s,d} + A_3 T_{s,d} + \frac{1}{2}\sum_{i=1}^{3} B_i u_i^2 \right] dt, \tag{6.30}$$

and the control set

$$\Delta = \left\{ (u_1,u_2,u_3) | u(t) \text{ is Lebesgue measurable on } [0,t_f], 0 \le u_i(t) \le 1, i = 1,2,3 \right\}.$$

The terms A_i, for $i = 1,2,3$, in the integrand J represent the benefit of $P_{s,d}, U_{s,d}$ and $T_{s,d}$ sub-populations, describing the comparative significance of the terms in the functional. For instance, a high value of A_1 means that it is more important to reduce the burden of HIV as reduce the costs related to all control strategies (Buonomo, 2011). Non-negative constants $B_i, i = 1,2,3$ are weights for protection, prevention and treatment respectively, which regularize the optimal control. In order to conform to work on optimal control studied in Buonomo (2011); Dias et al. (2015); Moulay et al. (2012); Zaman et al. (2008), we choose a linear function for the cost on infection, $A_1 P_{s,d}$, $A_2 U_{s,d}$, $A_3 T_{s,d}$ and quadratic forms for the cost on the controls $B_1 u_1^2$, $B_2 u_2^2$ and $B_3 u_3^2$. This is because an epidemiological control can be likened to an expenditure of energy by bringing to the applications of physics in control theory, minimize u_i is like minimize u_i^2, because $u_i > 0, i = 1,2,3$ and quadratic controls give rise to controls as feedback law, which is convenient for calculations.

6.7.1 Existence of an optimal control

Consider the control problem with system (6.3)–(6.4), there exists $u^* = (u_1^*, u_2^*, u_3^*)$ such that

$$J(u_1^*, u_2^*, u_3^*) = \min_{(u_1,u_2,u_3)\in \mathbf{U}} J(u_1, u_2, u_3). \tag{6.31}$$

Proof. To prove the existence of an optimal control, we employ the results in Fleming and Rishel (2012). Following Theorem 4.1 in Fleming and Rishel (2012), we check if the following conditions are met.

- The set of controls and corresponding state variables is non empty.
- The control set Δ is convex and closed.
- The right hand side of the state system is bounded by a linear function in the state and control.
- The integrand of the objective functional is convex.
- There exist constants $c_1 > 0, c_2 > 0,$ and $\beta > 1$ such that the integrand of the objective functional is bounded below by $c_1 \left(\sum_{i=1}^{3} |u_i|^2 \right) - c_2$.

To verify these conditions, we use the result from Lukes (1982) to give the existence of solutions for the state system (6.3)–(6.4) with bounded coefficients, which gives the first condition. Since by definition, the control set Δ is bounded , then the second condition is satisfied. The right hand side of the state system (6.3)–(6.4) satisfies the third condition since the state solutions are bounded. The integrand of our objective functional is clearly convex on Δ, which satisfies the forth condition. There are $c_1 > 0, c_2 > 0$ and $\beta > 1$ satisfying $A_1 P_{s,d} + A_2 U_{s,d} + A_3 T_{s,d} + \frac{1}{2}\sum_{i=1}^{3} B_i u_i^2 \geq c_1 \left(\sum_{i=1}^{2} |u_i|^2 \right) - c_2$ since the state variables are bounded hence the fifth condition is satisfied. Thus, we conclude that there exists an optimal control problem $u^* = (u_1^*, u_2^*, u_3^*)$ that minimizes the objective functional $J = (u_1, u_2, u_3)$. □

6.7.2 Characterization of an optimal control

The necessary conditions that an optimal control problem must satisfy are given by Pontryagin's Maximum Principle (PMP) (Pontryagin, 1987). Pontryagin's Maximum Principle converts the system (6.3)–(6.4) into a problem of minimizing point wise a Hamiltonian **H**, with respect to u_1, u_2, u_3, where

$$\begin{aligned}\mathbf{H} = {} & A_1 P_{s,d} + A_2 U_{s,d} + A_3 T_{s,d} + \frac{1}{2}\sum_{i=1}^{3} B_i u_i^2 + \chi_1[\Pi_1 + \xi_2 P_s + \kappa_2 S_d - \lambda_1^c S_s \\ & - (\mu + u_1(t)\xi_1 + \kappa_1)S_s] + \chi_2[\lambda_1^c S_s + \omega_2 U_d - (\alpha_1 u_3(t) + \omega_1 + \mu)U_s] + \chi_3[\alpha_1 u_3(t)U_s \\ & + \rho_2 T_d - (\rho_1 + \mu)T_s] + \chi_4[\xi_1 u_1(t)S_s + \gamma_2 P_d - (\gamma_1 + \xi_2 + \mu)P_s] + \chi_5[\Pi_2 + \kappa_1 S_s \\ & + \xi_4 P_d - (\lambda_2^c + \lambda_3^c)S_d - (\mu + \kappa_2 + u_1(t)\xi_3)S_d] + \chi_6[(\lambda_2^c + \lambda_3^c)S_d + \omega_1 U_s - (\alpha_2 u_3(t) \\ & + \omega_2 + \mu)U_d] + \chi_7[\alpha_2 u_3(t)U_d + \rho_1 T_s - (\rho_2 + \mu)T_d] + \chi_8[\xi_3 u_1(t)S_d + \gamma_1 P_s \\ & - (\gamma_2 + \xi_4 + \mu)P_d].\end{aligned} \tag{6.32}$$

Here, $\chi_i, i = 1, 2, \cdots, 8$ are the adjoint variables or co-state variables. The Hamiltonian H represents the flow of controls and the change in the infection rates. The adjoint variables are the marginal values of the state variables which measures change in infection with change in control input. Using Pontryagin's Maximum Principle, the following result is obtained.

Theorem 6.4. *Given an optimal control*

$$u^* = (u_1^*,\ u_2^*,\ u_3^*),$$

and solutions

$$S_s,\ U_s,\ T_s,\ P_s,\ S_d,\ U_d,\ T_d,\ P_d,$$

of the corresponding state system (6.3)–(6.4)*, there exist adjoint variables* $\chi_1,\ \chi_2,\ \chi_3,\ \chi_4,\ \chi_5,\ \chi_6,\ \chi_7,\ \chi_8$ *satisfying,*

$$
\left.
\begin{aligned}
\frac{d\chi_1(t)}{dt} &= (1-u_2)\lambda_1(\chi_1-\chi_2)+\kappa_1(\chi_1-\chi_5)+u_1\xi_1(\chi_1-\chi_4)+\chi_1\mu,\\
\frac{d\chi_2(t)}{dt} &= (1-u_2)\frac{\beta\psi}{N}\left(S_s(\chi_1-\chi_2)+\eta S_d(\chi_5-\chi_6)\right)+\alpha_1u_3(\chi_2-\chi_3)+\omega_1(\chi_2-\chi_6)+\chi_2\mu-A_2,\\
\frac{d\chi_3(t)}{dt} &= (1-u_2)\frac{\beta\psi\theta_1}{N}\left(S_s(\chi_1-\chi_2)+\eta S_d(\chi_5-\chi_6)\right)+\rho_1(\chi_3-\chi_7)+\chi_3\mu-A_3,\\
\frac{d\chi_4(t)}{dt} &= \xi_2(\chi_4-\chi_1)+\gamma_1(\chi_4-\chi_8)+\chi_4\mu-A_1,\\
\frac{d\chi_5(t)}{dt} &= (1-u_2)(\chi_5-\chi_6)(\lambda_2+\lambda_3)+\kappa_2(\chi_5-\chi_1)+u_1\xi_3(\chi_5-\chi_8)+\chi_5\mu,\\
\frac{d\chi_6(t)}{dt} &= (1-u_2)\frac{\beta\psi\theta_2}{N}\left(S_s(\chi_1-\chi_2)+\eta S_d(\chi_5-\chi_6)\right)+\alpha_2u_3(\chi_6-\chi_7)+\omega_2(\chi_6-\chi_2)\\
&\quad+(\chi_5-\chi_6)\frac{\delta(1+\tau(U_d-1))}{(1+\tau U_d)^2}S_d+\chi_6\mu-A_2,\\
\frac{d\chi_7(t)}{dt} &= (1-u_2)\frac{\beta\psi\theta_3}{N}\left(S_s(\chi_1-\chi_2)+\eta S_d(\chi_5-\chi_6)\right)+\rho_2(\chi_7-\chi_3)+\chi_7\mu-A_3,\\
\frac{d\chi_8(t)}{dt} &= \xi_4(\chi_8-\chi_5)+\gamma_2(\chi_8-\chi_4)+\chi_8\mu-A_1,
\end{aligned}
\right\} \tag{6.33}
$$

with the boundary conditions

$$
\chi_i(t_f)=0, \quad i=1,2,\cdots,8, \tag{6.34}
$$

as expressed as

$$
u_i^*=\begin{cases} 0 & \text{if } u_i\le 0,\\ u_i & \text{if } 0<u_i<1,\\ 1 & \text{if } u_i\ge 1. \end{cases} \tag{6.35}
$$

Furthermore, the control functions u_1^*, u_2^* and u_3^* are given by

$$
u_1^*=\max\left\{\min\left\{\frac{1}{B_1}\left[(\chi_1-\chi_4)\xi_1S_s^*+(\chi_5-\chi_8)\xi_3S_d^*\right],1\right\},0\right\}, \tag{6.36}
$$

$$
u_2^*=\max\left\{\min\left\{\frac{1}{B_2}\left[(\chi_2-\chi_1)\lambda_1^*S_s^*+(\chi_6-\chi_5)S_d^*(\lambda_2^*+\lambda_3^*)\right],1\right\},0\right\}, \tag{6.37}
$$

$$
u_3^*=\max\left\{\min\left\{\frac{1}{B_3}\left[\alpha_1I_s^*(\chi_2-\chi_3)+\alpha_2I_d^*(\chi_6-\chi_7)\right],1\right\},0\right\}. \tag{6.38}
$$

Proof. The differential equations governing the adjoint variables are obtained by differentiation of the Hamiltonian function, evaluated at the optimal control. Then the adjoint system

can be written as

$$\frac{d\chi_1}{dt} = -\frac{\partial H}{\partial S_s}, \quad \frac{d\chi_2}{dt} = -\frac{\partial H}{\partial U_s}, \quad \frac{d\chi_3}{dt} = -\frac{\partial H}{\partial T_s}, \quad \frac{d\chi_4}{dt} = -\frac{\partial H}{\partial P_s},$$
$$\frac{d\chi_5}{dt} = -\frac{\partial H}{\partial S_d}, \quad \frac{d\chi_6}{dt} = -\frac{\partial H}{\partial U_d}, \quad \frac{d\chi_7}{dt} = -\frac{\partial H}{\partial T_d}, \quad \frac{d\chi_8}{dt} = -\frac{\partial H}{\partial P_d},$$

with zero final time conditions (transversality). To get the characterization of the optimal control as expressed in (6.36)–(6.38), we follow the work done in Lenhart and Workman (2007); Omondi et al. (2017b); Rodrigues et al. (2014) and solve the equations on the interior of the control set,

$$\frac{\partial H}{\partial u_i} = 0, \quad i = 1,2,3.$$

Using the bounds on the controls, we obtain the desired characterization as defined in (6.33)-(6.38). □

6.8 Numerical results

The optimal control model is simulated with the initial data given in section 6.2.2 and detailed parameter values in Table 6.1. We use iterative scheme to solve the optimality system. First, we solve the system (6.3)–(6.4) with a guess for the controls over the simulated time using fourth order Runge-Kutta scheme in Matlab (MATLAB, 2019). Next, we use the current iterations solutions of the state equations (6.3)–(6.4) to solve the adjoint equations (6.33) by backward fourth order Runge-Kutta scheme. Lastly, we update the controls by using a convex combination of the previous controls and the values from the characterizations as expressed in (6.36)–(6.38). The values chosen for the weights in the objective functional J are given as $A_1 = A_2 = A_3 = 100, \quad B_1 = B_2 = B_3 = 1000$. We simulated the system (6.3)–(6.4) in a period of twenty five years $(t_f = 25)$. The following initial state variables are used to illustrate the effect of different optimal control strategies on the HIV infection within and between the two key populations. $S_s(0) = 2000, \quad U_s(0) = 200, \quad T_s(0) = 100, \quad P_s(0) = 100, \quad S_d(0) = 1200, \quad U_d(0) = 250, \quad T_d(0) = 100, \quad P_d(0) = 200$. We study the effect of combining control u_1 on PrEP, control u_2 on prevention and control u_3 on ART treatment. In

Figures 6.4(a) and 6.4(b), we observe that the control strategies resulted in a decrease in the number of infected individuals not on treatment compared to the case without control. In Figures 6.4(c) and 6.4(d) it is seen that with the control strategies, there is an increase in the number of infected individuals on treatment in comparison to the case without control. The results in Figures 6.4(e) and 6.4(f) indicate that there are more susceptible individuals on PrEP with the control strategies in place as opposed to the case without control. The results in Figure 6.5(c) show that optimal control u_3 is applied at the upper bound throughout the simulation period. This is suggestive of the fact that more emphasis should be put on ART treatment for the infected individuals so as to ensure the suppression of the viral load. On the other hand, in Figures 6.5(a) and 6.5(b), both controls for u_1 and u_2 dropped gradually from the upper bound to the lower bound after 17 years and 8 years, respectively. prevention as well as treatment. The results are suggestive that both prevention and treatment programs should be efficient and timely.

In Figures 6.5(d), 6.5(e) and 6.5(f) we give a comparison of infected individuals not on treatment, infected individuals on treatment (ART treatment) and susceptible individuals on PrEP for the optimal control model. There is observed higher severity of the infection in the injection drug users population compared to the commercial sex workers as shown in Figure 6.5(d). Thus, the infection reaches a self-limiting phase much earlier in the commercial sex workers population than in both the injection drug users. Furthermore, with the controls, more injection drug users could be enrolled on treatment (ART treatment) as compared to the commercial sex works according to the findings in Figure 6.5(e). Our model predicts that in the long term, higher proportion of susceptible individuals in the commercial sex workers, may be, may take up PrEP as a measure to protect themselves from acquiring infections, see Figure 6.5(f).

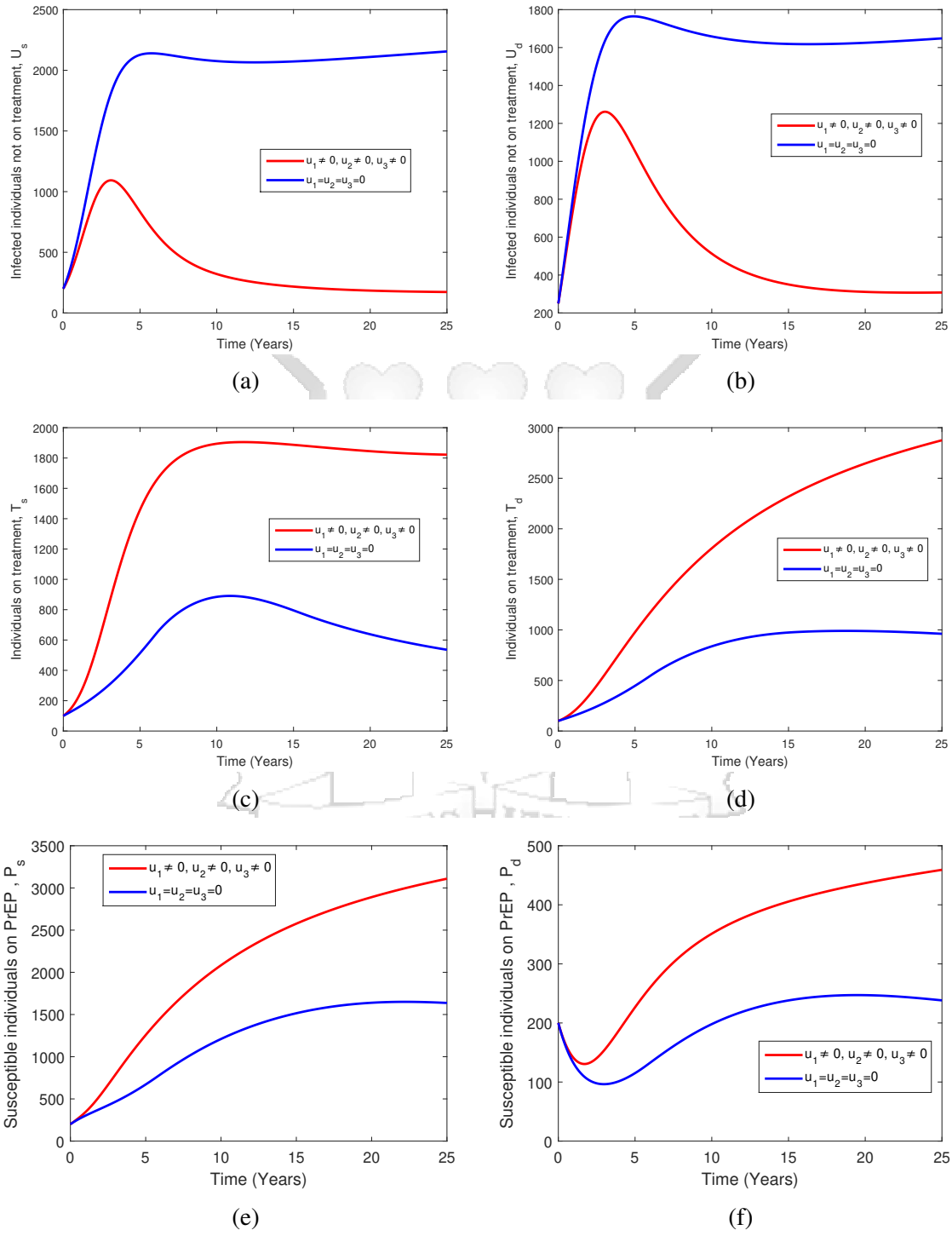

Figure 6.4: Simulation results of optimal control of the system (6.3)–(6.4). The panels (a)–(f), respectively, show the evolution of the $U_{s,d}$, $T_{s,d}$ and $P_{s,d}$.

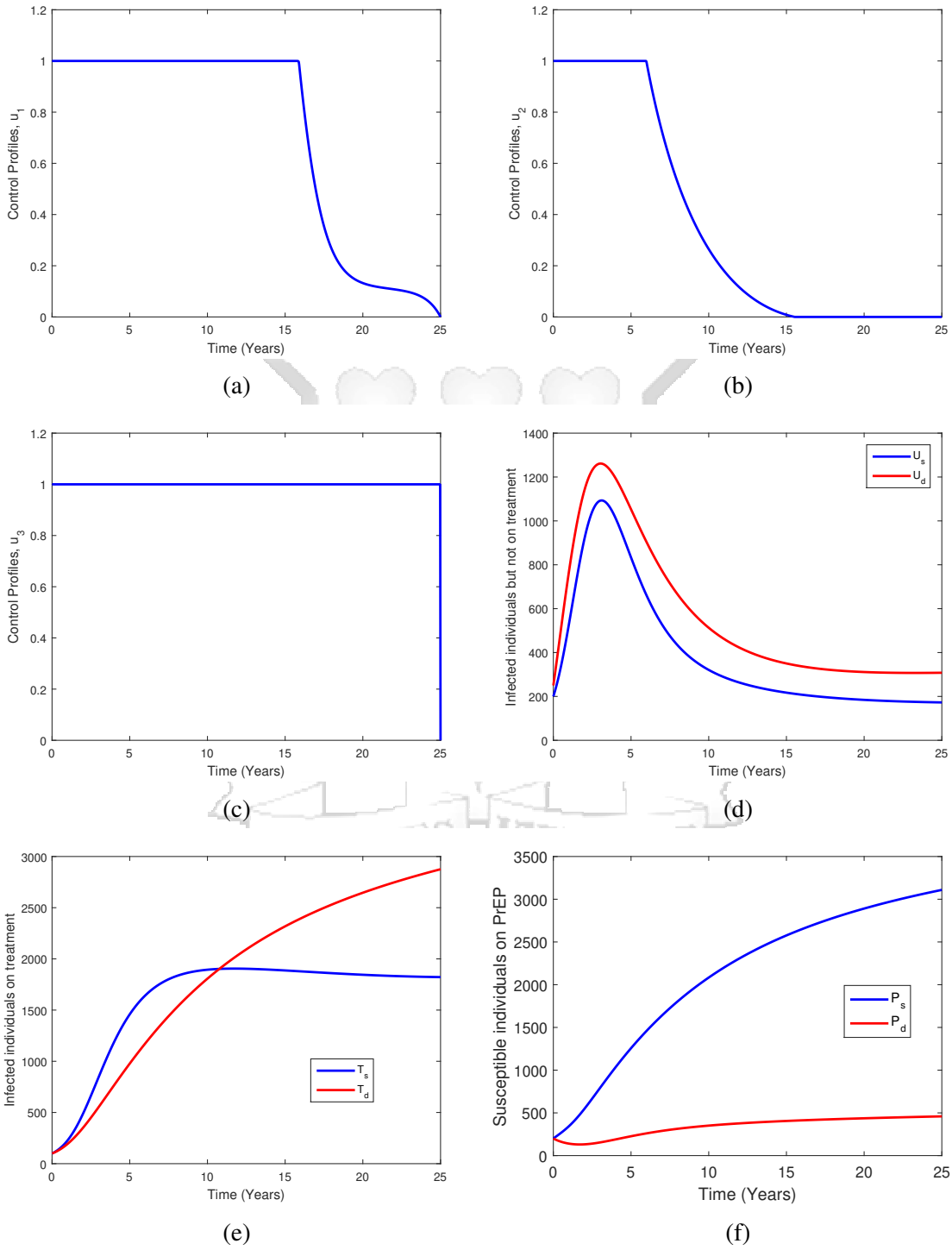

Figure 6.5: Panel (a) shows the evolution of the control strategy u_1, panel (b) shows that of the control strategy u_2 while panel (c) shows that of u_3. Comparison of infected individuals not on treatment, infected individuals on treatment (ART treatment), and the susceptible individuals on PrEP for the optimal control model are shown in panels (d), (e) and (f), respectively.

6.9 Conclusion

In this Chapter, a deterministic model for HIV dynamics between two key risk population (CSW, and IDU) is presented. Vital mathematical features which include; the invariant region of biological significance, key population specific disease thresholds for isolated, non-isolated key risk population connected by migration as well as the model disease threshold were presented. The analytical results indicate that $\mathscr{R}_{0d}$ is indeed the threshold for injection drug user when $\tau = 0$. When the saturation parameter $\tau > 0$, the system exhibits the phenomenon of backward bifurcation where a HIV-free equilibrium and two non-trivial equilibria coexist. A change in the qualitative behaviour of the system is observed when $\mathscr{R}_{0d} = 1$. At $\mathscr{R}_{0d} = 1$, the epidemic is sustained in the population since each existing infection causes one new infection. The appearance of backward bifurcation indicates that it is not sufficient to decrease the basic reproduction number below unity for the containment of HIV in the population. Thus, to effectively control the spread of HIV infection one has to reduce $\mathscr{R}_{0d}$ below another threshold referred to as the critical value of the basic reproduction number $\mathscr{R}^c_{0d}$. This is to mean that, HIV can be contained if $\mathscr{R}_{0d} < \mathscr{R}_{0d} < 1$. It is important to note that although the parameter τ might be present in the model, not every value of τ will lead to bi-stability. Instead τ has to be greater than a certain threshold $\tau_c = 0.20$. The results suggest that the saturation parameter τ is the one responsible for backward bifurcation. Thus, interventions that aim at limiting the accumulation of injection drug users in the community coupled with HIV treatment will be ideal in containing the proliferation of HIV.

We considered three time dependent controls as a way out, to ensure the control of the disease in a finite time. We performed optimal control analysis of the model. From the numerical results we concluded that the optimal strategy to effectively control HIV is the combination of PrEP, educational campaigns on the prevention of new infections and ART treatment. However, this conclusion must be taken with caution because of the uncertainties around the parameter values and to the budget/resource limitation. These results have the potential to help in the control programs against HIV infections within and between the key risk population by modifying the implementation of current interventions, or by adding new control mechanisms. The model presented in this chapter is a very simplified caricature

of a complex interaction of key risk populations and hence it has some cogent limitations. For example, the model does not take into account the ages of the individuals in the key risk populations. There is also paucity of experimental data for model verification. There are several ways to circumvent these limitations. First, there is a need to link the model to data for a clearer estimation of parameter values. Second, the development of mathematical models elucidating ages of the individuals in the key risk population will greatly advance our understanding of HIV dynamics within and between the key risk populations. Despite the highlighted limitations, the model results have significant bearings on HIV dynamics in the key risk populations.

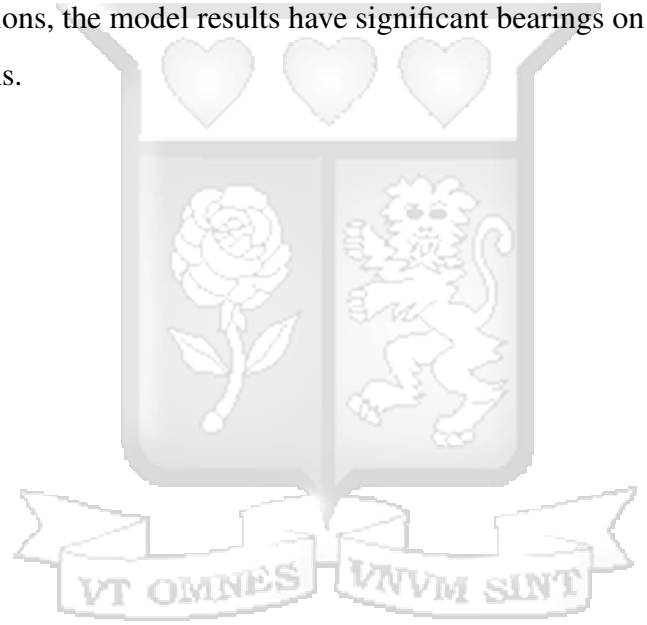

Chapter 7

Discussion and Conclusion

7.1 Introduction

In this thesis, mathematical models have been used to study HIV dynamics in Kenya with the main aim of determining the potential impact of HIV intervention strategies that include HTC, ART treatment and PrEP. Four key factors were considered, that is, the importance of PrEP uptake, HIV dynamics with movement between key populations that include commercial sex workers, injection drug users and males who have sex with males, sex orientation of the HIV patients and optimal control of the infection. Our study of HIV infection with focus on its control and eventual containment, HIV dynamics between key populations and optimal control of the infection in the model of HIV infection between key population is the first of the kind.

7.2 Discussion and conclusion

In Chapter 3, a mathematical model is presented to study the overall trend of HIV infection in Kenya factoring the main HIV intervention that mainly involves the use of ART. Based on the definition in Van den Driessche and Watmough (2002) and the subsequent computational procedure therein contained, the basic reproduction number, denoted by $\mathscr{R}_0$, for the model was computed. Global stability analysis of the disease-free equilibrium was carried out to prove that the infection would be contained if the basic reproduction number is less than unity and the infection would persist if it is greater than unity. Routine data from national survey is used to assess the variation of the new HIV infections in Kenya. Based on this data, least squares method was used to estimate the unknown parameters. The HIV incidence shows of

an infection at an endemic state implying of ceaseless problem. Furthermore, improvement in immunological status of the HIV patients on ART due to attrition, may lead to decline in HIV infection and be beneficial to the disease control. When comparing our model results to other models, we focused on the impact of test and treat. Most studies have modelled the impact of ART treatment on the spread of HIV (Isdory et al., 2015; Kiss et al., 2010; Podder et al., 2011; Sahu and Dhar, 2015). For example, Kiss et al. (2010), modelled HIV transmission and established that a proportion of the population that can respond to HIV by taking measures to avoid infection or if infected by seeking treatment early. Kok et al. (2015) findings suggested that optimal resource allocation favours routine testing in high prevalence settings over targeted testing and that a greater impact would be achieved by allocating more resources to routine testing in high prevalence settings. Our findings suggested that treatment with ART greatly aids the decline in HIV infections hence strengthening its intensity will effectively contribute to the disease control.

A mathematical model describing the dynamics of HIV transmission by incorporating sexual orientation of individuals is developed in in Chapter 4. Equilibrium points and the basic reproduction number are derived. The basic reproduction number provides a threshold that determines whether or not the disease fades away. The model, described by non-linear ODEs, shows existence of unique disease-free and disease-persistent equilibria. Least squares curve fitting is presented to quantitatively investigate the trend of infection within each gender. We further investigated the effect of the introduction of pre-exposure prophylaxis (PrEP) on the dynamics of the HIV. Other studies that have modelled the impact of PrEP have suggested that HIV can be effectively controlled if in addition to the current rate of administration of antiretroviral therapy in the community, at least 61-77% (with mean of about 70%) of the susceptible are on PrEP (Afassinou et al., 2017; Kim et al., 2014; Li et al., 2018; Podder et al., 2011; Silva and Torres, 2017; Simpson and Gumel, 2017). Our model results are indicative of a higher infectivity in the female population. Our findings show that the introduction of PrEP has had a positive effect on the limitation of spread of HIV when the coverage is maintained at slightly above 40%. Although our study assumes the same efficacy for both the males and females. Sensitivity analysis results show that control of effective contacts can result in control of the disease across gender divide. The model provides a unique

opportunity to influence policy on HIV treatment and management. A model by Simpson and Gumel (2017) showed that, if the current rate of administration of anti-retroviral treatment is maintained, HIV burden decreases with increasing PrEP coverage. This is, thus comparable to the reduction estimated by our model. What is new in our study is that we have considered test and treat as well as PrEP up-take.

In Chapter 5, we formulated and analysed a mathematical compartmental model of HIV transmission within and between two age groups in Kenya. We fitted the model to data using MCMC technique and inferred the parameters. Models that have used similar techniques in estimating parameters include (Sardar et al., 2016; Sasmal et al., 2018). We also estimated the reproduction numbers, namely within age group transmission and between age groups transmission basic reproduction numbers. When comparing our model to other models, we explicitly considered sex-oriented model stratified by age as motivated by the available Kenyan data. For instance, Mukandavire et al. (2009), modelled a sex-structured model for heterosexual transmission of HIV/AIDS with explicit incubation period and provided an in-depth and complete qualitative analysis. However, the model neglected stratification by age. In another study, Mukandavire and Garira (2007a) considered heterosexual interactions of males and females using integro-differential equations with a time delay due to incubation period. While they incorporated the effects of male and female condom use as the main mode of preventing HIV infection, no real-time surveillance data to establish the trend of infection. In addition, the model was not stratified by age. The analysis of the data revealed that there is significant difference in mean number of new HIV infections between males and females within the two age groups. More, particularly, females are highly infected with HIV as compared to their male counterparts. These results are comparable to the results obtained in (Ross et al., 2018). Calculation of the reproduction numbers within and between age groups provides insights into control that cannot be deduced simply from observations on the prevalence of infection. More specifically, the analysis showed that the per capita rate of HIV transmission was highest when there is interaction between young adults to adults and most HIV infections occurred in adult population. Furthermore, the sensitivity analysis demonstrated that the reproduction numbers depend mainly on the probabilities of infection. This results can be used to guide HIV interventions, PrEP distribution and antiretroviral

therapy. Precisely, the results can be used to educate the young adults on practising safe sex with their partners in order to contain the occurrence of new infections.

Our work in Chapter 6 attempts to study the transmission trend between commercial sex workers, and injection drug users. We formulated a deterministic model for the spread of HIV between these risk groups. The model is designed in such a way that it allows for free transition between the risk groups. The analytical results indicate that $\mathscr{R}_{0d}$ is indeed the threshold for injection drug user when $\tau = 0$. When the saturation parameter $\tau > 0$, the system exhibits the phenomenon of backward bifurcation where a HIV-free equilibrium and two non-trivial equilibria coexist. A change in the qualitative behaviour of the system is observed when $\mathscr{R}_{0d} = 1$. At $\mathscr{R}_{0d} = 1$, the epidemic is sustained in the population since each existing infection causes one new infection. The appearance of backward bifurcation indicates that it is not sufficient to decrease the basic reproduction number below unity for the containment of HIV in the population. These results are similar to the ones in Elbasha and Gumel (2006). Using data from literature related to the transmission dynamics of HIV, we carried out numerical simulations. The result showed that there is persistence of HIV in the populations when the basic reproduction number is greater than unity. This suggested that the control of the epidemic of HIV should be enhanced through a combination of PrEP use, individual protection, and treatment of infected with ART. Furthermore, we formulated an optimal control problem with the aim to determine the PrEP strategy that satisfies the mixed state control constraint and minimizes the number of HIV infection. We then considered three time dependent controls as a way out, to ensure the containment of HIV infection in a finite time. We performed optimal control analysis of the model. In this regard, we addressed the optimal control by deriving and analysing the conditions for optimal containment of HIV and in a situation where eradication is impossible or of less benefit compared to the cost of intervention, we also derived and analysed the necessary conditions for optimal control of the disease. We then provided numerical simulations, which show that it is possible to reduce the HIV incidence through PrEP and having into consideration the limitations related to the implementation of PrEP that include cost, epidemic context, program coverage and individual-level adherence. These results have the potential to help policy makers escalate programs against HIV infections in high risk populations by modifying the implementation

of current interventions, or by adding new control measures. It is also important to note that from many work on the optimal control of infectious diseases (*see for instance* Blayneh et al. (2009); Silva and Torres (2017)), and more particularly HIV infection (Gromov et al., 2017; Kwon et al., 2012; Okosun et al., 2013), optimal control analysis taking into consideration interaction between risk groups, to our knowledge, has not been done. This, therefore, represents a contribution to the study of optimal control models of HIV infection.

7.3 Policy recommendations

In spite of the intense and aggressive interventions from various governmental and non-governmental organisations, there is still growing number of new infections in Kenya especially amongst the youths aged 15-24 years. HIV/AIDS burden in Kenya accounts for approximately 29% of the adult deaths annually, 20% of the maternal mortality and 15% of deaths of children aged below five years. The findings from this research could be useful to organisations such as National AIDS Control Council (NACC), National AIDS and STIs Control Programme (NASCOP), Kenya Medical Research Institute (KEMRI), Centers for Disease Control and Prevention (CDC-Kenya) and the Ministry of Health (MoH), which are at the forefront in the fight against HIV/AIDS. These results have the potential to help in escalating programs against HIV infections in high risk populations by modifying the implementation of current interventions, or by adding new control measures. The following specific recommendations could be considered.

1. The uptake of PrEP is necessary for quick protection of individuals at high risk of HIV infections. This should not be limited to the key risk populations (commercial sex workers, males who have sex with males and injection drug users).

2. To reduce the chances of infections through sexual contacts with infected individuals at high risks of HIV infection, educational campaigns that encourage them to use preventive measures such as condoms should be particularly enhanced.

3. To achieve the WHO target of 90-90-90, the self test kits should be availed in all medical facilities and those who find themselves positive be immediately enrolled into ART treatment programmes.

4. The possibility of resistance to PrEP uptake provides a unique chance to monitor individual adherence. This provides an opportunity to look into the quality and standards of PrEP.

7.4 Study limitations

In the models used, stochasticity of the occurrence of HIV infection was not factored. Stochasticity that may be attributed to the environmental conditions that could influence the infection pattern. The noise resulting from such stochastic consideration may give a more realistic picture of the fluctuating non constant disease transmission rates. Furthermore, it is well known that the goodness of fit measures the discrepancy between observed data and values expected from the models. In this work, no goodness of fit tests were performed. Considering the importance of goodness of fit in fitting models to data, it can be an area of future research.

The models we used do not put into account the time delay between the time infection and when the infected person becomes infectious. It may be plausible to investigate the effect of delay on the transmission dynamics of the HIV in the presence of PrEP up-take. In addition the infection rate may not necessarily be constant throughout the epidemic period. We acknowledge the fact that considering time dependent parameter may give more insights into the HIV dynamics. The model that incorporates the key populations does not put into account the possibility of cross risk infection. This aspect may have a significant effect on the transmission dynamics and severity of the HIV and can be considered for future research.

References

Abate, A., Tiwari, A., and Sastry, S. (2009). Box invariance in biologically-inspired dynamical systems. *Automatica*, 45(7):1601–1610.

Afassinou, K., Chirove, F., and Govinder, K. S. (2017). Pre-exposure prophylaxis and antiretroviral treatment interventions with drug resistance. *Mathematical Biosciences*, 285:92–101.

AIDS (2015). AIDS info. Guidelines for the Use of Antiretroviral Agents in HIV-1-Infected Adults and Adolescents. https://aidsinfo.nih.gov/guidelines/html/1/adult-and-adolescent-arv-guidelines/458/plasma-hiv-1-rna--viral-load--and-cd4-count-monitoring, accessed April 2017.

AIDS (2016a). AIDS. Pre-Exposure Prophylaxis (PrEP). https://www.aids.gov/hiv-aids-basics/prevention/reduce-your-risk/pre-exposure-prophylaxis/, accessed April 2017.

AIDS (2016b). Global statistics. The Global HIV/AIDS Epidemic. https://www.aids.gov/hiv-aids-basics/hiv-aids-101/global-statistics/, accessed April 2017.

AIDS-Action (2005). When deciding which tests to use. https://aidsaction.net/pdf/ht/ht-section2.pdf, accessed March 2019.

AIDSINFO (2017). HIV/AIDS Glossary. Offering Information on HIV/AIDS Treatment, Prevention and Research. https://aidsinfo.nih.gov/understanding-hiv-aids/glossary/4597/binding/, accessed May 2017.

Aïnseba, B. and Benosman, C. (2010). Optimal control for resistance and suboptimal response in CML. *Mathematical Biosciences*, 227(2):81–93.

Aldila, D. (2018). Mathematical model for HIV spreads control program with ART treatment. In *Journal of Physics: Conference Series*, volume 974, page 012035. IOP Publishing.

Alsallaq, R. A., Cash, B., Weiss, H. A., Longini, I. M., Omer, S. B., Wawer, M. J., Gray, R. H., and Abu-Raddad, L. J. (2009). Quantitative assessment of the role of male circumcision in HIV epidemiology at the population level. *Epidemics*, 1(3):139–152.

Amornkul, P. N., Vandenhoudt, H., Nasokho, P., Odhiambo, F., Mwaengo, D., Hightower, A., Buvé, A., Misore, A., Vulule, J., and Vitek, C. (2009). HIV prevalence and associated risk factors among individuals aged 13-34 years in Rural Western Kenya. *PloS one*, 4(7):e6470.

Apenteng, O. O. and Ismail, N. A. (2017). Modelling the spread of HIV and AIDS epidemic trends in male and female populations. *World Journal of Modelling and Simulation*, 13(3):183–192.

Athithan, S. and Ghosh, M. (2014). Analysis of a sex-structured HIV/AIDS model with the effect of screening of infectives. *International Journal of Biomathematics*, 7(05):1450054.

Auvert, B., Buonamico, G., Lagarde, E., and Williams, B. (2000). Sexual behavior, heterosexual transmission, and the spread of hiv in Sub-Saharan Africa: a simulation study. *Computers and Biomedical Research*, 33(1):84–96.

Auvert, B., Taljaard, D., Lagarde, E., Sobngwi-Tambekou, J., Sitta, R., and Puren, A. (2005). Randomized, controlled intervention trial of male circumcision for reduction of HIV infection risk: the ANRS 1265 Trial. *PLoS Medicine*, 2(11):e298.

Auvert, B., Taljaard, D., Lagarde, E., Sobngwi-Tambekou, J., Sitta, R., and Puren, A. (2006). Correction: randomized, controlled intervention trial of male circumcision for reduction of HIV infection risk: the ANRS 1265 trial. *PLoS Medicine*, 3(5):e298.

AV (2017). Avert. Global information and Education on HIV and AIDS: HIV and AIDS in Kenya. Retrieved June, 2018 from https://www.avert.org/professionals/hiv-around-world/sub-saharan-africa/kenya.

AVERT (2018). HIV and AIDS in East and Southern Africa regional overview. https://www.avert.org/professionals/hiv-around-world/sub-saharan-africa/overview, accessed August 2018.

AVERT (2019). HIV and AIDS in Kenya. https://www.avert.org/professionals/hiv-around-world/sub-saharan-africa/kenya, accessed March 2019.

AVERTS (2007). Avert. Voluntary Medical Male Circumcision. https://www.avert.org/professionals/hiv-programming/prevention/voluntary-medical-male-circumcision#footnote1_og8311l4, accessed April 2017.

Bailey, R. C., Moses, S., Parker, C., et al. (2007). Male circumcision in HIV prevention. *Lancet*, 369(9573):1598–1598.

Barley, K., Murillo, D., Roudenko, S., Tameru, A., Tatum, S., et al. (2012). A mathematical model of HIV and malaria co-infection in Sub-Saharan Africa. *Journal of AIDS and Clinical Research*, 3(7):1–7.

Barouch, D. H. (2018). A step forward for HIV vaccines. *The Lancet HIV*, 5(7):e338–e339.

Baryarama, F., Mugisha, J., and Luboobi, L. (2006). A mathematical model for the dynamics of HIV/AIDS with gradual behaviour change. *Computational and Mathematical Methods in Medicine*, 7(1):15–26.

Beckerleg, S., Telfer, M., and Hundt, G. L. (2005). The rise of injecting drug use in East Africa: a case study from Kenya. *Harm Reduction Journal*, 2(1):12–21.

Beckerleg, S., Telfer, M., and Sadiq, A. (2006). A rapid assessment of heroin use in Mombasa, Kenya. *Substance Use & Misuse*, 41(6-7):1029–1044.

Bellan, S. E., Fiorella, K. J., Melesse, D. Y., Getz, W. M., Williams, B. G., and Dushoff, J. (2013). Extra-couple HIV transmission in sub-Saharan Africa: a mathematical modelling study of survey data. *The Lancet*, 381(9877):1561–1569.

Berman, A. and Plemmons, R. J. (1994). *Nonnegative matrices in the mathematical sciences*, volume 9. SIAM, Philadelphia.

Bhattacharjee, P., McClarty, L. M., Musyoki, H., Anthony, J., Kioko, J., Kaosa, S., Ogwang, B. E., Githuka, G., Sirengo, M., and Birir, S. (2015). Monitoring HIV prevention programme outcomes among key populations in Kenya: findings from a national survey. *PloS one*, 10(8):e0137007.

Bhunu, C. P., Mushayabasa, S., Kojouharov, H., and Tchuenche, J. (2011). Mathematical analysis of an HIV/AIDS model: impact of educational programs and abstinence in sub-Saharan Africa. *Journal of Mathematical Modelling and Algorithms*, 10(1):31–55.

Blaizot, S., Maman, D., Riche, B., Mukui, I., Kirubi, B., Ecochard, R., and Etard, J.-F. (2016). Potential impact of multiple interventions on HIV incidence in a hyperendemic region in Western Kenya: a modelling study. *BMC Infectious Diseases*, 16(1):189.

Blayneh, K., Cao, Y., and Kwon, H.-D. (2009). Optimal control of vector-borne diseases: treatment and prevention. *Discrete and Continuous Dynamical Systems B*, 11(3):587–611.

Blayneh, K. W. (2010). Backward bifurcation and optimal control in transmission dynamics of West Nile virus. *Bulletin of Mathematical Biology*, 72(4):1006–1028.

Blázquez, D., Ramos-Amador, J. T., Saínz, T., Mellado, M. J., García-Ascaso, M., De José, M. I., Rojo, P., Navarro, M. L., Muñoz-Fernández, M. Á., and Saavedra, J. (2015). Lipid and glucose alterations in perinatally-acquired HIV-infected adolescents and young adults. *BMC Infectious Diseases*, 15(1):119.

Bohner, M., Kenzhebaev, K., Lavrova, O., and Stanzhytskyi, O. (2017). Pontryagin's maximum principle for dynamic systems on time scales. *Journal of Difference Equations and Applications*, 23(7):1161–1189.

Boily, M., Desai, K., Masse, B., and Gumel, A. (2008). Incremental role of male circumcision on a generalised HIV epidemic through its protective effect against other sexually transmitted infections: from efficacy to effectiveness to population-level impact. *Sexually Transmitted Infections*, 84(Suppl 2):ii28–ii34.

Boily, M.-C., Baggaley, R. F., Wang, L., Masse, B., White, R. G., Hayes, R. J., and Alary, M. (2009). Heterosexual risk of HIV-1 infection per sexual act: systematic review and meta-analysis of observational studies. *The Lancet Infectious Diseases*, 9(2):118–129.

Braithwaite, R. S., Nucifora, K. A., Kessler, J., Toohey, C., Mentor, S. M., Uhler, L. M., Roberts, M. S., and Bryant, K. (2014). Impact of interventions targeting unhealthy alcohol use in Kenya on HIV transmission and AIDS-related deaths. *Alcoholism: Clinical and Experimental Research*, 38(4):1059–1067.

Buonomo, B. (2011). A simple analysis of vaccination strategies for rubella. *Mathematical Biosciences & Engineering*, 8:677–687.

Bush, S., Magnuson, D., Rawlings, M., Hawkins, T., McCallister, S., and Mera Giler, R. (2016). Racial characteristics of FTC/TDF for pre-exposure prophylaxis users in the US. *ASM Microbe*, pages 16–20.

Cann, A. J. and Karn, J. (1989). Molecular biology of HIV: new insights into the virus life-cycle. *AIDS*, 3(1):S19–34.

Capodici, J., Karikó, K., and Weissman, D. (2002). Inhibition of HIV-1 infection by small interfering RNA-mediated RNA interference. *The Journal of Immunology*, 169(9):5196–5201.

Castilho, C. (2006). Optimal control of an epidemic through educational campaigns. *Electronic Journal of Differential Equations*, 2006(125):1–11.

Castillo-Chavez, C., Cooke, K., Huang, W., and Levin, S. A. (1989). Results on the dynamics for models for the sexual transmission of the human immunodeficiency virus. *Applied Mathematics Letters*, 2(4):327–331.

Castillo-Chavez, C. and Song, B. (2004). Dynamical models of tuberculosis and their applications. *Mathematical Biosciences and Engineering*, 1(2):361–404.

CDC (2012). Progress in voluntary medical male circumcision service provision-kenya, 2008-2011. *MMWR. Morbidity and mortality weekly report*, 61(47):957.

CGD (2016). Global HIV / AIDS and the developing world. What are the impacts of HIV/AIDS in the developing world? https://www.cgdev.org/sites/default/files/2851_file_GLOBAL_HIV_AIDS1_0.pdf, accessed April 2017.

Chersich, M. and Rees, H. (2010). Causal links between binge drinking patterns, unsafe sex and HIV in South Africa: its time to intervene. *International Journal of STD & AIDS*, 21(1):2–7.

Claassen, M., Van Zyl, G., Korsman, S., Smit, L., Cotton, M., and Preiser, W. (2006). Pitfalls with rapid HIV antibody testing in HIV-infected children in the Western Cape, South Africa. *Journal of Clinical Virology*, 37(1):68–71.

De Cock, K. M. and Weiss, H. A. (2000). The global epidemiology of HIV/AIDS. *Tropical Medicine & International Health*, 5(7):A3–A9.

DeRiemer, K., Kawamura, L. M., Hopewell, P. C., and Daley, C. L. (2007). Quantitative impact of human immunodeficiency virus infection on tuberculosis dynamics. *American Journal of respiratory and critical care medicine*, 176(9):936–944.

Dias, W. O., Wanner, E. F., and Cardoso, R. T. (2015). A multiobjective optimization approach for combating aedes aegypti using chemical and biological alternated step-size control. *Mathematical Biosciences*, 269:37–47.

Diekmann, O. and Heesterbeek, J. A. P. (2000). *Mathematical epidemiology of infectious diseases: model building, analysis and interpretation*, volume 5. John Wiley & Sons.

Diekmann, O., Heesterbeek, J. A. P., and Metz, J. A. (1990). On the definition and the computation of the basic reproduction ratio r0 in models for infectious diseases in heterogeneous populations. *Journal of Mathematical Biology*, 28(4):365–382.

Doms, R. W. and Trono, D. (2000). The plasma membrane as a combat zone in the HIV battlefield. *Genes & Development*, 14(21):2677–2688.

Douraki, M. J. (2017). Continuous and discrete dynamics of a deterministic model of HIV infection. *arXiv preprint arXiv:1708.09462*.

Doyle, M., Greenhalgh, D., and Blythe, S. (1998). Equilibrium analysis of a mathematical model for the spread of AIDS in a two sex population with mixing constraints. *Journal of Biological Systems*, 6(02):159–185.

Elbasha, E. H. and Gumel, A. B. (2006). Theoretical assessment of public health impact of imperfect prophylactic HIV-1 vaccines with therapeutic benefits. *Bulletin of Mathematical Biology*, 68(3):577.

Eyawo, O., de Walque, D., Ford, N., Gakii, G., Lester, R. T., and Mills, E. J. (2010). HIV status in discordant couples in sub-Saharan Africa: a systematic review and meta-analysis. *The Lancet Infectious Diseases*, 10(11):770–777.

Fiebig, E. W., Wright, D. J., Rawal, B. D., Garrett, P. E., Schumacher, R. T., Peddada, L., Heldebrant, C., Smith, R., Conrad, A., and Kleinman, S. H. (2003). Dynamics of HIV viremia and antibody seroconversion in plasma donors: implications for diagnosis and staging of primary HIV infection. *AIDS*, 17(13):1871–1879.

Fleming, W. H. and Rishel, R. W. (2012). *Deterministic and Stochastic Optimal Control*, volume 1. Springer Science & Business Media, New York.

Forouzannia, F. and Gumel, A. B. (2014). Mathematical analysis of an age-structured model for malaria transmission dynamics. *Mathematical Biosciences*, 247:80–94.

Gardner, E. M., McLees, M. P., Steiner, J. F., del Rio, C., and Burman, W. J. (2011). The spectrum of engagement in HIV care and its relevance to test-and-treat strategies for prevention of HIV infection. *Clinical Infectious Diseases*, 52(6):793–800.

Garnett, G. P. (2002). An introduction to mathematical models in sexually transmitted disease epidemiology. *Sexually Transmitted Infections*, 78(1):7–12.

Geibel, S. (2012). Same-sex sexual behavior of men in Kenya: Implications for HIV prevention, programs, and policy. *Facts, views & vision in ObGyn*, 4(4):285–294.

Gelmon, L. (2009). *Kenya HIV prevention response and modes of transmission analysis*. National AIDS Control Council.

Ghimire, L., Smith, W. C. S., van Teijlingen, E. R., Dahal, R., and Luitel, N. P. (2011). Reasons for non-use of condoms and self-efficacy among female sex workers: a qualitative study in nepal. *BMC women's health*, 11(1):1–8.

Gillespie, S., Kadiyala, S., and Greener, R. (2007). Is poverty or wealth driving HIV transmission? *AIDS*, 21:S5–S16.

Gray, R. H., Makumbi, F., Serwadda, D., Lutalo, T., Nalugoda, F., Opendi, P., Kigozi, G., Reynolds, S. J., Sewankambo, N. K., and Wawer, M. J. (2007). Limitations of rapid HIV-1 tests during screening for trials in Uganda: diagnostic test accuracy study. *BMJ*, 335(7612):1–4.

Gromov, D., Bulla, I., Silvia Serea, O., and Romero-Severson, E. O. (2017). Numerical optimal control for HIV prevention with dynamic budget allocation. *Mathematical Medicine and Biology: a Journal of the IMA*, 35(4):469–491.

Guckenheimer, J. and Holmes, P. J. (2013). *Nonlinear oscillations, dynamical systems, and bifurcations of vector fields*, volume 42. Springer Science & Business Media.

Gumel, A., McCluskey, C. C., and van den Driessche, P. (2006). Mathematical study of a staged-progression HIV model with imperfect vaccine. *Bulletin of Mathematical Biology*, 68(8):2105–2128.

Gupta, N. and Rink, R. (1973). Optimum control of epidemics. *Mathematical Biosciences*, 18(3-4):383–396.

Gupta, R. K., Jordan, M. R., Sultan, B. J., Hill, A., Davis, D. H., Gregson, J., Sawyer, A. W., Hamers, R. L., Ndembi, N., and Pillay, D. (2012). Global trends in antiretroviral resistance in treatment-naive individuals with HIV after rollout of antiretroviral treatment in resource-limited settings: a global collaborative study and meta-regression analysis. *The Lancet*, 380(9849):1250–1258.

Hahn, J. A., Woolf-King, S. E., and Muyindike, W. (2011). Adding fuel to the fire: alcohol's effect on the HIV epidemic in Sub-Saharan Africa. *Current HIV/AIDS Reports*, 8(3):172–180.

Hallett, T. B., Gregson, S., Mugurungi, O., Gonese, E., and Garnett, G. P. (2009). Assessing evidence for behaviour change affecting the course of HIV epidemics: a new mathematical modelling approach and application to data from Zimbabwe. *Epidemics*, 1(2):108–117.

Hallett, T. B., Singh, K., Smith, J. A., White, R. G., Abu-Raddad, L. J., and Garnett, G. P. (2008). Understanding the impact of male circumcision interventions on the spread of HIV in Southern Africa. *PloS one*, 3(5):e2212.

Heffernan, J., Smith, R., and Wahl, L. (2005). Perspectives on the basic reproductive ratio. *Journal of the Royal Society Interface*, 2(4):281–293.

Hethcote, H. W. (1989). A model for HIV transmission and AIDS. In *Mathematical approaches to problems in resource management and Epidemiology*, pages 164–176. Springer.

Hethcote, H. W. (2000). The mathematics of infectious diseases. *SIAM Review*, 42(4):599–653.

HIV/AIDS (2016). HIV/AIDS. Pre-Exposure Prophylaxis (PrEP). https://www.cdc.gov/hiv/risk/prep/, accessed April 2017.

Huo, H.-F. and Feng, L.-X. (2013). Global stability for an HIV/AIDS epidemic model with different latent stages and treatment. *Applied Mathematical Modelling*, 37(3):1480–1489.

Isdory, A., Mureithi, E. W., and Sumpter, D. J. (2015). The impact of human mobility on HIV transmission in kenya. *PloS one*, 10(11):e0142805.

Janini, L. M. (1998). Horizontal and vertical transmission of human immunodeficiency virus type 1 dual infections caused by viruses of subtypes B and C. *Journal of Infectious Diseases*, 177(1):227–231.

Jaquet, A., Ekouevi, D. K., Bashi, J., Aboubakrine, M., Messou, E., Maiga, M., Traore, H. A., Zannou, M. D., Guehi, C., and Ba-Gomis, F. O. (2010). Alcohol use and non-adherence to antiretroviral therapy in HIV-infected patients in West Africa. *Addiction*, 105(8):1416–1421.

Kaur, N., Ghosh, M., and Bhatia, S. (2014). Mathematical analysis of the transmission dynamics of HIV/AIDS: Role of female sex workers. *Applied Mathematics & Information Sciences*, 8(5):2491–2501.

KD (2018). Kenya Demographics Profile 2018. Retrieved May, 2018 from https://www.indexmundi.com/kenya/demographics_profile.html.

Keeling, M. J. and Rohani, P. (2011). *Modeling infectious diseases in humans and animals*. Princeton University Press.

Kelvin, E. A., George, G., Kinyanjui, S., Mwai, E., Romo, M. L., Oruko, F., Odhiambo, J. O., Nyaga, E. N., Mantell, J. E., and Govender, K. (2019). Announcing the availability of oral HIV self-test kits via text message to increase HIV testing among hard-to-reach truckers in Kenya: a randomized controlled trial. *BMC public health*, 19(1):2–9.

Kharsany, A. B. and Karim, Q. A. (2016). HIV infection and AIDS in sub-Saharan Africa: current status, challenges and opportunities. *The open AIDS journal*, 10:34–48.

KHIS (2017). Kenya Health Information System. District Health Information System (DHIS2). https://hiskenya.org/, accessed September 2017.

Kim, S. B., Yoon, M., Ku, N. S., Kim, M. H., Song, J. E., Ahn, J. Y., Jeong, S. J., Kim, C., Kwon, H.-D., and Lee, J. (2014). Mathematical modeling of HIV prevention measures including pre-exposure prophylaxis on HIV incidence in South Korea. *PloS one*, 9(3):e90080.

Kirchhoff, F. (2013). HIV life cycle: overview. *Encyclopedia of AIDS. New York, NY: Springer*, pages 1–9.

Kiss, I. Z., Cassell, J., Recker, M., and Simon, P. L. (2010). The impact of information transmission on epidemic outbreaks. *Mathematical Biosciences*, 225(1):1–10.

KLGBTIR (2017). Kenya LGBTI Resources. Rights in exile programme. http://www.refugeelegalaidinformation.org/kenya-lgbti-resources, accessed April 2017.

KNASP (2009). Kenya National AIDS Strategic Plan 2009/10– 2012/13: Delivering on Universal Access to Services. http://siteresources.worldbank.org/INTHIVAIDS/Resources/375798-1151090631807/2693180-1151090665111/2693181-1155742859198/KenyaNationalStrategy.pdf, accessed January 2018.

KNBS (2015). Kenya National Bureau of Statistics. Demographic and Health Survey. https://dhsprogram.com/pubs/pdf/FR308/FR308.pdf, accessed April 2017.

KNBS (2017). Kenya National Bureau of Statistics. Publication. https://www.knbs.or.ke/, accessed September.

KNBS2 (2017). Kenya 1900. Population Pyramids of the World from 1950 to 2100. https://www.populationpyramid.net/kenya/1990/, accessed September, 2017.

Kok, S., Rutherford, A. R., Gustafson, R., Barrios, R., Montaner, J. S., Vasarhelyi, K., et al. (2015). Optimizing an HIV testing program using a system dynamics model of the continuum of care. *Health Care Management Science*, 18(3):334–362.

Kruskal, W. H. and Wallis, W. A. (1952). Use of ranks in one-criterion variance analysis. *Journal of the American statistical Association*, 47(260):583–621.

Kurth, A. E., Cleland, C. M., Des Jarlais, D. C., Musyoki, H., Lizcano, J. A., Chhun, N., and Cherutich, P. (2015). HIV prevalence, estimated incidence, and risk behaviors among people who inject drugs in Kenya. *JAIDS Journal of Acquired Immune Deficiency Syndromes*, 70(4):420–427.

Kuznetsov, Y. A. (2013). *Elements of applied bifurcation theory*, volume 112. Springer Science & Business Media.

Kwena, Z. A., Bukusi, E., Omondi, E., Ng'Ayo, M., and Holmes, K. K. (2012). Transactional sex in the fishing communities along Lake Victoria, Kenya: a catalyst for the spread of HIV. *African Journal of AIDS Research*, 11(1):9–15.

Kwon, H.-D., Lee, J., and Yang, S.-D. (2012). Optimal control of an age-structured model of HIV infection. *Applied Mathematics and Computation*, 219(5):2766–2779.

La Salle, J. P. (1976). *The stability of dynamical systems*. SIAM.

Lenhart, S. and Workman, J. T. (2007). *Optimal control applied to biological models*. Crc Press.

Li, J., Peng, L., Gilmour, S., Gu, J., Ruan, Y., Zou, H., Hao, C., Hao, Y., and Lau, J. T.-f. (2018). A mathematical model of biomedical interventions for HIV prevention among men who have sex with men in China. *BMC Infectious Diseases*, 18(1):2–9.

Lien, T. X., Tien, N. T., Chanpong, G. F., Cuc, C. T., Yen, V. T., Soderquist, R., Laras, K., and Corwin, A. (2000). Evaluation of rapid diagnostic tests for the detection of human immunodeficiency virus types 1 and 2, hepatitis B surface antigen, and syphilis in ho chi minh city, vietnam. *The American Journal of Tropical Medicine and Hygiene*, 62(2):301–309.

Liu, R., Wu, J., and Zhu, H. (2007). Media/psychological impact on multiple outbreaks of emerging infectious diseases. *Computational and Mathematical Methods in Medicine*, 8(3):153–164.

Lukes, D. L. (1982). *Differential equations: classical to controlled*. Elsevier.

Makinde, O. D. and Okosun, K. O. (2011). Impact of chemo-therapy on optimal control of malaria disease with infected immigrants. *Biosystems*, 104(1):32–41.

Manoukian, E. B. (1986). *Mathematical nonparametric statistics*. Gordon and Breach Science Publishers, Inc.

Marino, S., Hogue, I. B., Ray, C. J., and Kirschner, D. E. (2008). A methodology for performing global uncertainty and sensitivity analysis in systems biology. *Journal of Theoretical Biology*, 254(1):178–196.

MATLAB (2019). Runge Kutta 4th order ode. https://www.mathworks.com/matlabcentral/fileexchange/29851-runge-kutta-4th-order-ode?focused=3773771&tab=function, accessed March 2019.

McCurdy, S. A., Ross, M. W., Williams, M. L., Kilonzo, G. P., and Leshabari, M. T. (2010). Flashblood: blood sharing among female injecting drug users in Tanzania. *Addiction*, 105(6):1062–1070.

McNeil Jr, D. G. (2010). Desperate Addicts Inject others' Blood. *New York Times*, 13.

McPherson, T. D., Sobieszczyk, M. E., and Markowitz, M. (2018). Cabotegravir in the treatment and prevention of human immunodeficiency virus-1. *Expert opinion on investigational drugs*, 27(4):413–420.

Means, A. R., Risher, K. A., Ujeneza, E. L., Maposa, I., Nondi, J., and Bellan, S. E. (2016). Impact of Age and Sex on CD4+ Cell Count Trajectories following Treatment Initiation: An analysis of the Tanzanian HIV Treatment Database. *PloS one*, 11(10):e0164148.

Medscape (2010). HIV Testing Overview. https://emedicine.medscape.com/article/2061077-overview, accessed March 2019.

Mehra, B., Bhattar, S., Bhalla, P., and Rawat, D. (2014). Rapid tests versus ELISA for screening of HIV infection: our experience from a voluntary counselling and testing facility of a tertiary care centre in North India. *Isrn Aids*, 2014.

MOH (2014a). Kenya HIV Estimates. Retrieved May, 2018 from https://nacc.or.ke/wp-content/uploads/2018/11/HIV-estimates-report-Kenya-20182.pdf.

MOH (2014b). Kenyan Ministry of Health. Kenya HIV Prevention Revolution Road Map. http://reliefweb.int/sites/reliefweb.int/files/resources/Kenya_HIV_Prevention_Revolution_Road_Map.pdf, accessed April 2017.

MOH (2016a). Kenyan Ministry of Health. Kenya HIV County Profiles. http://nacc.or.ke/wp-content/uploads/2016/12/Kenya-HIV-County-Profiles-2016.pdf, accessed April 2017.

MOH (2016b). Kenyan Ministry of Health/National AIDS Control Council. Kenya AIDS Response Progress Report 2016. Retrieved May, 2018 from https://nacc.or.ke/wp-content/uploads/2016/11/Kenya-AIDS-Progress-Report_web.pdf.

Mojola, S. A. (2011). Fishing in dangerous waters: Ecology, gender and economy in HIV risk. *Social Science & Medicine*, 72(2):149–156.

Morison, L. (2001). The global epidemiology of HIV/AIDS. *British Medical Bulletin*, 58(1):7–18.

Morris, B. J., Wamai, R. G., Henebeng, E. B., Tobian, A. A., Klausner, J. D., Banerjee, J., and Hankins, C. A. (2016). Estimation of country-specific and global prevalence of male circumcision. *Population Health Metrics*, 14(1):1–13.

Moulay, D., Aziz-Alaoui, M., and Kwon, H.-D. (2012). Optimal control of chikungunya disease: larvae reduction, treatment and prevention. *Mathematical Biosciences & Engineering*, 9(2):369–392.

Mukandavire, Z., Chiyaka, C., Garira, W., and Musuka, G. (2009). Mathematical analysis of a sex-structured HIV/AIDS model with a discrete time delay. *Nonlinear Analysis: Theory, Methods & Applications*, 71(3):1082–1093.

Mukandavire, Z. and Garira, W. (2007a). Age and sex structured model for assessing the demographic impact of mother-to-child transmission of HIV/AIDS. *Bulletin of Mathematical Biology*, 69(6):2061–2092.

Mukandavire, Z. and Garira, W. (2007b). Sex-structured HIV/AIDS model to analyse the effects of condom use with application to zimbabwe. *Journal of Mathematical Biology*, 54(5):669–699.

Musyoki, H., Kellogg, T. A., Geibel, S., Muraguri, N., Okal, J., Tun, W., Raymond, H. F., Dadabhai, S., Sheehy, M., and Kim, A. A. (2015). Prevalence of HIV, sexually transmitted infections, and risk behaviours among female sex workers in Nairobi, Kenya: Results of a respondent driven sampling study. *AIDS and Behavior*, 19(1):46–58.

NACC (2009). The Kenya 2007 HIV and AIDS Estimates And interim projected HIV prevalence and incidence trends for 2008 to 2015. Retrieved in August 2017 from http://nacc.or.ke/wp-content/uploads/2016/03/Kenya-National-HIV-Estimates-projections-for-2008-20151.pdf.

NACC (2013). National AIDS Control Council and the National AIDS and STD Control Programme,March 2012. http://guidelines.health.go.ke:8000/media/National_HIV_Estimates_for_Kenya_2011-2015.pdf, accessed January, 2018.

NACC (2014a). Kenya National Aids Control Council. Kenya National AIDS Control Council 'Kenya AIDS Strategic Framework 2014/2015–2018/2019'. http://www.undp.org/content/dam/kenya/docs/Democratic%20Governance/KENYA%20AIDS%20STRATEGIC%20FRAMEWORK.pdf, accessed April 2017.

NACC (2014b). National Aids Control Council of Kenya. 'Kenya AIDS Response Progress Report 2014: Progress towards Zero'. http://nacc.or.ke/wp-content/uploads/2016/11/Kenya-AIDS-Progress-Report_web.pdf, accessed April 2017.

NACC (2016). Kenya National Aids Control Council. Kenya AIDS response progress report 2016. http://nacc.or.ke/wp-content/uploads/2016/11/Kenya-AIDS-Progress-Report_web.pdf, accessed April 2017.

Nanda, S., Moore, H., and Lenhart, S. (2007). Optimal control of treatment in a mathematical model of chronic myelogenous leukemia. *Mathematical Biosciences*, 210(1):143–156.

NIH (2019). First New HIV Vaccine Efficacy Study in Seven Years Has Begun: South Africa Hosts Historic NIH-Supported Clinical Trial. Retrieved in September 2019 from https://www.niaid.nih.gov/news-events/first-new-hiv-vaccine-efficacy-study-seven-years-has-begun.

Njagarah, J. B. and Nyabadza, F. (2014). A metapopulation model for cholera transmission dynamics between communities linked by migration. *Applied Mathematics and Computation*, 241:317–331.

Njeuhmeli, E., Forsythe, S., Reed, J., Opuni, M., Bollinger, L., Heard, N., Castor, D., Stover, J., Farley, T., and Menon, V. (2011). Voluntary medical male circumcision: modeling the impact and cost of expanding male circumcision for HIV prevention in eastern and Southern Africa. *PLoS Medicine*, 8(11):e1001132.

Nolan, D., Reiss, P., and Mallal, S. (2005). Adverse effects of antiretroviral therapy for HIV infection: a review of selected topics. *Expert Opinion on Drug Safety*, 4(2):201–218.

Nyabadza, F., Njagarah, J. B., and Smith, R. J. (2013). Modelling the dynamics of crystal meth ('tik') abuse in the presence of drug-supply chains in South Africa. *Bulletin of Mathematical Biology*, 75(1):24–48.

Okango, E., Mwambi, H., and Ngesa, O. (2016). Spatial modeling of HIV and HSV-2 among women in Kenya with spatially varying coefficients. *BMC Public Health*, 16(1):355–368.

Okongo, M., Kirimi, J., Murwayi, A., and Muriithi, D. (2013). Mathematical analysis of a comprehensive HIV/ AIDS model: Treatment versus vaccination. *Applied Mathematical Sciences*, 7(54):2687–2707.

Okosun, K., Makinde, O., and Takaidza, I. (2013). Impact of optimal control on the treatment of HIV/AIDS and screening of unaware infectives. *Applied Mathematical Modelling*, 37(6):3802–3820.

Okosun, K. O., Ouifki, R., and Marcus, N. (2011). Optimal control analysis of a malaria disease transmission model that includes treatment and vaccination with waning immunity. *Biosystems*, 106(2):136–145.

Omondi, E., Mbogo, R., and Luboobi, L. (2019). A mathematical modelling study of HIV infection in two heterosexual age groups in Kenya. *Infectious Disease Modelling*, 4(2019):183–98.

Omondi, E., Nyabadza, F., and Smith?, R. (2018a). Modelling the impact of mass administration of ivermectin in the treatment of onchocerciasis (river blindness). *Cogent Mathematics & Statistics*, 5(1):1–26.

Omondi, E. O., Mbogo, R., and Luboobi, L. (2018b). Mathematical modelling of the impact of testing, treatment and control of HIV transmission in Kenya. *Cogent Mathematics & Statistics*, 5(1):1–16.

Omondi, E. O., Mbogo, R. W., and Luboobi, L. S. (2018c). Mathematical analysis of sex-structured population model of HIV infection in Kenya. *Letters in Biomathematics*, 5(1):174–194.

Omondi, E. O., Mbogo, R. W., and Luboobi, L. S. (2018d). Modelling the Trend of HIV Transmission and Treatment in Kenya. *International Journal of Applied and Computational Mathematics*, 4(5):1–13.

Omondi, E. O., Nyabadza, F., Bonyah, E., and Badu, K. (2017a). Modeling the infection dynamics of onchocerciasis and its treatment. *Journal of Biological Systems*, 25(2):247–277.

Omondi, E. O., Orwa, T. O., and Nyabadza, F. (2017b). Application of optimal control to the onchocerciasis transmission model with treatment. *Mathematical Biosciences*, 297(2018):43–57.

OPTIONS (2016). OPTIONS Country Situation Analysis Interim Findings: Kenya. FSG in partnership with LVCT Health. http://www.prepwatch.org/wp-content/uploads/2016/05/Situation_Analysis_Kenya.pdf, accessed August 2016.

Oral-PrEP (2017). Uganda, Kenya carry out new trials in injectable HIV drug. https://www.theeastafrican.co.ke/scienceandhealth/Uganda-Kenya-carry-out-new-trials-in-injectable-HIV-drug-/3073694-4236652-ir7lkdz/index.html, accessed March 2019.

Overs, C. (2002). Sex workers: part of the solution. An analysis of HIV prevention programming to prevent HIV transmission during commercial sex in developing countries (Draft). Unpublished.

Pau, A. K. and George, J. M. (2014). Antiretroviral therapy: current drugs. *Infectious Disease Clinics*, 28(3):371–402.

PKPK (2014). Prioritization of key population in Kenya. Retrieved May, 2018 from http://icop.or.ke/wp-content/uploads/2016/09/Kenya-HIV-Prevention-Prioritization-evidence-note-11th-June-2014.pdf.

Podder, C., Sharomi, O., Gumel, A., and Moses, S. (2007). To cut or not to cut: a modeling approach for assessing the role of male circumcision in HIV control. *Bulletin of Mathematical Biology*, 69(8):2447–2466.

Podder, C., Sharomi, O., Gumel, A., and Strawbridge, E. (2011). Mathematical analysis of a model for assessing the impact of antiretroviral therapy, voluntary testing and condom use in curtailing the spread of HIV. *Differential Equations and Dynamical Systems*, 19(4):283–302.

Pontryagin, L. S. (1987). *Mathematical theory of optimal processes*. CRC Press.

POP (2017). Kenya Demographics Profile 2018. https://www.indexmundi.com/kenya/demographics_profile.html, accessed January, 2018.

Pretorius, C., Stover, J., Bollinger, L., Bacaër, N., and Williams, B. (2010). Evaluating the cost-effectiveness of pre-exposure prophylaxis (PrEP) and its impact on HIV-1 transmission in South Africa. *PloS one*, 5(11):e13646.

Prodger, J. L. and Kaul, R. (2017). The biology of how circumcision reduces HIV susceptibility: broader implications for the prevention field. *AIDS research and therapy*, 14(1):49.

Quinn, T. C., Wawer, M. J., Sewankambo, N., Serwadda, D., Li, C., Wabwire-Mangen, F., Meehan, M. O., Lutalo, T., and Gray, R. H. (2000). Viral load and heterosexual transmission of human immunodeficiency virus type 1. *New England Journal of Medicine*, 342(13):921–929.

Razali, N. M. and Wah, Y. B. (2011). Power comparisons of shapiro-wilk, kolmogorov-smirnov, lilliefors and anderson-darling tests. *Journal of Statistical Modeling and Analytics*, 2(1):21–33.

Robinson, J. and Yeh, E. (2011). Transactional sex as a response to risk in Western Kenya. *American Economic Journal: Applied Economics*, 3(1):35–64.

Rodrigues, H. S., Monteiro, M. T. T., and Torres, D. F. (2014). Vaccination models and optimal control strategies to dengue. *Mathematical Biosciences*, 247:1–12.

Ross, J. M., Ying, R., Celum, C. L., Baeten, J. M., Thomas, K. K., Murnane, P. M., van Rooyen, H., Hughes, J. P., and Barnabas, R. V. (2018). Modeling HIV disease progression and transmission at population-level: The potential impact of modifying disease progression in HIV treatment programs. *Epidemics*, 23:34–41.

Sahu, G. P. and Dhar, J. (2015). Dynamics of an SEQIHRS epidemic model with media coverage, quarantine and isolation in a community with pre-existing immunity. *Journal of Mathematical Analysis and Applications*, 421(2):1651–1672.

Sardar, T., Sasmal, S. K., and Chattopadhyay, J. (2016). Estimating dengue type reproduction numbers for two provinces of Sri Lanka during the period 2013–14. *Virulence*, 7(2):187–200.

Sasmal, S. K., Ghosh, I., Huppert, A., and Chattopadhyay, J. (2018). Modeling the Spread of Zika Virus in a Stage-Structured Population: Effect of Sexual Transmission. *Bulletin of Mathematical Biology*, 80(11):3038–3067.

Schmid, G. P., Buvé, A., Mugyenyi, P., Garnett, G. P., Hayes, R. J., Williams, B. G., Calleja, J. G., De Cock, K. M., Whitworth, J. A., and Kapiga, S. H. (2004). Transmission of HIV-1 infection in Sub-Saharan Africa and effect of elimination of unsafe injections. *The Lancet*, 363(9407):482–488.

Sethi, S. P. and Staats, P. W. (1978). Optimal control of some simple deterministic epidemic models. *Journal of the Operational Research Society*, pages 129–136.

Shapiro, S. S. and Wilk, M. B. (1965). An analysis of variance test for normality (complete samples). *Biometrika*, 52(3/4):591–611.

Sharp, P. M. and Hahn, B. H. (2011). Origins of HIV and the AIDS pandemic. *Cold Spring Harbor Perspectives in Medicine*, 1(1):a006841.

Shields, A. (2012). *Criminalizing Condoms: How policing practices put sex workers and HIV services at risk in Kenya, Namibia, Russia, South Africa, the United States, and Zimbabwe*. Open Society Foundations.

Sickinger, E., Jonas, G., Yem, A. W., Goller, A., Stieler, M., Brennan, C., Hausmann, M., Schochetman, G., Devare, S. G., and Hunt, J. C. (2008). Performance evaluation of the new fully automated human immunodeficiency virus antigen-antibody combination assay designed for blood screening. *Transfusion*, 48(4):584–593.

Silva, C. J. and Torres, D. F. (2017). Modeling and optimal control of HIV/AIDS prevention through PrEP. *arXiv preprint arXiv:1703.06446*.

Simpson, L. and Gumel, A. B. (2017). Mathematical assessment of the role of pre-exposure prophylaxis on HIV transmission dynamics. *Applied Mathematics and Computation*, 293:168–193.

Smith, H. L. and Waltman, P. (1995). *The theory of the chemostat*, volume 13. Cambridge University Press.

Soetaert, K., Petzoldt, T., et al. (2010). Inverse modelling, sensitivity and monte carlo analysis in R using package FME. *Journal of Statistical Software*, 33(3):1–28.

Stein, M. (1987). Large sample properties of simulations using Latin hypercube sampling. *Technometrics*, 29(2):143–151.

Stekler, J., Maenza, J., Stevens, C. E., Swenson, P. D., Coombs, R. W., Wood, R. W., Campbell, M. S., Nickle, D. C., Collier, A. C., and Golden, M. R. (2007). Screening for acute HIV infection: lessons learned. *Clinical Infectious Diseases*, 44(3):459–461.

Stephenson, K. E., T D'Couto, H., and Barouch, D. H. (2016). New concepts in HIV-1 vaccine development. *Current Opinion in Immunology*, 41:39–46.

Stoebenau, K., Heise, L., Wamoyi, J., and Bobrova, N. (2016). Revisiting the understanding of "transactional sex" in Sub-Saharan Africa: a review and synthesis of the literature. *Social Science & Medicine*, 168:186–197.

Su, Z., Dong, C., Li, P., Deng, H., Gong, Y., Zhong, S., Wu, M., Ruan, Y., Qin, G., and Yang, W. (2016). A mathematical modeling study of the HIV epidemics at two rural townships in the Liangshan Prefecture of the Sichuan Province of China. *Infectious Disease Modelling*, 1(1):3–10.

Tan, W.-Y. and Wu, H. (2005). *Deterministic and stochastic models of AIDS epidemics and HIV infections with intervention*. World Scientific.

Torane, V. and Shastri, J. (2008). Comparison of ELISA and rapid screening tests for the diagnosis of HIV, hepatitis B and hepatitis C among healthy blood donors in a tertiary care hospital in mumbai. *Indian Journal of Medical Microbiology*, 26(3):284–285.

Tukei, V. J., Asiimwe, A., Maganda, A., Atugonza, R., Sebuliba, I., Bakeera-Kitaka, S., Musoke, P., Kalyesubula, I., and Kekitiinwa, A. (2012). Safety and tolerability of antiretroviral therapy among HIV-infected children and adolescents in Uganda. *JAIDS Journal of Acquired Immune Deficiency Syndromes*, 59(3):274–280.

UNAIDS (2004). Making condoms work for HIV prevention. http://data.unaids.org/publications/irc-pub06/jc941-cuttingedge_en.pdf, accessed October 2017.

UNAIDS (2014). United Nations Programme on HIV/AIDS (UNAIDS) Progress reports submitted by countries. Kenya AIDS Response Progress Report 2014: Progress towards Zero'. http://www.unaids.org/en/dataanalysis/knowyourresponse/countryprogressreports/2014countries, accessed August 2016.

UNAIDS (2015a). 2015 estimates from the AIDSinfo online database. Additional disaggregations correspond to unpublished estimates for 2015 provided by UNAIDS, obtained from country-specific models of their AIDS epidemics. http://aidsinfo.unaids.org/, accessed April 2017.

UNAIDS (2015b). Global information and education on HIV and AIDS. HIV and AIDS in Kenya. https://www.avert.org/professionals/hiv-around-world/sub-saharan-africa/kenya#footnote5_jxd6oql, accessed April 2017.

UNAIDS (2015c). UNAIDS. HIV and AIDS estimates. http://www.unaids.org/en/regionscountries/countries/kenya, accessed April 2017.

UNAIDS (2016a). Global AIDS up date 2016. Global AIDS up date-UNAIDS 2016. http://www.unaids.org/sites/default/files/media_asset/global-AIDS-update-2016_en.pdf, accessed April 2017.

UNAIDS (2016b). Unaids report. Prevention Gap Report. http://www.unaids.org/sites/default/files/media_asset/2016-prevention-gap-report_en.pdf, accessed April 2017.

UNAIDS (2017). UNAIDS Fact sheet. Fact sheet – Latest statistics on the status of the AIDS epidemic. http://www.unaids.org/en/resources/fact-sheet, accessed April 2017.

UNAIDS (2018a). Global HIV & AIDS statistics - 2019 fact sheet. https://www.unaids.org/en/resources/fact-sheet, accessed January 2019.

UNAIDS (2018b). United Nations AIDS. Advocating for zero discrimination in health-care settings in Kenya. Retrieved June, 2018 from http://www.unaids.org/en/resources/presscentre/featurestories/2018/may/zero-discrimination-health-care-settings-kenya.

United Nations Programme on HIV/AIDS, J. (2014). 90-90-90: an ambitious treatment target to help end the AIDS epidemic. Geneva, Switzerland: Joint United Nations Programme on HIV. *AIDS*.

UNR-Med (2005). The HIV Life Cycle. https://med.unr.edu/Documents/unsom/statewide/aidsetc/HIVLifeCycle_FS_en.pdf, accessed March 2018.

Vaccine (2018). Study participants move HIV vaccine clinical trials forward. https://www.hvtn.org/en/media-room/news-releases/study-participants-move-hiv-vaccine-clinical-trials-forward.html, accessed March 2019.

Van den Driessche, P. and Watmough, J. (2002). Reproduction numbers and sub-threshold endemic equilibria for compartmental models of disease transmission. *Mathematical Biosciences*, 180(1):29–48.

Van Sighem, A., Vidondo, B., Glass, T. R., Bucher, H. C., Vernazza, P., Gebhardt, M., de Wolf, F., Derendinger, S., Jeannin, A., and Bezemer, D. (2012). Resurgence of HIV infection among men who have sex with men in Switzerland: mathematical modelling study. *PloS one*, 7(9):e44819.

Voeten, H. A., Egesah, O. B., Varkevisser, C. M., and Habbema, J. (2007). Female sex workers and unsafe sex in urban and rural Nyanza, Kenya: regular partners may contribute more to HIV transmission than clients. *Tropical Medicine & International Health*, 12(2):174–182.

Wamoyi, J., Stobeanau, K., Bobrova, N., Abramsky, T., and Watts, C. (2016). Transactional sex and risk for HIV infection in sub-Saharan Africa: a systematic review and meta-analysis. *Journal of the International AIDS Society*, 19(1):20992.

WB (2017). World Bank Data. Birth rate, crude (per 1,000 people). https://data.worldbank.org/indicator/SP.DYN.CBRT.IN, accessed October 2017.

Wechsberg, W. M., Luseno, W. K., and Lam, W. (2005). Violence against substance-abusing South African sex workers: intersection with culture and HIV risk. *AIDS Care*, 17(S1):55–64.

Weiss, H. A., Halperin, D., Bailey, R. C., Hayes, R. J., Schmid, G., and Hankins, C. A. (2008). Male circumcision for HIV prevention: from evidence to action? *AIDS*, 22(5):567–574.

WHO (2008). Male circumcision: global trends and determinants of prevalence, safety and acceptability.

WHO (2014). March 2014 supplement to the 2013 consolidated guidelines on the use of antiretroviral drugs for treating and preventing HIV infection: recommendations for a public health approach.

WHO (2015). *Guideline on when to start antiretroviral therapy and on pre-exposure prophylaxis for HIV*. World Health Organization.

WHO (2018). WHO. HIV/AIDS-Global Health Observatory (GHO) data. Retrieved January, 2018 from http://www.who.int/gho/hiv/en/.

WHO, UNAIDS, and UNICEF (2009). TOWARDS UNIVERSAL ACCESS: Scaling up priority HIV/AIDS interventions in the health sector.

WHR (2018). World Health Rankings. Live Longer Live Better. http://www.worldlifeexpectancy.com/kenya-life-expectancy, Accessed May 2018.

Williams, B. G. (2014). Optimizing control of HIV in Kenya. *arXiv preprint arXiv:1407.7801*.

Williams, B. G. and Dye, C. (2018). Dynamics and control of infections on social networks of population types. *Epidemics*, 23:11–18.

Williams, B. G., Hargrove, J. W., and Humphrey, J. H. (2010). The benefits of early treatment for HIV. *AIDS*, 24(11):1790–1791.

Wodarz, D. and Nowak, M. A. (2002). Mathematical models of HIV pathogenesis and treatment. *BioEssays*, 24(12):1178–1187.

World Bank (2019). World Bank Data. HIV / AIDS. Retrieved May, 2018 from https://ourworldindata.org/hiv-aids.

Wu, J., Dhingra, R., Gambhir, M., and Remais, J. V. (2013). Sensitivity analysis of infectious disease models: methods, advances and their application. *Journal of The Royal Society Interface*, 10(86):20121018.

Yan, X., Zou, Y., and Li, J. (2007). Optimal quarantine and isolation strategies in epidemics control. *World Journal of Modelling and Simulation*, 3(3):202–211.

Yang, W., Shu, Z., Lam, J., and Sun, C. (2017). Global dynamics of an HIV model incorporating senior male clients. *Applied Mathematics and Computation*, 311:203–216.

Yerly, S., Vora, S., Rizzardi, P., Chave, J.-P., Vernazza, P., Flepp, M., Telenti, A., Battegay, M., Veuthey, A.-L., Bru, J.-P., et al. (2001). Acute HIV infection: impact on the spread of HIV and transmission of drug resistance. *AIDS*, 15(17):2287–2292.

Young, R. M. and Meyer, I. H. (2005). The trouble with 'MSM' and 'WSW': Erasure of the sexual-minority person in public health discourse. *American Journal of Public Health*, 95(7):1144–1149.

Zaman, G., Kang, Y. H., and Jung, I. H. (2008). Stability analysis and optimal vaccination of an sir epidemic model. *BioSystems*, 93(3):240–249.

Zar, J. H. (2010). *Biostatistical Analysis, 5th ed*. Pearson Prentice Hall: Upper Saddle River, NJ.

Zeh, C., Inzaule, S. C., Ondoa, P., Nafisa, L. G., Kasembeli, A., Otieno, F., Vandenhoudt, H., Amornkul, P. N., Mills, L. A., and Nkengasong, J. N. (2016). Molecular epidemiology and transmission dynamics of recent and long-term HIV-1 infections in Rural Western Kenya. *PloS one*, 11(2):e0147436.

Appendix A

MATLAB

The MATLAB code used for curve fitting and simulations in Chapter 3 and Chapter 6.

A.1 Matlab curve fitting code

```
function HIVfit(do_estimation)
warning off;
%%% ====================loading data from excel ====================
Data=xlsread('HIV.xlsx');

%%% ========== The initial guess of the parameters=================
lambda = 1/30; mu = 1/60; kappa1 = 1/13; kappa2 = 1/14;
beta1 = 0.0523; beta2 = 0.0380; beta3 = 0.027; beta4 = 0.0120;
eta1 = 0.282; eta2 = 0.0282; delta1 = 0.0054; delta2 = 0.00465;
delta3 = 0.00613;
%%% ============== The initial conditions ========================
S0 = 20000000; I0 = 40702; T0 = 130000; W0 = 000; X0 = 000;
y0=[S0,I0,T0,W0,X0];
%%%============== year to start the model simulation ============
Istart=2000;
Iend=Istart + 17;
options=odeset('AbsTol',0.001,'RelTol',0.001,'MaxStep',1);
%%%============== The estimated parameters ======================
do_estimation=1;
```

```
if(do_estimation)
xdata=Data(:,1)'; ydata=Data(:,2)';
x0(1,1) = 1/30; x0(1,2) = 1/60; x0(1,3) = 1/13; x0(1,4) = 1/14;
x0(1,5) = 0.0523; x0(1,6) = 0.0380; x0(1,7) = 0.027; x0(1,8) = 0.0120;
x0(1,9) = 0.0282; x0(1,10) = 0.0282; x0(1,11) = 0.0054; x0(1,12) = 0.00465;
x0(1,13) = 0.00613;
%%% ====================== The upper and lower bounds ====================
LB=[0.025 0.014 0.0083 0.0083 0.0 0.0 0.0 0.0 0.060 0.05 0.0008 0.003 0.005];
UB=[0.050 0.020 0.0145 0.0145 1.9 1.9 1.9 1.9 0.9 0.8 0.052 0.09 0.05];
%%%=========================The least squares method ======================
x=lsqcurvefit(@Model_Inc,x0,xdata,ydata,LB,UB,optimset);
%%%======================== The estimation of parameters ==================
'estimated parameters'
lambda = x(1)
mu = x(2)
kappa1 =x(3)
kappa2 = x(4)
beta1 = x(5)
beta2 = x(6)
beta3 = x(7)
beta4 = x(8)
eta1 = x(9)
eta2 = x(10)
delta1 = x(11)
delta2 = x(12)
delta3 = x(13)
end
%%%====================== Solving the ODES with data======================
[t y] = ode45(@HIVfit,[000:1:(Iend-Istart)], y0);
S = y(:,1); I = y(:,2); T = y(:,3); W = y(:,4); X = y(:,5);
```

```
NN=sum(S+I+T+W+X);
%%%====================The incidence data (I)==============================
incidence= y(:,2);
close all;
%%% ====================model ploting ================================%%%
figure(1)
plot(Istart+t,incidence,'-r','LineWidth',1.5), hold on,
plot(Data(:,1),Data(:,2),'o','LineWidth',2.0),
xlabel ('Time (year)','fontsize',12),
ylabel ('New HIV infections ','fontsize',12),
hold off
legend('Model output','HIV data (aged 15+ years)','FontSize',8,'Location'
                                        ,'east')
ylim([0 80000])
xlim([xdata(1) 2018])
figure(2)
plot(Istart+t,I,'-r','LineWidth',1.5),
xlabel ('Time (year)','fontsize',12),
ylabel ('New HIV infections projection (aged 15+ years) ','fontsize',12),
ylim([0 80000])
xlim([xdata(1) 2030])
figure(3)
plot(Istart+t,(I*100)/N,'-r','LineWidth',1.5),
xlabel ('Time (year)','fontsize',12),
ylabel ('Estimated HIV incidence in % (aged 15+ years) ','fontsize',12),
ylim([0 0.35])
xlim([xdata(1) 2030])
%%% ================ The model system ==============================
function [ydot]=HIVfit(t,y)
S = y(1); I = y(2); T = y(3); W = y(4); X = y(5);
```

```
N=sum(y);
ydot(1) = lambda*N -(beta1*y(2)+beta2*y(3)+beta3*y(4)+beta4*y(5))*y(1)/N -
... mu*y(1);
ydot(2) = (beta1*y(2)+ beta2*y(3)+beta3*y(4)+beta4*y(5))*y(1)/N -...
 (delta1+eta1+mu)*y(2);
ydot(3) = delta1*y(2)-(eta2+mu+kappa1)*y(3);
ydot(4) = eta1*y(2) + delta3*y(5)-(delta2+mu)*y(4);
ydot(5) = eta2*y(3) + delta2*y(4)-(delta3+mu+kappa2)*y(5);
ydot=ydot';
end
function Inc=Model_Inc(x0,xdata)
  %%% ====== initialization of incidence not to have an empty array ========
Inc=0;
%%% ============== The order of the parameters =====================
lambda = x0(1);
mu = x0(2);
kappa1 =x0(3);
kappa2 = x0(4);
beta1 = x0(5);
beta2 = x0(6);
beta3 = x0(7);
beta4 = x0(8);
eta1 = x0(9);
eta2 = x0(10);
delta1 = x0(11);
delta2 = x0(12);
delta3 = x0(13);
%%%================= Initial values ================================
S0 = 20000000; I0 = 40702; T0 = 130000; W0 = 000; X0 = 000;
y0=[S0,I0,T0,W0,X0];
```

```
[t y] = ode45(@HIVfit, [0:1:Iend-Istart], y0);
S=y(:,1); I=y(:,2); T=y(:,3); W=y(:,4); X=y(:,5);
 incidence= y(:,2);
for i=1:length(xdata)
     ind=find(xdata(i)-Istart==t);
     S=y(ind,1); I=y(ind,2); T=y(ind,3); W=y(ind,4); X=y(ind,5);
%%%============== The incidence state variable ==================
Inc(i)= I;
end
end
end
```

A.2 Simulation code

```
function [yu]=risks
clc,
Istart=0;
Iend=Istart + 50;
%============ Fixed parameters ================================
Pi1 = 0.0161; Pi2 = 0.0161;  psi = 3;  mu = 0.0161; alpha1 = 0.39;
alpha2 =0.15;
%============ Transmission probabilities ======================
beta = 0.75; theta1 = 0.98; theta2 = 0.88; theta3 = 0.91;
tau = 0.28; eta = 0.58;  delta1 = 0.92;
%============= Transition parameters ==========================
omega1 = 0.0065; omega2 = 0.0085; kappa1 = 0.0055; kappa2 = 0.0075;
rho1 = 0.045; rho2 = 0.075; gamma1 = 0.0017; gamma2 = 0.0026;
%=============== PrEP uptake parameters =======================
xi1 = 0.9;   xi3 = 0.9;
```

```
%================ PrEP relapse parameters ========================
xi2 = 0.0512; xi4 = 0.0615;
%%=================== Initial conditions=========================
Ss0=110000; Us0=20000; Ts0=00000; Ps0=10000; Sd0=12000; Ud0=2500;
 Td0=2000;Pd0=2000;
y0=[Ss0,Us0,Ts0,Ps0,Sd0,Ud0,Td0,Pd0];
%%================================================================
function dy=system(t,y)
dy=zeros(8,1);
N = y(1)+ y(2)+y(3)+ y(4)+y(5)+y(6)+ y(7)+y(8);

lambda1 = psi*beta*(y(2)+theta1*y(3)+theta2*y(6)+theta3*y(7))/N;
lambda2 = psi*beta*eta*(y(2)+theta1*y(3)+theta2*y(6)+theta3*y(7))/N;
lambda3 = delta1*y(6)/(1+tau*y(6));
N1 = y(1)+ y(2)+y(3)+ y(4); N2 = y(5)+y(6)+y(7)+y(8);
dy(1) = Pi1*N1+xi2*y(4)+kappa2*y(5)-lambda1*y(1)-(mu+kappa1+xi1)*y(1);
dy(2) = lambda1*y(1)+omega2*y(6)-(alpha1+omega1+mu)*y(2);
dy(3) = alpha1*y(2)+rho2*y(7)-(rho1+mu)*y(3);
dy(4) = xi1*y(1)+gamma2*y(8)-(gamma1+xi2+mu)*y(4);
dy(5) = Pi2*N2+kappa1*y(1)+xi4*y(8)-(lambda2+lambda3)*y(5)-...
             (mu+kappa2+xi3)*y(5);
dy(6) = (lambda2+lambda3)*y(5)+omega1*y(2)-(alpha2+omega2+mu)*y(6);
dy(7) = alpha2*y(6)+rho1*y(3)-(rho2+mu)*y(7);
dy(8) = xi3*y(5)+gamma1*y(4)-(gamma2+xi4+mu)*y(8);
end
options = odeset('RelTol',1e-4,'AbsTol',1e-5*ones(1,8));
[T,Y] = ode45(@system,[000:1:(Iend-Istart)],y0,options);
Ss=Y(:,1);Us=Y(:,2);Ts=Y(:,3); Ps=Y(:,4); Sd=Y(:,5);Ud=Y(:,6); Td=Y(:,7);
Pd=Y(:,8);
% %----------------------------------------------------------------
```

```
% figure(1)
% hold on
% plot(Istart+T,Ss,'-b','LineWidth',1.5)
% hold on
% xlabel('Time (years)','fontsize',12);ylabel('Susceptible individuals,
%S_s','fontsize',12);
% % ylim([0,1000])
figure(2)
hold on
plot(Istart+T,Us,'--m','LineWidth',1.5)
hold on
xlabel('Time (years)','fontsize',12);ylabel('Infected individuals,
U_s','fontsize',12);
figure(3)
hold on
plot(Istart+T,Ts,'--m','LineWidth',1.5)
hold on
xlabel('Time (years)','fontsize',12);ylabel('Infected individuals on ART,
 T_s', 'fontsize',12);
figure(4)
hold on
plot(Istart+T,Ps,'--m','LineWidth',1.5)
hold on
xlabel('Time (years)','fontsize',12);ylabel('Susceptible individuals on
PrEP, P_s','fontsize',12);
% figure(5)
% hold on
% plot(Istart+T,(Us+Ts)/N1,'-b','LineWidth',1.5)
% hold on
% xlabel('Time (years)','fontsize',12);ylabel('Prevalence of HIV',
```

```
%'fontsize',12);
% figure(6)
% hold on
% plot(Istart+T,Sd,'-b','LineWidth',1.5)
% hold on
% xlabel('Time (years)','fontsize',12);ylabel('Susceptible individuals,
% S_d','fontsize',12);
% ylim([0,1000])
figure(7)
hold on
plot(Istart+T,Ud,'--m','LineWidth',1.5)
hold on
xlabel('Time (years)','fontsize',12);ylabel('Infected individuals,
 U_d','fontsize',12);
figure(8)
hold on
plot(Istart+T,Td,'--m','LineWidth',1.5)
hold on
xlabel('Time (years)','fontsize',12);ylabel('Infected individuals on ART,
 T_d','fontsize',12);
figure(9)
hold on
plot(Istart+T,Pd,'--m','LineWidth',1.5)
hold on
xlabel('Time (years)','fontsize',12);ylabel('Susceptible individuals on
PrEP, P_d','fontsize',12);
% figure(10)
% hold on
% plot(Istart+T,(Ud+Td)/N2,'-b','LineWidth',1.5)
% hold on
```

```
% xlabel('Time (years)','fontsize',12);ylabel('Prevalence of HIV',
%'fontsize',12);
%====================Compasiron plots ==========================
% figure(11)
% plot(Istart+T,Ss,'-b',Istart+T,Sd,'-r','LineWidth',2.0)
% xlabel('Time (Years)')
% ylabel('Infected individuals not on ART')
% legend('S_s', 'S_d')
%%%==========Computations of basic reproduction numbers ==========
Q1 = mu+kappa1+xi1; Q2 = alpha1+omega1+mu; Q3 = rho1+mu; Q4 = gamma1+xi2+mu;
Q5 = mu+kappa2+xi3; Q6 = alpha2+omega2+mu; Q7 = rho2+mu; Q8 = rho2+xi4+ mu;
Q9 = kappa1*kappa2*Q4*Q8+xi1*xi2*Q5*Q8; Phi1 = (xi1*xi2)/(Q1*Q4);
Phi2 = (xi3*xi4)/(Q5*Q8); Phi3 = (xi2*xi3)/(gamma1*kappa2);
Phi4 = (xi1*xi4)/(gamma2*kappa1); Phi5 = (kappa1*kappa2)/(Q1*Q5);
Phi6 = gamma1*gamma2*(kappa2*Pi2*(1-Phi3)+Pi1*Q5);
Phi7 = kappa1*kappa2*Q4*Q8-xi1*xi2*Q5*Q8;
Phi8 = delta1*(Pi1+Pi2)*Q7+beta*eta*mu*psi*(theta2*Q7+alpha2*theta3);
R01 = (beta*psi*(mu +xi2)*(Q3+alpha1*theta1))/(Q2*Q3*(mu +xi2+xi1))
R02 = ((mu +xi4)*(Q7*delta1+beta*psi*eta*(Q7*theta2+alpha2*theta3)))
/(Q6*Q7*(mu +xi4+xi3))
R0s = (beta*psi*mu*(Q3+alpha1*theta1)*(Q4*Q8*(kappa2*Pi2+Pi1*Q5*(1-Phi2))
-Phi6))/((Pi1+Pi2)*Q2*Q3*(gamma1*gamma2*kappa1*kappa2*(1-Phi3)*(1-Phi4)
-Q1*Q5*(gamma1*gamma2-Q4*Q8*(1-Phi2))-Phi7))
R0d = (Phi8*((gamma1*gamma2*kappa1*Pi1*(1-Phi4)+Q4*Q8*(kappa1*Pi1+Pi2*Q1)
+Pi2*(gamma1*gamma2*Q1+xi1*xi2*Q8))))/((Pi1+Pi2)*Q6*Q7*(gamma1*gamma2
*kappa1*kappa2*(1-Phi3)*(1-Phi4)-Q1*Q5*(gamma1*gamma2-Q4*Q8*(1-Phi2))-Phi7))
R0 = max([R0s,R0d])
end
```

Appendix B

R code

The **R** code used for descriptive analysis, curve fitting and simulations in Chapter 4 and Chapter 5.

B.1 Descriptive analysis code

```
#==============Setting the working directory=======================
setwd("C:/Users/eomondi/Desktop/PHD-code/Sex-model")
dir()
# ============== Loading the necessary packages====================
library(deSolve) # library for solving differential equations
library(reshape2) # library for reshaping data
library(ggplot2) #library for plotting
library(minpack.lm)
library(gridExtra)
library(tidyr)
library(rcompanion)
library(FSA)
###
#====== Loading the data=========================================
MyData <- read.csv("Adults.csv", header = T)
colnames(MyData) = c("time","Male","Female","Total")
### =====Converting the data HIV.data1 to long data=================
MyData.long  <- gather(data = MyData, key = Gender, value = Number,
```

```
                -c(time))
###### ======== Plots for the row data of the HIV infections =======
Raw.data<-MyData[,c(1,2,3)] # Subset of the main data
Raw.long.data  <- gather(data = Raw.data, key = Gender, value = Number,
                         -c(time))
Plot1<-ggplot(data=Raw.long.data,aes(x=time,y=Number,color=Gender))+
  geom_point(size=2) +theme_bw() +theme(axis.title
      = element_text(face  = "bold")) +  xlab("Time in years")
      +ylab("Cases of new infections")+ xlim(2000,2020)+ylim(0,80000)
Plot1
### ==========Error bar/ ggplot to describe the data ==================
Sum = groupwiseMean(Number ~ Gender,data   = MyData.long,conf   = 0.95,
         digits = 3)
Sum
bar1<-qplot(x    = Gender,y = Mean,data = Sum) +
  geom_errorbar(aes(ymin  = Trad.lower,ymax  = Trad.upper,width = 0.15))
  +theme_bw() +theme(axis.title   = element_text(face  = "bold"))+
  ylab("Mean number of new infections")+ylim(0,100000)
bar1
bar2<-ggplot(Sum, aes(x = Gender, y = Mean)) +
  geom_errorbar(aes(ymin = Trad.lower,ymax = Trad.upper), width = 0.05,
  size  = 0.5) +  geom_point(shape = 15,size  = 3) +theme_bw()
  +theme(axis.title   = element_text(face  = "bold"))
  + ylab("Mean number of new infections")+ylim(0,100000)
bar2
## =========Simple error bargraph of the mean ====================
Table = as.table(Sum$Mean)
rownames(Table) = Sum$Gender
par(mfrow=c(1,1))
barplot(Table,ylab="Mean number of new infections",xlab="Sex")
```

```
bar3<-qplot(x    = Gender,y= Mean,data = Sum)
 + geom_bar(stat ="identity",fill = "gray")
 +  geom_errorbar(aes(ymin  = Trad.lower, ymax  = Trad.upper,
 width = 0.15))+  geom_point(shape = 15,size  = 3)+theme_bw()
 +theme(axis.title   = element_text(face  = "bold")) +
  ylab("Mean number of new infections")+ylim(0,100000)
#dev.off()
bar3
#### =============The density plot ==============================
data.den<-MyData[,c(1,2,3)]
data.den.long<-gather(data = data.den, key = Gender, value = Number,
                      -c(time))
ggplot(data.den.long, aes(x = Number, fill = Gender))+
  geom_density(alpha=.5)+ scale_fill_manual(values=c("red","blue"))+
  theme_bw() +theme(axis.title   = element_text(face  = "bold"))+
  xlab("Number of new cases of HIV infection")
### ============ The statistical test for the difference===========
wiltest<-wilcox.test(data.den.long$Number ~ data.den.long$Gender,
                     paired=FALSE)
wiltest
sum(rank(c(MyData$Female,MyData$Male))[1:17])
### ===================== End ===================================
```

B.2 Curve fitting code

```
setwd("~/OneDrive - Strathmore University/Documents/PhD/PHD-code/Sex-model")
# ============ Loading the necessary packages======================
library(deSolve) # library for solving differential equations
library(reshape2) # library for reshaping data (tall-narrow <-> short-wide)
```

```
library(ggplot2) #library for plotting
library(minpack.lm); library(gridExtra); library(tidyr); library(rcompanion)
library(FSA); library(FME); library(stargazer); library(plotly)
library(dplyr); library(devtools); library(Rmisc); library(data.table)
library(DescTools); library(agricolae); require(PMCMR); library(pastecs)
### Loading the data=======================================
HIV.data <- read.csv("HIVA.csv", header = T)
##========== Subsetting the data of interest and plotting===========
HIV.data1<-HIV.data[,c(5,11,12)] # Subset of the main data
HIV.long.data  <-gather(data=HIV.data1, key=Gender, value=Number,-c(Year))
HIV.plot<-ggplot(data=HIV.long.data,aes(x=Year,y=Number,color=Gender))+
geom_point(size=2)+theme_bw()+theme(axis.title = element_text(face="bold"))
+xlab("Year")+ylab("New cases of HIV infection")+xlim(2010,2018)
                      +ylim(0,30000)
HIV.plot
#================== FSW function ====================================
FSW.ode = function(t,y,p){
  with(as.list(c(y,p)),{
  #===========The baseline model parameters (fixed parameters) ===========
  Lambda = 0.001245; mu =0.00139; delta_1 =  0.009125;   delta_2 = 0.00725
  c_m1 = 3;   c_m2 = 2;   c_m3 = 2;   c_m4 = 2; c_f1 = 3;   c_f2 = 2
  c_f3 = 2;   c_f4 = 2;   alpha = 0.49
  #=============PrEP intervention introduced in May 2017 ==============
  if(t<=2017.333333){  #
    phi=0
  }else {
    phi=0.40
  }
    ## ==================The population of each gender=================
  N_m =  S_m+I_m1+I_m2+T_m1+T_m2; N_f =  S_f+I_f1+I_f2+T_f1+T_f2
```

```
    #==================The infection terms ============================
  lambda_m =(1-phi)*((beta_f1*c_m1*I_f1+beta_f2*c_m2*I_f2+
                beta_f3*c_m3*T_f1+beta_f4*c_m4*T_f2)/N_m)
  lambda_f =(1-phi)*((beta_m1*c_f1*I_m1+beta_m2*c_f2*I_m2+
                beta_m3*c_f3*T_m1+beta_m4*c_f4*T_m2)/N_f)
  #========== ODE system of equations ============================
  dS_m = alpha*Lambda*N_m-lambda_m* S_m- mu*S_m
  dI_m1 =lambda_m*S_m-(gamma_1+tau_1+mu)*I_m1
  dI_m2 = gamma_1*I_m1-(tau_2+mu+delta_1)*I_m2
  dT_m1 = tau_1*I_m1+ omega_1*T_m2-(psi_1+mu)*T_m1
  dT_m2 = tau_2*I_m2+psi_1*T_m1-(omega_1+mu+delta_2)*T_m2
  dS_f =(1-alpha)*Lambda*N_f-lambda_f*S_f-mu*S_f
  dI_f1 = lambda_f*S_f-(gamma_2+tau_3+mu)*I_f1
  dI_f2 = gamma_2*I_f1-(tau_4+mu+delta_1)*I_f2
  dT_f1 = tau_3*I_f1+omega_2*T_f2-(psi_2+mu)*T_f1
  dT_f2 = tau_4*I_f2+psi_2*T_f1-(omega_2+mu+delta_2)*T_f2
  #=========== packagin the ODES as a list ======================
  list(c(dS_m,dI_m1,dI_m2,dT_m1,dT_m2,dS_f,dI_f1,dI_f2,dT_f1,dT_f2),
       N_m,N_f, lambda_m, lambda_f)})
}
#========= model parameters to be fitted ========================
prm=c(beta_m1 =2.232372e-01,beta_m2 =6.861681e-03,beta_m3=2.840410e-03,
beta_m4=2.358015e-01, beta_f1=8.415809e-01, beta_f2 =9.512583e-03,
beta_f3 =1.109097e-02,beta_f4=3.322502e-03, gamma_1=5.038317e-01,
gamma_2 = 9.881907e-01,tau_1=9.886510e-01,tau_2=9.992431e-01,
tau_3 =9.895523e-01,tau_4=9.987893e-01,psi_1=1.822176e-04,
psi_2 =9.998650e-01,omega_1= 9.999946e-01,omega_2=2.166125e-05)
# prm=c(beta_m1 = 0.8703, beta_m2 = 0.703, beta_m3 = 0.6703,beta_m4 = 0.5703,
#       beta_f1 =  0.8703,beta_f2 = 0.703, beta_f3 = 0.6703,beta_f4 = 0.5703,
#       gamma_1 = 0.5231,gamma_2 = 0.5231,tau_1 =  0.623,tau_2 =  0.623,
```

```
#       tau_3 = 0.623, tau_4 = 0.623, psi_1 = 0.271, psi_2 = 0.271,
#       omega_1 = 0.057, omega_2 = 0.036)
#===================initial conditions==============================
init = c(z0=12000000,z1=500,z2=35000,z3=30000,z4=45000,z5=11000000,z6=530,
         z7=40000,z8=35000,z9=50000)

inits=c(S_m=init[[1]],I_m1=init[[2]],I_m2=init[[3]],T_m1=init[[4]],
T_m2=init[[5]],S_f=init[[6]],I_f1=init[[7]],I_f2=init[[8]],T_f1=init[[9]],
T_f2=init[[10]])
#==============output times ================================
tm = seq(2011,2030,by=1/12)
##tm = HIV.data1$Year
#======================ODE output================================
pra = as.data.frame(lsoda(inits,tm,FSW.ode,prm))
results1<-pra[,c(1:11)]
results2<-pra[,c(1,12,13)]
results3<-pra[,c(1,14,15)]
###======Plotting the initial output============================
HIV.pra  <- gather(data=results1, key=Population, value=Number,-c(time))
HIV.pra1  <- gather(data=results2, key = Total, value = Number,-c(time))
HIV.pra2  <- gather(data=results3, key = Force, value = Number,-c(time))
HIV.pra.plot<-ggplot(data=HIV.pra,aes(x=time,y=Number,color=Population))+
  geom_line(size=1.2)+theme_bw() +theme(axis.title=element_text(face="bold"))
  +xlab("Time in years")+ylab("Population profile")+ xlim(2010,2030)
  +ylim(0,15000000)
HIV.pra.plot
##### ======The plots to the total population and forces of infection=====
ggplot(data=HIV.pra1,aes(x=time,y=Number,color=Total))+
  geom_line(size=1.2)+theme_bw() +theme(axis.title=element_text(face= "bold"))
  +xlab("Time in years")+ylab("Total population")+ xlim(2010,2030)
```

```
ggplot(data=HIV.pra2,aes(x=time,y=Number,color=Force))+
  geom_line(size=1.2)+theme_bw() +theme(axis.title=element_text(face="bold"))
  +xlab("Time in years")+ylab("Force of infection")+ xlim(2010,2030)
#==============HIV incidence  data ==============================
Data<-HIV.data[,c(5,12,11)] #5,11,12
colnames(Data) = c("time","I_m1","I_f1")
DataF<-as.data.frame(Data)
### =======The objective function for fitting the data =============
Objective = function(x, parset = names(x)) {
  prm[parset] = x
  ## ====================== output times ============================
  ###tout <- HIV.data1$Year
  tout = seq(2011,2030,by=1/12)
  ## ==================initial conditions ====================
  inits0=c(S_m=init[[1]],I_m1=init[[2]],I_m2=init[[3]],T_m1=init[[4]],
  T_m2=init[[5]],S_f=init[[6]],I_f1=init[[7]],I_f2=init[[8]],T_f1=init[[9]],
  T_f2=init[[10]])
  out = lsoda(inits0,tout,FSW.ode,prm)
  ## ====================Model cost ==========================
  return(modCost(obs = Data, model = out))
}
 ##=============== fitting the model ==========================
LL = c(0.0,0.0,0.0,0.0,0.0,0.0,0.0,0.0,0.0,0.0,0.0,0.0,0.0,0.0,0.0,0.0,0.0,0.0,0.0)
UL=c(2.0,2.0,2.0,2.0,2.0,2.0,2.0,2.0,1.0,1.0,1.0,1.0,1.0,1.0,1.0,1.0,1.0,1.0,1.0)
parms = c(beta_m1 =2.232372e-01,beta_m2 =6.861681e-03,beta_m3=2.840410e-03,
          beta_m4=2.358015e-01, beta_f1=8.415809e-01, beta_f2 =9.512583e-03,
          beta_f3 =1.109097e-02,beta_f4=3.322502e-03, gamma_1=5.038317e-01,
          gamma_2 = 9.881907e-01,tau_1=9.886510e-01,tau_2=9.992431e-01,
          tau_3 =9.895523e-01,tau_4=9.987893e-01,psi_1=1.822176e-04,
          psi_2 =9.998650e-01,omega_1= 9.999946e-01,omega_2=2.166125e-05)
```

```
# ,z0=12000000,z1=500,z2=35000,z3=30000,
# z4=45000,z5=11000000,z6=530,z7=40000,z8=35000,z9=50000
Fit = modFit(p = parms, f = Objective,lower = LL,upper=UL)
betafit = Fit$par
prmfit1    = c(betafit)
print(prmfit1)
inits1=c(S_m=init[[1]],I_m1=init[[2]],I_m2=init[[3]],T_m1=init[[4]],
T_m2=init[[5]],S_f=init[[6]],I_f1=init[[7]],I_f2=init[[8]],T_f1=init[[9]],
T_f2=init[[10]])
#==============ODE output==============================
praF = as.data.frame(lsoda(inits1,tm,FSW.ode,prmfit1))
## ================Extracting the data for plot ==================
Male<-praF[,c(1,3)]
colnames(Male) = c("time","Model")
Male1<-HIV.data[,c(5,12)] #5,11,12
colnames(Male1) = c("time","Data")
Female<-praF[,c(1,8)]
colnames(Female) = c("time","Model")
Female1<-HIV.data[,c(5,11)] #5,11,12
colnames(Female1) = c("time","Data")
# =======Overlay predicted profile with experimental data ===========
  ##### Male
base = ggplot(data=Male, aes(x=time,Model)) + geom_line(color='#CC0000',size=1)
base = base+geom_point(data=Male1,aes(time,Data),size=1,colour="blue")
base = base+ theme_bw() +theme(axis.title=element_text(face="bold")) +
  xlab("Time (years)")+ylab("New cases of infection (male)")+ xlim(2010,2018)
  + ylim(0,20000)
print(base)
## Female
```

```
base1=ggplot(data=Female, aes(x=time,Model)) + geom_line(color='#CC0000',size=1)
base1 = base1+geom_point(data=Female1,aes(time,Data),size=1,colour="blue")
base1 =base1+theme_bw() +theme(axis.title=element_text(face="bold"))
+ xlab("Time (years)")+ylab("New cases of infection (female)")+ xlim(2010,2018)
  + ylim(0,30000)
print(base1)
###=====comparing male and female fits============================
Comp_data<-praF[,c(1,3,8)]
colnames(Comp_data) = c("time","Male","Female")
Comp_data2  <- gather(data=Comp_data, key = Gender, value = Number,-c(time))
ggplot(data=Comp_data2,aes(x=time,y=Number,color=Gender))+
  geom_line(size=1.2)+ theme_bw() +theme(axis.title=element_text(face="bold"))
  +xlab("Time (years)")+ylab("New cases of infection ")+ xlim(2010,2030)
  + ylim(0,20000)
## =========Summary and coeficients of the params estimates==========
p_st<-coef(Fit)
SF<-summary(Fit)
Var0 <- SF$modVariance # model variance
covIni <- SF$cov.scaled*2.4^2/2 # model covariance
## =========Generating the table of the parameters ================
stargazer(SF$par)
###=======    Sensitivity analysis ============================
##======== Global sensitivity analysis ================
min = c(0.0,0.0,0.0,0.0,0.0,0.0,0.0,0.0,0.0,0.0,0.0,0.0,0.0,0.0,0.0,0.0,
0.0,0.0,0.0)
max =c(2.0,2.0,2.0,2.0,2.0,2.0,2.0,2.0,1.0,1.0,1.0,1.0,1.0,1.0,1.0,1.0,
1.0,1.0,1.0)
parRanges <- data.frame(min, max)
rownames(parRanges) <- c("beta_m1", "beta_m2", "beta_m3","beta_m4","beta_f1",
                         "beta_f2","beta_f3","beta_f4","gamma_1","gamma_2",
```

```
                        "tau_1", "tau_2", "tau_3", "tau_4", "psi_1",
                        "psi_2","omega_1","omega_2")
parRanges

tout = seq(2011,2030,by=1/12)
print(system.time(
  sR <- sensRange(func = Objective, parms = prm, dist = "grid",
    sensvar =c("I_m1","I_f1"), parRange=parRanges[1,],num=84)))
head(summary(sR))
summ.sR <- summary(sR)
par(mfrow=c(2, 2))
plot(summ.sR, xlab = "Year", ylab = "Cases of infection",
     legpos = "topright", mfrow = NULL)
plot(summ.sR, xlab = "Year", ylab = "Cases of infection", mfrow = NULL,
     quant = TRUE, col = c("lightblue", "darkblue"), legpos = "topright")
mtext(outer = TRUE, line = -1.5, side = 3, "Sensty to beta_m1", cex = 1.25)
par(mfrow = c(1, 1))
###======global for all the parameters ==========================
Sens2 <- summary(sensRange(func = Objective, parms = prm,dist = "latin",
 sensvar = "I_m1", parRange = parRanges, num = 1000))
plot(Sens2, main = "Sensitivity of all params", xlab = "Year",
     ylab = "Number of infections")
##============Local sensitivity analysis ==================
HIVfit<-sensFun(func = Objective,parms=prm,sensvar =c("I_m1","I_f1"),
 varscale = 1)
head(HIVfit)
plot(HIVfit,which = c("I_m1", "I_f1"), col = c("blue", "green"))
###==================Univariate sensitivity====================
summary(HIVfit)
summary(sensFun(Objective, prm, varscale = 1), var = TRUE)
```

```
###===========Bivariate sensitivity and collinearity============
cor1<-cor(HIVfit[ ,-(1:2)])
cor1
collin(HIVfit,parset = 1:18)
Coll <- collin(HIVfit)
Coll
par(mfrow=c(1,1))
plot(Coll,log = "y")
abline(h=20,col="red")
ident<-collin(SF)
head(ident,n=20)
pairs(HIVfit, which = c("I_m1", "I_f1"), col = c("blue", "green"))
###=========Run the MCMC================================
LB = c(0.0,0.0,0.0,0.0,0.0,0.0,0.0,0.0,0.0,0.0,0.0,0.0,0.0,0.0,0.0,
0.0,0.0,0.0)
UB=c(2.0,2.0,2.0,2.0,2.0,2.0,2.0,2.0,1.0,1.0,1.0,1.0,1.0,1.0,1.0,
1.0,1.0,1.0)
MCMC <- modMCMC(p=p_st,f=Objective,niter=5000,lower=LB,upper=UB,
 jump = NULL,var0=Var0,wvar0 = 1,updatecov=40,burninlength=100)
#============analysing the MCMC chain ==========================
plot(MCMC,cex = 1.25)
plot(MCMC, Full = TRUE) #Results of the MCMC application
par(mar=c(4, 4, 3, 1) + .1)
plot(MCMC, Full = TRUE)
#===============plots of the posterior distributions===================
hist(MCMC)
#=========plotting correlations of your parameters=============
pairs(MCMC)
pairs(MCMC,cex.labels=1.4,cex=0.7)
#=========== Sample parameters from the MCMC chain ==============
```

```
q_par<-summary(as.mcmc(MCMC$par))
q_par
stat.desc(MCMC$par)
#===========The best parameter from MCMC =================
p_mcmc<-MCMC$bestpar
p_mcmc
#========ODE solving============================
inits2=c(S_m=init[[1]],I_m1=init[[2]],I_m2=init[[3]],T_m1=init[[4]],
         T_m2=init[[5]],S_f=init[[6]],I_f1=init[[7]],I_f2=init[[8]],
         T_f1=init[[9]],T_f2=init[[10]])
pra2 = lsoda(inits2,tm,FSW.ode,p_mcmc)
praF2 = as.data.frame(lsoda(inits2,tm,FSW.ode,p_mcmc))
#============Plotting====================================
par(mfrow=c(1,1))
plot(tm,(praF$I_m1),type="l",col =c("blue"),lwd=c(2),lty = 1,
     xlab = "Time (years)", ylab = "HIV prevalence",xlim=c(2010,2030))
lines(tm,(praF2$I_m1),col =c("red"),lwd=c(2),lty = 1 )
points(DataF$time,DataF$I_m1)
legend("topright", c("Least squares","MCMC"),lty = c(1,1),bty="n",
col =c("blue","red"), lwd = c(2,2),cex = 0.6)
par(mfrow=c(1,1))
#===========extract quantiles for your 95% CIs===============
UBq<-q_par$quantiles[1:length(p_mcmc),5]
Median=q_par$quantiles[1:length(p_mcmc),3]
LBq<-q_par$quantiles[1:length(p_mcmc),1]
praF3 = as.data.frame(lsoda(inits2,tm,FSW.ode,LBq))
praF4 = as.data.frame(lsoda(inits2,tm,FSW.ode,Median))
praF5 = as.data.frame(lsoda(inits2,tm,FSW.ode,UBq))
plot(tm,(praF3$I_m1),type="l",ylim=c(0,20000),col =c("black"),lwd=c(2),
lty = 1,xlab = "Time (years)", ylab = "HIV prevalence",xlim=c(2010,2030))
```

```
lines(tm,(praF5$I_m1),col =c("black"),lwd=c(2),lty = 1 )
polygon(c(tm, rev(tm)), c(praF3$I_m1, rev(praF5$I_m1)), col = "grey",
border = NA)
lines(tm,(praF4$I_m1),col =c("brown"),lwd=c(2),lty = 2 )
points(DataF$time,DataF$I_m1)
```

Appendix C

Publications derived from the works in this thesis

Int. J. Appl. Comput. Math (2018) 4:123
https://doi.org/10.1007/s40819-018-0558-y

ORIGINAL PAPER

Modelling the Trend of HIV Transmission and Treatment in Kenya

E. O. Omondi[1] · **R. W. Mbogo**[1] · **L. S. Luboobi**[1]

Abstract
HIV infection remains a major contributor to disease burden and a global leading cause of death. Although progress is being made to control HIV infections, Kenya still remains one of the high HIV burden countries in Sub-Sahara Africa. A deterministic model was proposed to describe the trend of HIV infection in Kenya and suggest some control strategies. The basic reproduction number, $\mathcal{R}_0$, is derived and global asymptotic stability analysis of the disease-free equilibrium carried out. We proved that HIV infections will be contained if the reproduction number is kept below one. Routine data from national survey is used to assess the variation of the new HIV infections in Kenya. Based on this data, least squares method was used to estimate the unknown parameters. The HIV incidence shows of an infection at an endemic state implying of ceaseless problem. Furthermore, improvement in immunological status of the HIV patients on ART due to attrition, may lead to decline in HIV infection and be beneficial to the disease control. The findings suggested that treatment with ART greatly aids the decline in HIV infections hence strengthening its intensity will effectively contribute to the disease control.

Keywords HIV transmission · Reproduction number · Least squares curve fitting · Simulations

Introduction

HIV epidemic has been evolving in Kenya since the detection of the first case in 1984. Kenya has the fourth highest number of HIV infections globally alongside South Africa and Nigeria [28]. The reports from Kenyan National Aids Control Council (NACC) approximated that 1.6 million people were living with HIV by end of year 2015 with 36,000 deaths resulting from AIDS-related illness [25,28]. Based on the sentinel surveillance data, the highest HIV prevalence was reported to be at 10.5% at the end of the year 1996 and fell to approximately 6.0% by end 2015 [12]. Adults aged 15–49 years constitute about 51% of the new infections in Kenya [12].

E. O. Omondi
eomondi@strathmore.edu

[1] Institute of Mathematical Sciences, Strathmore University, P.O. Box 59857-00200 Nairobi, Kenya

Published online: 14 September 2018

A lot of research has been carried out on transmission of HIV using mathematical models [3,17,33]. These models have focused on steady states and their stability as well as computer simulations. None of the existing mathematical models, however, explicitly considers the HIV trends data specific to Kenya. For example, Okongo et al. [18] used a mathematical model to investigated the effects of social behaviour, treatment and vaccination of HIV. The model's stability analysis was determined and numerical simulations carried out. They established that treatment which does not reduce infectivity may not reduce spread of HIV. The incorporation of practical control measures such as behaviour change and treatment in models present an opportunity to assess the benefits of the intervention of public health authorities [26,34]. Liu et al. [11] studied the psychological impact on epidemic outbreaks. They established that an increment in the infection level decreases the effective contacts. Kiss et al. [7] developed a deterministic model to study the impact of information transmission on sexually transmitted diseases. Their model accounted for the diffusion of health information disseminated as a result of the presence of a disease and an 'active' host population that can respond to it by taking measures to avoid infection or if infected by seeking treatment early. However, in their findings they concluded that only a proportion of the population chooses to respond to the risks by limiting effective contacts and subsequently seeking immediate treatment. Other models pertinent to this study include [2,4,6,15,20,22]. While these models incorporated the effects of HIV prevention through such means as behaviour change and as well as treatment with ART, they did not consider the immediate enrolment of new HIV infected individuals to treatment following the WHO and UNAIDS recommendation for HIV treatment centred on 90–90–90 [29]. In our modelling attempt, we consider the case where HIV patients are linked to ART treatment irrespective of their $CD4^+$T cell counts in addition to studying the trend of HIV infections.

To our knowledge, no deterministic model has focused on the study of trend of HIV infection in Kenya. Thus, in the current paper, we aim to develop a mathematical model to integrate to real-time series of HIV infection data amongst the people aged 15 years and above. This is the aged group that significantly contributes to high HIV burden in Kenya through heterosexual means [12]. Our aim is to examine the trend of HIV in Kenya so as to devise effective strategies to combat HIV epidemic in order to achieve the vision 2030. Under this vision, Kenya aims to eradicate HIV infections so as to end AIDS epidemic. Furthermore, we aim to examine the global behaviour of the proposed HIV transmission model.

We organise the work in this paper as follows, second section introduces the model used. We carry out analysis of the mathematical model in third section. In fourth section, we fit the model to data and provide further numerical results. In fifth section, the findings of the study are discussed and conclusions drawn.

Model

Model Formulation

To study the trend of HIV infection in Kenya, we propose a five state compartmental model. The structure of the model is such that it comprises susceptible individuals (S) who are at high risk of HIV infection. Upon acquiring infection, individuals in class S move to infection class which is divided into two stages according to $CD4^+$T cell counts in the blood. These include: stage 1 comprising of individuals with $CD4^+$T cell counts $\geq 350/\mu L$, (I_1). The infected individuals in (I_1) are assumed to be having lower viral load hence considered to be the new

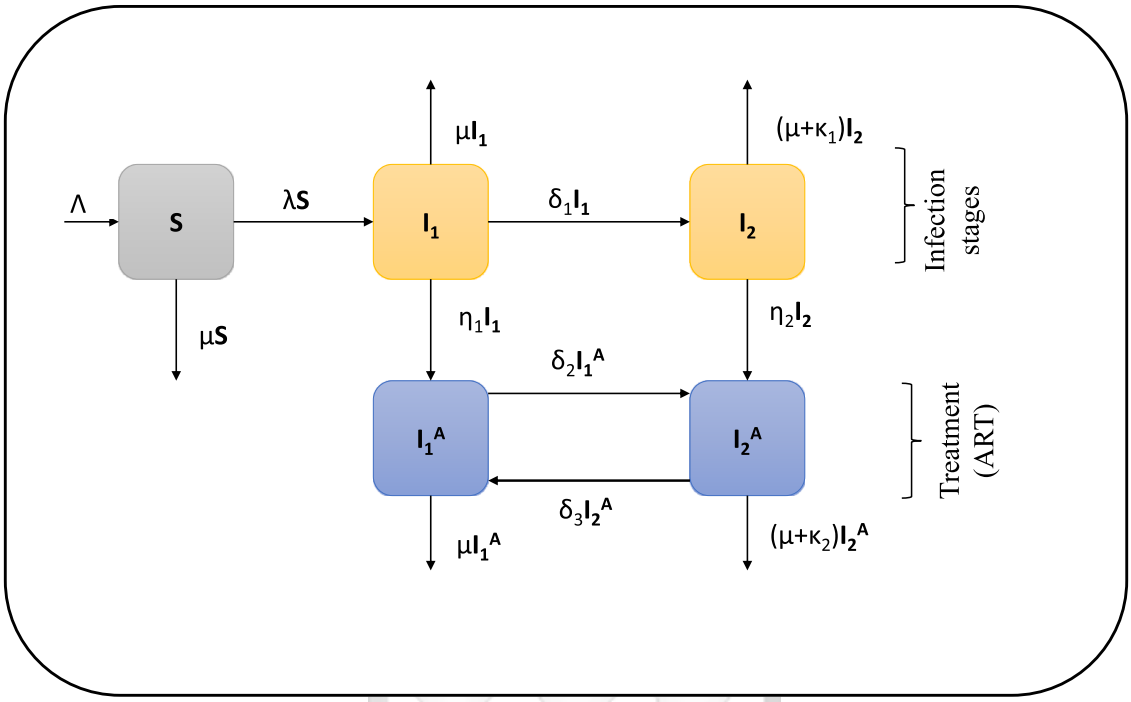

Fig. 1 Schematic diagram of HIV transmission

infections. The second stage of infection consists of individuals with $200/\mu L < CD4^+T$ cell counts $< 350/\mu L$, (I_2). Individuals in this stage are assumed to be having high viral load. HIV positive individuals in stages I_1 and I_2 enter into I_1^A and I_2^A if they receive antiviral therapy treatment (ART) respectively. This is consistent with the WHO recommendation of immediate enrolment into ART irrespective of the $CD4^+T$ cell counts in the blood in order to achieve viral load suppression [1,32]. The AIDS class is not considered in this model given that full blown AIDS patients are usually hospitalised and/or sexually inactive. It is assumed that they are not able to engage in HIV transmission activities hence do not contribute to HIV infection. Figure 1 shows the schematic flow diagram of the model structure. The variable population denoted by N(t) is described by (1).

$$N(t) = S(t) + I_1(t) + I_2(t) + I_1^A(t) + I_2^A(t). \tag{1}$$

We assume that the susceptible individuals are recruited into the system at a constant rate Λ. The susceptible individuals then acquire infections at the rate λ, expressed as

$$\lambda = \frac{\beta_1 I_1 + \beta_2 I_2 + \beta_3 I_1^A + \beta_4 I_2^A}{N}. \tag{2}$$

Here, β_i, where $(i = 1, 2, 3, 4)$, define the effective contact rates between susceptible individuals and infectious individuals in the classes I_1, I_2, I_1^A and I_2^A, respectively. Different effective contact rates are used based on the assumption that infected individuals in different stages may have different effective contact rates due to difference in $CD4^+T$ cell counts in the blood, ART treatment and behaviour change. The natural death rate for all classes is μ. The progression rate from I_1 stage I_2 is given by δ_1. The progression rates from I_1 stage to I_1^A stage and from I_2 stage to I_2^A stage are given by η_1 and η_2 upon enrolment to ART treatment respectively. The rates δ_2 and δ_3 refers to the movement from I_1^A to I_2^A and from I_2^A to I_1^A. This movement is assumed to be bi-directional due to adherence of HIV patients to ART treatment and improvement or decline of the immunological status of the HIV patients

on ART treatment. The disease related death rate is assumed to be κ_1 and κ_2 for I_2 and I_2^A respectively.

Model Equations

The following non-linear ordinary differential equations are obtained.

$$\left.\begin{aligned}
\frac{dS}{dt} &= \Lambda - \lambda S - \mu S,\\
\frac{dI_1}{dt} &= \lambda S - (\delta_1 + \eta_1 + \mu) I_1,\\
\frac{dI_2}{dt} &= \delta_1 I_1 - (\eta_2 + \mu + \kappa_1) I_2,\\
\frac{dI_1^A}{dt} &= \eta_1 I_1 + \delta_3 I_2^A - (\delta_2 + \mu) I_1^A,\\
\frac{dI_2^A}{dt} &= \delta_2 I_1^A + \eta_2 I_2 - (\delta_3 + \mu + \kappa_2) I_2^A.
\end{aligned}\right\} \tag{3}$$

We assume that at $t = 0$, $S(0) > 0$, $I_1(0) \geq 0$, $I_2(0) \geq 0$, $I_1^A(0) \geq 0$ and $I_2^A(0) \geq 0$.

Model Basic Properties

In this section, we explore the basic dynamical features of the system (3). For the system (3) to be mathematically tractable and epidemiologically meaningful, it is important to prove that that all the state variables and all the associated parameters are non-negative for all time $t > 0$.

Theorem 1 *The feasible region Ω represented by the set*

$$\Omega := \left\{ (S, I_1, I_2, I_1^A, I_2^A) \in \mathbb{R}_+^5 : S + I_1 + I_2 + I_1^A + I_2^A \leq \max\left\{ N(0), \frac{\Lambda}{\mu} \right\} \right\},$$

with initial conditions $S(0) > 0, I_1(0) \geq 0, I_2(0) \geq 0, I_1^A(0) \geq 0$ and $I_2^A(0) \geq 0$, is attracting and positively invariant with respect to the flow of the model system (3).

Proof If $S(0), I_1(0), I_2(0), I_1^A(0), I_2^A(0)$ are non-negative, so are $S(t), I_1(t), I_2(t), I_1^A(t), I_2^A(t)$ for all time $t > 0$. The total population evolves according to the following expression.

$$\frac{dN(t)}{dt} = \Lambda - \mu N(t). \tag{4}$$

Using, the standard comparison theorem as given in [27], we can easily deduce that the solution to the expression (4) is given by

$$N(t) \leq \frac{\Lambda}{\mu} + \left(N(0) - \frac{\Lambda}{\mu} \right) \exp(-\mu t), \quad \text{for all } t \geq 0. \tag{5}$$

The solution in (5) yields two possible scenarios in studying the behaviour of $N(t)$. In the first scenario, we consider $N(0) > \frac{\Lambda}{\mu}$ so that, at time $t = 0$, the right-hand side of (5) experiences the largest possible value of $N(0)$. That is, $N(t) \leq N(0)$ for all time $t \geq 0$. In the second scenario, we consider $N(0) < \frac{\Lambda}{\mu}$, so that the largest possible value of the right-hand

side of (5) approaches $\frac{\Lambda}{\mu}$ as time t tends infinity. Thus, $N(t) \leq \frac{\Lambda}{\mu}$ for all time $t \geq 0$. From these two scenarios, we conclude that $N(t) \leq \max\left\{N(0), \frac{\Lambda}{\mu}\right\}$ for all time $t \geq 0$.

□

The solutions in Ω are all non-negative and bounded. Hence the domain of biological significance is positively invariant and attracting. Thus, all solutions starting in Ω remain in Ω. Furthermore, the system (3) is well-posed epidemiologically and we will consider dynamic behaviour of the system (3) in Ω.

Theorem 2 *The solutions of system* (3) *exist and are non-negative for any given positive initial conditions for all* $t \in [0, \infty)$.

Proof Here, we prove that all the stated variables remain non-negative and the solutions of the system (3) with non-negative initial conditions will remain positive for all $t > 0$. Following the work in [16,23], assume that

$$\hat{t} = \sup\{t > 0 : S > 0, I_1 > 0, I_2 > 0, I_1^A > 0, I_2^A > 0)\} \in (0, t].$$

Thus $\hat{t} > 0$, and it follows directly from the first equation of the system (3) that

$$\dot{S} = \Lambda - \lambda S - \mu S = \Lambda - (\lambda + \mu)S. \tag{6}$$

Equation (6) can be written as

$$\frac{d}{dt}\left(S \exp\left\{\int_0^t \lambda(u)du + \mu t\right\}\right) = \Lambda \exp\left\{\int_0^t \lambda(u)du + \mu(t)\right\},$$

Integrating both sides from $t = 0$ to $t = \hat{t}$, we obtain

$$S(\hat{t}) \exp\left\{\int_0^{\hat{t}} \lambda(u)du + \mu\hat{t}\right\} - S(0) = \int_0^{\hat{t}} \Lambda \exp\left\{\int_0^x \lambda(x)dx + \mu y\right\} dy,$$

then multiplying both sides by $\exp\left\{-\int_0^{t^*} \lambda(u)du - \mu_v\hat{t}\right\}$, we have

$$\begin{aligned} S(\hat{t}) = S(0) \exp\left\{-\int_0^{\hat{t}} \lambda(u)du - \mu\hat{t}\right\} + \exp\left\{-\int_0^{\hat{t}} \lambda_v(u)du - \mu\hat{t}\right\} \\ \times \int_0^{\hat{t}} \Lambda \exp\left\{\int_0^x \lambda(x)dx + \mu y\right\} dy > 0. \end{aligned} \tag{7}$$

Since, the right-hand side of the expression (7) is always positive, the solution $S(t)$ will always remain positive for all $t > 0$. Using the same argument, it can be shown that the quantities I_1, I_2, I_1^A, and I_2^A are positive for all $t > 0$.

□

Stability of Analysis

Basic Reproduction Number

The disease-free steady state (DFE) of system (3) is given by

$$\mathcal{E}_0 = \{S_0, 0, 0, 0, 0\}.$$

$S_0 = \frac{\Lambda}{\mu}$, represents the susceptible individuals when no one is infected with HIV. To obtain basic reproduction number, denoted by $\mathcal{R}_0$, we employ the next generation method [30]. Adopting the matrix notations as given in [30], we have

$$\mathbf{F} = \begin{pmatrix} \beta_1 & \beta_2 & \beta_3 & \beta_4 \\ 0 & 0 & 0 & 0 \\ 0 & 0 & 0 & 0 \\ 0 & 0 & 0 & 0 \end{pmatrix} \quad \text{and} \quad \mathbf{V} = \begin{pmatrix} Q_1 & 0 & 0 & 0 \\ -\delta_1 & Q_2 & 0 & 0 \\ -\eta_1 & 0 & Q_3 & -\delta_3 \\ 0 & -\eta_2 & -\delta_2 & Q_4 \end{pmatrix}.$$

Thus, $\mathcal{R}_0$ is the dominant eigenvalue of $\mathbf{FV}^{-1}$ given by

$$\mathcal{R}_0 = \mathcal{R}_1 + \mathcal{R}_2 + \mathcal{R}_1^A + \mathcal{R}_2^A, \tag{8}$$

where

$$\mathcal{R}_1 = \frac{\beta_1}{Q_1}, \quad \mathcal{R}_2 = \frac{\beta_2\delta_1}{Q_1Q_2}, \quad \mathcal{R}_1^A = \frac{\beta_3(Q_2Q_4 + \delta_1\delta_3\eta_2)}{Q_1Q_2Q_3Q_4(1-\Phi_1)},$$
$$\mathcal{R}_2^A = \frac{\beta_4(Q_2\delta_2\eta_1 + Q_3\delta_1\eta_2)}{Q_1Q_2Q_3Q_4(1-\Phi_1)}$$

with

$$Q_1 = \delta_1+\eta_1+\mu, \quad Q_2 = \eta_2+\mu+\kappa_1, \quad Q_3 = \delta_2+\mu, \quad Q_4 = \delta_3+\mu+\kappa_2, \quad \Phi_1 = \frac{\delta_2\delta_3}{Q_3Q_4}.$$

Note that $0 < \Phi_1 < 1$. The expression for $\mathcal{R}_0$ in (8) is carefully written to reflect the contribution of each stage of the infected individuals in the initiation of new infections. That is, $\mathcal{R}_1$, $\mathcal{R}_2$, $\mathcal{R}_1^A$ and $\mathcal{R}_2^A$ define the contribution of I_1, I_2, I_1^A and I_2^A, respectively, in the generation of new infections. Here, $\mathcal{R}_0$ is interpreted as the expected cases of secondary HIV infections arising from a single HIV infected individual during his or her entire infectious period, in an otherwise disease-free population [5,21,24,30].

From Theorem 2 in [30], we establish following result.

Theorem 3 *The disease-free equilibrium of system* (3) *is locally asymptotically stable whenever* $\mathcal{R}_0 < 1$ *and unstable otherwise.*

Theorem 3 implies that HIV infection will disappear from the population when $\mathcal{R}_0 < 1$ if the initial sizes of the of the sub-populations of the system (3) are in the basin of attraction of the disease-free equilibrium.

Existence of Endemic Equilibrium

The results in Theorem 3, shows that the system (3) has an disease-free steady state when $\mathcal{R}_0 < 1$. When $\mathcal{R}_0 > 1$, the disease-free steady state ($\mathcal{E}_0$), is unstable and the system (3) has a non-trivial endemic equilibrium. Let the endemic equilibrium be represented by the phase space

$$\mathcal{E}_1 = \left(S^*, I_1^*, I_2^*, I_1^{A*}, I_2^{A*}\right) \in \mathbb{R}_+^5.$$

Therefore, solving system (3) in terms of the force of infection in (2), we obtain

$$S^* = \frac{\Lambda}{\lambda^*+\mu}, \quad I_1^* = \frac{\Lambda\lambda}{Q_1(\lambda^*+\mu)}, \quad I_2^* = \frac{\Lambda\lambda\delta_1}{Q_1Q_2(\lambda^*+\mu)},$$
$$I_1^{A*} = \frac{\Lambda\lambda^*(Q_2Q_4\eta_1 + \delta_1\delta_3\eta_2)}{Q_1Q_2Q_3Q_4(1-\Phi_1)(\lambda^*+\mu)}, \quad I_2^{A*} = \frac{\Lambda\lambda^*(Q_2\delta_2\eta_1 + Q_3\delta_1\eta_2)}{Q_1Q_2Q_3Q_4(1-\Phi_1)(\lambda^*+\mu)}.$$

Substituting the expressions for I_1^*, I_2^*, I_1^{A*} and I_2^{A*} into (2) at the equilibrium, we either obtain $\lambda^* = 0$, which corresponds to the disease-free equilibrium previously obtained or

$$\lambda^* = \frac{\mu(\mathcal{R}_0 - 1)}{Q_1 Q_2 Q_3 Q_4 (1 - \Phi_1)}. \tag{9}$$

Since the solution of the system (3) is only feasible in the invariant region Ω, the expression (9) is only feasible when $\mathcal{R}_0 > 1$. Hence the system (3) has a unique endemic equilibrium whenever $\mathcal{R}_0 > 1$ and this equilibrium approaches zero as $\mathcal{R}_0$ tends to one. These results are summarized in the following lemma.

Lemma 1 *The model system* (3) *has a unique endemic equilibrium whenever* $\mathcal{R}_0 > 1$ *and no positive endemic equilibrium otherwise.*

Global Stability Analysis DFE

In this section, we study the global stability of system (3) by construction of Lyapunov functions. Thus, we begin by stating the following theorem.

Theorem 4 *The disease-free steady state,* $\mathcal{E}_0$*, of the model system* (3) *is globally asymptotically stable when* $\mathcal{R}_0 < 1$ *and unstable otherwise.*

Proof We define a candidate Lyapunov function as follows

$$L(I_1, I_2, I_1^A, I_2^A) = \Psi_1 I_1 + \Psi_2 I_2 + \Psi_3 I_1^A + \Psi_4 I_2^A, \tag{10}$$

where Ψ_1, Ψ_2, Ψ_3 and Ψ_4 are non-negative constants to be determined. The derivative of (10) is given by

$$\begin{aligned}
\frac{dL}{dt} &= \Psi_1 \frac{dI_1}{dt} + \Psi_2 \frac{dI_2}{dt} + \Psi_3 \frac{dI_1^A}{dt} + \Psi_4 \frac{dI_2^A}{dt}, \\
&= \Psi_1 \left[\left(\frac{\beta_1 I_1 + \beta_2 I_2 + \beta_3 I_1^A + \beta_4 I_2^A}{N} \right) S - Q_1 I_1 \right] + \Psi_2 \left[\delta_1 I_1 - Q_2 I_2 \right] \\
&\quad + \Psi_3 \left[\eta_1 I_1 + \delta_3 I_2^A - Q_3 I_1^A \right] + \Psi_4 \left[\delta_2 I_1^A + \eta_2 I_2 - Q_4 I_2^A \right], \\
&\leq \Psi_1 \left[\beta_1 I_1 + \beta_2 I_2 + \beta_3 I_1^A + \beta_4 I_2^A - Q_1 I_1 \right] + \Psi_2 \left[\delta_1 I_1 - Q_2 I_2 \right] \\
&\quad + \Psi_3 \left[\eta_1 I_1 + \delta_3 I_2^A - Q_3 I_1^A \right] + \Psi_4 \left[\delta_2 I_1^A + \eta_2 I_2 - Q_4 I_2^A \right], \\
&= [\Psi_1 \beta_1 + \Psi_2 \delta_1 + \Psi_3 \eta_1 - \Psi_1 Q_1] I_1 + [\Psi_1 \beta_2 + \Psi_4 \eta_2 - \Psi_2 Q_2] I_2 \\
&\quad + [\Psi_1 \beta_3 + \Psi_4 \delta_2 - \Psi_3 Q_3] I_1^A + [\Psi_1 \beta_4 + \Psi_3 \delta_3 - \Psi_4 Q_4] I_2^A.
\end{aligned}$$

Setting the coefficients of I_2, I_1^A and I_2^A to zero and solving, we get

$$\begin{aligned}
&\Psi_1 = Q_2 Q_3 Q_4 (1 - \Phi_1), \quad \Psi_2 = Q_3 Q_4 \beta_2 (1 - \Phi_1) + \eta_2 (\beta_3 \delta_3 + \beta_4 Q_3), \\
&\Psi_3 = Q_2 (\beta_3 Q_4 + \beta_4 \delta_2), \Psi_4 = Q_2 (Q_3 \beta_4 + \beta_3 \delta_3).
\end{aligned}$$

Using these coefficients, the time derivative of (10) can be expressed as

$$\frac{dL}{dt} \leq Q_1 Q_2 Q_3 Q_4 (1 - \Phi_1)[\mathcal{R}_0 - 1]. \tag{11}$$

Table 1 Reported new HIV infections in Kenya

Year	2000	2001	2002	2003	2004	2005	2006	2007	2008
HIV+	77,219	72,329	71,875	74,074	77,729	81,523	85,201	91,082	105,292
Year	2009	2010	2011	2012	2013	2014	2015	2016	2017
HIV+	108,764	105,072	98,263	91,949	85,569	90,986	71,034	69,491	70,570

Clearly from (11), when $\mathcal{R}_0 \leq 1$, $\frac{dL}{dt}$ is negative semi-definite, with equality at $\mathcal{R}_0 = 1$. In addition, $\frac{dL}{dt} = 0$ if and only if $I_1 = I_2 = I_1^A = I_2^A = 0$. Hence, the largest compact invariant set in $\{(S, I_1, I_2, I_1^A, I_2^A) \in \Omega : \frac{dL}{dt} = 0\}$, when $\mathcal{R}_0 \leq 1$ is the singleton $\mathcal{E}_0$. Thus, $\mathcal{E}_0$ is the only steady state when $\mathcal{R}_0 \leq 1$. Using LaSalle Invariance Principle [10], this implies that $\mathcal{E}_0$ is globally attractive in Ω if $\mathcal{R}_0 \leq 1$. □

Epidemiological implications of Theorem 4 is that when $\mathcal{R}_0 < 1$, a small influx of HIV infected individuals into the community will not result in an outbreak. The subsequent numbers of those infected will be less than that of their predecessors and eventually the disease will be annihilated.

Data and Parameter Estimation

To fit system (3) to data, we determine the baseline values of known parameters from the literature that correspond to available experimental data and biological facts. The unknown parameters are estimated intuitively and their corresponding ranges and point values obtained through curve fitting given in Table 2. The known parameter baseline values are approximated as follows: Λ which is defined as the recruitment rate into the susceptible is estimated based on the birth rate given as 23.9 births/1000 population [31]. Thus the constant recruitment rate $\Lambda = 0.0239N$ per year. The natural death rate μ is estimated based on life expectancy which is reported to be 58 years [31]. Thus, $\mu = 0.0172$. AIDS related death rate in I_2, κ_1 is estimated at 0.089 while that in class I_2^A, κ_2 is estimated at 0.095 [19].

The initial conditions are estimated as follows.

(i) $N = 17{,}528{,}707$, adult population that were found in 2000 [8,9].
(ii) $S(0) = N - I_1(0) - I_2(0) - I_1^A(0) - I_2^A(0) = 17{,}196{,}488$.
(iii) $I_1(0) = 77{,}219$, reported number of new HIV infections at the end of 2000 [14].
(iv) $I_2(0) = 150{,}000$ (assumed), $I_1^A(0) = 60{,}000$ and $I_2^A(0) = 45{,}000$ (assumed).

The data used in this paper was obtained from National AIDS Control Council [13] and is given in Table 1. The data was extracted for the period spanning 17 years from the year 2000–2017. This data represents new infections for the adults aged 15 years and above.

Results

Curve Fitting

Curve fitting can be defined as a process that enables us to quantitatively estimate the trend of the outcomes. In this process, equations of approximating curves are fitted to raw data. In

Table 2 Estimated parameter ranges per unit year and parameter point values generated from the curve fitting

Parameter	Description	Min	Max	Point value
β_1	Contact for susceptible with I_1	0.0	2.0	0.912
β_2	Contact for susceptible with I_2	0.0	2.0	0.894
β_3	Contact for susceptible with I_1^A	0.0	2.0	0.095
β_4	Contact for susceptible with I_2^A	0.0	2.0	0.091
η_1	Progression rate from I_1 to I_1^A	0.1	1.5	0.084
η_2	Progression rate from I_1 to I_2^A	0.1	1.0	0.091
δ_1	Progression rate from I_1 to I_2	0.1	1.0	1.000
δ_2	Progression rate from I_1^A to I_2^A	0.1	1.0	0.096
δ_3	Progression rate from I_2^A to I_1^A	0.1	1.0	0.112

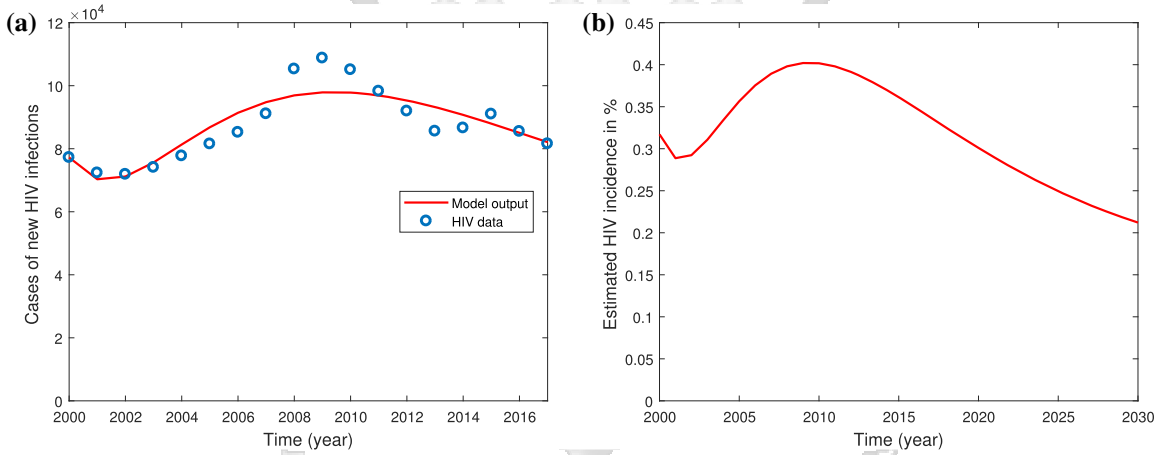

Fig. 2 Model system (3) fitted to data for the reported new HIV positive cases. **a** Shows the model fit to HIV data. **b** Gives the estimated disease incidence

order to fit the system (3) to data, we employ least squares method in Matlab where unknown parameters are given both lower and upper bounds from which obtain parameter values that provide the best fit. These set of parameter values are presented in Table 2.

Figure 2 presents the results of the curve fitting where the trend of the data as reported in Table 1 and the curve representing the estimated values given the model for the new HIV infected persons. It is seen that the cases of new HIV infections estimated by the model for the set of parameter values in Table 2 are closer to the reported new HIV infection data in Kenya. Figure 2b shows HIV incidence as estimated by the incidence function λS. It is seen that the estimated incidence reached the peak between 2010–2014. Our results show of a short-term increase of HIV epidemic in which there is a significant rise in new HIV infections for a considerably short time, followed by a significant decline in the generation of new cases. Nonetheless, this may not give a similar pattern with regards to prevalence, since recovery from HIV is not possible due to HIV being incurable. Hence, the cases of HIV infection is projected to remain significantly high over a long time. It is therefore suggested educational campaigns on safe sex be increased so as to stop further spread.

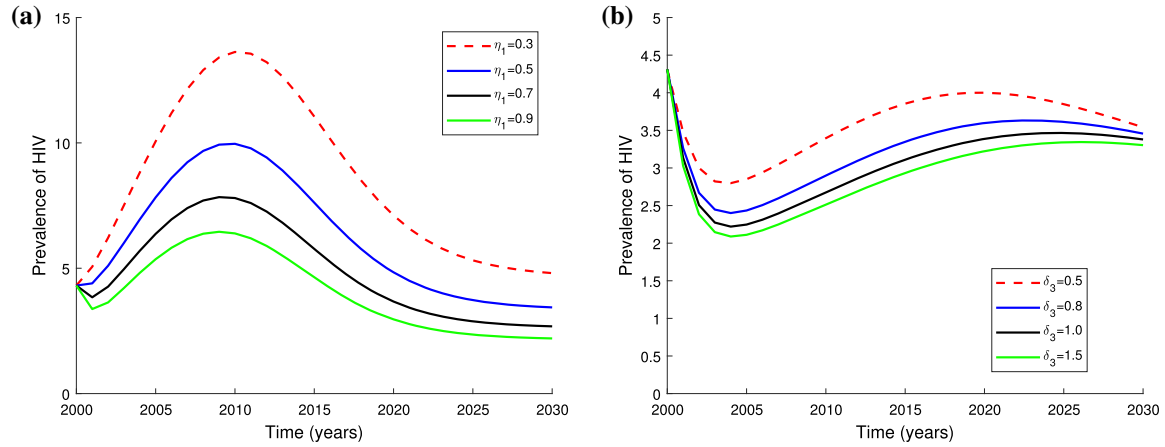

Fig. 3 Shows the impact of linkage to ART and improvement in the immunological status of HIV patient on the HIV prevalence. **a** Gives the impact of linkage to ART of the new infections on prevalence of HIV and **b** gives the impact of improvement in the immunological status on prevalence of HIV

Numerical Simulations

In this section, we carry out numerical simulations to see the dynamical behaviour of the system (3) using the following initial data.

$$S(0) = 200{,}000, \quad I_1(0) = 10{,}000, \quad I_2(0) = 15{,}000, \quad I_1^A(0) = 2000, \quad I_2^A(0) = 5000.$$

The numerical results depend on the parameter values in Table 2. To investigate the contribution of linkage of new infected individuals to ART as well as the effectiveness of ART treatment on increasing the $CD4^+T$ cell counts, we show the variation over time of prevalence of HIV for different rates of η_1 and δ_3. This is shown in Fig. 3a, b respectively. We note an increase in the values of η_1 decreases the prevalence of HIV. The decrease in prevalence can be attributed to the protective effect of ART in increasing the level of $CD4^+T$ cell counts. Similarly, an improvement in the immunological status of HIV patients in I_2 following effectiveness of ART maintaining the level of $CD4^+T$ cell counts high results in a decrease in the HIV prevalence as shown by the effect of δ_3. This shows that effectiveness in the up-take of ART reduces the risk at which an infected individual may spread HIV.

The results in Fig. 4 indicate that $\mathcal{R}_0$ exponentially decreases with the increase in the rate of progression from I_1 to I_2, that is, η_1 and progression rate from I_2^A to I_1^A, that is, δ_3. Therefore, increasing the treatment with ART and its effective up-take reduces the chances of a susceptible person being infected with HIV through contact with HIV patients on ART treatment. The reduction in the likelihood of infection is due to the fact that high ART efficacy increases the level of $CD4^+T$ cell counts in the blood and as a result lowers the disease viral load. It is imperative to note that, eventhough increased drug efficacy may reduce incidence and consequently prevalence of HIV, it does not lead to its subsequent eradication from the community.

Discussion

In the current work, a model that takes into account new cases of HIV infections as well as HIV patients on ART was formulated to study the trend of HIV infection in Kenya amongst adults aged 15 years and above. The basic reproduction number was derived and the model's stability

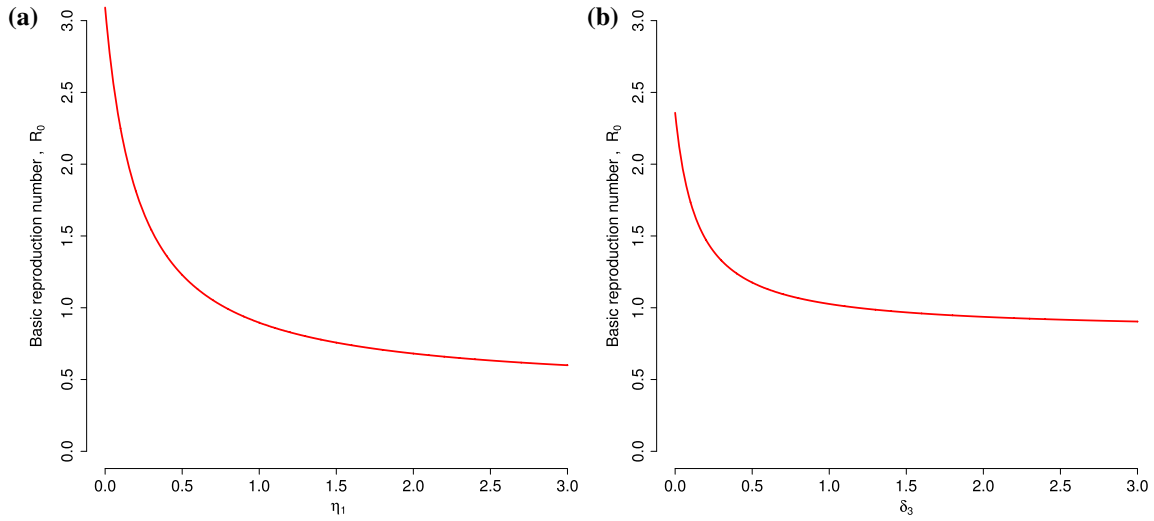

Fig. 4 Effect of η_1 and δ_3 on $\mathcal{R}_0$

analysis carried out. It is shown that when $\mathcal{R}_0$ is less than 1, the disease-free equilibrium is globally asymptotically stable. This implies that whenever $\mathcal{R}_0$ is less than 1, then the generation of the infections is less than their predecessor hence the disease cannot invade the community. This suggests that, HIV infection can be easily controlled or eliminated from the community if control programmes are directed towards reducing $\mathcal{R}_0$ to a value less than 1.

With the help of least squares method in Matlab, the model was fitted to data on cases of new HIV infections for the patients aged 15 years and above. The parameter values obtained from the curve fitting have been used to predict future infection trends. The results suggest that there is a general decline in the HIV infection which is predicted to eventually converge asymptotically over the next few years. The most important observation from our findings is that there is a short-term rise in HIV infection in which there is a significant increase in new HIV infections followed by a significant decline in the generation of new infections. Both treatment of the new infected individuals and the drug effectiveness is seen to greatly reduce HIV prevalence. Therefore, treatment applied immediately to someone who is found to have acquired HIV as well close attention to ART effectiveness in limiting new infections is paramount.

The model presented in this study is not exhaustive and may be extended to involve the study of transmission of HIV within and between different risk groups as well as studying the effect of testing, roll out of PrEP, ART up-take and other HIV intervention measures. Furthermore, the model did not consider immigration. Taking into account these suggestions will undoubtedly enhance the understanding of HIV transmission and control in Kenya. Thus, the future work will involve developing an extended dynamical model of the epidemic in order to further test the ideas and suggestions discussed here and at the same time project future time trends of the epidemic and to carry out detailed cost benefit analyses.

Acknowledgements The authors acknowledge, with thanks, the support of Institute of Mathematical Sciences, Strathmore University for the production of this manuscript. Authors are also very grateful to the referees and the editor for the constructive and valuable comments and recommendations and for making us pay attention to certain references.

Author contributions All authors worked together to produce the results and read and approved the final manuscript.

Compliance with ethical standards

Conflict of interest All authors declare that they have no conflict of interest.

References

1. AIDS: AIDS info. Guidelines for the Use of Antiretroviral Agents in HIV-1-Infected Adults and Adolescents (2015). Retrieved April, 2017 from https://aidsinfo.nih.gov/guidelines/html/1/adult-and-adolescent-arv-guidelines/458/plasma-hiv-1-rna--viral-load--and-cd4-count-monitoring
2. Baggaley, R.F., Ferguson, N.M., Garnett, G.P.: The epidemiological impact of antiretroviral use predicted by mathematical models: a review. Emerg. Themes Epidemiol. **2**(1), 9 (2005)
3. Baryarama, F., Mugisha, J., Luboobi, L.: A mathematical model for the dynamics of HIV/AIDS with gradual behaviour change. Comput. Math. Methods Med. **7**(1), 15–26 (2006)
4. Bórquez, A., Cori, A., Pufall, E.L., Kasule, J., Slaymaker, E., Price, A., Elmes, J., Zaba, B., Crampin, A.C., Kagaayi, J.: The incidence patterns model to estimate the distribution of new HIV infections in Sub-Saharan Africa: development and validation of a mathematical model. PLoS Med. **13**(9), e1002121 (2016)
5. Heffernan, J., Smith, R., Wahl, L.: Perspectives on the basic reproductive ratio. J. R. Soc. Interface **2**(4), 281–293 (2005)
6. Isdory, A., Mureithi, E.W., Sumpter, D.J.: The impact of human mobility on HIV transmission in Kenya. PLoS ONE **10**(11), e0142805 (2015)
7. Kiss, I.Z., Cassell, J., Recker, M., Simon, P.L.: The impact of information transmission on epidemic outbreaks. Math. Biosci. **225**(1), 1–10 (2010)
8. KNBS: Kenya National Bureau of Statistics (2017). Retrieved September, 2017 from https://www.knbs.or.ke/
9. KNBS2: Kenya 1900. Population Pyramids of the World from 1950 to 2100 (2017). Retrieved September, 2017 from https://www.populationpyramid.net/kenya/1990/
10. La Salle, J.P.: The Stability of Dynamical Systems. SIAM, Philadelphia (1976)
11. Liu, R., Wu, J., Zhu, H.: Media/psychological impact on multiple outbreaks of emerging infectious diseases. Comput. Math. Methods Med. **8**(3), 153–164 (2007)
12. NACC: Kenya National Aids Control Council. Kenya AIDS response progress report 2016 (2016). Retrieved April, 2017 from http://nacc.or.ke/wp-content/uploads/2016/11/Kenya-AIDS-Progress-Report_web.pdf
13. NACC: Kenya National Aids Control Council. Kenya National AIDS Control Council 'Kenya AIDS Strategic Framework 2014/2015–2018/2019' (2017a). Retrieved April, 2017 from http://www.undp.org/content/dam/kenya/docs/Democratic%20Governance/KENYA%20AIDS%20STRATEGIC%20FRAMEWORK.pdf
14. NACC: National AIDS Control Council and the National AIDS and STD Control Programme,March 2012. HIV/AIDS report (2017b). Retrieved January, 2018 from http://guidelines.health.go.ke:8000/media/National_HIV_Estimates_for_Kenya_2011-2015.pdf
15. Naresh, R., Tripathi, A., Sharma, D.: Modelling and analysis of the spread of aids epidemic with immigration of HIV infectives. Math. Comput. Model. **49**(5), 880–892 (2009)
16. Nyabadza, F., Njagarah, J.B., Smith, R.J.: Modelling the dynamics of crystal meth (tik) abuse in the presence of drug-supply chains in South Africa. Bull. Math. Biol. **75**(1), 24–48 (2013)
17. Okango, E., Mwambi, H., Ngesa, O.: Spatial modeling of HIV and HSV-2 among women in Kenya with spatially varying coefficients. BMC Public Health **16**(1), 355–368 (2016)
18. Okongo, M., Kirimi, J., Murwayi, A., Muriithi, D.: Mathematical analysis of a comprehensive HIV/ AIDS model: treatment versus vaccination. Appl. Math. Sci. **7**(54), 2687–2707 (2013)
19. Okosun, K., Makinde, O., Takaidza, I.: Impact of optimal control on the treatment of HIV/AIDS and screening of unaware infectives. Appl. Math. Model. **37**(6), 3802–3820 (2013)
20. Olney, J.J., Braitstein, P., Eaton, J.W., Sang, E., Nyambura, M., Kimaiyo, S., McRobie, E., Hogan, J.W., Hallett, T.B.: Evaluating strategies to improve HIV care outcomes in Kenya: a modelling study. Lancet HIV **3**(12), e592–e600 (2016)
21. Omondi, E.O., Mbogo, R., Luboobi, L.: Mathematical modelling of the impact of testing, treatment and control of HIV transmission in Kenya. Cogent Math. Stat. **5**(1), 1475590 (2018a)
22. Omondi, E.O., Mbogo, R.W., Luboobi, L.S.: Mathematical analysis of sex-structured population model of HIV infection in Kenya. Lett. Biomath. **5**(1), 174–194 (2018b)

23. Omondi, E.O., Nyabadza, F., Bonyah, E., Badu, K.: Modeling the infection dynamics of onchocerciasis and its treatment. J. Biol. Syst. **25**(2), 247–277 (2017a)
24. Omondi, E.O., Orwa, T.O., Nyabadza, F.: Application of optimal control to the onchocerciasis transmission model with treatment. Math. Biosci. **297**(2018), 43–57 (2017b)
25. OPTIONS: OPTIONS Country Situation Analysis Interim Findings: Kenya. FSG in partnership with LVCT Health (2016). Retrieved August, 2016 from http://www.prepwatch.org/wp-content/uploads/2016/05/Situation_Analysis_Kenya.pdf
26. Sahu, G.P., Dhar, J.: Dynamics of an SEQIHRS epidemic model with media coverage, quarantine and isolation in a community with pre-existing immunity. J. Math. Anal. Appl. **421**(2), 1651–1672 (2015)
27. Smith, H.L., Waltman, P.: The Theory of the Chemostat, vol. 13. Cambridge University Press, Cambridge (1995)
28. UNAIDS: UNAIDS. HIV and AIDS estimates (2015). Retrieved April, 2017 from http://www.unaids.org/en/regionscountries/countries/kenya
29. United Nations Programme on HIV/AIDS, J.: 90–90–90: an ambitious treatment target to help end the AIDS epidemic. Joint United Nations Programme on HIV AIDS, Geneva, Switzerland (2014)
30. Van den Driessche, P., Watmough, J.: Reproduction numbers and sub-threshold endemic equilibria for compartmental models of disease transmission. Math. Biosci. **180**(1), 29–48 (2002)
31. WB: World Bank Data. Birth rate, crude (per 1000 people) (2017). Retrieved October, 2017 from https://data.worldbank.org/indicator/SP.DYN.CBRT.IN
32. Williams, B.G.: Optimizing control of HIV in Kenya (2014). arXiv preprint arXiv:1407.7801
33. Wodarz, D., Nowak, M.A.: Mathematical models of HIV pathogenesis and treatment. BioEssays **24**(12), 1178–1187 (2002)
34. Yan, X., Zou, Y., Li, J.: Optimal quarantine and isolation strategies in epidemics control. World J. Model. Simul. **3**(3), 202–211 (2007)

LETTERS IN BIOMATHEMATICS
2018, VOL. 5, NO. 1, 174–194
https://doi.org/10.1080/23737867.2018.1506712

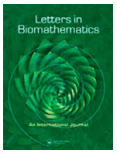

Taylor & Francis
Taylor & Francis Group

Mathematical analysis of sex-structured population model of HIV infection in Kenya

E. O. Omondi, R. W. Mbogo and L. S. Luboobi

Institute of Mathematical Sciences, Strathmore University, Nairobi, Kenya

ABSTRACT

In this paper, we develop a mathematical model describing the dynamics of HIV transmission by incorporating sexual orientation of individuals. Equilibrium points and the basic reproduction number are derived. The basic reproduction number provides a threshold that determines whether or not the disease fades away. The model, described by non-linear ODEs, shows existence of unique disease-free and disease-persistent equilibria. Least squares curve fitting is presented to quantitatively investigate the trend of infection within each gender. The results are indicative of a higher infectivity in the female population. We further investigated the effect of the introduction of pre-exposure prophylaxis (PrEP) on the dynamics of the HIV. Our results show that the introduction of PrEP has had a positive effect on the limitation of spread of HIV. Sensitivity analysis results show that control of effective contacts can result in control of the disease across gender divide. The model provides a unique opportunity to influence policy on HIV treatment and management.

ARTICLE HISTORY
Received 2 April 2018
Accepted 25 July 2018

KEYWORDS
HIV; PrEP; ART; equilibrium; reproduction number; sensitivity; curve fitting

1. Introduction

HIV remains a major global health problem affecting approximately 70 million people worldwide causing significant morbidity and mortality (WHO, 2018). In Kenya, the number of persons living with HIV was approximated to be 1.6 million in the year 2016, with women accounting for 910,000 (OPTIONS, 2016; UNAIDS, 2016a). The main transmission route is through heterosexual means with estimated 30% of the new infections deeply rooted among sex workers (National Aids Control Council of Kenya [NACC], 2014a). High HIV infections among sex workers in Kenya is attributed to unprotected sex. According to Shields (2012), most sex workers are constantly harrased by the police in which they are physically and sexually abused for carrying condoms. In addition, the sex workers have no power to negotiate for safe sex. This is due to the fact that clients may decline to pay if they have to use condom and hence use intimidation or violence to force unsafe sex (Ghimire, Smith, van Teijlingen, Dahal & Luitel, 2011). Furthermore, the clients may offer more money for unprotected sex, a proposal that is unlikely to be rejected by the sex workers. According to National Aids Control Council of Kenya (NACC, 2014b) an estimated

CONTACT E. O. Omondi eomondi@strathmore.edu, evansotieno@aims.ac.za Institute of Mathematical Sciences, Strathmore University, P.O Box 59857-00200, Nairobi, Kenya

29.3% of female sex workers were living with HIV in 2011. In addition, the findings from the Sex Workers Outreach Project reported a HIV prevalence of 30% among female sex workers and 40% among male sex workers in 2011 (UNAIDS, 2015).

Young women are more than three times more likely to be exposed to sexual violence than young man (Kenya National Bureau of Statistics [KNBS], 2015). Among women aged 15–19 years, HIV prevalence was 23.0%, compared to 3.5% among men of the same age (KNBS, 2015; Voeten, Egesah, Varkevisser, & Habbema, 2007). Approximately 33% of the girls in Kenya have been raped by the time they reach 18 years with about 22% aged 15–19 years reporting that their first sexual encounter was forced (NACC, 2014a). In addition, women continue to face discrimination in terms of access to education, employment and healthcare (UNAIDS, 2018). Consequently, men often dominate sexual relationships, with women not always able to practice safer sex even when they know the risks involved (UNAIDS, 2015, 2018). For instance, in 2014, 35% of adult women (aged 15–49) who were or had been married had experienced spousal violence and 14% had experienced sexual violence (UNAIDS, 2018). Although progress is being made to control new HIV infections, Kenya still remains one of the six high HIV burdened countries in Africa (UNAIDS, 2014). The main treatment received by HIV patients is the uptake of ART which refers to the use of a combination of three or more ARVs to achieve the suppression of the viral load (WHO, 2014). The drugs do not kill or cure the virus and is a lifelong treatment for HIV patients to reduce the risk of dying (Williams, 2014; Williams, Hargrove, & Humphrey, 2010). In its efforts to reduce HIV infections, in 2015, Kenya began to adopt 2015 WHO recommendations to immediately offer treatment to people diagnosed with HIV in order to increase the ART access. It is estimated that about 826,000 adults and 71,500 children were receiving ART treatment by end of 2015 (UNAIDS, 2016b).

In the recent years, quite a number of mathematical models have been developed to investigate the dynamics of HIV transmission and spread in the population (Athithan & Ghosh, 2014; Baryarama, Mugisha, & Luboobi, 2006; Doyle, Greenhalgh, & Blythe, 1998; Kaur, Ghosh, & Bhatia, 2014; Okango, Mwambi, & Ngesa, 2016; Omondi, Mbogo, & Luboobi, 2018b; Van Sighem et al., 2012; Wodarz & Nowak, 2002). However, to the authors knowledge, none of these existing mathematical models has explicitly considered incorporating sexual orientation of individuals using real-time series of HIV infection trend data. For example, the mathematical models in Mukandavire and Garira (2007a, 2007b) describe the heterosexual interactions of males and females using integro-differential equations with a time delay due to incubation period. While these two models incorporated the effects of male and female condom use as the main mode of preventing HIV infection, they did not consider applying real-time surveillance data to establish the trend of infection. Additionally, in our modelling attempt, we consider a scenario in which individuals with HIV are linked to ART treatment. A study by Mukandavire, Chiyaka, Garira, and Musuka (2009) modelled a sex-structured model for heterosexual transmission of HIV/AIDS with explicit incubation period and provided an in-depth and complete qualitative mathematical analysis. However, there was no numerical results to show the effect HIV prevention intervention measures as well as trend within these two sexes. Bhunu, Mushayabasa, Kojouharov, and Tchuenche (2011) derived a HIV model and examined the effect of counselling and testing coupled with decrease in sexual activity on HIV spread in resource-limited communities. The results from this model suggested that effective counselling and testing have a great potential to partially control

the epidemic especially when HIV positive individuals willingly withdraw from sexual activities.

While these models elucidated the importance of prevention to reduce HIV burden, they did not take into account the fact that the immediate linkage of HIV patients to ART treatment can reduce the risk of dying as well as preventing further occurrence of new infections. Our proposed model aims to integrate data on HIV within males and females in Kenya so as to develop a better understanding of the epidemic. In this study, we analyse the model and apply it to data for male and female. Our main goals are: first, to develop a mathematical model that takes into account the treatment of HIV patients with ART and carry out qualitative mathematical analysis of the model and find the necessary threshold for controlling the spread of the disease. Second, to fit the model to observed data of new infections to show the trend between males and females using the parameter values that produce the best fit to the data. The model can help in planning and designing effective control measures to reduce the risk of new infections. In addition, the model and its predictions provides a framework for evaluating the success or failure of the current HIV intervention measures.

2. Methods

2.1. Model formulation

The model proposed in this work is an extension of the previous models studied in Mukandavire et al. (2009); Mukandavire and Garira (2007a, 2007b). We keep the model as simple as possible consistent with the available data. The model proposed here represents the sexually mature age group in Kenya (age 15 years and over). It is believed that this is the age group that is responsible for the spread of HIV (UNAIDS, 2015). It is assumed that the male and female populations are divided into compartments described by time-dependent state variables. These compartments are: Susceptible (S_i), infected individuals with CD4 cell counts $\geq$ 350/μL who are considered to be new infections (I_{i1}) and infected individuals with CD4 cell counts $<$ 350/μL (I_{i2}). The infected individuals are then enrolled on ART which is divided into two depending the CD4 cell counts, that is, T_{i1} and T_{i2}. This is consistent with the WHO recommendation of immediate treatment with ART of HIV to attain viral load suppression (AIDS, 2015; Williams, 2014). Here, $i = m, f$ denoting male and female, respectively. The total variable population at time t , denoted by $N(t)$ is described by (1).

$$N(t) = N_m(t) + N_f(t), \tag{1}$$

where

$$N_m(t) = S_m(t) + I_{m1}(t) + I_{m2}(t) + T_{m1}(t) + T_{m2}(t) \quad \text{and}$$
$$N_f(t) = S_f(t) + I_{f1}(t) + I_{f2}(t) + T_{f1}(t) + T_{f2}(t).$$

The recruitment in the population is at the constant rate Λ of which a proportion α are assumed to be males and $(1 - \alpha)$ are assumed to be females. The newly recruited individuals enter the susceptible compartment S_i. Each individual compartment goes out from the dynamics at natural mortality rate μ. The susceptible in either male or female populations is decreased following infection, which can be acquired via effective contact with

an infectious person at the respective rates given by λ_m and λ_f. These rates are obtained as follows the probability that a male or female person chooses a particular partner can be assumed as $1/N_m$ and $1/N_f$, respectively. Thus, a male or female receives in average $c_{mj}N_f/N_m$ and $c_{fj}N_m/N_f$ partners per unit of times, respectively. Then, the infection rate per susceptible male or female are, respectively, given by

$$\left.\begin{aligned}\lambda_m &= \frac{\left(\frac{N_f}{N_m}\right)\left[\sum_{j=k=1}^{j=k=2}\beta_{fj}c_{mj}I_{fk} + \sum_{j=3,k=1}^{j=4,k=2}\beta_{fj}c_{mj}T_{fk}\right]}{N_f},\\ \lambda_f &= \frac{\left(\frac{N_m}{N_f}\right)\left[\sum_{j=k=1}^{j=k=2}\beta_{mj}c_{fj}I_{mk} + \sum_{j=3,k=1}^{j=4,k=2}\beta_{mj}c_{fj}T_{mk}\right]}{N_m}.\end{aligned}\right\} \tag{2}$$

Here, $k=1,2$ representing the two stages of infectious population, β_{ij}, where $i = m, f$ and $j = 1, \ldots, 4$, are the probabilities of HIV transmission per partnership and c_{ij} are the rates at which an individual acquires sexual partners associated with the four infectious compartments respectively. Thus, the expressions in (2) can be simplified to the following

$$\left.\begin{aligned}\lambda_m &= \left(\frac{\beta_{f1}c_{m1}I_{f1} + \beta_{f2}c_{m2}I_{f2} + \beta_{f3}c_{m3}T_{f1} + \beta_{f4}c_{m4}T_{f2}}{N_m}\right),\\ \lambda_f &= \left(\frac{\beta_{m1}c_{f1}I_{m1} + \beta_{m2}c_{f2}I_{m2} + \beta_{m3}c_{f3}T_{m1} + \beta_{m4}c_{f4}T_{m2}}{N_f}\right).\end{aligned}\right\} \tag{3}$$

Infectious individuals in class (I_{i1}) progress to class (I_{i2}) at rate γ_h, for $h=1,2$. Infectious individuals in classes (I_i^1) and (I_{i2}) move to (T_{i1}) and (T_{i2}) at a constant rate τ_p, for $p = 1, \ldots, 4$, as consequence of treatment with ART. The infectious individuals on ART in class (T_{i1}) progress to (T_{i2}) at a rate ψ_h as a result of decline in the immunological status. Similarly, infectious individuals on ART in class (T_{i2}) progress to (T_{i1}) at a rate ω_h as a consequence of improvement in the immunological status. Infectious individuals in classes I_{i2} and T_{i2} may die as a consequence of infection, at a disease-induced death rate δ_1 and δ_2, respectively.

2.1.1. Model assumptions

The following key assumptions have been made.

(i) The proportion of the infected individuals on treatment is bi-directional due to attrition or adherence to ART and decline or improvement of immunological status.
(ii) The standard HIV transmission incidence has been used to model the disease transmission. This is the form most commonly used for sexually transmitted diseases (Hethcote, 2000).
(iii) There is homogeneous mixing and the transmission of HIV is assumed to be mainly through heterosexual means.
(iv) An exit due to death as a consequence of development of AIDS has been included hence AIDS class is considered redundant and thus left out. Furthermore, AIDS patients are usually too ill to remain sexually active and they are unable to transmit HIV through sexual activity.

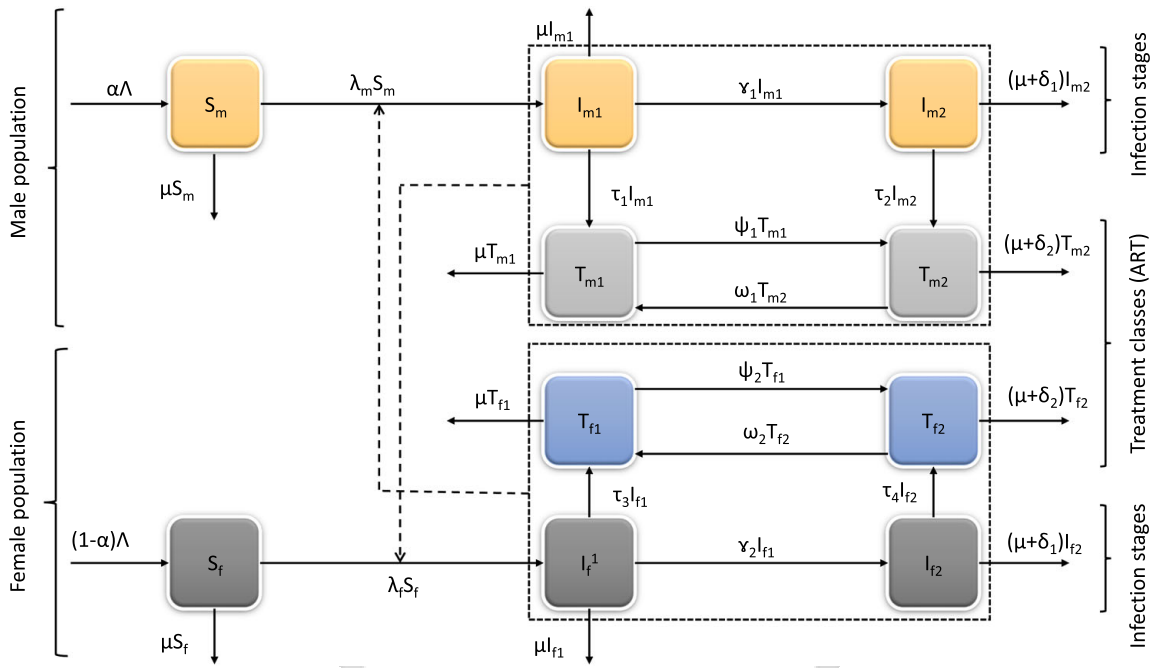

Figure 1. A compartmental model for the transmission dynamics of HIV, which takes into account treatment with ART.

In 2016, Kenya issued full regulatory approval of PrEP, becoming the second country in Sub-Saharan Africa after South Africa, to make such approval (UNAIDS, 2016b). PrEP is used by people who do not have HIV but are at high risk of acquiring it to prevent HIV infection (AIDS, 2016; HIV/AIDS, 2016). The successes of PrEP use in Kenya are yet to be reported since research into the uptake and impact of PrEP, specifically with young women and girls in high-incidence areas is still on-going (UNAIDS, 2016b). The challenges posed by the continued occurrence of new infections call for a better understanding of the disease transmission and development of effective strategies for prevention and control of the spread of HIV. Therefore, we add control $0 \leq \phi \leq 1$ to measure the effectiveness of PrEP in the prevention measurements against acquiring HIV infection. Thus the infection terms given in (3) are, respectively, modified as follows

$$\lambda_{mq} = (1-\phi)\lambda_m \quad \text{and} \quad \lambda_{fq} = (1-\phi)\lambda_f. \tag{4}$$

Figure 1 shows the schematic diagram for the compartmental model structure.

2.1.2. Model equations

The above assumptions lead to the following 10 non-linear system of ordinary differential equations.

$$\left.\begin{aligned}
\frac{dS_m}{dt} &= \alpha\Lambda - \lambda_{mq}S_m - \mu S_m, & \frac{dS_f}{dt} &= (1-\alpha)\Lambda - \lambda_{fq}S_f - \mu S_f,\\
\frac{dI_{m1}}{dt} &= \lambda_{mq}S_m - (\gamma_1 + \tau_1 + \mu)I_{m1}, & \frac{dI_{f1}}{dt} &= \lambda_{fq}S_f - (\gamma_2 + \tau_3 + \mu)I_{f1},\\
\frac{dI_{m2}}{dt} &= \gamma_1 I_{m1} - (\tau_2 + \mu + \delta_1)I_{m2}, & \frac{dI_{f2}}{dt} &= \gamma_2 I_{f1} - (\tau_4 + \mu + \delta_1)I_{f2},\\
\frac{dT_{m1}}{dt} &= \tau_1 I_{m1} + \omega_1 T_{m2} - (\psi_1 + \mu)T_{m1}, & \frac{dT_{f1}}{dt} &= \tau_3 I_{f1} + \omega_2 T_{f2} - (\psi_2 + \mu)T_{f1},\\
\frac{dT_{m2}}{dt} &= \tau_2 I_{m2} + \psi_1 T_{m1} - (\omega_1 + \mu + \delta_2)T_{m2}, & \frac{dT_{f2}}{dt} &= \tau_4 I_{f2} + \psi_2 T_{f1} - (\omega_2 + \mu + \delta_2)T_{f2},
\end{aligned}\right\} \tag{5}$$

Table 1. Description of the state variables of model (5). The information on how the initial population estimates have been made is given in Section 3.3.2.

Variable	Male	Female	Source
S	11,589,991	11,764,344	National Aids Control Council of Kenya (NACC, 2017)
I_1	500	530	KHIS (2017)
I_2	35,000	40,000	Assumed
T_1	30,000	35,000	NACC (2017)
T_2	45,000	50,000	Assumed

Table 2. Description and range of parameters of model (5) given per month.

Parameter	Min	Max	Source
Λ	0.0013N	0.00265N	WB (2017)
β_{ij}	0.0	1.0	Assumed
c_{ij}	1.0	4.0	Estimated
α	0.35	0.60	POP (2017)
μ	0.00119	0.00167	WB (2017) and POP (2017)
δ_h	0.0069	0.0104	Okosun, Makinde, and Takaidza (2013)
γ_h	0.18	1.0	Estimated
τ_p	0.1	1.0	Estimated
ψ_h	0.1	1.0	Estimated
ω_h	0.1	0.8	Estimated

subject to the following initial conditions

$$S_i(0) \geq 0, \quad I_{i1}(0) \geq 0, \quad I_{i2}(0) \geq 0, \quad T_{i1}(0) \geq 0, \quad T_{i2}(0) \geq 0, \quad \text{for } i = m, f. \tag{6}$$

The description of state variables and parameters of model (5) are given in Tables 1 and 2, respectively.

The total population of both male and female sub-populations, respectively, evolve according to the following

$$\frac{\mathrm{d}N_m}{\mathrm{d}t} = \alpha\Lambda - \mu N_m \quad \text{and} \quad \frac{\mathrm{d}N_f}{\mathrm{d}t} = (1-\alpha)\Lambda - \mu N_f. \tag{7}$$

The solutions to each of the equations in system (7) are given by

$$N_m = \frac{\alpha\Lambda}{\mu} + \left[N_{0m} - \frac{\alpha\Lambda}{\mu}\right]\exp(-\mu t) \quad \text{and}$$
$$N_f = \frac{(1-\alpha)\Lambda}{\mu} + \left[N_{0f} - \frac{(1-\alpha)\Lambda}{\mu}\right]\exp(-\mu t),$$

respectively. Here, N_{0m} and N_{0f} are the initial populations for the males and females. The solution of all the equations from system (5) all remain non-negative for all $t \geq 0$. The total population $\{N_m; N_f\}$ in each of the sub-populations is bounded by $\alpha\Lambda/\mu$ and $((1-\alpha)\Lambda)/\mu$, respectively. The total population in both sub-populations is given by $N = N_m + N_f$ such that the evolution of the total population over a specified period is

given by

$$\frac{dN}{dt} = \Lambda - \mu N. \quad \text{It can easily be seen that } \limsup_{t\to\infty} N \leq \frac{\Lambda}{\mu}.$$

Therefore, the phase space of the system (5) is given by

$$\Omega := \left\{ (S_i, I_{i1}, I_{i2}, T_{i1}, T_{i2}) : S_i + I_{i1} + I_{i2} + T_{i1} + T_{i2} \leq \frac{\Lambda}{\mu} \right\}.$$

The solutions in Ω are all non-negative and bounded. Hence the domain of biological significance is positively invariant and attracting. Therefore, all solutions starting in Ω remain in Ω.

3. Equilibrium points

To better understand the dynamics of the proposed model, we begin by examining the model's behaviour about the steady states. This analysis is crucial for identifying the parameters of the model that help to achieve a HIV-free state. Since the rate of change in each compartment is constant at equilibrium, we set the right-hand side of equations in the system (5) to zero and solve for the state variables in terms of the infection terms λ_{mq} and λ_{fq} and obtain the following

$$\left.\begin{aligned}
S_m^* &= \frac{\alpha\Lambda}{\mu+\lambda_{mq}^*}, \quad I_{m1}^* = \frac{\alpha\Lambda\lambda_{mq}^*)}{Q_1(\mu+\lambda_{mq}^*)}, \quad I_{m2}^* = \frac{\alpha\gamma_1\Lambda\lambda_{mq}^*}{Q_1Q_2(\mu+\lambda_{mq}^*)},\\
T_{m1}^* &= \frac{\alpha\Lambda\lambda_{mq}^*(\gamma_1\tau_2\omega_1 + Q_2Q_4\tau_1)}{Q_1Q_2Q_3Q_4(\mu+\lambda_{mq}^*)(1-\Phi_1)}, \quad T_{m2}^* = \frac{\alpha\Lambda\lambda_{mq}^*(\gamma_1Q_3\tau_2 + Q_2\tau_1\psi_1)}{Q_1Q_2Q_3Q_4(\mu+\lambda_{mq}^*)(1-\Phi_1)},\\
S_f^* &= \frac{(1-\alpha)\Lambda}{\mu+\lambda_{fq}^*}, \quad I_{f1}^* = \frac{(1-\alpha)\Lambda\lambda_{fq}^*}{Q_5(\mu+\lambda_{fq}^*)}, \quad I_{f2}^* = \frac{(1-\alpha)\gamma_2\Lambda\lambda_{fq}^*}{Q_5Q_6(\mu+\lambda_{fq}^*)},\\
T_{f1}^* &= \frac{(1-\alpha)\Lambda\lambda_{fq}^*(\gamma_2\tau_4\omega_2 + Q_6Q_8\tau_3)}{Q_5Q_6Q_7Q_8(\lambda_{fq}^*+\mu)(1-\Phi_2)}, \quad T_{f2}^* = \frac{(1-\alpha)\Lambda\lambda_{fq}^*(\gamma_2Q_7\tau_4 + Q_6\tau_3\psi_2)}{Q_5Q_6Q_7Q_8(\lambda_{fq}^*+\mu)(1-\Phi_2)},
\end{aligned}\right\} \tag{8}$$

where

$$\begin{aligned}
Q_1 &= \gamma_1 + \tau_1 + \mu, \quad Q_2 = \tau_2 + \mu + \delta_1, \quad Q_3 = \psi_1 + \mu,\\
Q_4 &= \omega_1 + \mu + \delta_2, \quad \Phi_1 = \frac{\psi_1\omega_1}{Q_3Q_4},\\
Q_5 &= \gamma_2 + \tau_3 + \mu, \quad Q_6 = \tau_4 + \mu + \delta_1, \quad Q_7 = \psi_2 + \mu,\\
Q_8 &= \omega_2 + \mu + \delta_2, \quad \Phi_2 = \frac{\psi_2\omega_2}{Q_7Q_8}.
\end{aligned}$$

Substituting the expressions for the state variables $I_{i1}^*, I_{i2}^*, T_{i1}^*$ and T_{i2}^* in (8) into infection terms in (4) then simplifying, the following polynomial is obtained.

$$\lambda_{mq}^*[A_1\lambda_{mq}^* + A_0] = 0, \tag{9}$$

where

$$
\begin{aligned}
A_0 &= -Q_1Q_2Q_3Q_4Q_5Q_6Q_7Q_8\mu(1-\Phi_1)(1-\Phi_2)(1-\alpha)[\mathcal{R}_0-1],\\
A_1 &= Q_5Q_6Q_7Q_8(1-\Phi_2)[(1-\phi)\alpha(Q_3Q_4(1-\Phi_1)(Q_2\beta_{m1}c_{f1}+\gamma_1\beta_{m2}c_{f2})\\
&\quad +(Q_2Q_4\tau_1+\gamma_1\tau_2\omega_1)\beta_{m3}c_{f3}+(Q_3\gamma_1\tau_2Q_2\tau_1\psi_1)\beta_{m4}c_{f4})\\
&\quad +Q_1Q_2Q_3Q_4\mu(1-\Phi_1)(1-\alpha)].
\end{aligned}
$$

The expression for $\mathcal{R}_0$ is computed in (13). Note that the case $\lambda^*_{mq}=0$ corresponds to the disease-free equilibrium which can be expressed as

$$\mathcal{E}_0=\left[\frac{\alpha\Lambda}{\mu},0,0,0,0,\frac{(1-\alpha)\Lambda}{\mu},0,0,0,0\right]. \tag{10}$$

The disease-free equilibrium is refers to a scenario in which HIV infection is not present in a population. The solutions to the remaining part of (9), given by Equation (11) gives possible disease-persistent state ($\mathcal{E}_1$).

$$A_1\lambda^*_{mq}+A_0=0. \tag{11}$$

The existence of disease-persitent state refers to a scenario in which HIV infection persists in the population. We note that $A_0>0$ if $\mathcal{R}_0<1$ and expression (11) does not have a positive solution. However, $A_0<0$ if $\mathcal{R}_0>1$ and expression (11) does have a positive solution implying that there exists a unique endemic equilibrium if and only if $\mathcal{R}_0>1$.

3.1. The basic reproduction number

The basic reproduction number is defined as the average number of new infections generated by one infected individual, via heterosexual means, in a completely susceptible population (Van den Driessche, & Watmough, 2002). The basic reproduction number, R_0, which is a measure of the infection on the susceptible populations, for the system (5) is obtained using the next generation method described in Van den Driessche, and Watmough (2002). This method has been explored in many papers, for instance, Feng, Ruan, Teng, and Wang (2015); Munz, Hudea, Imad, and Smith (2009); Nyabadza, Njagarah, and Smith (2013); Omondi, Nyabadza, and Smith (2018a); Omondi, Nyabadza, Bonyah, and Badu (2017). Following the explanation given in Van den Driessche, and Watmough (2002), we obtain $\mathbf{F}$ which is the matrix of new infections and $\mathbf{V}$ which is the matrix of transfers between compartments given by

$$\mathbf{F}=\begin{bmatrix}\mathbf{F}_1 & \mathbf{F}_2\\ \mathbf{F}_3 & \mathbf{F}_4\end{bmatrix} \text{ and}$$

$$\mathbf{V}=\begin{bmatrix}
Q_1 & 0 & 0 & 0 & 0 & 0 & 0 & 0\\
-\gamma_1 & Q_2 & 0 & 0 & 0 & 0 & 0 & 0\\
-\tau_1 & 0 & Q_3 & -\omega_1 & 0 & 0 & 0 & 0\\
0 & -\tau_2 & -\psi_1 & Q_4 & 0 & 0 & 0 & 0\\
0 & 0 & 0 & 0 & Q_5 & 0 & 0 & 0\\
0 & 0 & 0 & 0 & -\gamma_2 & Q_6 & 0 & 0\\
0 & 0 & 0 & 0 & -\tau_3 & 0 & Q_7 & -\omega_2\\
0 & 0 & 0 & 0 & 0 & -\tau_4 & -\psi_2 & Q_8
\end{bmatrix}, \tag{12}$$

where

$$\mathbf{F}_1 = \begin{bmatrix} 0 & 0 & 0 & 0 \\ 0 & 0 & 0 & 0 \\ 0 & 0 & 0 & 0 \\ 0 & 0 & 0 & 0 \end{bmatrix},$$

$$\mathbf{F}_2 = \begin{bmatrix} (1-\phi)c_{m1}\beta_{f1} & (1-\phi)c_{m2}\beta_{f2} & (1-\phi)c_{m3}\beta_{f3} & (1-\phi)c_{m4}\beta_{f4} \\ 0 & 0 & 0 & 0 \\ 0 & 0 & 0 & 0 \\ 0 & 0 & 0 & 0 \end{bmatrix}$$

$$\mathbf{F}_3 = \begin{bmatrix} (1-\phi)c_{f1}\beta_{m1} & (1-\phi)c_{f2}\beta_{m2} & (1-\phi)c_{f3}\beta_{m3} & (1-\phi)c_{f4}\beta_{m4} \\ 0 & 0 & 0 & 0 \\ 0 & 0 & 0 & 0 \\ 0 & 0 & 0 & 0 \end{bmatrix},$$

$$\mathbf{F}_4 = \begin{bmatrix} 0 & 0 & 0 & 0 \\ 0 & 0 & 0 & 0 \\ 0 & 0 & 0 & 0 \\ 0 & 0 & 0 & 0 \end{bmatrix}.$$

If there is an existence of an infection in the population, then the corresponding threshold number for the persistence or eradication of HIV obtained from the spectral radius of $\mathbf{FV}^{-1}$ is given by

$$R_0 = \sqrt{\mathcal{R}_0} = \sqrt{\mathcal{R}_{0m}\mathcal{R}_{0f}}, \tag{13}$$

where

$$\mathcal{R}_{0m} = \mathcal{R}_{0m1} + \mathcal{R}_{0m2} + \mathcal{R}_{0m3} + \mathcal{R}_{0m4}, \quad \mathcal{R}_{0f} = \mathcal{R}_{0f1} + \mathcal{R}_{0f2} + \mathcal{R}_{0f3} + \mathcal{R}_{0f4},$$

with

$$\mathcal{R}_{0m1} = \left(\frac{1-\phi}{Q_1}\right)\beta_{m1}c_{f1}, \quad \mathcal{R}_{0m2} = \left(\frac{1-\phi}{Q_1Q_2}\right)\gamma_1\beta_{m2}c_{f2},$$

$$\mathcal{R}_{0m3} = \left(\frac{(Q_2Q_4\tau_1 + \gamma_1\tau_2\omega_1)(1-\phi)}{Q_1Q_2Q_3Q_4(1-\Phi_1)}\right)\beta_{m3}c_{f3},$$

$$\mathcal{R}_{0m4} = \left(\frac{(Q_3\gamma_1\tau_2 + Q_2\tau_1\psi_1)(1-\phi)}{Q_1Q_2Q_3Q_4(1-\Phi_1)}\right)\beta_{m4}c_{f4},$$

$$\mathcal{R}_{0f1} = \left(\frac{1-\phi}{Q_5}\right)\beta_{f1}c_{m1}, \quad \mathcal{R}_{0f2} = \left(\frac{1-\phi}{Q_5Q_6}\right)\gamma_2\beta_{f2}c_{m2},$$

$$\mathcal{R}_{0f3} = \left(\frac{(Q_6Q_8\tau_3 + \gamma_2\tau_4\omega_2)(1-\phi)}{Q_5Q_6Q_7Q_8(1-\Phi_2)}\right)\beta_{f3}c_{m3},$$

$$\mathcal{R}_{0f4} = \left(\frac{(Q_7\gamma_2\tau_4 + Q_6\tau_3\psi_2)(1-\phi)}{Q_5Q_6Q_7Q_8(1-\Phi_2)}\right)\beta_{f4}c_{m4}.$$

The components of the basic reproduction numbers, $\mathcal{R}_{0i}$, for $i = m,f$, are explained as follows:-

(i) $\mathcal{R}_{0mj}$, for $j = 1, \ldots, 4$, represents the basic reproductive number of the associated with each category of the male infected patients in compartments I_{mk} and T_{mk}, for $k = 1,2$, when introduced into a population, respectively.
(ii) $\mathcal{R}_{0fj}$, for $j = 1, \ldots, 4$, represents the basic reproductive number of the associated with each category of the female infected patients in compartments I_{fk} and T_{fk}, for $k = 1,2$, when introduced into a population, respectively.

The term $\Phi_1 = \psi_1\omega_1/Q_3Q_4$ indicates the fraction of male individuals in compartments T_{m1} and T_{m2} who move from either the compartments due to either improvement or decline in their immunological status. The same explanation applies to the term $\Phi_2 = \psi_2\omega_2/Q_7Q_8$ in the female population. The values $(1/Q_3)$, $(1/Q_4)$ indicate the average time male individuals in compartments T_{m1} and T_{m2} stay in their respective compartments. A similar explanation is given for the values $(1/Q_7)$, $(1/Q_8)$ in the female population. Therefore, $(1 - \Phi_1)$ and $(1 - \Phi_2)$ refer to the fraction of individuals who do not cycle between compartments T_{i1} and T_{i2} in the male and female populations, respectively. Note that the square-root arises due to the fact that it takes two generations for infected individuals to produce new infections.

From Theorem 2 in Van den Driessche, and Watmough (2002), fundamental results about the equilibria analyses of the system (5) are given by the following propositions.

Proposition 3.1: *The disease-free equilibrium point $\mathcal{E}_0$ is locally asymptotically stable when $R_0 < 1$ and unstable otherwise.*

Remark 3.1: It is important to note that If $\mathcal{R}_0 < 1$, then on average, an infected individual produces less than one new infected individual over the course of its infectious period and the infection cannot grow. Conversely, if $\mathcal{R}_0 > 1$, then each infected individual produces, on average, more than one new infection. As a result, the infection will spread and become endemic in the population.

Proposition 3.2: *The disease-persistent equilibrium point $\mathcal{E}_1$ given by the solution of expression (11) is locally asymptotically stable in Ω when $R_0 > 1$ and unstable otherwise.*

Proof: The local stability of the disease-persistent equilibrium point $\mathcal{E}_1$ is proved based on the centre manifold theory as described in Castillo-Chavez and Song (2004). We avoid restating the theorem and compute the components of **a** and **b** as explained in the theorem. Let $\vartheta = \beta_{m1}c_{f1}$ be our bifurcation parameter so that for

$$\mathcal{R}_0 = 1, \quad \vartheta = \vartheta^* = \left[\frac{Q_1}{1-\phi}\right]\left[\frac{1}{\mathcal{R}_{0f1} + \mathcal{R}_{0f2} + \mathcal{R}_{0f3} + \mathcal{R}_{0f4} - (\mathcal{R}_{0m2} + \mathcal{R}_{0m3} + \mathcal{R}_{0m4})}\right]. \tag{14}$$

Furthermore, to linearize the system (5), we define

$$S_m = x_1, \quad I_{m1} = x_2, \quad I_{m2} = x_3, \quad T_{m1} = x_4, \quad T_{m2} = x_5,$$
$$S_f = x_6, \quad I_{f1} = x_7, \quad I_{f2} = x_8, \quad T_{f1} = x_9, \quad T_{f2} = x_{10},$$

and

$$\frac{\mathrm{d}x}{\mathrm{d}t} = f(x, \vartheta), \quad f : \mathbb{R}^{10} \times \mathbb{R} \to \mathbb{R} \quad \text{and} \quad f \in \mathbf{C}^2(\mathbb{R}^{10} \times \mathbb{R}).$$

Thus, we linearize the system (5) at disease-free equilibrium with the bifurcation parameter ϑ to obtain

$$\mathbf{J} = \begin{bmatrix} J_1 & J_2 \\ J_3 & J_4 \end{bmatrix} \tag{15}$$

where

$$J_1 = \begin{bmatrix} -\mu & 0 & 0 & 0 & 0 \\ 0 & -Q_1 & 0 & 0 & 0 \\ 0 & \gamma_1 & -Q_2 & 0 & 0 \\ 0 & \tau_1 & 0 & -Q_3 & \omega_1 \\ 0 & 0 & \tau_2 & \psi_1 & -Q_4 \end{bmatrix}, \quad J_4 = \begin{bmatrix} -\mu & 0 & 0 & 0 & 0 \\ 0 & -Q_5 & 0 & 0 & 0 \\ 0 & \gamma_2 & -Q_6 & 0 & 0 \\ 0 & \tau_3 & 0 & -Q_7 & \omega_2 \\ 0 & 0 & \tau_4 & \psi_2 & -Q_8 \end{bmatrix}.$$

$$J_2 = \begin{bmatrix} 0 & -\frac{(1-\phi)\beta_{f1}c_{m1}S_m^*}{N_m} & -\frac{(1-\phi)\beta_{f2}c_{m2}S_m^*}{N_m} & -\frac{(1-\phi)\beta_{f3}c_{m3}S_m^*}{N_m} & -\frac{(1-\phi)\beta_{f4}c_{m4}S_m^*}{N_m} \\ 0 & \frac{(1-\phi)\beta_{f1}c_{m1}S_m^*}{N_m} & \frac{(1-\phi)\beta_{f2}c_{m2}S_m^*}{N_m} & \frac{(1-\phi)\beta_{f3}c_{m3}S_m^*}{N_m} & \frac{(1-\phi)\beta_{f4}c_{m4}S_m^*}{N_m} \\ 0 & 0 & 0 & 0 & 0 \\ 0 & 0 & 0 & 0 & 0 \\ 0 & 0 & 0 & 0 & 0 \end{bmatrix},$$

$$J_3 = \begin{bmatrix} 0 & -\frac{(1-\phi)\beta_{m1}c_{f1}S_f^*}{N_f} & -\frac{(1-\phi)\beta_{m2}c_{f2}S_f^*}{N_f} & -\frac{(1-\phi)\beta_{m3}c_{f3}S_f^*}{N_f} & -\frac{(1-\phi)\beta_{m4}c_{f4}S_f^*}{N_f} \\ 0 & \frac{(1-\phi)\beta_{m1}c_{f1}S_f^*}{N_f} & \frac{(1-\phi)\beta_{m2}c_{f2}S_f^*}{N_f} & \frac{(1-\phi)\beta_{m3}c_{f3}S_f^*}{N_f} & \frac{(1-\phi)\beta_{m4}c_{f4}S_f^*}{N_f} \\ 0 & 0 & 0 & 0 & 0 \\ 0 & 0 & 0 & 0 & 0 \\ 0 & 0 & 0 & 0 & 0 \end{bmatrix}.$$

It is important to note that with the bifurcation parameter expressed in (14), the linearised system (15) has a zero eigenvalue while the rest of the eigenvalues are negative. The left eigenvector of (15), $\mathbf{V} = (v_1, v_2, v_3, v_4, v_5, v_6, v_7, v_8, v_9, v_{10})$ and the right eigenvector $\mathbf{W} = (w_1, w_2, w_3, w_4, w_5, w_6, w_7, w_8, w_9, w_{10})^{\mathrm{T}}$ both associated to the eigenvalue zero are solutions of the linearised system (15) such that $\mathbf{VJ} = [0, 0, 0, 0, 0, 0, 0, 0, 0, 0]$, $\mathbf{JW} = [0, 0, 0, 0, 0, 0, 0, 0, 0, 0]^{\mathrm{T}}$ and $\mathbf{VW} = 1$. The associated left eigenvectors are given by

$$\left.\begin{aligned} &v_1 = v_6 = 0, \quad v_7 = 1, \quad v_2 = \frac{Q_5Q_6(Q_7(\delta_2+\mu)+\mu\omega_2)}{\mu(1-\phi)(Q_9+Q_{10}+Q_{11})}, \\ &v_3 = \frac{(1-\phi)(\omega_1(\mu c_{f2}\beta_{m2}+\tau_2 c_{f3}\beta_{m3})+Q_3((\delta_2+\mu)c_{f2}\beta_{m2}+\tau_2 c_{f4}\beta_{m4}))}{Q_2(\mu\omega_1+Q_3(\delta_2+\mu))}, \\ &v_4 = \frac{(1-\phi)(Q_4 c_{f3}\beta_{m3}+\psi_1 c_{f4}\beta_{m4})}{\mu\omega_1+Q_3(\delta_2+\mu)}, \quad v_5 = \frac{(1-\phi)(\omega_1 c_{f3}\beta_{m3}+Q_3 c_{f4}\beta_{m4})}{\mu\omega_1+Q_3(\delta_2+\mu)}, \\ &v_8 = \frac{Q_5(\beta_{f2}c_{m2}(\mu\omega_2+Q_7(\delta_2+\mu))+\tau_4(\omega_2\beta_{f3}c_{m3}+Q_7\beta_{f4}c_{m4}))}{(Q_9+Q_{10}+Q_{11})}, \\ &v_9 = \frac{Q_5Q_6(Q_8\beta_{f3}c_{m3}+\psi_2\beta_{f4}c_{m4})}{(Q_9+Q_{10}+Q_{11})}, \quad v_{10} = \frac{Q_5Q_6(\omega_2\beta_{f3}c_{m3}+Q_7\beta_{f4}c_{m4})}{(Q_9+Q_{10}+Q_{11})}, \end{aligned}\right\}$$

while the associated right eigenvectors are given by

$$\left.\begin{aligned} w_1 &= \frac{-Q_1}{\mu}, \quad w_2 = 1, \quad w_3 = \frac{\gamma_1}{Q_2}, \quad w_4 = \frac{\gamma_1\tau_2\omega_1 + Q_2Q_4\tau_1}{Q_2(\mu\omega_1 + Q_3(\mu+\delta_2))},\\ w_5 &= \frac{Q_2\tau_1\omega_1 + Q_3\gamma_1\tau_2}{Q_2(\mu\omega_1 + Q_3(\mu+\delta_2))}, \quad w_6 = \frac{-Q_1Q_5Q_6(\mu\omega_2 + Q_7(\delta_2+\mu))}{\mu(1-\phi)(Q_9+Q_{10}+Q_{11})},\\ w_7 &= \frac{Q_1Q_6(Q_7(\delta_2+\mu)+\mu\omega_2)}{\mu(1-\phi)(Q_9+Q_{10}+Q_{11})}, \quad w_8 = \frac{(Q_1\gamma_2(Q_7(\delta_2+\mu)+\mu\omega_2)}{\mu(1-\phi)(Q_9+Q_{10}+Q_{11})},\\ w_9 &= \frac{Q_1(\gamma_2\tau_4\omega_2 + Q_6Q_8\tau_3)}{\mu(1-\phi)(Q_9+Q_{10}+Q_{11})}, \quad w_{10} = \frac{(Q_1(Q_7\gamma_2\tau_4 + Q_6\tau_3\psi_2)}{\mu(1-\phi)(Q_9+Q_{10}+Q_{11})}, \end{aligned}\right\}$$

with

$$Q_9 = (\mu\omega_2 + Q_7(\delta_2+\mu))(Q_6\beta_{f1}c_{m1} + \gamma_2\beta_{f2}c_{m2}), \quad Q_{10} = \beta_{f3}c_{m3}(\gamma_2\tau_4\omega_2 + Q_6Q_8\tau_3),$$
$$Q_{11} = \beta_{f4}c_{m4}(\gamma_2Q_7\tau_4 + Q_6\tau_3\psi_2).$$

According Castillo-Chavez and Song (2004), the local dynamics of the system (5) around zero is governed by the the signs of **a** and **b**, where

$$\mathbf{a} = \sum_{k,i,j=1}^{n} v_k w_i w_j \frac{\partial^2 f_k}{\partial x_i \partial x_j}(0,0), \quad \mathbf{b} = \sum_{k,i=1}^{n} v_k w_i \frac{\partial^2 f_k}{\partial x_i \partial \vartheta}(0,0). \tag{16}$$

To compute **a** and **b** we, respectively, evaluate the non-zero second-order mixed derivatives with respect to variables and the non-zero partial derivatives with respect to bifurcation parameter. These are given by

$$\frac{\partial^2 f_7}{\partial x_6 \partial x_2} = \frac{\partial^2 f_7}{\partial x_2 \partial x_6} = \frac{\mu\vartheta}{(1-\alpha)\Lambda}, \quad \frac{\partial^2 f_7}{\partial x_2 \vartheta} = 1. \tag{17}$$

Now, substituting the expressions into (16) and simplifying, we obtain

$$\left.\begin{aligned} \mathbf{a} &= -\frac{Q_1Q_5Q_6(\mu\omega_2 + Q_7(\delta_2+\mu))[Q_1Q_2Q_3Q_4Q_5Q_6Q_7Q_8(1-\Phi_1)(1-\Phi_2) - \Psi_1]}{Q_3Q_4\Lambda(1-\alpha)(1-\phi)^3(1-\Phi_1)(Q_9+Q_{10}+Q_{11})\Psi_2},\\ \mathbf{b} &= 1, \end{aligned}\right\} \tag{18}$$

where

$$\left.\begin{aligned} \Psi_1 = (1-\phi)^2(&\gamma_1Q_3Q_4(1-\Phi_1)c_{f2}\beta_{m2} + c_{f3}\beta_{m3}(\gamma_1\tau_2\omega_1 + Q_2Q_4\tau_1)\\ &+ c_{f4}\beta_{m4}(\gamma_1Q_3\tau_2 + Q_2\tau_1\psi_1))(Q_6Q_7Q_8\beta_{f1}c_{m1}(1-\Phi_2)\\ &+ \beta_{f3}c_{m3}(Q_6Q_8\tau_3 + \gamma_2\tau_4\omega_2)\\ &+ Q_7Q_8\beta_{f2}c_{m2}\gamma_2(1-\Phi_2) + \beta_{f4}c_{m4}(Q_7\gamma_2\tau_4 + Q_6\tau_3\psi_2)),\\ \Psi_2 = (&Q_6Q_7Q_8\beta_{f1}c_{m1}(1-\Phi_2) + \beta_{f3}c_{m3}(Q_6Q_8\tau_3 + \gamma_2\tau_4\omega_2)\\ &+ Q_7Q_8\beta_{f2}c_{m2}\gamma_2(1-\Phi_2) + \beta_{f4}c_{m4}(Q_7\gamma_2\tau_4 + Q_6\tau_3\psi_2)). \end{aligned}\right\}$$

From expressions in (18), it can be seen that $\mathbf{a} < 0$ and $\mathbf{b} > 0$ for all parameter values. Therefore, the disease-persistent equilibrium point $\mathcal{E}_1$ is locally asymptotically stable close to $\mathcal{R}_0 = 1$. ■

3.2. Parameter estimation

Some of the parameters ranges used in this paper have been estimated from previously published articles, while others are estimated intuitively. The baseline parameter values are obtained through curve fitting are presented under the caption of Figure 4. The full list of parameter ranges used in the simulation is given in Table 2.

3.3. Data

3.3.1. HIV data

The data were obtained from Kenya Health Information System (KHIS) (KHIS, 2017). The data used represent new HIV infection for both males and females in Kenya. Data are collected routinely on a monthly basis and was retrieved for the period beginning January 2011 to December 2017. Only variables of interest were pulled out to excel spreadsheet. Data were stored in excel and thereafter analysed in **R**. The pictorial representation of the raw data is given in Figure 2.

3.3.2. Initial conditions

To fit and validate the model (5) to the data on reported cases of new HIV infections in Kenya, the initial conditions are set as follows. The total population of Kenya at the end of 2010 was estimated to be 41.35 million according to KNBS (2015). Of this 57.6% of the population was aged 15 years and above. Therefore, the total population (N) considered in this paper is 23.8176 million. The population of male (N_m) is estimated to be 49% and that of female (N_f) is estimated at 51%. The reported number of adults living with HIV in January 2011 was 1.2 million with approximated 661,515 on ART treatment (NACC, 2017). From here, the number of new HIV infections (I_{m1} and I_{fm}) have been estimated based on the data reported in January 2011 to be 500 and 530, respectively (KHIS, 2017). The

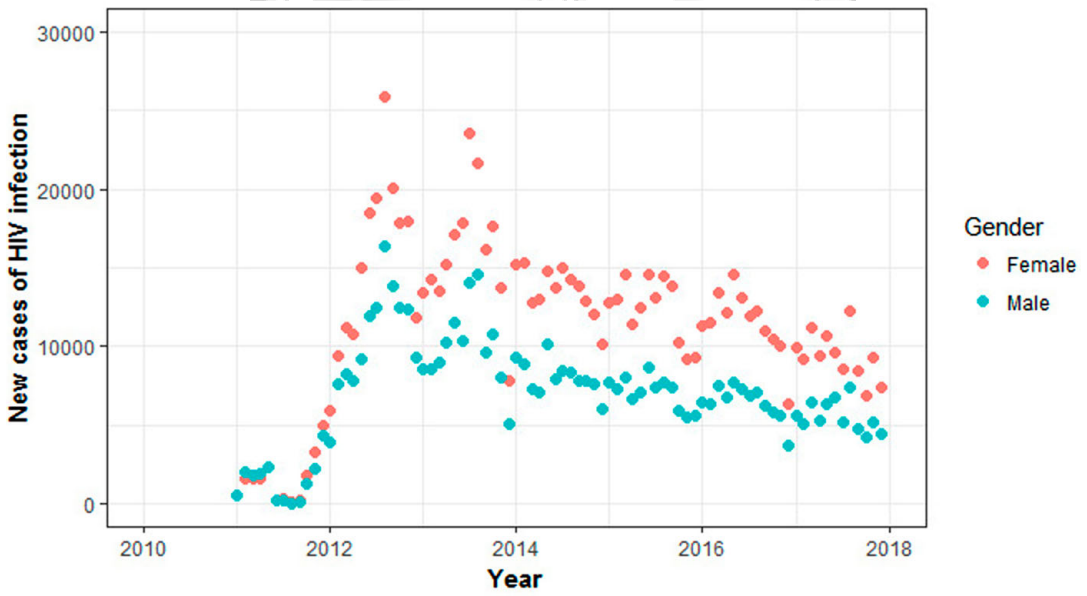

Figure 2. The graphical representation of the data for the new cases of HIV infections in Kenya in the male and female populations.

susceptible population for each gender is estimated using the following relations

$$S_m = N_m - \sum_{k=1}^{2} I_{mk} - \sum_{k=1}^{2} T_{mk} \quad \text{and} \quad S_f = N_f - \sum_{k=1}^{2} I_{fk} - \sum_{k=1}^{2} T_{fk}.$$

The breakdown of the initial populations used in the curve fitting is given in Table 1. We therefore resort to curve fitting and numerical simulation to understand the effect of PrEP in the evolution of HIV.

4. Results

4.1. Data input description

Input data were summarized using error bar and density plot to illustrate the extent of variability and presented in Figure 3. For process indicators, the mean number of infections are reported and the 95% confidence intervals are presented using the error bar in Figure 3(a). The results suggest that there appears a significant difference in HIV infections between males and females. This is supported by the non-overlapping standard deviation error bars. Furthermore, it can easily be seen that the mean number of new cases of infections in the female population is higher than the mean number of new cases of infection in the male population. From result in Figure 3(b), it can clearly be seen that the data for the two sets do not follow a normal distribution. Thus, there is need to perform further tests to establish any significance difference. To establish whether there is significant difference in the male and female infections, Mann–Whitney U-test is used. This is a non-parametric test that is used to compare means of two groups that do not follow a normal distribution as suggested by the results in Figure 3(b). The results in Table 3 show that there is significant difference in the mean infections between male and female given that the p-value $= 3.686e - 10 < 0.05$, performed at 95% confidence level.

4.2. Curve fitting

In this section, we fit system (5) to data to determine the trend of HIV in male and female populations. Curve fitting is a process that allows us to quantitatively estimate the trend of

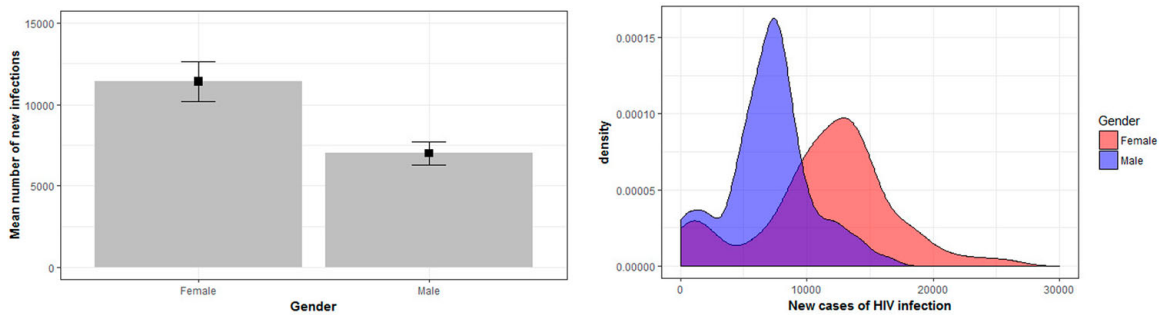

Figure 3. A graphical representations of the variability of the data. (a) The means with error bars for two variables (females and males): $n = 84$ for each variable. The column denotes the data mean (M). The bars show confidence interval (CI). CI error bars encompass 95% of the data. (b) The density distribution of the data.

Table 3. Wilcoxon test.

w	*p*-value
5504	3.686e−10

the outcomes. The curve fitting process fits equations of approximating curves to the raw field data. However, for a given set of data, the fitting curves of a given type are generally not unique. Thus, a curve with a minimal deviation from all data points is desired. This best-fitting curve can be obtained by the method of least squares. In this method, the parameters not known are approximated through minimization of the sum of the squared deviations between the data and the model. It minimizes the sum of squared distances between the observed values and the model values. This can be mathematically expressed as

$$RSS = \sum_{i=1}^{n} \theta_i^2 = \sum_{i=1}^{n} (y_1 - \hat{y})^2,$$

where $\theta_i = (y - \bar{y})$ and n refers to the data points and RSS refers to the sum of square error estimate which is assumed to follow a normal distribution.

The FME package (A flexible modelling environment for inverse modelling, sensitivity, identifiability and Monte Carlo Analysis) in **R** is used to fit the model to data. A **R** code is used in which, the parameters with unknown values are given lower and upper bounds from which the set of parameter values that produce the best fit are obtained. The following parameters were fixed at the following values: $\Lambda = 0.0014N, \mu = 0.00139, \delta_1 = 0.00915, \delta_2 = 0.00725, c_{m1} = c_{f1} = 3, c_{m2} = c_{m3} = c_{m4} = c_{f2} = c_{f3} = c_{f4} = 2, \alpha = 0.49$. The parameter ranges/values in Table 2 are used in the curve fitting and the resulting point values estimated are presented under the caption of Figure 4.

We observe in Figure 4(a,b) that the model fits well with the data. It is important to observe that the cases of new infection peaked in the year 2014. The results show that there was a rise in HIV infection between 2011 and 2014, accompanied by a noticeable decline in the occurrences of of new cases of HIV infection. The estimated trends in Figure 5(b) show that infection will decline towards 2030 when PrEP uptake is maintained slightly above 40%. Note that the government of Kenya approved PrEP uptake in 2017 and much of its successes are yet to be reported. The effect of introduction of PrEP is seen in Figure 5(b) where there is a sudden fall in 2017 following the government approval. Thus, there is need to emphasise on preventive measures through educational campaigns and social programmes that ensure minimal or reduced infections. Although, the population shows a general fall in HIV infections, the female population will still continue to be disproportionately affected by the epidemic compared to the the male population as reflected in Figure 5(a). This finding agrees with the finding in the report by Kenya National AIDS Control Council (NACC) (Kenyan Ministry of Health [MOH], 2016; NACC, 2016) .

In order to establish the correlation between the parameters with respect to variables I_{m1} and I_{f1}, we present pairs plot of the markov chain monte carlo (MCMC) samples for the model parameters. As seen Figure 6, the scatter plot matrix in the upper panel describes the pairwise relationship between parameters with corresponding correlation coefficients shown in the lower panel. The marginal distribution for each parameter is shown on the

diagonal. The scatter in blue and green correspond to I_{m1} and I_{f1}, respectively. It is shown in Figure 6 there is a negative correlation between β_{m1} and ω_1 as well as β_{f1} and ω_2. Implying that an increase in the drug efficacy (ART) results to a decrease in the infection terms. This is particular true with regards to treatment of HIV due to the fact that an increase in the drug efficacy results to an increase in viral load suppression which in turn lowers the chances of infection through heterosexual means.

4.3. Sensitivity analysis

We perform sensitivity analysis to examine the output's (basic reproduction number) response to the simultaneous variation of the parameter values within a range in the parameter space is described in Table 2. Following the work in Marino, Hogue, Ray, and Kirschner (2008), Wu, Dhingra, Gambhir, and Remais (2013), and Stein (1987), we use Latin Hypercube Sampling (LHS) to determine the Partial Rank Correlation Coefficients (PRCCs) with 5000 simulations per run. PRCC takes values between -1 and $+1$ in which the sign indicates how the model output is qualitatively related to each model parameter. The parameters are assumed to be random variables with uniform distribution with

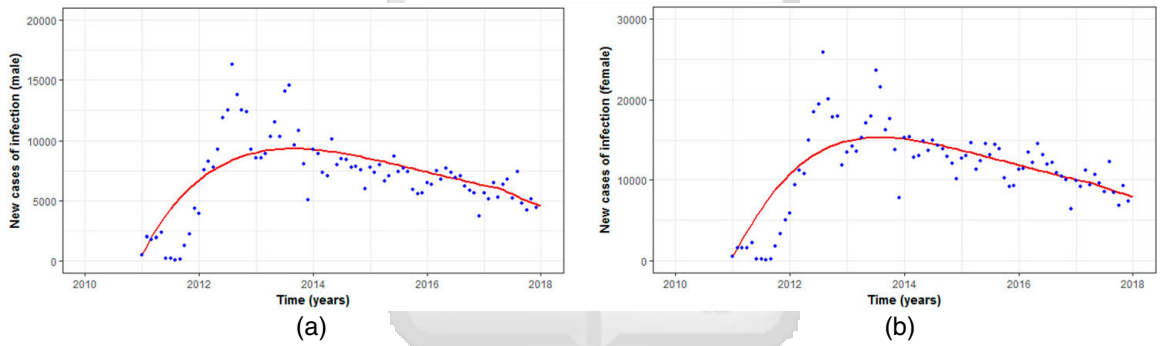

Figure 4. Model system (5) fitted to data for the reported new cases of HIV infection. (a) shows the model fitted to the data for the male while (b) shows the model fitted to data for the female. The blue dots indicate the actual data and the red line indicates the model fit to the data. The baseline parameter values obtained from the curve fitting are: $\beta_{m1} = 0.110, \beta_{m2} = 0.0031, \beta_{m3} = 0.0062, \beta_{m4} = 0.149, \beta_{f1} = 0.243, \beta_{f2} = 0.127, \beta_{f3} = 0.003, \beta_{f4} = 0.0014, \gamma_1 = 0.550, \gamma_2 = 0.126, \tau_1 = 0.999, \tau_2 = 1.000, \tau_3 = 0.613, \tau_4 = 0.483, \psi_1 = 0.005, \psi_2 = 0.002, \omega_1 = 0.540, \omega_2 = 0.002$.

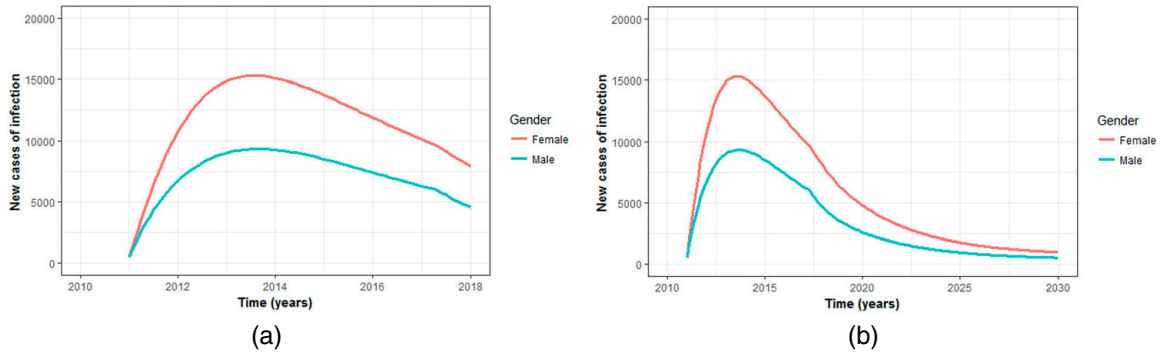

Figure 5. (a) shows the comparison of the new cases of infections between male and females as fitted to the data while the (b) shows the projection of infection to 2030 with a constant uptake of PrEP at 40% following its approval and its subsequent use in 2017 by the Kenyan government.

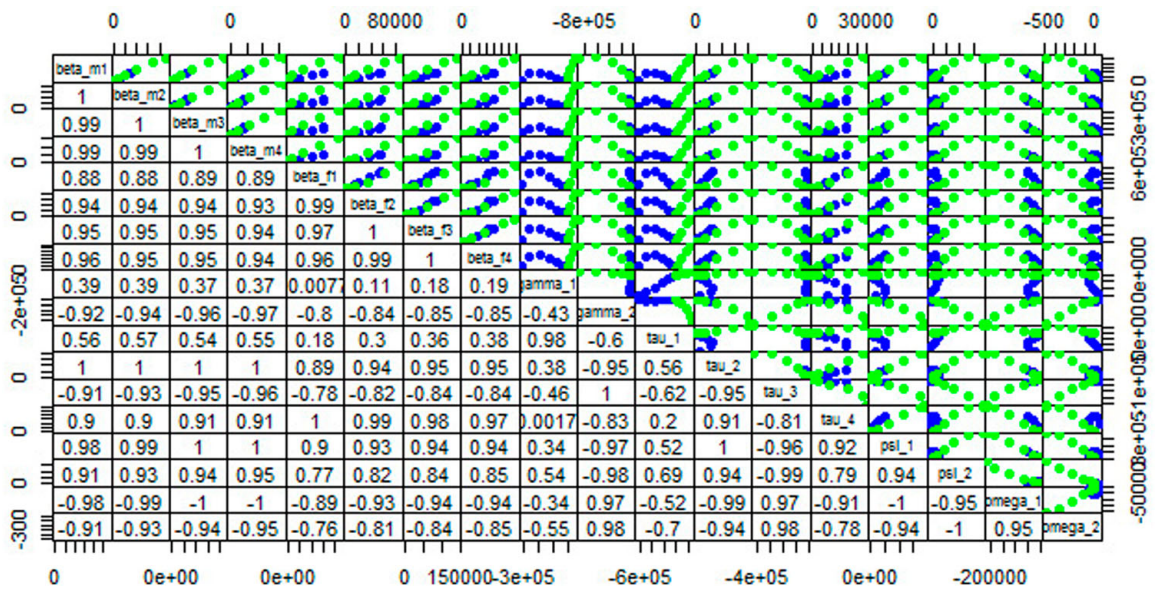

Figure 6. Pairs plot of the markov chain monte carlo (MCMC) samples for the model parameters.

their range values given in Table 2 and point values given under the caption of Figure 4. We observe from Figure 7 that the parameters with the greatest potential to increase the HIV infection are the effective person to person contact rates. Moreover, the uptake of PrEP, ϕ is the parameter with the greatest potential to make the epidemic better when increased. This is supported by the results in Figure 5(b).

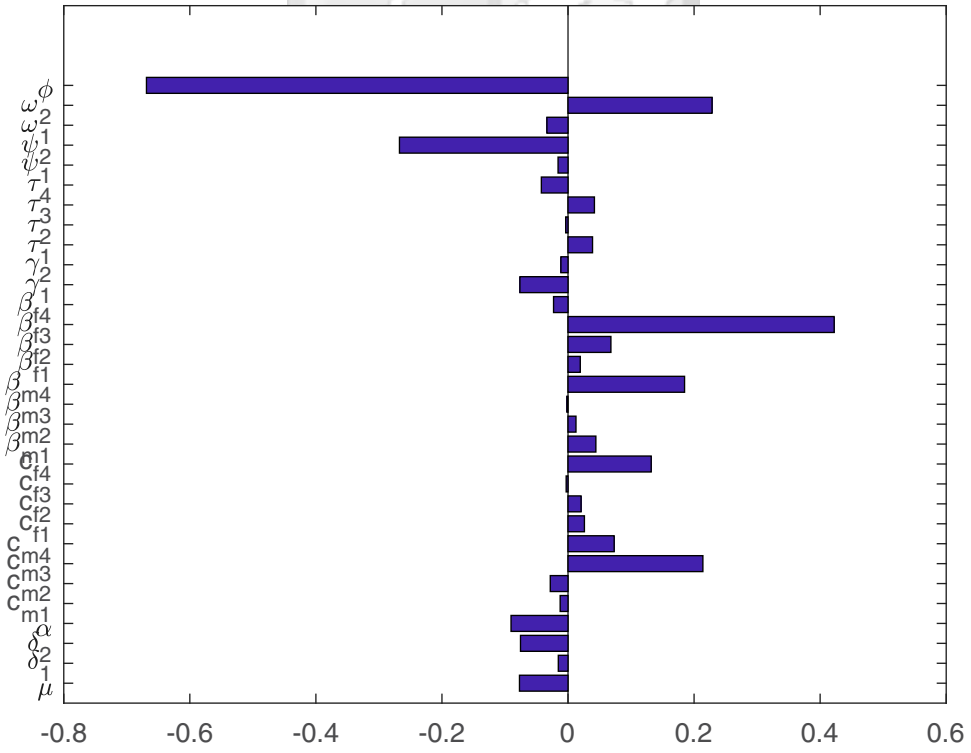

Figure 7. Sensitivity indices of the model parameters with I_{m1} and I_{f1} taken as baseline PRCC analysis variables. Analysis was computed based on the parameter values presented under the caption of Figure 4.

5. Discussion

In this paper, we have analysed a sex-structured population model and studied the HIV infection trends in males and females. The model has assumed that the main mode of HIV transmission is heterosexual. The basic reproduction number and equilibrium points are computed. From our computation, it therefore suffices to deduce that the model exhibits two equilibria namely the disease-free equilibrium and the endemic equilibrium. The data representing new cases of HIV infection for both males and females has been extracted from Kenya Health Information System (KHIS) and analysed. The descriptive statistics of the data shows that there exists a higher number of cases of infection in females as opposed to males. This difference has been established to be significant through Mann–Whitney *U*-test. The model has been fitted to data using least squares method in **R**. The trend shows that the females are still disproportionately affected with HIV as compared to males. In order to establish the impact of the recent roll-out of PrEP, we investigated its role in limiting HIV infection. We fixed the rate of PrEP use to zero for the period before May 2017 when the PrEP use was launched in Kenya and after May 2017, the rate of PrEP use was fixed at 0.40 representing 40% coverage. From the trend projection to year 2030, it suffices to conclude that PrEP plays an important role in reducing the number of new cases of HIV. We notice that when the value of parameter (ϕ) is fixed at 0.40, the cases of infection declines towards 2030 to a near complete eradication of HIV. This implies that controlling and eventual eradication of HIV in Kenya requires aggressive campaigns by the Kenyan government in favour of PrEP use. Furthermore, sensitivity analysis has been carried out using Latin Hypercube Sampling (LHS) technique. It is seen that the model output (basic reproduction number) is highly sensitive to the effective contact rates suggesting that efforts made to reduce the contacts between uninfected individuals and the infected individuals will be most appropriate in limiting the occurrence of new infections.

In conclusion, we show that prevention of HIV infection still remains the most vital way of curbing further spread. HIV patients under ART treatment are possibly capable of aiding the eradication of HIV by convincing their sexual partners of the need to adhere to protection via use of PrEP or any other protection means and ART treatment. The model presented in this paper is a very simplified description of HIV infection in Kenya and therefore it has some cogent limitation. The model presented in this study does not take into account the full stages of HIV. Even though, the model recognizes the fact that there is need for immediate treatment once an individual is found to be positive in line with WHO regulations of 2015 based on viral load suppression, the model did not factor in the viral load levels. This limitation can be circumvented in various ways. First,there is a need to link the model to laboratory experiments for a clearer determination of parameter values based on the viral load of the patients. Second, the development of mathematical models elucidating all the HIV stages will greatly advance our understanding of HIV spread in Kenya. Despite the limitations highlighted, the model results have significant bearings on HIV dynamics and its treatment with ART.

Acknowledgments

The authors acknowledge, with thanks, the support of Strathmore University, Institute of Mathematical Sciences for the production of this manuscript. EO participated in formulating the model, carried out the mathematical analysis of the model, performed the numerical analysis and drafted

the manuscript. RW participated in the mathematical analysis and numerical analysis. LL conceived of the study, and participated in model formulation and helped to draft the manuscript. All authors read and approved the final manuscript.

Disclosure statement

No potential conflict of interest was reported by the authors.

ORCID

E. O. Omondi http://orcid.org/0000-0002-1779-1043
R.W. Mbogo http://orcid.org/0000-0003-1639-1360
L.S. Luboobi http://orcid.org/0000-0002-8256-8593

References

AIDS. (2015). *AIDS info. Guidelines for the use of antiretroviral agents in HIV-1-Infected adults and adolescents*. Retrieved from https://aidsinfo.nih.gov/guidelines/html/1/adult-and-adolescent-arv-guidelines/458/plasma-hiv-1-rna-viral-load-and-cd4-count-monitoring.

AIDS. (2016). *Pre-Exposure Prophylaxis (PrEP)*. Retrieved from https://www.aids.gov/hiv-aids-basics/prevention/reduce-your-risk/pre-exposure-prophylaxis/.

Athithan S., & Ghosh M. (2014). Analysis of a sex-structured HIV/AIDS model with the effect of screening of infectives. *International Journal of Biomathematics*, *7*(05), 1450054.

Baryarama F., Mugisha J. Y. T., & Luboobi L. S. (2006). A mathematical model for the dynamics of HIV/AIDS with gradual behaviour change. *Computational and Mathematical Methods in Medicine*, *7*(1), 15–26.

Bhunu C. P., Mushayabasa S., Kojouharov H., & Tchuenche J. (2011). Mathematical analysis of an HIV/AIDS model: Impact of educational programs and abstinence in Sub-Saharan Africa. *Journal of Mathematical Modelling and Algorithms*, *10*(1), 31–55.

Castillo-Chavez C., & Song B. (2004). Dynamical models of tuberculosis and their applications. *Mathematical Biosciences and Engineering*, *1*(2), 361–404.

Doyle M., Greenhalgh D., & Blythe S. (1998). Equilibrium analysis of a mathematical model for the spread of AIDS in a two sex population with mixing constraints. *Journal of Biological Systems*, *6*(02), 159–185.

Feng X., Ruan S., Teng Z., & Wang K. (2015). Stability and backward bifurcation in a malaria transmission model with applications to the control of malaria in china. *Mathematical Biosciences*, *266*, 52–64.

Ghimire L., Smith W. C. S., van Teijlingen E. R., Dahal R., & Luitel N. P. (2011). Reasons for non-use of condoms and self-efficacy among female sex workers: A qualitative study in Nepal. *BMC Women's Health*, *11*(1), 42.

Hethcote H. W. (2000). The mathematics of infectious diseases. *SIAM Review*, *42*(4), 599–653.

HIV/AIDS. (2016). *Pre-Exposure Prophylaxis (PrEP)*. Retrieved from https://www.cdc.gov/hiv/risk/prep/.

Kaur N., Ghosh M., & Bhatia S. (2014). Mathematical analysis of the transmission dynamics of HIV/AIDS: Role of female sex workers. *Applied Mathematics & Information Sciences*, *8*(5), 2491.

Kenya Health Information System. (2017). *District Health Information System (DHIS2)*. Retrieved from https://hiskenya.org/.

Kenyan Ministry of Health. (2016). *Kenya HIV county profiles*. Retrieved from http://nacc.or.ke/wp-content/uploads/2016/12/Kenya-HIV-County-Profiles-2016.pdf.

Kenya National Bureau of Statistics. (2015). *Demographic and health survey*. Retrieved from https://dhsprogram.com/pubs/pdf/FR308/FR308.pdf.

Marino S., Hogue I. B., Ray C. J., & Kirschner D. E. (2008). A methodology for performing global uncertainty and sensitivity analysis in systems biology. *Journal of Theoretical Biology*, *254*(1), 178–196.

Mukandavire Z., Chiyaka C., Garira W., & Musuka G. (2009). Mathematical analysis of a sex-structured HIV/AIDS model with a discrete time delay. *Nonlinear Analysis: Theory, Methods & Applications*, *71*(3), 1082–1093.

Mukandavire Z., & Garira W. (2007a). Age and sex structured model for assessing the demographic impact of mother-to-child transmission of HIV/AIDS. *Bulletin of Mathematical Biology*, *69*(6), 2061–2092.

Mukandavire Z., & Garira W. (2007b). Sex-structured HIV/AIDS model to analyse the effects of condom use with application to Zimbabwe. *Journal of Mathematical Biology*, *54*(5), 669–699.

Munz P., Hudea I., Imad J., & Smith R. J. (2009). When zombies attack! Mathematical modelling of an outbreak of zombie infection. *Infectious Disease Modelling Research Progress*, *4*, 133–150.

National Aids Control Council of Kenya. (2014a). *Kenya AIDS strategic framework 2014/2015–2018/2019*. Retrieved from http://www.undp.org/content/dam/kenya/docs/Democratic%20Governance/KENYA%20AIDS%20STRATEGIC%20FRAMEWORK.pdf.

National Aids Control Council of Kenya. (2014b). *Kenya AIDS response progress report 2014: Progress towards zero*. Retrieved from http://nacc.or.ke/wp-content/uploads/2016/11/Kenya-AIDS-Progress-Report_web.pdf.

National Aids Control Council of Kenya. (2016). *Kenya AIDS response progress report 2016*. Retrieved from http://nacc.or.ke/wp-content/uploads/2016/11/Kenya-AIDS-Progress-Report_web.pdf.

National Aids Control Council of Kenya. (2017). *National AIDS Control Council and the National AIDS and STD Control Programme, March 2012*. HIV/AIDS report. Retrieved from http://guidelines.health.go.ke:8000/media/National_HIV_Estimates_for_Kenya_2011-2015.pdf.

Nyabadza F., Njagarah J. B., & Smith R. J. (2013). Modelling the dynamics of crystal meth ('tik') abuse in the presence of drug-supply chains in South Africa. *Bulletin of Mathematical Biology*, *75*(1), 24–48.

Okango E., Mwambi H., & Ngesa O. (2016). Spatial modeling of HIV and HSV-2 among women in Kenya with spatially varying coefficients. *BMC Public Health*, *16*(1), 355–368.

Okosun K. O., Makinde O. D., & Takaidza I. (2013). Impact of optimal control on the treatment of HIV/AIDS and screening of unaware infectives. *Applied Mathematical Modelling*, *37*(6), 3802–3820.

Omondi E., Nyabadza F., & Smith R. (2018a). Modelling the impact of mass administration of ivermectin in the treatment of onchocerciasis (river blindness). *Cogent Mathematics & Statistics*, *5*(1), 1429700.

Omondi E. O., Mbogo R., & Luboobi L. (2018b). Mathematical modelling of the impact of testing, treatment and control of hiv transmission in Kenya. *Cogent Mathematics & Statistics*, *5*(1), 1475590.

Omondi E. O., Nyabadza F., Bonyah E., & Badu K. (2017). Modeling the infection dynamics of onchocerciasis and its treatment. *Journal of Biological Systems*, *25*(02), 247–277.

OPTIONS. (2016). *OPTIONS country situation analysis interim findings: Kenya. FSG in partnership with LVCT health*. Retrieved from http://www.prepwatch.org/wp-content/uploads/2016/05/Situation_Analysis_Kenya.pdf.

POP. (2017). *Kenya demographics profile 2018. Demographic profiles of the world*. Retrieved from https://www.indexmundi.com/kenya/demographics_profile.html.

Shields A. (2012). *Criminalizing Condoms: How policing practices put sex workers and HIV services at risk in Kenya, Namibia, Russia, South Africa, the United States, and Zimbabwe*. New York: Open Society Foundations.

Stein M. (1987). Large sample properties of simulations using Latin hypercube sampling. *Technometrics*, *29*(2), 143–151.

UNAIDS. (2014). *United Nations Programme on HIV/AIDS (UNAIDS) progress reports submitted by countries*. Kenya AIDS Response Progress Report 2014: Progress towards Zero. Retrieved from http://www.unaids.org/en/dataanalysis/knowyourresponse/countryprogressreports/2014countries.

UNAIDS. (2015). *Global information and education on HIV and AIDS*. HIV and AIDS in Kenya. Retrieved from https://www.avert.org/professionals/hiv-around-world/sub-saharan-africa/kenya#footnote5_jxd6oql.

UNAIDS. (2016a). *UNAIDS. HIV and AIDS estimates*. Retrieved from http://www.unaids.org/en/regionscountries/countries/kenya.

UNAIDS. (2016b). UNAIDS report (Prevention gap report). Retrieved from http://www.unaids.org/sites/default/files/media_asset/2016-prevention-gap-report_en.pdf.

UNAIDS. (2018). *United Nations AIDS. Advocating for zero discrimination in health-care settings in Kenya*. Retrieved from http://www.unaids.org/en/resources/presscentre/featurestories/2018/may/zero-discrimination-health-care-settings-kenya.

Van den Driessche P., & Watmough J. (2002). Reproduction numbers and sub-threshold endemic equilibria for compartmental models of disease transmission. *Mathematical Biosciences*, *180*(1), 29–48.

Van Sighem A., Vidondo B., Glass T. R., Bucher H. C., Vernazza P., Gebhardt M., de Wolf F., Derendinger S., Jeannin A., & Bezemer D. (2012). Resurgence of HIV infection among men who have sex with men in Switzerland: Mathematical modelling study. *PLoS One*, *7*(9), e44819.

Voeten H. A., Egesah O. B., Varkevisser C. M., & Habbema J. (2007). Female sex workers and unsafe sex in urban and rural Nyanza, Kenya: Regular partners may contribute more to HIV transmission than clients. *Tropical Medicine & International Health*, *12*(2), 174–182.

WB. (2017). *World Bank Data. Birth rate, crude (per 1000 people)*. Retrieved from https://data.worldbank.org/indicator/SP.DYN.CBRT.IN.

WHO. (2014). *March 2014 supplement to the 2013 consolidated guidelines on the use of antiretroviral drugs for treating and preventing HIV infection: recommendations for a public health approach*. Geneva: World Health Organization.

WHO. (2018). *HIV/AIDS-Global Health Observatory (GHO) data*. Retrieved from http://www.who.int/gho/hiv/en/.

Williams B. G. (2014). Optimizing control of HIV in Kenya. *arXiv preprint arXiv:1407.7801*.

Williams B. G., Hargrove J. W., & Humphrey J. H. (2010). The benefits of early treatment for HIV. *AIDS*, *24*(11), 1790–1791.

Wodarz D., & Nowak M. A. (2002). Mathematical models of HIV pathogenesis and treatment. *BioEssays*, *24*(12), 1178–1187.

Wu J., Dhingra R., Gambhir M., & Remais J. V. (2013). Sensitivity analysis of infectious disease models: Methods, advances and their application. *Journal of The Royal Society Interface*, *10*(86), 20121018.

Infectious Disease Modelling 4 (2019) 83–98

Contents lists available at ScienceDirect

Infectious Disease Modelling

journal homepage: www.keaipublishing.com/idm

A mathematical modelling study of HIV infection in two heterosexual age groups in Kenya

E.O. Omondi*, R.W. Mbogo, L.S. Luboobi

Institute of Mathematical Sciences, Strathmore University, P.O Box 59857-00200, Nairobi, Kenya

ARTICLE INFO

Article history:
Received 19 December 2018
Received in revised form 13 April 2019
Accepted 15 April 2019
Available online 21 April 2019
Handling Editor: Y. Shao

Keywords:
Heterosexual transmission (HIV)
Basic reproduction number
MCMC
Probability distribution
Kruskal–Wallis test
Correlation

ABSTRACT

The control of HIV demands different interventions for different age groups. In the present manuscript, we formulate and analyze a mathematical compartmental models of HIV transmission within and between two age groups in Kenya. We fitted the model to data using MCMC technique and inferred the parameters. We also estimate the reproduction numbers, namely within age group transmission and between age groups transmission basic reproduction numbers. The analysis of the data revealed that there is significant difference in mean number of new HIV infections between males and females within the two age groups. More, particularly, females are highly infected with HIV as compared to their male counterparts. Calculation of the reproduction numbers within and between age groups provides insights into control that cannot be deduced simply from observations on the prevalence of infection. More specifically, the analysis showed that the per capita rate of HIV transmission was highest when there is interaction between young adults to adults and most HIV infections occurred in adult population. Furthermore, the sensitivity analysis demonstrated that the reproduction numbers depend mainly on the probabilities of infection. This results can be used to guide HIV interventions, condom distribution and antiretroviral therapy. Precisely, the results can be used to educate the young adults on practicing safe sex with their partners in order to contain the occurrence of new infections.

1. Introduction

Kenya has the joint fourth-largest HIV epidemic in the world (alongside Mozambique and Uganda) with 1.5 million people living with HIV in 2017 (AV, 2017). In the same year, 35,000 people died from AIDS-related illnesses, while this is still high it has declined steadily from 64,000 in 2010 (WHO, 2018). Kenya's HIV epidemic is driven by sexual transmission and is generalized, meaning it affects all sections of the population including children, young people, adults, women and men (AV, 2017). In 2010, the prevalence of HIV in the female population was 6.5% and 5.6% in the male population (WHO, 2018). While the prevalence of HIV infection has considerably reduced to 6.0 in 2010 from 10% in 1996, women still continue to be disproportionately affected by the HIV infections since men often dominate sexual relationships, with women not always able to practice safer sex even when they know the risks (AV, 2017). Young women are almost twice as likely to acquire HIV as their

* Corresponding author.
E-mail address: eomondi@strathmore.edu (E.O. Omondi).
Peer review under responsibility of KeAi Communications Co., Ltd.

https://doi.org/10.1016/j.idm.2019.04.003

male counterparts. At the end of 2015 young women accounted for 33% of the total number of new infections in comparison to young men that accounted for 16% (MOH, 2016).

Antiretroviral therapy (ART) is the current standard of care for patients living with HIV infection (WHO, 2014). It has led to significant reduction in AIDS related morbidity and mortality (Chow, Leong, Chow, & Hooi, 2007; Omondi, Mbogo, & Luboobi, 2018a; Williams, 2014). The control of HIV demands different interventions for different age groups. HIV education and awareness is an important component of HIV prevention. In Kenya, 73% of young women and 82% of young men in 2014 demonstrated adequate knowledge of HIV prevention (MOH, 2016). However, incorrect perception of HIV risk, and having unprotected sexual intercourse under influence of alcohol or drugs have been cited as some of the factors that contribute to the rise in HIV infection among young people (AV, 2017). HIV testing and counselling (HTC) has become a major feature of Kenya's HIV response. Targeted community-based HIV testing, door-to-door testing campaigns, and the introduction of self-testing kits are some of the innovative approaches to HIV testing adopted in recent years (UNAIDS, 2016). By 2015, about 9.9 million had been tested. Nonetheless, there remains a significant disparity between men and women. In 2014, 53% of women had tested for HIV in the past 12 months and received their results, compared to 45% of men (KNBS, 2014). In its effort to reduce HIV infections in Kenya, the government introduced self-testing kits in May 2017, the Kenya, as part of their 'Be Self Sure' campaign as well as PrEP which uses antiretroviral drugs to protect HIV-negative people from HIV before potential exposure to the virus (UNAIDS, 2017a).

Mathematical modelling is a common tool for understanding and studying the dynamics of infectious disease, and propose mitigation measures to control disease outbreaks (Keeling & Rohani, 2011). As such a number of HIV models have been constructed and analyzed to understand the transmission dynamics of the disease. Recently, Aldila (2018) studied the HIV transmission dynamics using a compartmental model. He considered the awareness of individuals both infected and uninfected with HIV as well as ART treatment intervention. Omondi, Mbogo, and Luboobi (2018b) modelled the impact of testing, treatment and control of HIV transmission that include anti-retroviral interventions in Kenya that among the adult population. They used the basic reproduction number and both the local and global stability to understand how HIV might spread. They established that an infection might suppress with the use of combination of testing, Pre-Exposure Prophylaxis and antiretroviral treatment intervention. In another study, Kim et al. (2014) studies HIV prevention measures including Pre-Exposure Prophylaxis on HIV incidence and established that PrEP use was more beneficial in prevention of HIV infection in South Korea. Omondi, Mbogo, and Luboobi (2018c) studied the trend of HIV transmission and treatment in Kenya. However, their model was not stratified to include gender and age. Mukandavire, Chiyaka, Garira, and Musuka (2009) modelled a sex-structured model for heterosexual transmission of HIV/AIDS with explicit incubation period and provided an in-depth and complete qualitative analysis. However, the model neglected stratification by age. In another study, Mukandavire and Garira (2007) considered heterosexual interactions of males and females using integro-differential equations with a time delay due to incubation period. While they incorporated the effects of male and female condom use as the main mode of preventing HIV infection, no real-time surveillance data to establish the trend of infection. In addition, the model was not stratified by age. To the best of our knowledge, all the above research works mentioned focused on the mathematical analysis of the models and few papers of HIV infection exist, where gender and age is modelled using real-time surveillance. It is important to note that the mentioned studies did not attempt to use inference methods to fit the models to data and estimate model parameters. While both the impact and the cost of different combinations of interventions vary, we are concerned in this paper with the population impact that can be achieved for a given reduction in the individual risk of transmission irrespective of how it is brought about. This analysis focuses on the spread of an HIV epidemic in Kenya, as described by data collected. Thus, we develop a within and between age groups model of HIV transmission. The model is mathematically analyzed, fitted to data of new cases of HIV infections in Kenya and parameters are inferred.

This paper is organized as follows: In Section 2, we develop mathematical model. In Section 3, we find the expressions for basic reproductive numbers for within and between age groups. Results are presented in Section 4. Finally, the paper ends with a conclusion in Section 5.

2. Methods

2.1. Model formulation

We consider a simple mathematical model to understand the dynamics of HIV within and between two different age categories in Kenya. In our modelling framework, it is assumed that HIV transmission is mainly through heterosexual means. The population is divided into young adults (aged 15–24) and adult (age 25 and over) sub-populations. Each sub-population is divided into susceptible individuals (S), infected individuals (I) and those who have been enrolled into treatment programme mainly ART (T). We assume that all the infected individuals are connected to ART treatment. The AIDS class is not considered in this model given that full blown AIDS patients are usually hospitalized and/or sexually inactive. It is assumed that they are not able to engage in HIV transmission activities hence do not contribute to HIV infection. The total variable population at time t is described by

$$N(t) = N_m(t) + N_f(t), \tag{1}$$

where the subscripts m and f denote male and female and the individual sex oriented population described by

$$\left.\begin{aligned} N_m(t) &= S_{dm} + S_{am} + I_{dm} + I_{am} + T_{dm} + T_{am}, \\ N_m(t) &= S_{df} + S_{af} + I_{df} + I_{af} + T_{df} + T_{af}. \end{aligned}\right\} \tag{2}$$

here, d and a represent the young adults (aged between 15 and 24 years) and the adults (aged over 25 years), respectively. Individuals move from one class to the other as their status evolve with respect to the infection. The population of the susceptible young adults is generated at the rate Π via maturation into adulthood or immigration of which a proportion τ are assumed to be males and $(1-\tau)$ are assumed to be females. Since the current study is looking at the trend of new HIV infections within and between these two age groups, it is assumed that there is no vertical transmission. The population is reduced by young adults maturation at the rate α and by natural death at the rate μ_d. The infection rate of the young adults in both males and females is respectively, given by

$$\lambda_{dm} = \frac{\beta_1\gamma_1\left(I_{df} + \theta_1 I_{af} + \theta_2 T_{df} + \theta_3 T_{af}\right)}{N_m} \text{ and } \lambda_{df} = \frac{\beta_2\gamma_2(I_{dm} + \theta_4 I_{am} + \theta_5 T_{dm} + \theta_6 T_{am})}{N_f}. \tag{3}$$

The parameters β_1, and β_2 are the probabilities of HIV infection through contacts with individuals in Iij and T_{ij}, and $\theta_1, \theta_2, \theta_3, \theta_4, \theta_5$, and θ_6 are modification factors in transmission probabilities, where i,j refers to young adults and adults, respectively. The infected young adults for both males and females are connected to ART treatment and care at the rates ϕ_1 and δ_1, respectively. The male and female adults acquire infection at the rates, respectively given by

$$\lambda_{am} = \frac{\beta_3\gamma_3\left(I_{df} + \eta_1 I_{af} + \eta_2 T_{df} + \eta_3 T_{af}\right)}{N_m} \text{ and } \lambda_{af} = \frac{\beta_4\gamma_4(I_{dm} + \eta_4 I_{am} + \eta_5 T_{dm} + \eta_6 T_{am})}{N_f}, \tag{4}$$

where the parameters β_3, and β_4 are the probabilities of HIV infection through contacts with individuals in Iij and T_{ij}, respectively, and $\eta_1, \eta_2, \eta_3, \eta_4, \eta_5$, and η_6 are modification factors in transmission probabilities. The infected male and female adults are connected to ART treatment and care at the respective rates given by ϕ_2 and δ_2. The adult classes are reduced by the natural death rate μ_a. The parameters γ_k, for $k = 1, \cdots, 4$, are the rate at which individuals in each age category acquire sexual partners. These compartments have been schematically illustrated in Fig. 1.

Given the above descriptions and assumptions, the dynamics of HIV in the population is given by the following deterministic system of non-linear differential equations.

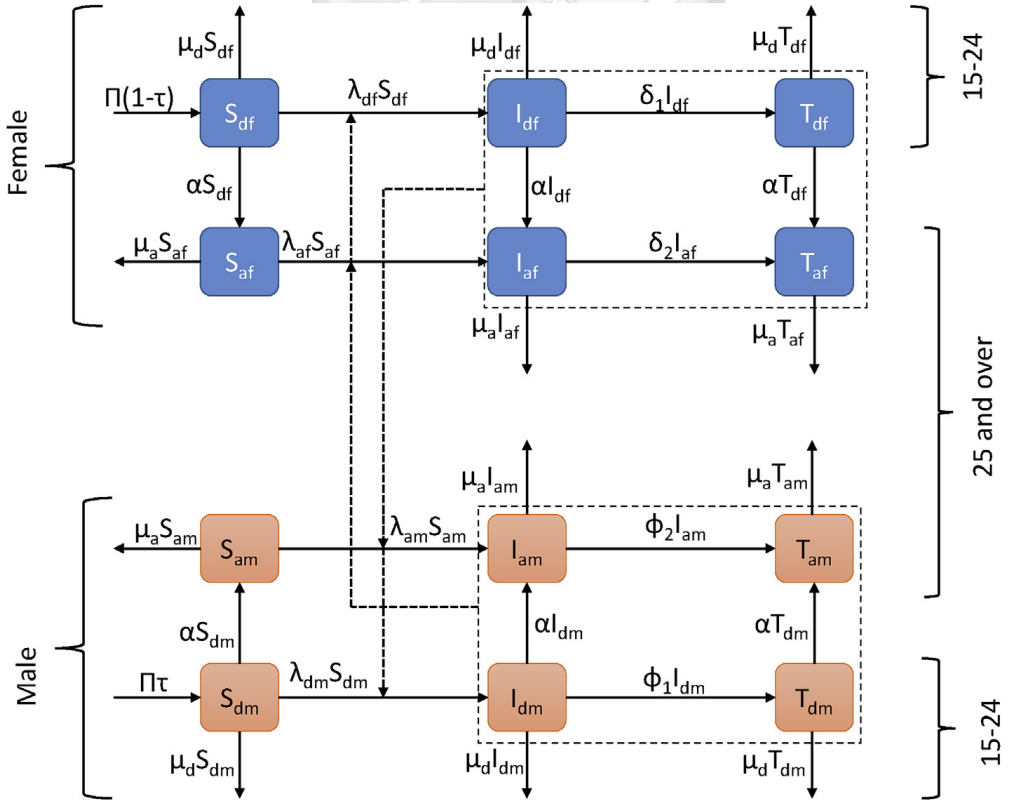

Fig. 1. Schematic diagram of HIV model in the presence of ART.

$$\left.\begin{aligned}
\frac{dS_{dm}}{dt} &= \Pi\tau - \lambda_{dm}S_{dm} - (\mu_d+\alpha)S_{dm}, & \frac{dS_{df}}{dt} &= \Pi(1-\tau) - \lambda_{df}S_{df} - (\mu_d+\alpha)S_{df},\\
\frac{dI_{dm}}{dt} &= \lambda_{dm}S_{dm} - (\phi_1+\alpha+\mu_d)I_{dm}, & \frac{dI_{df}}{dt} &= \lambda_{df}S_{df} - (\alpha+\delta_1+\mu_d)I_{df},\\
\frac{dT_{dm}}{dt} &= \phi_1 I_{dm} - (\alpha+\mu_d)T_{dm}, & \frac{dT_{df}}{dt} &= \delta_1 I_{df} - (\alpha+\mu_d)T_{df},\\
\frac{dS_{am}}{dt} &= \alpha S_{dm} - \lambda_{am}S_{am} - \mu_a S_{am}, & \frac{dS_{af}}{dt} &= \alpha S_{df} - \lambda_{af}S_{af} - \mu_a S_{af},\\
\frac{dI_{am}}{dt} &= \lambda_{am}S_{am} + \alpha I_{dm} - (\phi_2+\mu_a)I_{am}, & \frac{dI_{af}}{dt} &= \lambda_{af}S_{af} + \alpha I_{df} - (\delta_2+\mu_a)I_{af},\\
\frac{dT_{am}}{dt} &= \phi_2 I_{am} + \alpha T_{dm} - \mu_a T_{am}, & \frac{dT_{af}}{dt} &= \delta_2 I_{af} + \alpha T_{df} - \mu_a T_{af},
\end{aligned}\right\} \tag{5}$$

subject to the following initial conditions

$$S_{ijm}(0)\geq 0, I_{ijm}(0)\geq 0, T_{ijm}(0)\geq 0, S_{ijf}(0)\geq 0, I_{ijf}(0)\geq 0, T_{ijf}(0)\geq 0, \text{ for } i,j = d,a. \tag{6}$$

3. Model dynamics

3.1. Well-posedness of the model

In this section, we show that the system (5) is mathematically well defined and biologically feasible. The system (5) can be rewritten in the following form

$$\frac{dX}{dt} = A(X)X + F,$$

where $X = (S_{dm}, I_{dm}, T_{dm}, S_{am}, I_{am}, T_{am}, S_{df}, I_{df}, T_{df}, S_{af}, I_{af}, T_{af})^t$. Let $Q_1 = \mu_d+\alpha$, $Q_2 = \phi_1+\alpha+\mu_d$, $Q_3 = \phi_2+\mu_a$, $Q_4 = \alpha+\delta_1+\mu_d$, $Q_5 = \delta_2+\mu_a$. Thus, the matrix A is given by

$$A(X) = \begin{bmatrix}
-Q_6 & 0 & 0 & 0 & 0 & 0 & 0 & 0 & 0 & 0 & 0 & 0\\
\lambda_{dm} & -Q_2 & 0 & 0 & 0 & 0 & 0 & 0 & 0 & 0 & 0 & 0\\
0 & \phi_1 & -Q_1 & 0 & 0 & 0 & 0 & 0 & 0 & 0 & 0 & 0\\
\alpha & 0 & 0 & -Q_7 & 0 & 0 & 0 & 0 & 0 & 0 & 0 & 0\\
0 & \alpha & 0 & \lambda_{am} & -Q_3 & 0 & 0 & 0 & 0 & 0 & 0 & 0\\
0 & 0 & \alpha & 0 & \phi_2 & -\mu_a & 0 & 0 & 0 & 0 & 0 & 0\\
0 & 0 & 0 & 0 & 0 & 0 & -Q_8 & 0 & 0 & 0 & 0 & 0\\
0 & 0 & 0 & 0 & 0 & 0 & \lambda_{df} & -Q_4 & 0 & 0 & 0 & 0\\
0 & 0 & 0 & 0 & 0 & 0 & 0 & \delta_1 & -Q_1 & 0 & 0 & 0\\
0 & 0 & 0 & 0 & 0 & 0 & 0 & 0 & 0 & -Q_9 & 0 & 0\\
0 & 0 & 0 & 0 & 0 & 0 & 0 & 0 & 0 & \lambda_{af} & -Q_5 & 0\\
0 & 0 & 0 & 0 & 0 & 0 & 0 & 0 & 0 & \alpha & \delta_2 & -\mu_a
\end{bmatrix}$$

and $F = (\Pi\tau, 0, 0, 0, 0, 0, \Pi(1-\tau), 0, 0, 0, 0, 0)^T$. Here, $Q_6 = (\lambda_{dm}+Q_1)$, $Q_7 = (\lambda_{am}+\mu_a)$, $Q_8 = (\lambda_{df}+Q_1)$, $Q_9 = (\lambda_{af}+\mu_a)$. It is important to note that $A(X)$ is a Metzler matrix, that is, a matrix such that off diagonal entries non-negative, for all $Y\in\mathbb{R}^{12}_+$. Thus, using the fact that $F\geq 0$, the system (5) is positively invariant in $\mathbb{R}^{12}_+$ (see, Abate, Tiwari, and Sastry (2009); Berman and Plemmons (1994)). This implies that any trajectory of the system (5) starting from an initial state in $\mathbb{R}^{12}_+$ forever remains in $\mathbb{R}^{12}_+$. The evolution of the system (5) is described by $\frac{dN}{dt} = \Pi - \mu N$. Thus, solving for $N(t)$ we get

$$N(t) \leq \frac{\Pi}{\mu} + e^{-\mu t}\left(N(0) - \frac{\Pi}{\mu}\right). \tag{7}$$

There are two possible cases in studying the behaviour of $N(t)$ in (7). In the first case, we consider $N(0) > \frac{\Pi}{\mu}$ so that, at time t = 0, the right-hand side (RHS) of (7) experiences the largest possible value of $N(0)$. That is, $N(t)\leq N(0)$ for all time $t\geq 0$. In the second case, we consider $N(0) < \frac{\Pi}{\mu}$, so that the largest possible value of the RHS of (7) approaches $\frac{\Pi}{\mu}$ as time t approaches

infinity. Thus, $N(t) \leq \frac{\Pi}{\mu}$ for all time $t \geq 0$. From these two cases, we conclude that $N(t) \leq \max\left\{N(0), \frac{\Pi}{\mu}\right\}$ for all time $t \geq 0$. Therefore, we can study the system (5) in the feasible region given by

$$\Omega = \left\{ \left(S_{ijm}(t), I_{ijm}(t), T_{ijm}(t), S_{ijf}(t), I_{ijf}(t), T_{ijf}(t)\right) \in \mathbb{R}_+^{12} : N(t) \leq \max\left\{N(0), \frac{\Pi}{\mu}\right\}\right\},$$

which is positively invariant with respect to systems (5). This implies that the systems (5) is well posed epidemiologically and all the solutions starting in Ω remain in Ω for all $t \geq 0$.

3.2. Basic reproduction number

According to Diekmann and Heesterbeek (2000); Diekmann, Heesterbeek, and Metz (1990), the basic reproduction number commonly denoted as $\mathscr{R}_0$ is defined as the number of secondary cases of infections arising from the introduction of a single infected individual in a wholly susceptible population. The system (5) has a unique disease-free equilibrium given by

$$\mathscr{E}_0 = \left(\frac{\Pi\tau}{Q_1}, 0, 0, \frac{\alpha\Pi\tau}{Q_1\mu_a}, 0, 0, \frac{\Pi(1-\tau)}{Q_1}, 0, 0, \frac{\alpha\Pi(1-\tau)}{Q_1\mu_a}, 0, 0\right). \tag{8}$$

Since the model system (5) allows for free mixing of the individuals from the two stated age groups, there are two ways of the disease transmission. These are within age group transmission and between age groups transmission. We begin by finding the reproduction numbers within the age groups. For the young adults, the disease-free equilibrium is given by

$$\mathscr{E}_d = \left(\frac{\Pi\tau}{\mu_d}, 0, 0, \frac{\Pi(1-\tau)}{\mu_d}, 0, 0\right). \tag{9}$$

Following the approach given in Van den Driessche and Watmough (2002), we let $F(t)$ and $V(t)$ be the matrices of new infections and transmission, respectively. Thus, at the disease-free equilibrium defined in (9), these matrices are respectively given by

$$F(t) = \begin{bmatrix} 0 & 0 & \beta_1\gamma_1 & \beta_1\gamma_1\theta_2 \\ 0 & 0 & 0 & 0 \\ \beta_2\gamma_2 & \beta_2\gamma_2\theta_5 & 0 & 0 \\ 0 & 0 & 0 & 0 \end{bmatrix}, \quad V(t) = \begin{bmatrix} \mu_d + \phi_1 & 0 & 0 & 0 \\ -\phi_1 & \mu_d & 0 & 0 \\ 0 & 0 & \delta_1 + \mu_d & 0 \\ 0 & 0 & -\delta_1 & \mu_d \end{bmatrix}.$$

The young adults transmission reproduction number which is the spectral radius of the next-generation matrix (NGM) for the epidemic of HIV given by $FV^{-1}(t)$ is obtained as

$$\mathscr{R}_{0d} = \sqrt{\left[\frac{\beta_1\gamma_1(\delta_1\theta_2 + \mu_d)}{\mu_d(\mu_d + \phi_1)}\right]\left[\frac{\beta_2\gamma_2(\mu_d + \theta_5\phi_1)}{\mu_d(\mu_d + \delta_1)}\right]}. \tag{10}$$

Similarly, the disease-free equilibrium within the adult age group is defined as

$$\mathscr{E}_a = \left(\frac{\Pi\tau}{\mu_d}, 0, 0, \frac{\Pi(1-\tau)}{\mu_d}, 0, 0\right). \tag{11}$$

The matrices of new infections and transmission within adult (age group 25+) evaluated at disease-free in (11) are, respectively given as

$$F(t) = \begin{bmatrix} 0 & 0 & \beta_3\gamma_3\eta_1 & \beta_3\gamma_3\eta_3 \\ 0 & 0 & 0 & 0 \\ \beta_4\gamma_4\eta_4 & \beta_4\gamma_4\eta_6 & 0 & 0 \\ 0 & 0 & 0 & 0 \end{bmatrix}, \quad V(t) = \begin{bmatrix} \mu_a + \phi_2 & 0 & 0 & 0 \\ -\phi_2 & \mu_a & 0 & 0 \\ 0 & 0 & \delta_2 + \mu_a & 0 \\ 0 & 0 & -\delta_2 & \mu_a \end{bmatrix}.$$

Therefore, the transmission reproduction number is given by

$$\mathscr{R}_{0a} = \sqrt{\left[\frac{\beta_3\gamma_3(\eta_1\mu_a + \delta_2\eta_3)}{\mu_a(\mu_a + \phi_2)}\right]\left[\frac{\beta_4\gamma_4(\eta_4\mu_a + \eta_6\phi_2)}{\mu_a(\mu_a + \delta_2)}\right]}. \tag{12}$$

If the HIV infection exists in a single age group connected to another age group through maturation, then the movement of the individuals must be reflected in the basic reproduction number. The matrices for new infection terms and the transfer terms at the disease-free equilibrium (8) are given by

$$F(t) = \begin{bmatrix} 0 & 0 & \frac{\beta_1\gamma_1\theta_1\mu_a}{\alpha+\mu_a} & \frac{\beta_1\gamma_1\theta_3\mu_a}{\alpha+\mu_a} \\ 0 & 0 & 0 & 0 \\ \frac{\alpha\beta_4\gamma_4}{\alpha+\mu_a} & \frac{\alpha\beta_4\gamma_4\eta_5}{\alpha+\mu_a} & 0 & 0 \\ 0 & 0 & 0 & 0 \end{bmatrix}, \quad V(t) = \begin{bmatrix} Q_2 & 0 & 0 & 0 \\ -\phi_1 & Q_1 & 0 & 0 \\ 0 & 0 & Q_5 & 0 \\ 0 & 0 & -\delta_2 & \mu_a \end{bmatrix}$$

Thus, the basic reproduction number between the male young adults and the female adults (aged 25 + years) is given by

$$\mathscr{R}_{0mdfa} = \sqrt{\left[\frac{\alpha\beta_4\gamma_4(\eta_5\phi_1 + Q_1)}{Q_1Q_2(\mu_a+\alpha)}\right]\left[\frac{\beta_1\gamma_1(\theta_1\mu_a + \delta_2\theta_3)}{Q_5(\mu_a+\alpha)}\right]}. \tag{13}$$

On the other hand, the matrices for new infection terms and the transfer terms at the disease-free equilibrium in (8) for the female young adults and male adults are given by

$$F = \begin{bmatrix} 0 & 0 & \frac{\alpha\beta_3\gamma_3}{\alpha+\mu_a} & \frac{\alpha\beta_3\gamma_3\eta_2}{\alpha+\mu_a} \\ 0 & 0 & 0 & 0 \\ \frac{\beta_2\gamma_2\theta_4\mu_a}{\alpha+\mu_a} & \frac{\beta_2\gamma_2\theta_6\mu_a}{\alpha+\mu_a} & 0 & 0 \\ 0 & 0 & 0 & 0 \end{bmatrix}, \quad V = \begin{bmatrix} Q_3 & 0 & 0 & 0 \\ -\phi_2 & \mu_a & 0 & 0 \\ 0 & 0 & Q_4 & 0 \\ 0 & 0 & -\delta_1 & Q_1 \end{bmatrix}.$$

Hence, the basic reproduction number between the female young adults and the male adults is given by

$$\mathscr{R}_{0fdma} = \sqrt{\left[\frac{\beta_2\gamma_2(\theta_4\mu_a + \theta_6\phi_2)}{Q_3(\mu_a+\alpha)}\right]\left[\frac{\alpha\beta_3\gamma_3(\delta_1\eta_2 + Q_1)}{Q_1Q_4(\mu_a+\alpha)}\right]}. \tag{14}$$

The basic reproduction number, $\mathscr{R}_0$, of the between the age groups of the system (5) is given as the maximum of the between age groups specific reproduction numbers. Thus, we have

$$\mathscr{R}_0 = \max\left\{\mathscr{R}_{0mdfa}, \mathscr{R}_{0fdma}\right\}.$$

It is important to note that due to mathematical intractability we are unable to explicitly express the basic reproduction number of the whole system without splitting the model into within and between age groups. To understand the trend of HIV infection, we perform data analysis and present results in section 4.

4. Results

4.1. Epidemiological data and ethical considerations

To study the extent and trend of HIV infection, we analyze the confirmed cases of new infections in Kenya from January 2011 to September 2018. The data analyzed was routinely collected on a monthly basis and retrieved from Kenya Health information System available at KHIS. Only variables of interest were pulled out to excel spreadsheet and thereafter analyzed in **R**. The data analyzed is publicly available. Thus, the datasets used in our study were de-identified and fully anonymized in advance, and the analysis of publicly available data without identity information does not require ethical approval.

4.2. Parameter inference and estimation

The natural death rate was estimated to be $\mu_d = 0.0013, \mu_a = 0.00128$ based on the life expectancy in Kenya (WH, 2018). The young adults maturation at the rate $\alpha = 0.0083$. The rate at young adults acquire sexual partners is assumed to be 3, that is, $\gamma_1 = \gamma 2 = 3$, while that of the adults has been assumed to be 2 ($\gamma_3 = \gamma_4 = 2$). Initiating and staying on treatment is particularly problematic for young adults. In 2014, it was estimated that only 34,800 out of 141,000 young adults with known HIV positive status were on ART (AV, 2017). Thus, the rates at which adolescents (males and females) are connected to ART

treatment are assumed to be $\phi_1 = 0.24$ and $\delta_1 = 0.28$, respectively. On the other hand, based on the estimates from AV (2017), the rates at which the male and female adults are connected to ART treatment is assumed to be $\phi_2 = 0.58$ and $\delta_2 = 0.68$, respectively. Table 1 gives the description of the parameters and the initial conditions estimates used in this work. The initial conditions for S_{dm}, S_{df}, S_{am} and S_{af} are estimated from Kenya demographics profile of both 2010 and 2018 (see KD (2018)) while other initial conditions for $I_{dm}, T_{dm}, I_{df}, T_{fm}, I_{am}, T_{am}, I_{af}$ and T_{af} are estimated based on the retrieved data that is used in curve fitting.

The unknown parameters, that is, $\beta_1, \beta_2, \beta_3, \beta_4, \theta_1, \theta_2, \theta_3, \theta_4, \theta_5, \theta_6, \eta_1, \eta_2, \eta_3, \eta_4, \eta_5$ and η_6, were estimated on the basis of the available data as earlier described. Bayesian approach that is implemented to the Markov Chain Monte Carlo (MCMC) technique is used in parameter estimation. We minimize the sum of the squared error between the model and data, which is given by

$$SS\left(\widehat{\vartheta}\right) = \sum_{i=1}^{n} \left(Y_h - P\left(t_h, \widehat{\vartheta}\right)\right)^2, \tag{15}$$

where

$$P\left(t_h, \widehat{\vartheta}\right) = P\left(t, \widehat{\vartheta}\right) = \int_{t-1}^{t} p\left(\lambda_{dm} S_{dm} + \lambda_{df} S_{df} + \lambda_{am} S_{am} + \lambda_{af} S_{af}\right) dt,$$

which is the number of new HIV cases of infection for each age group. Note that, there are D independent observations from the dataset that represent the number of new HIV cases of infection at the hth month, for $h = 1, 2, 3, \cdots, D$. Now considering ε is the error of fit, which follows an independent Gaussian distribution having unknown variance σ^2, then it follows from (15) that

$$Y_h = P\left(t_h, \widehat{\vartheta}\right) + \varepsilon, \quad \varepsilon \sim \mathcal{N}\left(0,\ I_{ij}^{*}\sigma^2\right),$$

with $*$ referring to males and females, i and j remain as earlier defined. We assume an independent Gaussian prior specification for the unknown parameters $\widehat{\vartheta}$, that is, $\vartheta_r \sim \mathcal{N}(\nu_r,\ \psi_r^2)$, where $r = 1, 2, 3, \cdots, D$. Furthermore, it is assumed that the inverse of the error variance follows a Gaussian distribution as prior taking the following form

$$\upsilon\left(\sigma^{-2}\right) \sim \Gamma\left(\frac{x_0}{2}, \frac{x_0 S_0^2}{2}\right).$$

here, x_0 and S_0^2 respectively, give the prior accuracy and prior mean of σ^2. Considering the conditional conjugacy property of Gamma distribution (*see*, Sardar, Sasmal, and Chattopadhyay (2016)), the conditional distribution of $\upsilon(\sigma^{-2}|Y, \widehat{\vartheta})$ is also a Gamma distribution with

Table 1
Description of the parameters and the initial conditions estimates for the system (5). The parameters are given per month.

Par/var	Range	Value	Source	Par	Range	Value	Source
$S_{dm}(0)$	4,148,153–4,552,448	Est.	KD (2018)	β_1	0.0–1.0	Est.	
$I_{dm}(0)$	0–8,000	Est.		β_2	0.0–1.0	Est.	
$T_{dm}(0)$	0–6,000	Est.		β_3	0.0–1.0	Est.	
$S_{df}(0)$	4,147,896–4,567,894	Est.	KD (2018)	β_4	0.0–1.0	Est.	
$I_{df}(0)$	0–11,000	Est.		θ_1	0.0–1.0	Est.	
$T_{fm}(0)$	0–8,000	Est.		θ_2	0.0–1.0	Est.	
$S_{am}(0)$	8,460,138–9,641,107	Est.	KD (2018)	θ_3	0.0–1.0	Est.	
$I_{am}(0)$	0–11,000	Est.		θ_4	0.0–1.0	Est.	
$T_{am}(0)$	0–9,000	Est.		θ_5	0.0–1.0	Est.	
$S_{af}(0)$	8,624,799–9,799,146	Est.	KD (2018)	θ_6	0.0–1.0	Est.	
$I_{af}(0)$	0–17,000	Est.		η_1	0.0–1.0	Est.	
$T_{af}(0)$	0–14,000	Est.		η_2	0.0–1.0	Est.	
Π	40,000–85,000	44,000	KD (2018)	η_3	0.0–1.0	Est.	
τ	0.0–1.0	0.48	WH (2018)	η_4	0.0–1.0	Est.	
μ_d	0.0011–0.0017	0.0013	WH (2018)	η_5	0.0–1.0	Est.	
μ_a	0.0011–0.0017	0.00128	WH (2018)	η_6	0.0–1.0	Est.	
γ_1	1–4	3	Assumed	γ_2	1–4	3	Assumed
γ_3	1–4	2	Assumed	γ_4	1–4	2	Assumed
ϕ_1	0.0–1.0	0.24	AV (2017)	ϕ_2	0.0–1.0	0.58	AV (2017)
δ_1	0.0–1.0	0.28	AV (2017)	δ_2	0.0–1.0	0.68	AV (2017)
α		0.0083					

$$\upsilon\left(\sigma^{-2}\middle|Y,\widehat{\vartheta}\right)=\Gamma\left(\frac{x_0+R}{2},\frac{x_0S_0^2+SS\left(\widehat{\vartheta}\right)}{2}\right).$$

The above property makes it possible to sample and update σ^{-2} within each Metropolis Hastings simulation step for the other parameters. Since an independent Gaussian prior specification for $\widehat{\vartheta}$ is assumed, the prior sum of squares for $\widehat{\vartheta}$ is given by

$$SS_{\text{pri}}\left(\widehat{\vartheta}\right)=\sum_{h=1}^{D}\left(\frac{\vartheta_h-\nu_h}{\psi_h}\right)^2.$$

For a fixed value of σ^2, the posterior distribution of $\widehat{\vartheta}$ is given by

$$\upsilon\left(\widehat{\vartheta}\middle|Y,\sigma^2\right)\propto\exp\left[-\frac{1}{2}\left(\frac{SS\left(\widehat{\vartheta}\right)}{\sigma^2}+SS_{\text{pri}}\left(\widehat{\vartheta}\right)\right)\right],$$

with the posterior ratio needed in the Metropolis-Hastings acceptable probability given as

$$\frac{\upsilon\left(\widehat{\vartheta^1}\middle|Y,\sigma^2\right)}{\upsilon\left(\widehat{\vartheta^2}\middle|Y,\sigma^2\right)}=\exp\left[-\frac{1}{2}\left(\left(\frac{SS\left(\widehat{\vartheta^1}\right)}{\sigma^2}-\frac{SS\left(\widehat{\vartheta^2}\right)}{\sigma^2}\right)+\frac{1}{2}\left(SS_{\text{pri}}\left(\widehat{\vartheta^2}\right)+SS_{\text{pri}}\left(\widehat{\vartheta^1}\right)\right)\right)\right].$$

The modCost, modFit and modMCMC routine in package FME package (A flexible modelling environment for inverse modelling, sensitivity, identifiability and Monte Carlo Analysis) in **R** is used to estimate the unknown ϑ for the model. A **R** code is used in which, the unknown parameter values are given a lower bound and an upper bound from which the set of parameter values that produce the best fit are obtained. The parameter estimates and other results arising from the model fitting to data are given in Section 4.4.

4.3. Statistical analysis

4.3.1. The basic description of data

In this section, we carry out simple descriptive statistical analysis of the dataset and results presented in Table 2.

The mean number of new HIV infections in the male young adults age group is 1336.9 (95% Confidence Intervals (CI), 1114.0,1559.8) while the average number of new infections in the females of the same age group is 3164.7 (95% Confidence Intervals (CI), 2775.3,3554.1), for the period from January 2011 to September 2018. The average number of new infections in male and female adults are given by 5319.2 (95% Confidence Intervals (CI), 4817.9,5820.5) and 7692.5 (95% Confidence Intervals (CI), 6951.9,8433.4), respectively. Overally, the mean number of HIV infections in males is 3328.1 while that in females is 5428.6. It can be seen that females in both age categories are disproportionately affected with HIV more than the males. In order to establish the extent of variation in the mean number of cases of infections in the two age categories along the gender line, an error bar is plotted and presented in Fig. 2. It can be seen that the non-overlapping error bars may be significantly different. This implies that further test is required to indicate the nature of differences means. Thus, in section 4.3.2, we carry out probability distribution test in order to choose an appropriate test to establish the mean differences.

Table 2
Descriptive characteristics of the dataset retrieved for the duration spanning from January 2011 to September 2018.

Age group	Male				Female			
	Mean	SD	SE	95% CI[a]	Mean	SD	SE	95% CI[a]
15–24 years	1336.9	1082.4	112.2	[1114.0,1559.8]	3164.7	1891.0	196.1	[2775.3,3554.1]
25 + years	5319.2	2434.3	252.4	[4817.9,5820.5]	7692.5	3597.4	373.0	[6951.9,8433.4]
d[b] and a[c]	3328.1	2741.5	201.0	[2931.5,3724.7]	5428.6	3656.1	268.1	[4899.7,5957.5]

[a] 95% Confidence Interval.
[b] The young adults aged 15–24 years.
[c] The adults aged 25 and over years.

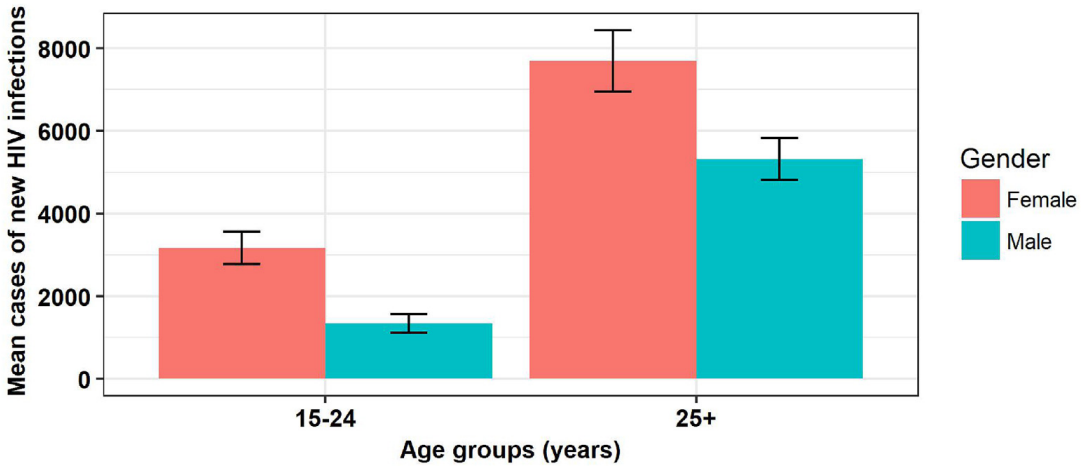

Fig. 2. A graph showing the distribution of the average number of new HIV infections in two age groups for males and females. Error bars are 95% confidence intervals.

4.3.2. The probability distribution of the data

The probability distribution of the given dataset plays an important role in determining which tests between parametric and non-parametric to conduct. There are various methods used to test for the probability distribution of a given dataset. The methods can be to test for normality or any other distribution. For normality tests, methods used include kolmogorov-smirnov, Anderson Darling, Shapiro Wilk and Lilliefors test (Shapiro & Wilk, 1965). In this study, we use the Shapiro Wilk test. This is the most powerful test when compared to the Anderson Darling, Kolmogorov-Smirnov and Lilliefors tests (Razali et al., 2011). The test statistics proposed in Shapiro and Wilk (1965) is given by

$$W = \frac{(a'y)^2}{S^2} = \frac{\left(\sum_{q=1}^{n} a_q y_q\right)^2}{\sum_{q=1}^{n} \left(y_q - \bar{y}\right)^2},$$

where a' are set of weights given by

$$a' = (a_1, \cdots, a_n) = \frac{m'V^{-1}}{\sqrt{(m'V^{-1}V^{-1}m)}}.$$

here, y_q, for $q = 1, 2, \cdots, n$, is the ith order statistics whose similarity scores are sorted in either descending or ascending order, $\bar{y}$ is the sample mean similarity score, $m = (m_1, \cdots, m_n)'$ are the first moments of the order statistics which are independent and identically normally distributed random variables, S^2 is the estimator for the population variance σ^2 and V is the covariance matrix of the order statistics. The dataset is assumed not to follow a normal distribution when the test statistics W is small, that is, $0 < \frac{na_1^2}{n-1} \leq W \leq 1$ or when p-value $< \alpha$, the significance level. Otherwise the dataset follows a normal distribution.

Table 3 shows results from Shapiro Wilk test for normality of the dataset. The test was carried out at alpha level equal to 0.05, that is, at 95% Confidence Interval. Given that the p-value for each age category for males and females is less than 0.05, then the null hypothesis that the data are normally distributed is rejected. Thus, there is no enough evidence to assume that the data follows a normal distribution. Fig. 3 shows density plot to visualise the distribution of data. This chart uses kernel smoothing to plot values, allowing for smoother distributions by smoothing out the noise. The peaks of a density plot help

Table 3
Shapiro Wilk test for normality of the dataset.

Age group	Male		Female	
	W	P-value	W	P-value
15–24 years	0.8585	0.0000	0.9549	0.0028
25 + years	0.9692	0.0268	0.9600	0.0061

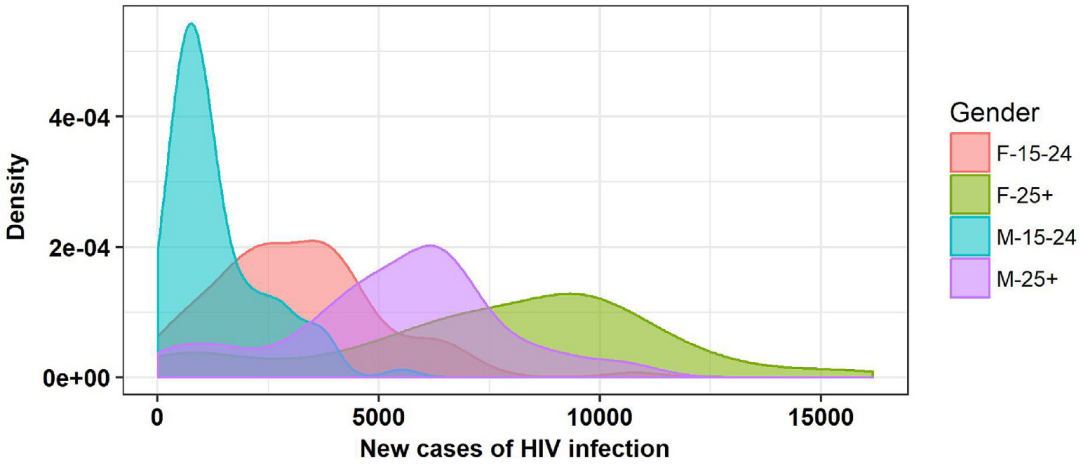

Fig. 3. Density distribution of the dataset.

display where values are concentrated over the interval. It can be easily seen that the data are positively skewed. Since the results show that the data does not follow a normal distribution, we conduct Friedman test, a non-parametric test, to establish if there exists any significant differences in mean number of HIV infections between the two age groups for the males and females.

4.3.3. Kruskal–Wallis test

Kruskal–Wallis's test is a non-parametric method for testing the equality of several independent samples. It is useful in analyzing experimental data from completely randomized designs (Kruskal & Wallis, 1952). To compute the Kruskal–Wallis test statistic, all the observations are first ranked in ascending order where the smallest observation takes rank 1 and the largest observation takes rank N. The sum and average of the ranks of the observations pertaining to each sample are obtained next. If the sample effects are equal, then the average ranks are expected to be the same and if there is any difference then that is due to sampling fluctuations. The Kruskal–Wallis test statistic is based on the assessment of the differences among the average ranks. That is, let R_{ij} be the rank of $y_{ij}, i = 1, 2, 3, \cdots, b;\ j = 1, 2, \cdots, t$ where b refers to the samples (treatments) and the ith treatment is replicated t_1 times, $i = 1, 2, \cdots, b, R_i = \sum_{j=1}^{t} R_{ij}$ be the sum of the ranks of the observations pertaining to the ith treatment, $\overline{R}_i = \frac{R_i}{t_i}$ be the average of the ranks of the observations pertaining to the ith treatment, and $\overline{R}$ be the mean of all the $\overline{R}_i$. The Kruskal–Wallis test statistic is then given by

$$H = \frac{12}{N(N+1)} \sum_{i=1}^{b} t_i (\overline{R}_i - \overline{R})^2 \sim \chi^2_{b-1}. \tag{16}$$

Since $\sum_{i=1}^{b} R_i = \frac{N(N+1)}{2}$, it follows that $\overline{R} = \frac{N+1}{2}$. Thus, expression (16) reduces to

$$H = \frac{12}{N(N+1)} \sum_{i=1}^{b} \frac{R_i^2}{t_i} - 3(N+1) \sim \chi^2_{b-1}. \tag{17}$$

Note that the coefficient $\frac{12}{N(N+1)}$ is known as a suitable normalization factor (see, Manoukian (1986)). The expressions in (16) and (17) are computed if there are no ties in the observations. In the event there are ties, each observation is given the mean of the ranks for which it is tied. The Kruskal–Wallis statistics in (17) is then divided by the correction factor given by

$$cf = 1 - \frac{\sum_{i=1}^{k} (m_i^3 - m_i)}{N^3 - N},$$

where m_i refers to the number of ties in ith group of k tied groups. Hence, the corrected Kruskal–Wallis test statistic for ties is expressed as

$$H^m = \frac{12}{N(N+1)}\sum_{i=1}^{b}\frac{R_i^2}{t_i} - \frac{3N(N+1)^2(N-1)}{N(N^2-1)-\sum_{i=1}^{k}\left(m_i^3-m_i\right)} \sim \chi^2_{b-1}.$$

It is important to note that the correction factor is included when there are ties to increase the value of the test statistics so as to make the results more significant. Furthermore, the Kruskal–Wallis test statistic has a chi-square distribution with $(b-1)$ degrees of freedom under the null hypothesis. The test results obtained in **R** are given as:

$$\text{Kruskal} - \text{Wallis chi} - \text{squared} \;=\; 180.11,\ \text{df} \;=\; 3,\ \text{p} - \text{value} < 2.2e-16.$$

The results give $\chi^2_{3,\alpha=0.05} = 180.11$ and p-value< 0.05, the level of significance. There is very strong evidence to suggest a significant difference in HIV infection between at least one pair of the groups. Since there is a significant difference in HIV infections as the results suggest, a post-hoc analysis is performed to determine which group of the individuals differ from each other in HIV infections. We use Nemenyi test which is appropriate for groups with equal number of observations as in our case (Zar, 2010). The results are presented in Table 4. Since all the p-values are less that 0.05, the level of significance, there are significant differences in HIV infections between the groups.

4.4. Model fitting

The results in Fig. 4 clearly show that the model fits well with the available data points. It is important to observe that the cases of infection peaked in the year 2013. The results show that there was a rise in HIV infection between 2011 and 2013, followed by a significant slow down in the occurrences of new cases of HIV infection. In Fig. 5, we make a comparison of new cases of HIV infection for the two groups. Our results are indicative of a long-term fall in cases of HIV infection in which there is a significant decline in the cases of infection by 2030. However, it can be clearly seen that the occurrence of new cases of HIV infection is more prominent in the adult population as compared to the young adults' population. The most important observation is there is high number of cases of HIV infection amongst the female adults (aged 25 and over) in comparison to the remaining groups. It is known that women in this group are disproportionately affected by the HIV infections since it is men often dominate sexual relationships leaving women with no ability to always practice safer sex despite the known risks involved (AV, 2017). The results show that new cases of HIV infection amongst the young male adults would be contained by 2025 while that of their female counterparts is likely to be contained after 2030 should the current interventions against HIV in Kenya be maintained. Tables 5–7 give the estimated variable values, estimated parameter values and the transmission reproduction numbers, respectively. The computation of the reproduction numbers within and between age groups in Table 7 provides insights into control that cannot be deduced simply from observations on the prevalence of infection. More specifically, the analysis showed that the per capita rate of HIV transmission was highest when there is interaction between young adults to adults and most HIV infections occurred in adult population.

4.4.1. Sensitivity analysis

Sensitivity analysis is introduced to study the strength of the basic reproduction numbers as listed in Table 7 for the model parameters. Here, we perform sensitivity analysis to examine the model's response to parameter variation within a wider range in the parameter space. Following the work by Marino, Hogue, Ray, and Kirschner (2008), partial rank correlation coefficients (PRCC) between the basic reproduction number R_0 and each parameter are derived from 1,000 runs of the Latin hypercube sampling (LHS) method (Stein, 1987). The parameters are assumed to be random variables with uniform distributions with their mean value listed in Tables 1 and 6. Tornado plots for the normalised sensitivity index for different parameters are given in Fig. 6.

If the sensitivity index is positive, then the reproduction number increases along with increasing value of the parameter. On the other hand, if the sensitivity index is negative, then reproduction decreasing with the increasing value of the parameter. Fig. 6a and b are produced assuming that the HIV infection is localised only the young adults (15–24 years) and adults (15 + years) age groups respectively. From the figures, the parameters related to the probabilities of HIV transmission

Table 4
Pairwise comparisons using Tukey and Kramer (Nemenyi) test. F-15-24 and M-15-24 means the female and male young adults while F-25 + and M-25 + means the female and male adults, respectively. The lower triangles of the matrices respectively contain the χ^2 and p-values of the pairwise comparisons.

	χ^2 output				P-value		
	F-15-24	F-25+	M-15-24		F-15-24	F-25+	M-15-24
F-25+	10.978			F-25+	0.0000		
M-15-24	6.828	17.806		M-15-24	0.00001	0.0000	
M-25+	6.377	4.601	13.205	M-25+	0.00004	0.006	0.0000

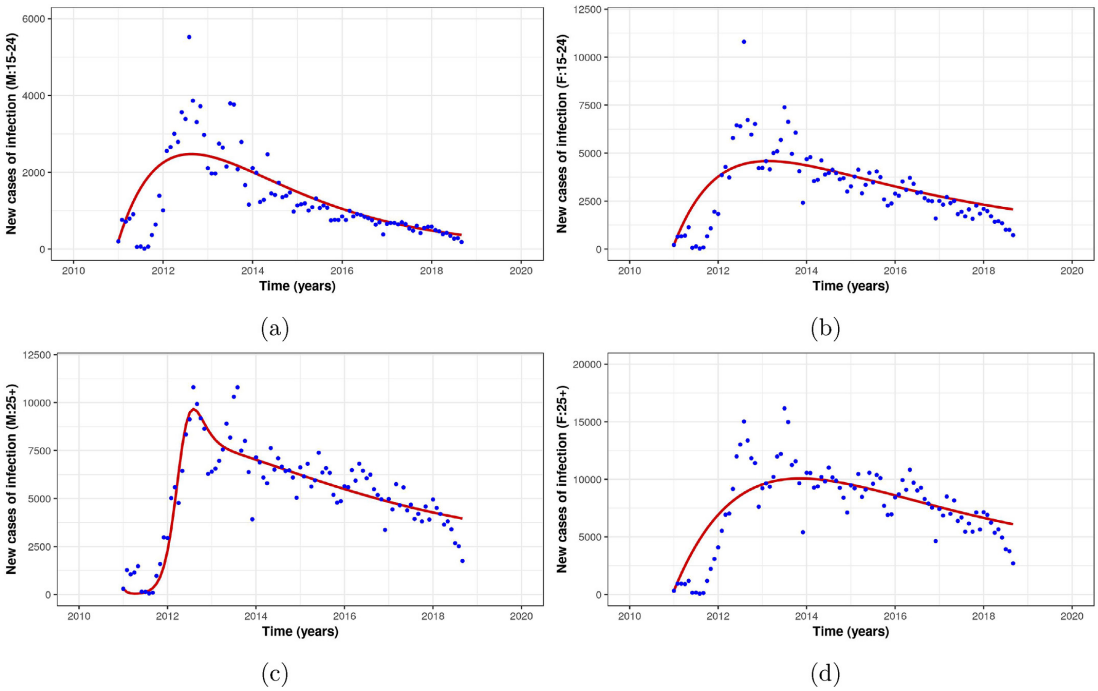

Fig. 4. Model system (5) fitted to data for the reported new cases of HIV infection. 4a shows the model fitted to the data for the young male adults (aged 15−24 years) while 4b shows the model fitted to data for the young female adults (aged 15−24 years). On the other hand 4c shows the model fitted to the data for the male adults (aged 25 + years) while 4d shows the model fitted to data for the female adults (aged 25 + years). The blue dots indicate the actual data and the red line indicates the model fit to the data. All the fitted curves are done with 95% confidence limits.

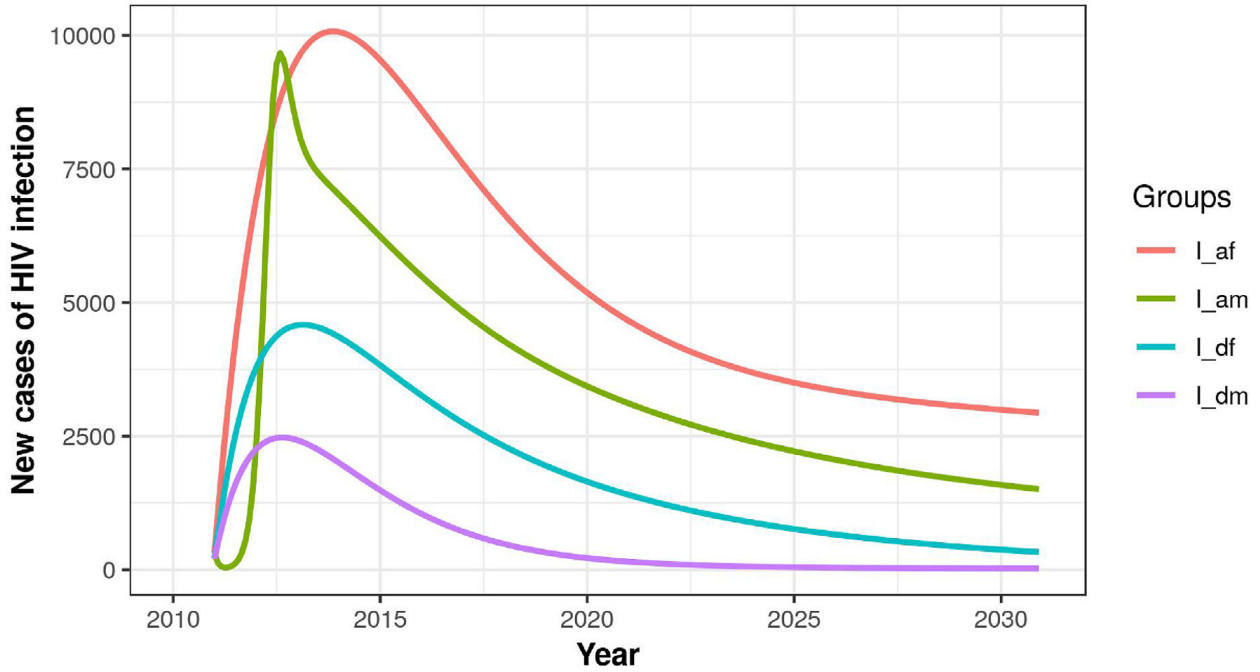

Fig. 5. The projected cases of new HIV infection within the age groups as fitted in Fig. 4.

Table 5
Estimated variable values from the model fitting to data for the period January 2011 to September 2018.

	Male			Female		
	Mean	SE	95% CI[a]	Mean	SE	95% CI[a]
S_d	4326140	1665	[4325114, 4327166]	4333384	548.6	[4332309, 4334459]
I_d	180	0.4845	[179.05, 180.95]	191	1.766	[187.54, 194.46]
T_d	105	0.4625	[104.09, 105.91]	126	0.2417	[125.53, 126.47]
S_a	9011930	1418	[9009150, 9014710]	9312839	1417	[9310062, 9315616]
I_a	665	1.671	[661.73, 668.28]	370	0.9102	[368.22, 371.78]
T_a	144	0.4261	[143.16, 144.84]	333	0.6121	[331.8, 334.2]

[a] 95% Confidence Interval.

Table 6
Estimated parameter values of the system (5) obtained from model fitting for the period January 2011 to September 2018.

Par	Mean	SE	95% CI	Par	Mean	SE	95% CI
β_1	0.3743	7.8e-4	[0.3728, 0.3758]	β_2	0.4.01e-3	5.0e-6	[4.0e-3, 4.02e-3]
β_3	4.2e-5	5.33e-8	[4.23e-5, 4.25e-5]	β_4	0.7451	0.0015	[0.7421, 0.7481]
θ_1	0.1698	2.86e-4	[0.1693, 0.1704]	θ_2	2.76e-4	4.57e-7	[2.7e-4, 2.8e-4]
θ_3	1.282e-5	8.2e-9	[1.28e-5, 1.29e-5]	θ_4	0.0422	1.301e-4	[0.0419, 0.0425]
θ_5	0.0248	7.531e-5	[0.0246, 0.0250]	θ_6	0.2195	2.712e-4	[0.2189, 0.2202]
η_1	0.0432	1.167e-4	[0.0429, 0.0434]	η_2	0.6256	1.0704e-3	[0.6235, 0.6277]
η_3	0.0680	1.078e-4	[0.0678, 0.0683]	η_4	5.181e-4	1.181e-6	[5.15e-4, 5.2e-4]
η_5	5.494e-3	1.735e-5	[5.46e-3, 5.53e-3]	η_6	0.2169	2.392e-4	[0.2165, 0.2174]

Table 7
Estimation of young adults transmission reproduction number $\mathscr{R}_{0d}$, adults transmission reproduction number $\mathscr{R}_{0a}$, basic reproduction number between the male young adults and the female adults $\mathscr{R}_{0mdfa}$, basic reproduction number between the female young adults and the male adults $\mathscr{R}_{0fdma}$ and the system (5) basic reproduction number $\mathscr{R}_0$.

Statistics	$\mathscr{R}_{0d}$	$\mathscr{R}_{0a}$	$\mathscr{R}_{0mdfa}$	$\mathscr{R}_{0fdma}$
Mean	1.135	1.921	2.432	2.432
Std. error	0.000035	0.00014	0.00089	0.00089
95% Confidence Interval	1.131–1.139	1.901–1.941	2.397–2.467	2.397–2.467

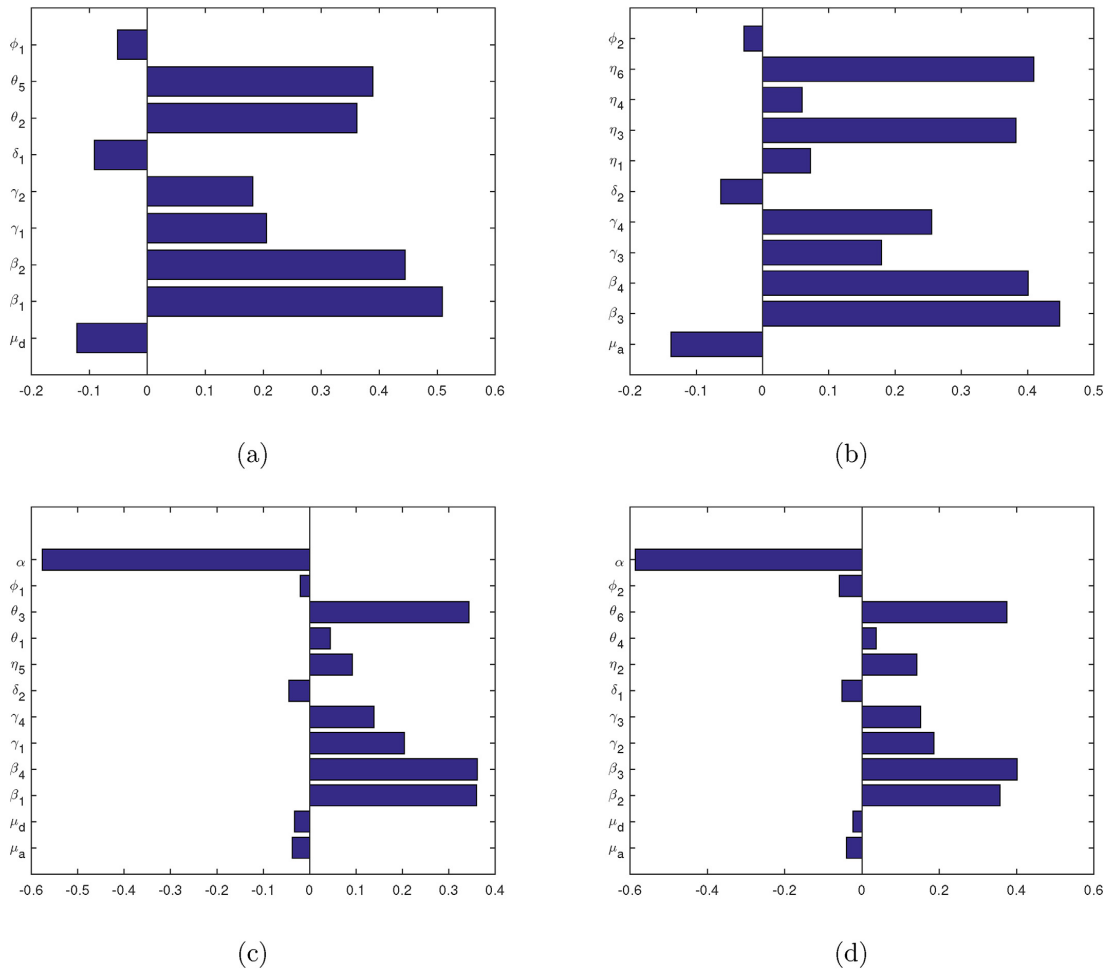

Fig. 6. Tornado plots showing PRCCs for the different parameter values. 6a and 6b are produced assuming that the HIV infection is localised only the young adults (15−24 years) and adults (15 + years) age groups respectively. On the other hand 6c and 6d are produced assuming that there is interaction between young male adults (15−24 years) and adult females (15 + years) and young female adults (15−24 years) and male adults (15 + years), respectively.

have reasonably significant PRCCs and cannot be ignored. The parameters ϕ_1, δ_1, ϕ_2 and δ_2 have the lowest PRCCs with respect to the corresponding disease thresholds. However, their direction of influence is clearly visible. In this regard, since no effort toward reducing disease spread is rendered insignificant, any action that increases the number of individuals under ART treatment reduces the infection. Fig. 6c and d are produced assuming that there is interaction between young male adults (15–24 years) and adult females (15 + years) and young female adults (15–24 years) and male adults (15 + years), respectively. It is also seen that probabilities of HIV transmission have the potential of making the epidemic worse if increased while parameters related to treatment of infected individuals into ART have the potential of reducing infections.

5. Conclusion

The HIV epidemic has been evolving in Kenya since the detection of the first case in 1984. Kenya has the fourth highest number of HIV infection globally alongside South Africa and Nigeria (UNAIDS, 2015). The number of people living with HIV was estimated to be 1.6 million in the year 2015 with 36,000 deaths resulting from AIDS-related illness (OPTIONS, 2016; UNAIDS, 2015). In its efforts to reduce HIV spread, HIV testing and counselling has been adopted through targeted community-based testing and door-to-door testing initiatives and use of preventive measures such as condoms encouraged. In 2016, an estimated 64% of the people living with HIV were receiving antiretroviral treatment (ART) of whom 51% were virally supressed (UNAIDS, 2017b). Furthermore, according to UNAIDS (2017b), 73% of men and 55% of women used a condom the last time they engaged in sex with a non-marital as well as non-cohabiting partner. Despite the intense and aggressive interventions against HIV, there is still growing number of new infections in Kenya especially amongst the young adults. Thus, in this work, we attempt to model the trend of new HIV infections in Kenya, for which a considerable amount of data is available. A deterministic model for HIV dynamics within and between age groups that takes into consideration the sexual orientation of individuals is presented. Vital mathematical characteristics of the model have been presented. These include the invariant region of biological significance, the age group specific basic transmission numbers and inter age group specific basic transmission numbers. MCMC method has been used to estimate the parameter values based on the available data. The basic descriptive and inferential statistics of the data have been computed and presented. Our analysis of the data shows that females in both age categories are disproportionately affected with HIV more than the males. This is supported by the Kruskal-Wallis results which are indicative of very strong evidence that there exist significant differences in HIV infections between the groups.

The model was then fitted to on the new cases of HIV infections with the objective of using the model parameters that give the best fit to examine the trend of HIV infection. It has been established that the occurrence of new cases of HIV infection is more prominent in the adult population as compared to the young adults' population. It is important to note that there is high number of cases of HIV infection amongst the female adults (aged 25 and over). This can be attributed to the fact that men often dominate sexual relationships leaving women with no ability to always practice safer sex despite the known risks involved. The results show that new cases of HIV infection amongst the young male adults would be contained by 2025 while that of their female counterparts is likely to be contained after 2030 should the current interventions against HIV in Kenya be maintained. Furthermore, computation of the reproduction numbers within and between age groups provides insights into control that cannot be deduced simply from observations on the prevalence of infection. More specifically, the analysis showed that the per capita rate of HIV transmission was highest when there is interaction between young adults to adults and most HIV infections occurred in adult population.

Sensitivity of parameters was also considered. The results demonstrate that the transmission probabilities and treatment rates have the greatest impacts on the reproduction numbers. This suggests that control of HIV pivots around transmission prevention programs. Programs aimed at individuals at high risks of HIV infection that encourage them to use preventive measures such as condoms and PrEP will be particularly effective. Furthermore, enrolling more infected individuals on ART treatment would be ideal in reducing the cases of new infections for it is known that it helps in suppressing the viral load in the body thus limiting further HIV infections. It is thus critical to devote more resources to education on HIV preventive measures and treatment programs that are especially targeted to both the susceptible and infected individuals.

The model considered in this paper is consistent with the dynamics of HIV infection in Kenya and it has some lucid limitations. In fact, lack of sufficient data on the number of HIV patients enrolled in ART treatment and care limited the numerical analysis and interpretation. This work has only considered the new cases of HIV infections. It is well known that the goodness of fit measures the discrepancy between observed data and values expected from the model. In this work, no goodness of fit tests were performed. However, we relied on the MCMC method for the model fitting. We argue that MCMC method of fitting models to data provides useful insights into how the model can be linked to data despite the challenge of using statistical tools to test the goodness of fit of the model.

Author contributions

All authors conceived and developed the study. All authors read and approved the final version of the manuscript.

Disclosure statement

The authors declare that there are no competing interests regarding the publication of this paper.

Funding

The authors received no direct funding for this research.

Acknowledgment

The authors acknowledge, with thanks, the support of Strathmore University, Institute of Mathematical Sciences for the production of this manuscript.

References

Abate, A., Tiwari, A., & Sastry, S. (2009). Box invariance in biologically-inspired dynamical systems. *Automatica, 45*(7), 1601–1610.
Aldila, D. (2018). Mathematical model for HIV spreads control program with ART treatment. In *Journal of physics: Conference series* (vol. 974, p. 012035). IOP Publishing.
AV. (2017). *Avert. Global information and education on HIV and AIDS: HIV and AIDS in Kenya*. Retrieved June, 2018 from https://www.avert.org/professionals/hiv-around-world/sub-saharan-africa/kenya.
Berman, A., & Plemmons, R. J. (1994). *Nonnegative matrices in the mathematical sciences* (vol. 9). Philadelphia: SIAM.
Chow, Y., Leong, C., Chow, H., & Hooi, L. (2007). Lactic acidosis in hiv patients receiving highly active antiretroviral therapy. *Medical Journal of Malaysia, 62*(1), 78.
Diekmann, O., & Heesterbeek, J. A. P. (2000). *Mathematical epidemiology of infectious diseases: Model building, analysis and interpretation* (vol. 5). John Wiley & Sons.
Diekmann, O., Heesterbeek, J. A. P., & Metz, J. A. (1990). On the definition and the computation of the basic reproduction ratio r_0 in models for infectious diseases in heterogeneous populations. *Journal of Mathematical Biology, 28*(4), 365–382.
KD. (2018). *Kenya demographics profile 2018*. Retrieved May, 2018 from https://www.indexmundi.com/kenya/demographics_profile.html.
Keeling, M. J., & Rohani, P. (2011). *Modeling infectious diseases in humans and animals*. Princeton University Press.
Kim, S. B., Yoon, M., Ku, N. S., Kim, M. H., Song, J. E., Ahn, J. Y., et al. (2014). Mathematical modeling of HIV prevention measures including pre-exposure prophylaxis on HIV incidence in South Korea. *PLoS One, 9*(3), e90080.
KNBS. (2014). *Kenya demographic and health survey 2014*. Retrieved May, 2018 from https://dhsprogram.com/pubs/pdf/FR308/FR308.pdf.
Kruskal, W. H., & Wallis, W. A. (1952). Use of ranks in one-criterion variance analysis. *Journal of the American Statistical Association, 47*(260), 583–621.
Manoukian, E. B. (1986). *Mathematical nonparametric statistics*.
Marino, S., Hogue, I. B., Ray, C. J., & Kirschner, D. E. (2008). A methodology for performing global uncertainty and sensitivity analysis in systems biology. *Journal of Ttheoretical Biology, 254*(1), 178–196.
MOH. (2016). *Kenyan ministry of health/national AIDS control council. Kenya AIDS response progress report 2016*. Retrieved May, 2018 from https://nacc.or.ke/wp-content/uploads/2016/11/Kenya-AIDS-Progress-Report_web.pdf.
Mukandavire, Z., Chiyaka, C., Garira, W., & Musuka, G. (2009). Mathematical analysis of a sex-structured HIV/AIDS model with a discrete time delay. *Nonlinear Analysis: Theory, Methods & Applications, 71*(3–4), 1082–1093.
Mukandavire, Z., & Garira, W. (2007). Age and sex structured model for assessing the demographic impact of mother-to-child transmission of HIV/AIDS. *Bulletin of Mathematical Biology, 69*(6), 2061–2092.
Omondi, E., Mbogo, R., & Luboobi, L. (2018a). Mathematical analysis of sex-structured population model of hiv infection in Kenya. *Letters in Biomathematics, 5*(1), 174–194.
Omondi, E., Mbogo, R., & Luboobi, L. (2018b). Mathematical modelling of the impact of testing, treatment and control of HIV transmission in Kenya. *Cogent Mathematics & Statistics*, 1475590.
Omondi, E., Mbogo, R., & Luboobi, L. (2018c). Modelling the trend of HIV transmission and treatment in Kenya. *International Journal of Applied and Computational Mathematics, 4*(5), 123.
OPTIONS. (2016). *OPTIONS country situation analysis interim findings: Kenya*. FSG in partnership with LVCT Health. http://www.prepwatch.org/wp-content/uploads/2016/05/Situation_Analysis_Kenya.pdf Accessed August 2016.
Razali, N. M., & Wah, Y. B. (2011). Power comparisons of shapiro-wilk, Kolmogorov-smirnov, lilliefors and anderson-darling tests. *Journal of Statistical Modeling and Analytics, 2*(1), 21–33.
Sardar, T., Sasmal, S. K., & Chattopadhyay, J. (2016). Estimating dengue type reproduction numbers for two provinces of Sri Lanka during the period 2013–14. *Virulence, 7*(2), 187–200.
Shapiro, S. S., & Wilk, M. B. (1965). An analysis of variance test for normality (complete samples). *Biometrika, 52*(3/4), 591–611.
Stein, M. (1987). Large sample properties of simulations using Latin hypercube sampling. *Technometrics, 29*(2), 143–151.
UNAIDS. (2015). *UNAIDS. HIV and AIDS estimates*. http://www.unaids.org/en/regionscountries/countries/kenya Accessed April 2017.
UNAIDS. (2016). *Prevention gap report*. Retrieved May, 2018 from http://www.unaids.org/sites/default/files/media_asset/2016-prevention-gap-report_en.pdf.
UNAIDS. (2017a). *Global information and education on HIV and AIDS*. Retrieved June, 2018 from https://www.avert.org/professionals/hiv-around-world/sub-saharan-africa/kenya#footnote41_8o0cqle.
UNAIDS. (2017b). *UNAIDS Fact sheet. Fact sheet – latest statistics on the status of the AIDS epidemic*. http://www.unaids.org/en/resources/fact-sheet Accessed April 2017.
Van den Driessche, P., & Watmough, J. (2002). Reproduction numbers and sub-threshold endemic equilibria for compartmental models of disease transmission. *Mathematical Biosciences, 180*(1), 29–48.
WH. (2018). *World health rankings. Live longer live better*. Retrieved May, 2018 from http://www.worldlifeexpectancy.com/kenya-life-expectancy.
WHO. (2014). *March 2014 supplement to the 2013 consolidated guidelines on the use of antiretroviral drugs for treating and preventing HIV infection: Recommendations for a public health approach*. Geneva: World Health Organization.
WHO. (2018). *WHO. HIV/AIDS-Global health observatory (GHO) data*. Retrieved October, 2018 from http://www.who.int/gho/hiv/en/.
Williams, B. G. (2014). *Optimizing control of HIV in Kenya*. arXiv:1407.7801.
Zar, J. H. (2010). *Biostatistical analysis* (5th ed.). Upper Saddle River, NJ: Pearson Prentice Hall.

Appendix D

Originality report

D.1 Similarity index

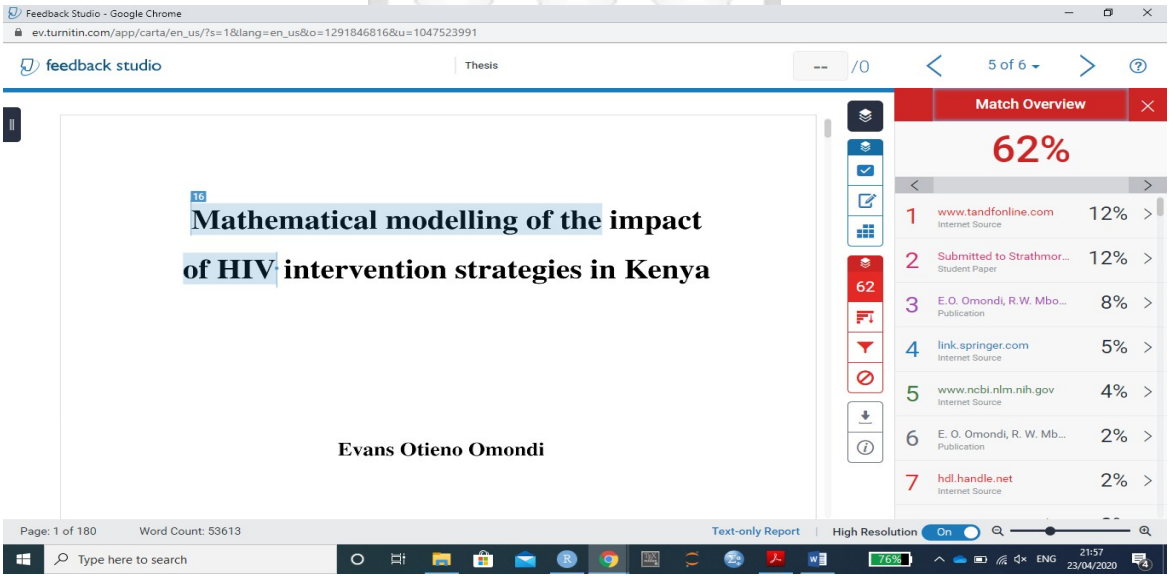

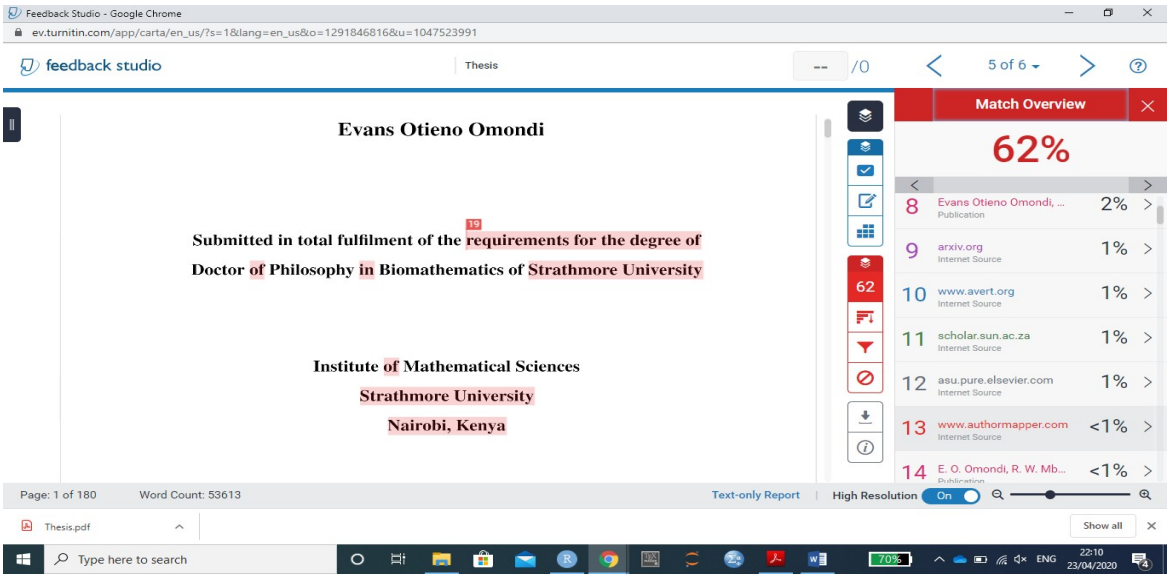

D.2 Similarity index contribution

The 62% similarity index is largely as a result of the publications from this thesis as follows:

- 12% from www.tandfone.com comes from the publication “Mathematical analysis of sex-structured population model of HIV infection in Kenya”. This is entirely my chapter four in the thesis.
- 12% from “submitted to Strathmore University” are names and guidelines of the thesis that I can’t change. For example, I can’t change the way the title page appears, declaration page and individual names and some of the work that originated from this thesis that were presented at Strathmore University.
- 9% and 4% (www.ncbi.nlm.nih.gov) come from “E.O. Omondi, R.W. Mbogo, L.S. Luboobi. A mathematical modelling study of HIV infection in two heterosexual age groups in Kenya, Infectious Disease Modelling, 2019" is another publication from this thesis which is entirely from the chapter 5 of this thesis.
- 5% and 2% that come from “link.springer.com" and E. O. Omondi, R. W. Mbogo, L. S. Luboobi. “Modelling the Trend of HIV Transmission and Treatment in Kenya", International Journal of Applied and Computational Mathematics, 2018. This is another publication which is entirely chapter three of this thesis.
- 2% from Evans Otieno Omondi, Rachel Mbogo, Livingstone Luboobi. “Mathematical modelling of the impact of testing, treatment and control of HIV transmission in Kenya", Cogent Mathematics & Statistics, 2018" is another publication that originated from the work in this thesis.
- The remaining indices are either mathematical theorems and symbols that characterize the mathematical modelling. Other areas that could be similar are either definitions or statements that are properly cited from the sources. This has been done throughout the thesis.

The above similarity indices contribute to 46% of the 62%. This essentially implies that the similarity index of this thesis is 62%-46%= 16%.